Fortschritt-Berichte VDI

VDI

Reihe 1

Konstruktionstechnik/
Maschinenelemente

Nr. 438

Dipl.-Wirtsch.-Ing. (Univ.) Benjamin Schleich,
Erlangen

Skin Model Shapes: A new Paradigm for the Tolerance Analysis and the Geometrical Variations Modelling in Mechanical Engineering

Lehrstuhl für
Konstruktionstechnik
Friedrich-Alexander-Universität Erlangen-Nürnberg
Prof. Dr.-Ing. Sandro Wartzack

Skin Model Shapes:
A new Paradigm for the Tolerance Analysis and the Geometrical Variations Modelling in Mechanical Engineering

Skin Model Shapes: Ein neues Paradigma für die Toleranzanalyse
und die Modellierung geometrischer Abweichungen im Maschinenbau

Der Technischen Fakultät
der Friedrich-Alexander-Universität
Erlangen-Nürnberg
zur Erlangung des Doktorgrades

DOKTOR-INGENIEUR

vorgelegt von
Benjamin Schleich
aus Fürth

Als Dissertation genehmigt von
der Technischen Fakultät der
Friedrich-Alexander-Universität Erlangen-Nürnberg

Tag der mündlichen Prüfung: 20. März 2017
Vorsitzender des Promotionsorgans: Prof. Dr.-Ing. Reinhard Lerch

Gutachter: Prof. Dr.-Ing. Sandro Wartzack
Prof. Luc Mathieu

Fortschritt-Berichte VDI

Reihe 1

Konstruktionstechnik/
Maschinenelemente

Dipl.-Wirtsch.-Ing. (Univ.)
Benjamin Schleich, Erlangen

Nr. 438

Skin Model Shapes: A new Paradigm for the Tolerance Analysis and the Geometrical Variations Modelling in Mechanical Engineering

Lehrstuhl für
Konstruktionstechnik
Friedrich-Alexander-Universität Erlangen-Nürnberg
Prof. Dr.-Ing. Sandro Wartzack

Schleich, Benjamin
Skin Model Shapes:
A new Paradigm for the Tolerance Analysis and the Geometrical Variations Modelling in Mechanical Engineering
Fortschr.-Ber. VDI Reihe 1 Nr. 438. Düsseldorf: VDI Verlag 2017.
256 Seiten, 173 Bilder, 19 Tabellen.
ISBN 978-3-18-343801-3, ISSN 0178-949X,
€ 90,00/VDI-Mitgliederpreis € 81,00.

Für die Dokumentation: Simulation – Toleranzanalyse – Toleranzmanagement – Produktentwicklung – Konstruktion – Robust Design – Unsicherheit – Dimensional Management – Geometrische Produktspezifikation – Skin Model Shapes

Die vorliegende Arbeit wendet sich an Ingenieure und Wissenschaftler aus dem Bereich der virtuellen Produktentwicklung und angrenzender Disziplinen mit Schwerpunkt auf dem Toleranzmanagement. Sie stellt ein umfassendes Rahmenwerk für die Toleranzsimulation unter Berücksichtigung von Formabweichungen in Übereinstimmung mit internationalen Normen zur Geometrischen Produktspezifikation vor. Hierzu werden Algorithmen für die Erzeugung abweichungsbehafteter Punktwolken und Oberflächennetze (Skin Model Shapes), für deren Skalierung sowie deren Montagesimulation erarbeitet. Darüber hinaus behandelt die Arbeit die Toleranzanalyse bewegter Mechanismen und stellt einen Software-Prototypen für die Toleranzsimulation mittels Oberflächennetzen vor. Auf Basis der kritischen Gegenüberstellung von Ergebnissen des erarbeiteten Verfahrens mit bestehenden Toleranzanalysemethoden für typische Problemfälle wird gezeigt, dass durch die Berücksichtigung von Formabweichungen bei der Toleranzanalyse die Einflüsse von Bauteilabweichungen auf die Funktion und Qualität mechanischer Baugruppen und bewegter Systeme deutlich realitätsnäher bestimmt und dadurch Toleranzentscheidungen optimiert werden können.

Bibliographische Information der Deutschen Bibliothek
Die Deutsche Bibliothek verzeichnet diese Publikation in der Deutschen Nationalbibliographie; detaillierte bibliographische Daten sind im Internet unter http://dnb.ddb.de abrufbar.

Bibliographic information published by the Deutsche Bibliothek
(German National Library)
The Deutsche Bibliothek lists this publication in the Deutsche Nationalbibliographie (German National Bibliography); detailed bibliographic data is available via Internet at http://dnb.ddb.de.

D 29

Als Manuskript gedruckt. Printed in Germany.

ISSN 0178-949X

ISBN 978-3-18-343801-3

Preface

The current work was developed during my time as an academic counsellor at the Institute of Engineering Design KTmfk of the FAU Erlangen-Nürnberg. During that time, I received great support from and I was influenced by many persons, to whom I am sincerely grateful.

Particularly, I thank Prof. Dr.-Ing. Sandro Wartzack for offering me the opportunity to conduct my work under his guidance at the Institute of Engineering Design, for his professional supervision, and his constant support in scientific as well as personal affairs. The last five years have been not only busy, productive, and educational, but they have also been a pleasant expedition covering successful projects, minor detours, and much fun. I deeply thank Sandro for shaping this time and for providing me with responsibilities, scope for development, and unconditional trust during this period.

Moreover, I thank Prof. Luc Mathieu as a highly acknowledged expert and researcher in tolerancing and production engineering for sharing his professional expertise and personal advice, for contributing numerous valuable suggestions during the last years, and for agreeing to act as the co-examiner.

Additionally, I thank Prof. Dr. sc. ETH Alexander Hasse for his interest in my work and for acting as the chairperson of the examination committee. I also thank Prof. Dr. Michael Stingl for his interest in my work and for acting as a further member of the examination committee.

Beside this, my special thank goes to all past and present colleagues of the KTmfk, particularly to the tolerancing and robust design group, for the countless professional discussions, the constructive feedback, as well as for the optimal technical and collegial working environment. Only the working in such a strong and dedicated team allowed us to master many challenging tasks and projects. Moreover, I want to express my deep appreciation to those students, who have contributed to this work in any manner.

Furthermore, I want to express my deepest gratitude to Dr. Nabil Anwer for taking the time for numerous discussions and web-meetings during the last years, for sharing his professional experience, and for the fruitful and friendly cooperation.

I also thank all colleagues from national and international research laboratories and the computer-aided tolerancing community, who encouraged me in my work. Particularly, I thank Dr. Alex Ballu as one of the conceptual fathers of the Skin Model, Prof. Jean-Yves Dantan, and Prof. Rikard Söderberg for their favourable support and encouragement as well as many discussions and conversations during conferences and meetings. I also like to offer my thanks to all colleagues and partners from industry, who provided me with valuable comments and feedback as well as encouragement during the last years.

Last but most important, I owe my sincere and deepest gratitude to my beloved Juli, my parents, my brother, my sister-in-law, and the rest of my family for their patience and for providing me with unconditional love, support, motivation, and welcome diversion. All the efforts and hardships would not have been worthwhile without you.

March 2017 Benjamin Schleich

— Meinen Eltern —

Contents

Abbreviations and Symbols

Abbreviations

ANOVA	Analysis of Variance
ASME	American Society of Mechanical Engineers
BC	Before Christ
BRep	Boundary Representation
CAD	Computer-Aided Design
CAM	Computer-Aided Manufacturing
CAPP	Computer-Aided Process Planning
CAT	Computer-Aided Tolerancing
CLTE	Closed-Loop Tolerance Engineering
CMM	Coordinate Measuring Machine
CSG	Constructive Solid Geometry
CZ	Common Zone
D	Dimension
DIN	Deutsches Institut für Normung (German Institute for Standardization)
DLM	Direct Linearisation Method
DoF	Degree of Freedom
E. g.	Exempli Gratia
(E)FAST	(Extended) Fourier Amplitude Sensitivity Test
FEA	Finite Element Analysis
GD&T	Geometric Dimensioning and Tolerancing
GPS	Geometrical Product Specification
GUI	Graphical User Interface
I. a.	Inter alia
I. e.	Id est
I. i. d.	Independent and Identically Distributed
ICDF	Inverse Cumulative Distribution Function
ICP	Iterative Closest Point
IGES	Initial Graphics Exchange Specification
ISO	International Organization for Standardization
ITP	Integrated Tolerancing Process
KC	Key Characteristic
KDE	Kernel Density Estimate
LHS	Latin Hypercube Sampling
LSC	Least-Squares Circle/Cylinder
LSL	Lower Specification Limit
MBD	Model-based Definition
MCC	Minimum Circumscribed Circle/Cylinder
MIC	Maximum Inscribed Circle/Cylinder

MZC	Minimum Zone Circle/Cylinder
NC	Numerically Controlled
NURB	Non-Uniform Rational B-Spline
(K)PCA	(Kernel) Principal Component Analysis
PCFR	Place, Clamp, Fasten, and Release
PDF	Probability Density Function
PDM	Point Distribution Model
PMI	Product and Manufacturing Information
RD(M)	Robust Design (Methodology)
SDT	Small Displacement Torsor
SMS	Skin Model Shapes
SPC	Statistical Process Control
SSA	Statistical Shape Analysis
STEP	Standard for the Exchange of Product Model Data
STL	STereoLithography File Format
TC	Technical Committee
TCA	Tooth Contact Analysis
TTRS	Technologically and Topologically Related Surfaces
USL	Upper Specification Limit
VDA	Verband der Automobilindustrie (German Assoc. of the Automotive Industry)
VDI	Verein Deutscher Ingenieure (Association of German Engineers)
WC	Worst-Case
WP	Workpiece

Symbols

a, b, m, k, K	Cost-Function Parameters
$\boldsymbol{b}$	Scores, Axis Direction
$\tilde{\boldsymbol{b}}$	Random Scores
c	Cost (Tolerance-related)
c_a	Process Accuracy Index
c_p	Process Precision Index
c_{pk}	Process Capability Index
c_{pm}	"Taguchi" Index
d	Dimension, Distance
d^r	Radial Distance
d_{PS}	Projected (signed) Distance
d_{PSN}	Normal Distance
f	Tolerance Analysis Function, Probability Density, Facet of the Convex Hull
f	Stochastic Process with Approximation $\boldsymbol{f}$
h	Systematic Deviations (Point-wise), Height
l_ρ	Correlation Length
m	Module
n	(Vertex) Normal Vector

p	Point $\in \mathbb{R}^3$
$\boldsymbol{r}$	Rotations
$\boldsymbol{t}$	Tolerance, Point in Time, Translations
$\boldsymbol{w}$	Assembly Direction
x	Point $\in \mathbb{R}^3$
$\hat{x}$	Center of a Skin Model Shape
$\hat{x}^{\mathrm{f}}$	Center of a Skin Model Shape Feature
$\tilde{x}$	Point $x \in \mathbb{R}^3$ with systematic Deviations
$\check{x}$	Point $x \in \mathbb{R}^3$ with systematic and random Deviations
$\underline{x}$	Footpoint
C	Total Cost (Tolerance-related), Covariance Function
$\boldsymbol{C}$	Correlation Matrix
CV	Convex Hull Volume
$\boldsymbol{F}$	Force Slope of the Assembly Force
F_r	Runout Error
K	Cost Coefficient (Quality Loss)
L	Quality-Loss
P	Precision Factor
$\boldsymbol{P}$	Force Application Point of the Assembly Force
R^2	Coefficient of Determination
$\boldsymbol{S}$	Difference Surface
$\boldsymbol{X}$	Skin Model Shape as a Set of Points in $\mathbb{R}^3$
$\boldsymbol{X}^{\mathrm{f}}$	Skin Model Shape Feature ($\boldsymbol{X}^{\mathrm{f}} \subset \boldsymbol{X}$)
$\overline{\boldsymbol{X}}$	Mean (Skin Model) Shape
$\tilde{\boldsymbol{X}}$	Approximation of $\boldsymbol{X}$
Y	Key Characteristic
α	Rotation Angle
$\boldsymbol{\alpha}$	Rigid Body Transformation
α^E	Transmission Error
β	Regression Coefficients
$\boldsymbol{\beta}$	Parameter Vector
δ	Moment-independent Sensitivity Measure
ζ	Euclidean Distance
μ	Expectation, Sample Mean
ξ	Linearity Coefficient
$\boldsymbol{\xi}$	Gaussian Random Variables (i. i. d.)
ρ	Correlation Function
σ	Standard Deviation, Sample Standard Deviation
$\boldsymbol{\tau}$	Small Displacement Torsor
$\boldsymbol{\chi}$	Random Variables (Spatially correlated)

$\boldsymbol{\psi}$	Standard Gaussian Random Variables (i. i. d.)
ω	Weights
$\boldsymbol{\omega}$	Rotations (Small Displacement Torsor) with $\alpha \equiv r_x, \beta \equiv r_y, \gamma \equiv r_z$
Δp	Displacement of p
Δt	Time Discretization
$\boldsymbol{\Phi}$	Main Modes of Variation

Indices

i, n	$1, 2, 3, \ldots$	Counting Indices
ψ	$1, 2, 3, \ldots$	Assembly Steps

Zusammenfassung

In Zeiten scharfen internationalen Wettbewerbs steigt der Druck auf Unternehmen qualitativ hochwertige Produkte mit moderaten Fertigungskosten anzubieten. Obgleich moderne Fertigungsverfahren stetig steigende Fertigungsgenauigkeiten erreichen, sind dennoch die Produktqualität und die Montierbarkeit als wesentlicher Treiber für die Fertigungskosten durch geometrische Bauteilabweichungen beeinflusst, die zwangsläufig an jedem gefertigten Bauteil zu beobachten sind. Daher existiert eine dringende Notwendigkeit für Unternehmen, diese Abweichungen und deren Auswirkungen entlang des Produktlebenszyklus zu steuern. Um dies innerhalb der Zeit- und Kostenbudgets umzusetzen, werden Produkt- und Prozessentwickler durch Toleranzsimulationsprogramme unterstützt, die die frühzeitige Vorhersage der Auswirkungen von geometrischen Bauteilabweichungen auf Produkteigenschaften ohne zeit- und kostenintensive physikalische Prototypen erlauben. Allerdings bringen bekannte Methoden und Werkzeuge zur Toleranzanalyse und deren zugrundeliegende mathematische Ansätze zur Abbildung geometrischer Abweichungen, Spezifikationen und Anforderungen schwerwiegende Nachteile in Hinblick auf die Berücksichtigung von Formabweichungen mit sich und sind nicht vollständig konform zu internationalen Tolerierungsnormen.

Als Antwort auf diese Nachteile wurde das Konzept der Skin Model Shapes als neues Paradigma für die Modellierung von Produktgeometrie unter Berücksichtigung geometrischer Abweichungen entwickelt. Es nutzt punktbasierte Modelle zur Abbildung der Produktgeometrie in Anbetracht aller Arten geometrischer Abweichungen. Die vorliegende Arbeit untersucht die Grundlagen des Konzepts der Skin Model Shapes, demonstriert seine Potentiale für die Abbildung von abweichungsbehafteter Produktgeometrie entlang des Produktlebenszyklus und zeigt wesentliche Anwendungsfelder dieses Konzepts im Kontext des Toleranzmanagements auf. Zudem wird ein Toleranzanalyseansatz auf Basis von Skin Model Shapes vorgestellt, der verschiedene Algorithmen für die Erzeugung und Verarbeitung von Bauteilrepräsentanten in diskreter Geometrie nutzt und die realistische Vorhersage der Auswirkungen von geometrischen Bauteilabweichungen auf funktions- und qualitätskritische Schließmaße erlaubt. Die vorgestellten Ergebnisse dieses Ansatzes zur Toleranzanalyse für verschiedene Problemfälle belegen, dass Formabweichungen deutlichen Einfluss auf verschiedene Produkteigenschaften haben und dass das Konzept der Skin Model Shapes sowie der vorgestellte Toleranzanalyseansatz ein theoretisch fundiertes Rahmenwerk bilden, das die Nachteile bekannter Toleranzanalyseverfahren überwindet.

Abstract

In times of fierce international competition, the need for companies increases to deliver high-quality products manufactured at moderate costs. However, even though modern manufacturing processes offer steadily increasing accuracy, the product quality as well as the product assemblability as a main driver for the manufacturing costs are influenced by geometrical part deviations, which are inevitably observed on every manufactured workpiece. Thus, there exists a strong need for companies to manage these deviations and their effects throughout the whole product life-cycle. In order to perform this within time and cost constraints, computer-aided tolerancing tools support product and process development teams by enabling the early prediction of the effects of geometrical part deviations on product characteristics without the need for cost and time expensive physical mock-ups. However, established tools for the tolerance analysis and their underlying mathematical approaches for the representation of geometrical deviations, geometrical specifications, and geometrical requirements imply severe shortcomings regarding the consideration of form deviations and lack of a full conformance to international tolerancing standards.

As a response to these shortcomings, the concept of Skin Model Shapes has been developed as a new paradigm for the modelling of product geometry considering shape variability. It employs point-based models for the representation of part geometry considering all different kinds of geometrical deviations. The present work explores the fundamentals of the concept of Skin Model Shapes, demonstrates its potentials for the representation of product geometry considering geometrical variations along the product life-cycle, and illustrates main applications of this concept in the context of geometrical variations management. Moreover, a tolerance analysis approach utilising the concept of Skin Model Shapes is proposed, which employs various algorithms for the generation and processing of discrete geometry Skin Model Shapes and which allows the realistic prediction of the effects of geometrical variations and tolerance specifications on product key characteristics. The results obtained by this novel tolerance analysis approach for various study cases highlight, that form deviations have distinct effects on geometrical product characteristics and that the concept of Skin Model Shapes and the tolerance analysis based thereon offer a sound theoretical framework and theory, which overcomes severe shortcomings of established tolerance analysis approaches.

1 Introduction

The form and shape of physical artefacts pervade all aspects of our daily life as our visual and tactile senses permanently perceive the shape and geometry of objects, that surround us. Based on these perceptions, we classify and arrange the objects, we implicitly try to derive their affordances, and we decide if the objects satisfy our subjective feeling of pleasure. Moreover, these perceptions often unconsciously guide us when assessing the quality of physical products, when forming our opinions about brands and companies, and when making purchasing decisions.

1.1 The Context: Geometrical Variations Management

Consequently, due to its omnipresence in the physical world, "geometry plays a crucial role in nearly all design and production activities in the discrete goods industries" [VR77] and companies are required to control geometrical part variations, which are inevitably observed on every manufactured artefact, and their effects on the product quality throughout the whole product life-cycle in order to live up to the ever tightening product requirements[1] [MB07]. In modern value added chains, which are increasingly based on specialisation and external procurement, this involves many different activities, that are performed by various actors. These actors, in turn, are to specify, communicate, and process the various requirements on the part and product geometry. The concepts of dimensional and geometrical tolerances, which are anchored in international tolerancing standards, such as the standards for the geometrical product specification (GPS) by the International Standardization Organization (ISO) and the standards for geometric dimensioning and tolerancing (GD&T) by the American Society of Mechanical Engineers (ASME), offer a means of communication between them and provide a "language" for the specification, communication, and verification of geometrical product requirements [Sri91]. In this context, it is widely accepted, that particularly functional tolerancing, which consists of specifying such tolerances in order to ensure the required product quality [DBM08], is a highly important and responsible task in geometrical variations management, since the geometrical part specifications are ubiquitous throughout the product life-cycle and "profoundly impact the quality and cost" [QDS+12] of a product. Consequently, functional tolerancing "has become an important issue in [the] product design process" [DBM08], especially for "automotive and aircraft industries" [DBM08].

In order to perform this task within time, cost, and quality constraints, there is "a critical need for a quantitative design tool" [DGD+12], that "brings the engineering design requirements and manufacturing capabilities together in a common model, where the effects of tolerance specifications on both design and manufacturing requirements can be evaluated quantitatively" [DGD+12]. This quantitative design tool is commonly referred to as tolerance analysis, which enables the virtual prediction of the effects of geometrical part deviations on geometrical product requirements and "is a key element in industry for improving product quality" [DGD+12].

[1] As one prominent example for tightening geometrical requirements on consumer products, Jonathan Ive, Chief Design Officer at Apple Inc., highlighted at the introduction of the iPhone 5 in 2012, that "The variances from product to product, we now measure in microns".

1.2 The Essence: The Concept of Skin Model Shapes as a new Paradigm for Modelling Geometrical Variations

Nowadays, the efficient execution of product development, manufacturing, and inspection activities relies inevitably on the extensive use of computer-aided tools for the modelling and analysis of parts, assemblies, and products as well as the simulation of manufacturing and inspection processes. In this context, computer-aided design (CAD) and solid modelling are key technologies to designing the nominal product geometry during virtual product development and have been increasingly introduced in various industries during the last decades. They allow the modelling of the nominal product geometry, whereas the functionalities of these tools have steadily increased over the past decades[2]. However, they lack of a realistic representation of product shape variability considering inevitable geometrical part deviations, which also holds for established tolerance analysis approaches. In this regard, the main shortcomings of these tools and their underlying approaches for the virtual representation of part geometry are the lacking consideration of form deviations and, as a consequence, the insufficient conformance to international tolerancing standards. As a response to these shortcomings, the concept of Skin Model Shapes has been developed as a new paradigm for the modelling of product geometry considering shape variability based on discrete geometry representation schemes (see Figure 1.1) [SAMW14]. It stems from international standards for the geometrical product specification (GPS) [ISO17450-1], grounds on the Skin Model [ABM13], which is a model of the physical interface between a workpiece and its environment and which can be considered as a fundamental concept of modern GPS standards, and is to convey the concept of the "Digital Twin"[3] [Gri14] to geometrical variations management.

As its essence, the present work explores the fundamentals of the concept of Skin Model Shapes, demonstrates its potentials for the representation of product geometry considering geometrical variations along the product life-cycle, and illustrates main applications of this concept in the context of geometrical variations management and, in particular, in tolerance analysis.

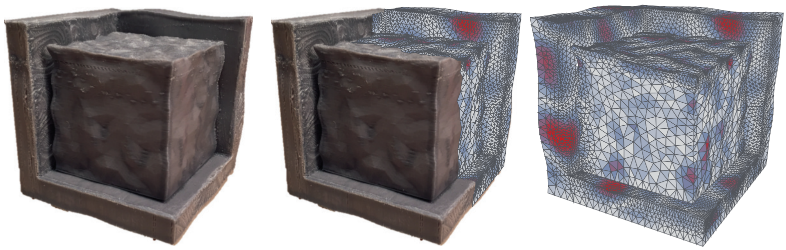

(a) Picture of Physical Parts (b) "Digital Twins" (c) Skin Model Shapes

Figure 1.1: The Essence: The Concept of Skin Model Shapes as a novel Paradigm for Modelling and Assessing Geometrical Variations

[2] It has been argued that solid modellers shifted from being design *tools* to design *systems* [LvHB$^+$14].

[3] The concept of the "Digital Twin" can be understood as a "virtual representation of what has been produced" [Gri14], while the underlying idea is to "compare a Digital Twin to its engineering design to better understand what was produced versus what was designed" [Gri14].

1.3 The Aim: A Framework for the Tolerance Analysis based on Skin Model Shapes

In times of fierce international competition and decreasing times-to-market, there is a strong ambition for shifting problem identification and solving to early design stages in order to shorten the product development lead time [TF00]. These ambitions coupled with the high cost responsibility in early design stages[4] dictate the use of advanced computer-aided tools to virtually predict the effects of design decisions on the product behaviour without the need for costly and time-expensive physical mock-ups. Among these various computer-aided tools, computer-aided tolerancing and tolerance simulation tools do not rank as mere niche applications, but are increasingly applied in various industries, since they allow the prediction of the effects of tolerance specifications on assembly and product key characteristics. Indeed, "as the geometric tolerances are complex, so too are the algorithms using these tolerances" [MB07] and many established computer-aided tolerance analysis tools are not fully conform to international tolerancing standards.

As a response, the aim of the current work is the utilisation of the concept of Skin Model Shapes for the tolerance analysis to provide a valuable design tool based on a sound mathematical framework, that overcomes the shortcomings of established tolerance analysis approaches and allows the realistic prediction of the effects of geometrical variations and tolerance specifications on product key characteristics and the product behaviour (see Figure 1.2).

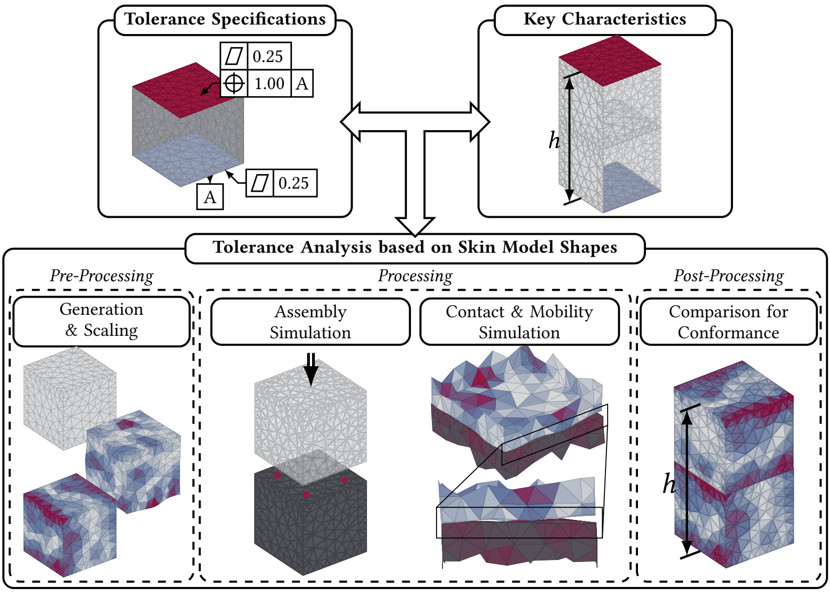

Figure 1.2: The Aim: Utilisation of the Concept of Skin Model Shapes for Tolerance Analysis

[4]It has been reported, that up to 70% of the final product costs can be traced back to decisions made in early design stages [VDI2235, BDK94].

1.4 The Approach: Scope and Outline of the Work

In order to tackle the illustrated challenges, the work is structured as follows (see Figure 1.3). Firstly, the context of this work, namely the issue of geometrical variations management, is introduced. Moreover, the standards for the geometrical product specification as the predominant means of communication in geometrical variations management are reviewed and the state of the art regarding tolerancing, particularly focusing on the computer-aided tolerance analysis, is presented. Thereafter, based on the provided context and state of the art, the need for research is identified. Following this, the concept of Skin Model Shapes is conceptualised, approaches for its representation and visualisation are highlighted, a framework for the generation of Skin Model Shapes is provided, and potential applications for this concept in geometrical variations management are carved out. Based thereon, a framework for the tolerance analysis employing the concept of Skin Model Shapes is detailed, which comprises various approaches for the processing of Skin Model Shapes, such as the scaling and the assembly simulation. After that, the prototype implementation of a tolerance analysis tool using these approaches is explained. Furthermore, the tolerance analysis approach based on Skin Model Shapes is applied to various case studies and the results are critically discussed. Finally, a conclusion is given and perspectives for future research are highlighted.

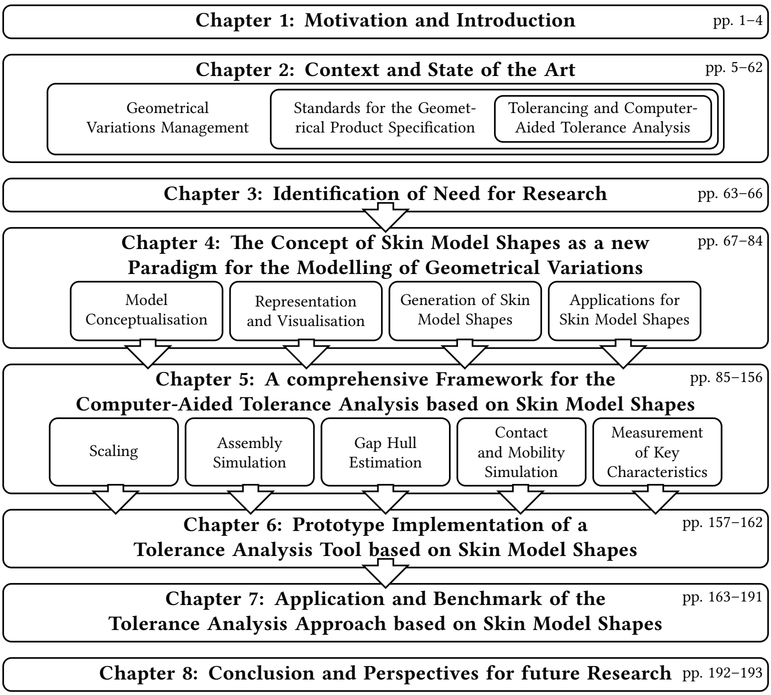

Figure 1.3: Outline of the Work

2 Context and State of the Art

Since geometrical deviations are observed on every manufactured artefact due to the axioms of manufacturing imprecision and measurement uncertainty [Sri06], there exists a strong need for modern companies to manage these deviations and their effects on product assemblability, product quality, and product function along the whole product life-cycle [MB07]. This requires many activities and tasks to be performed by different departments and various actors, with manifold computer-aided tolerancing tools having been developed to support these activities. Among these different tasks, the tolerance analysis is a key activity, since it aims at assessing the effects of geometrical deviations on product characteristics already during product design, and not least its importance becomes apparent from the high number of computer-aided tolerance analysis approaches, that have been proposed during the last decades.

The aim of this chapter is to provide an overview of the different tasks and activities in the context of geometrical variations management, to give a brief introduction to the standards for the geometrical product specification as the predominantly used toolbox for specifying and communicating geometrical product requirements, and to highlight different approaches and tools for the computer-aided tolerancing with a focus on the computer-aided tolerance analysis.

2.1 Geometrical Variations Management throughout the Product Life-Cycle

The Need for Geometrical Variations Management Though modern manufacturing processes achieve steadily increasing accuracy [Tan83, HCHC06, DL08], geometrical deviations[5] compared to the nominal and intended geometry are observed on every physical artefact and are ubiquitous at all stages of the physical product origination process [She30, DQA$^+$13]. These geometrical deviations have various process-related sources[6] and can be classified as deviations of dimension, surface texture, form, orientation, location, and runout (see Figure 2.1) [ISO4287, ISO14405-1, ISO1101]. Beside this classification, international standards [ISO8785] define different terms for the description of surface imperfections and [DIN4760] differentiates form errors according to the ratio between the distance and depths of the surface irregularities as form deviations, waviness, and surface roughness (see also [Wec14]). These geometrical deviations are technically-economically inevitable and vary even for parts of the same production lot. Furthermore, they have distinct effects not only on the product function [Buc21, She30, WCH$^+$88], but also on the perceived product quality [FS10, FKS13, QKFS13, HDS13a,

[5] In the following, the term "deviation" according to ISO 1101:2012 [ISO1101] is used interchangeably with the term "variation" according to ASME Y14.5-2009 [ASM09].

[6] The attempt to discuss all these process-related sources of geometrical deviations would result in a non-exhaustive list. However, some further information on the effects of process variables on geometrical deviations can be found in [HSB$^+$99, LV03, WB06, TD13] for machining processes, in [SZCZ08] for high-speed milling, in [HNX$^+$14, LLK98a, LLK98b, MSP14] for layered and additive manufacturing, in [LLDM15] for sheet forming, in [VMW10] for casting, in [ISO8062-1, ISO8062-2, ISO8062-3] for moulding, and in [WSL13, LCE$^+$14] for spot and sheet metal welding.

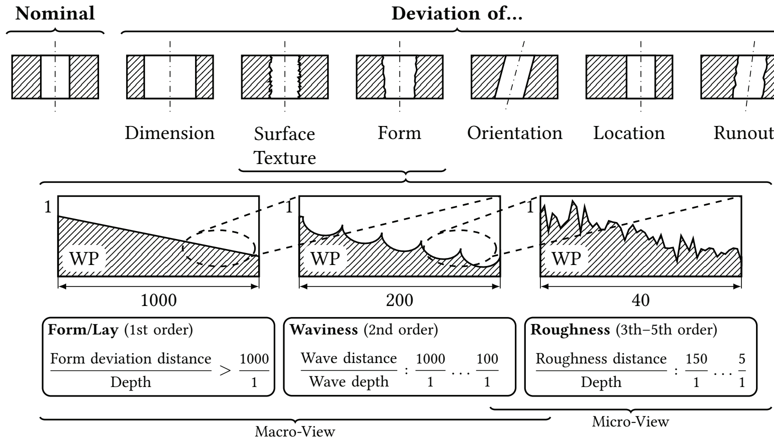

Figure 2.1: Classification of Geometrical Deviations for a Drill-Hole freely adapted from [ISO4287, ISO14405-1, ISO1101, DIN4760, JS14]

HDS15] and the economic and environmental sustainability [HDS13b, HDS14]. Moreover, they add up with further deviations caused by physical phenomena, such as wear, thermal expansion, or part deformations [JHC02, BA11, AS13, SW13a, WSW13, WW13, PTN14] and hence further deteriorate the product quality during use. Consequently, there is a strong need for companies to manage these geometrical deviations along the whole product life-cycle [MB07, WMS+11].

Geometrical Variations Management then and now Prior to the first industrial revolution, when products were made by artisans and the different steps of product origination from design, to manufacturing, assembly, and testing were physically unified [SWM96, Voe98], the management of geometrical part deviations was usually simply performed by fitting parts to their mating parts [Jur62, Eva74] and thus by manually reducing the "relative" deviations between parts for every single entity. Since then, triggered by the introduction of the concept of interchangeable parts as a basis of present-day production by Christopher Polhem, Jean-Baptiste Vaquette de Gribeauval, Honoré Blanc, and Eli Whitney in the 18th century [Woo60, MCB98, Dan14], i. a. the ambition for efficient fabrication of physical artefacts in mass production, the increasing product complexity, and the diversification of customer needs, have led to a disruption of design, manufacturing, assembly, and inspection, to an increasing specialisation of these disciplines, and particularly to a dichotomy between design and manufacturing [SWM96]. To this day, this disruption becomes apparent in modern series manufacturing chains, which are considerably based on the concepts of total or partial part interchangeability[7], process independence, and external procurement [Voe98]. Thus, in contrast to former times, industry is facing the current situation, in which many departments and different act-

[7] Total part interchangeability allows the exchange of a part with any other good part, whereas partial part interchangeability requires a part of the same accuracy class ("selective fitting") [FGE91, Wit11, JS14].

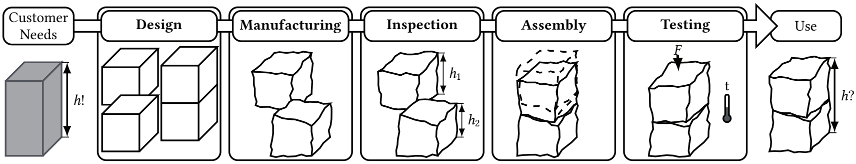

Figure 2.2: Geometrical Variations Management Stages throughout the Product Life-Cycle

ors from product design, to manufacturing, inspection, assembly, and testing (see Figure 2.2), are involved in the **geometrical variations management** process, which covers all activities related to controlling geometrical deviations throughout the product life-cycle in order to ensure quality goals. These different actors in geometrical variations management perform manifold activities related to controlling geometrical deviations using specialized tools (see e. g. [MC10]) and they are to decide about manifold issues (see Figure 2.3), such as the product structure, the part design, and the manufacturing, inspection, and assembly plans and processes. In order to perform these tasks, they are required to communicate (and often fiercely discuss) about how precisely parts should be manufactured, how they should be inspected, and how they should be positioned and assembled to finally ensure, that the product requirements are met during product use in spite of geometrical part deviations.

Communication in Geometrical Variations Management As the product realization process changed from job-shop to mass production and the number of actors in geometrical variations management increased, it soon became clear, that the communication between them required the specification not only of the design intent and the nominal product geometry by engineering drawings or a physical reference part, called a "masterpiece" [Har14], but also of the *set* of acceptable non-ideal product geometries by expressing allowable limits through symbols on the engineering drawings [VR77, Hop92, Voe93, Sri99, MB03]. Moreover, in order to avoid confusion due to multiple different versions of such specifications, it seemed appropriate to appoint only one department in a company to be in charge of authoring and issuing these specifications (being the design department in most engineering companies), which should then be disseminated to all other departments and actors [Jur62].

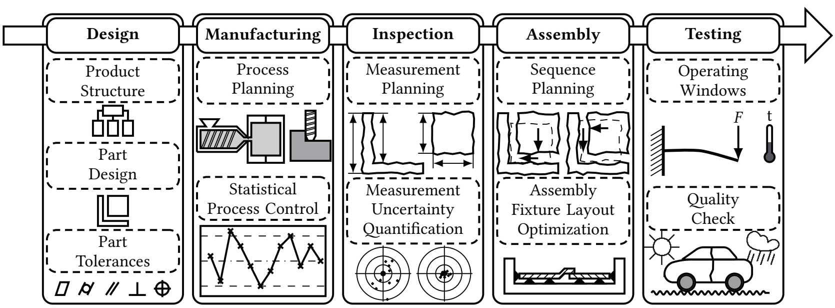

Figure 2.3: Important Issues in Geometrical Variations Management

However, in the course of time, companies encountered many problems related to the insufficient communication between the different involved persons in geometrical variations management, such as quality problems, high scrap rates with need for rework, high manufacturing and inspection costs, as well as delays due to unnecessary iterations within and between the different stages in the product origination process [Dan14]. This was because their specifications allowed different expressions and interpretations of the allowable limits of the non-ideal product geometry and of how to verify if a workpiece was conform to these limits [BM96, Dan14]. Thus, there was a need for enabling an unambiguous communication in geometrical variations management within and between companies by establishing a univocal language for the specification and verification of non-ideal product geometry [BM96].

As a response to this need, starting from simple plus/minus limits on product dimensions and a general definition of a **specification** "as a quantity called characteristic, which is limited in a given range" [MB03], the concept of a **geometrical specification** as "a condition, which must be satisfied by a part or a set of parts" and which "is expressed from a geometrical characteristic between geometrical features or on geometrical features"[8,9] [BMD03] evolved. The evolution of this concept has led to the current practice for the specification of the allowable limits of product geometry and for the communication of these geometrical specifications in industry, which is based on the application of geometrical dimensioning and tolerancing standards (**GD&T**)[10]. They provide "a symbolic language used to specify the size, shape, orientation, and location of part features" [Dan14] and introduce the concept of dimensional and geometrical **tolerances**, which "define the limit boundaries within which the real workpieces produced must fit to function as intended" [Cha13, ISO286-1]. During the last decades, these GD&T standards have been continuously revised and improved and offer a sound and versatile toolbox for the specification of non-ideal product geometry [WS93, PJH$^+$14].

The Role of Tolerances in Geometrical Variations Management and the Product Life-Cycle Thus, the concept of dimensional and geometrical tolerances evolved from the need for the unambiguous communication between the various actors in geometrical variations management regarding the specification and verification of non-ideal product geometry. As indicated, this communication is often perceived as being unidirectional *from* design, where tolerances are annotated as symbols and numerical quantities on technical drawings or on three-dimensional solid models per model-based definition (MBD) of product and manufacturing information (PMI) [QRP$^+$10, LL15], *to* manufacturing and inspection, where they have to be adhered to and verified.

[8] This may serve as a preliminary definition. The definition of the term "geometrical specification" according to international standards for the geometrical product specification is introduced in section 2.2.

[9] In the context of engineering design, the term "feature" is often defined with some similarity to SHAH: "Features are generic shapes with which engineers associate certain properties or attributes and knowledge useful in reasoning about the product" [Sha91]. However, in the context of this work, a feature is defined in a strict geometrical sense according to ISO 17450-1:2011: "A feature is a point, line, surface, or volume or a set of these elements" [ISO17450-1]. Moreover, a distinction between ideal, non-ideal, integral, and derived features will be introduced in section 2.2.

[10] In the following, the term GD&T is defined in analogy to [Dan14] and refers collectively to both the standards for the geometrical product specification by the International Organisation for Standardisation (ISO) [ISO1101], to which an overview is given in section 2.2, and their American counterpart, the Dimensioning and Tolerancing Standard Y14.5 by the American Society of Mechanical Engineers (ASME) [ASM09].

However, in fact, as tolerances link the product function and the design intent with the manufacturing and measurement precision [SWM96, Dan14], they serve as a multi-directional connection and are hence a means to overcome the disruption of the different disciplines in geometrical variations management and to reintegrate them by knowledge and information sharing [SWM96]. Consequently, tolerances are ubiquitous throughout the product life-cycle as they affect nearly every aspect of the product origination (see Figure 2.4) [CP91, RLW91, Sri94, HC02a] and they are required by many actors in downstream activities for different purposes, e. g. for the tolerance transfer, the computer-aided process planning (CAPP) [LLH99, ElM93, EN14], the tolerance verification, and the performance correlation [KPMW03]. In this regard, tolerances are a critical link between design, manufacturing, inspection, and assembly as they have distinct effects on the product function and quality as well as on the manufacturing, inspection, and assembly costs [Jur62, Pet70, BG70a, BG70b, CM88, ATLD14, MP14].

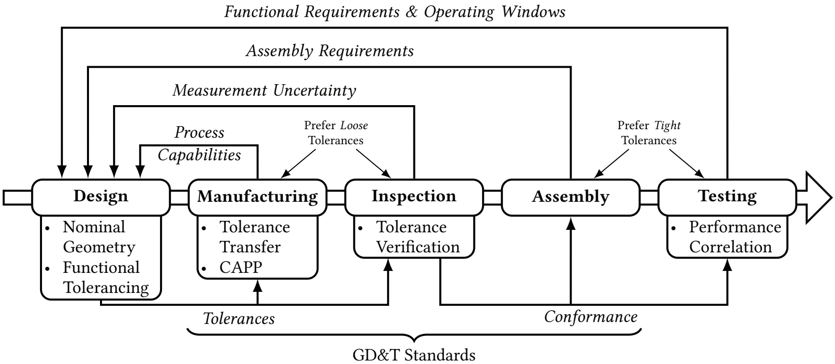

Figure 2.4: The ubiquitous Role of Tolerances and the Utilization and Transfer of Tolerance Information during the Product Life-Cycle (freely adapted from [CP91, RLW91, HC02a, KPMW03])

The Importance of integrated Tolerancing Activities during Design Due to the ubiquitous role of tolerances in the product life-cycle and the far-reaching impacts of tolerancing decisions, design teams are required to choose carefully between *tight* tolerances, which certainly ensure the product requirements, but lead to high manufacturing and inspection costs due to additional manufacturing steps, costly and time-intensive measurement operations, and an increased scrap rate, and *loose* tolerances, which allow cheap fabrication of products, but probably lead to increased assembly costs as well as non-functioning products and deteriorated quality [CP91]. Keeping in mind, that up to 70% of the product costs is due to decisions made in the design stage [VDI2235, BDK94] and that up to 70% of all design changes[11] are related to geometrical variations [CS95], it is thus not exaggerated to state, that specifying tolerances during design can be compared to "drawing a check on the company treasury" [Jur62]. In order to cope with this cost and quality responsibility, design teams have to consider various requirements of downstream activities, such as manufacturing capabilities, avail-

[11]These design changes, in turn, lead to costs for the change of manufacturing and inspection equipment [FGE91].

able inspection capabilities, measurement uncertainties, assembly requirements[12], admissible operating conditions, and, of course, quality as well as functional requirements, when performing the tolerancing activities. In times of fierce international competition and decreasing times-to-market, the simultaneous consideration of all these contradictory requirements and constraints in product design — summarized under the term “Design for X” [Mee94] — requires integrated product and process development approaches, concurrent engineering workflows [RLW91, Soh92, GRDN97, Smi97], and predictive engineering strategies [War00]. Moreover, the ambition for shifting problem identification and solving to early design stages in order to shorten the product development lead time, often depicted as “front-loading” [TF00], dictates the use of advanced computer-aided tools to virtually predict the effects of design decisions on the product behaviour without the need for costly and time-expensive physical mock-ups. Particularly, in the automotive industry, the application of simulations and computer models has been identified as an important capability to speeding up and reducing the cost of design iterations and thus to increase the product development performance [Tho98]. These computer-aided tools thrive on the rapid growth of computer technology and the steadily evolving application of computers in industry [Bre96, Tho98]. Consequently, there is a strong need for companies to introduce and apply computer-aided tolerancing tools to support the tolerancing activities during design.

In summary, considering the vast importance of the concept of dimensional and geometrical tolerances as an enabler of part interchangeability in modern series manufacturing chains, their ubiquitous role in the product life-cycle, and the immense cost and quality responsibility coming along with tolerancing, it is indispensable for companies to pay specific attention to the tolerancing activities during design. Moreover, there is a strong need to support these activities by adequate computer-aided tolerancing tools in order to allow the integration of all other geometrical variations management activities performed throughout the product life-cycle and to finally shorten the product development lead time and to increase the product development performance.

In the following, as a background for the further work, an introduction to the international standards for the geometrical product specification as the established means of communicating the specification and verification of product geometry is provided, before the tolerancing activities during design and computer-aided tolerancing tools are highlighted in section 2.3.

2.2 Standards for the Geometrical Product Specification as the predominant Means of Communication in Geometrical Variations Management

Every form of human communication and exchange as well as cultural interaction requires shared concepts and meanings [Wen10]. In this regard, standardisation as an age-old process aiming at establishing such shared concepts, called standards[13], “has always been a central component of transnational and transcultural exchange” [Wen10]. The importance of stand-

[12] These assembly requirements comprise product assemblability, but also requirements related to the ease and cost of assembly operations and the flexibility of assembly systems [BB08, AJF15].

[13] The European Commission defines standards as “technical specifications defining requirements for products, production processes, services or test-methods” [Com16].

ardisation is widely accepted, as the Council of the European Union acknowledges, that standardisation "has contributed in a significant way to the functioning of the single market, the protection of health and safety, the competitiveness of industry and the promotion of international trade, and has been supporting an increasing range of community policies" [Con00]. Moreover, it has contributed to the economic growth of nations [Mio09]. Despite its importance, the first systematic attempts to standardisation began not until the end of the eighteenth century, during the French Revolution, when the French revised their weights and measures using a science- and conference-based standardisation process, that became later "the primary way to set and maintain international standards" [Wen10].

In this context, particularly the standardisation of weights and measures [Ada21] as well as of product geometry has always been of great importance [Sri99], which is further increasing with the use of computer-aided tools at all stages of the product life-cycle [BM96]. In this regard, it can be seen from the very first standard issued by the International Organization for Standardization (ISO), the ISO 1:2002 "Geometrical Product Specifications (GPS) – Standard reference temperature for geometrical product specification and verification" [ISO1], which was last revised in 2002, that the standards for the geometrical product specification (GPS) "form some of the earliest standards of the information age" [Sri08]. These GPS standards are a set of international standards for the description, specification, and verification of workpieces, so that they can be manufactured and measured independently as single parts or assembly groups in such a manner that they will assemble interchangeably without the need for rework while still fulfilling their intended function [WH01]. They cover many documents, which are nowadays under responsibility of a single ISO Technical Committee (TC), the ISO/TC 213[14] (Dimensional and geometrical product specifications and verification), "which is charged with the standardization of dimensioning, tolerancing, surface finish and related metrological principles and practices" [Sri08], and are widely applied in industry [Sri99, Sri08, Cha13]. Some of these GPS standards are the ISO 14638:2014 (Geometrical product specifications (GPS) – Matrix model), which is "a fundamental ISO GPS standard and explains the concept of Geometrical Product Specification (ISO GPS)" [ISO14638], the ISO 8015:2011 (Geometrical product specifications (GPS) – Fundamentals – Concepts, principles and rules), which "specifies fundamental concepts, principles and rules valid for the creation, interpretation and application of all other International Standards, Technical Specifications and Technical Reports concerning geometrical product specifications (GPS) and verification" [ISO8015], and the ISO 1101:2012 (Geometrical product specifications (GPS) – Geometrical tolerancing – Tolerances of form, orientation, location and run-out), which "contains basic information and gives requirements for the geometrical tolerancing of workpieces and represents the initial basis and defines the fundamentals for geometrical tolerancing" [ISO1101]. The set of GPS standards provides terms and definitions for a univocal description, specification, and verification of product geometry and is thus often considered as a fundamental engineering language regarding geometric di-

[14] The scope of the ISO TC 213 is defined by the ISO as follows: "Standardization in the field of geometrical product specifications (GPS), i.e. macro- and microgeometry specifications covering dimensional and geometrical tolerancing, surface properties and the related verification principles, measuring equipment and calibration requirements including the uncertainty of dimensional and geometrical measurement. The standardization includes the basic layout and explanation of drawing indications (symbols). " [ISOTC16]

mensioning and tolerancing (GD&T) [DBM08]. In this context, it has been argued, that these standards ”provide both the syntax and the semantics of the GD&T language” [Sri08]. Consequently, they serve as the basic form of communication between all persons and company departments, which are involved in and interrelated by tolerancing activities and geometrical variations management [BM96, BMD03, Cha13].

Since the modern standards for the geometrical product specification cover more than 100 different documents, many of them issued and thoroughly revised in recent years, it is certainly not easy to speak the "GD&T language" fluently and to fully comprehend all the concepts and backgrounds required for proper application. In this regard, as Srinivasan clarifies, "the best way to understand the past and look clearly into the future is to follow the history of development of these standards" [Sri08]. Thus, the next section will provide a brief history of the standards for the geometrical product specification, before the fundamentals and basic concepts of these standards are highlighted. After that, some current research and education trends are illustrated and, for the sake of completeness, further approaches for the specification of product geometry are briefly looked at.

2.2.1 A Brief History of the Standards for the Geometrical Product Specification

The standards for the geometrical product specification have evolved over the last 75 years from company practices to the predominant means of communication in geometrical variations management [Sri13]. In this regard, they form a symbol language, which is used by designers to express the limits of geometrical part deviations, that are still allowable without deteriorating the intended function, and to communicate these limits to manufacturing, inspection, and testing. Hence, this language has to be embeddable in the form of communication used to convey the design intent to all the downstream activities. Moreover, as the geometrical part deviations are to be measured during inspection in order to verify, if a manufactured workpiece is conform to the specifications, it is essential, that the specifications made allow their verification using the available inspection capabilities. Thus, the language used to express the specifications has to consider the current state of the art regarding the verification[15].

Consequently, the standards for the geometrical product specification have always been caught between the restrictions imposed by the predominant means of *technical communication* (i. e. sketches, engineering drawings, or solid models) and the possibilities offered by available *verification technologies*[16] used to perform the verification of the specifications. Thus, when retracing the history of the GPS standards, it is important to keep in mind the technological progress in both of these domains. In the following, some of these developments are briefly highlighted in order to illustrate the historical background of the GPS standards (see Figure 2.5) with a focus upon the most relevant milestones.

[15] As Hook highlights, "we know now that the results one obtains vary with the measurement process used" [Hoo93].

[16] The term "verification technology" is used here instead of "measurement technology" to take account of the fact, that for example gauges are a means of verification, but not necessarily of measurement.

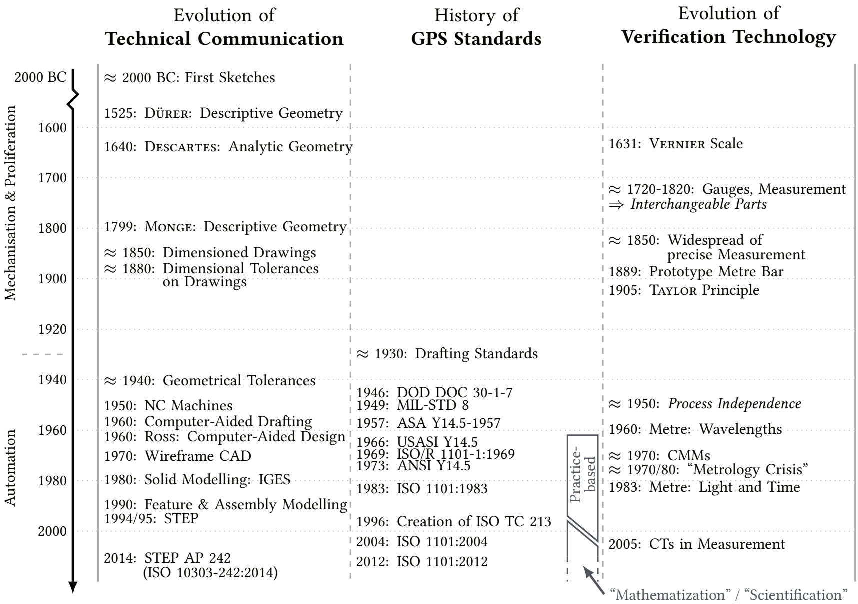

Figure 2.5: The History of GPS Standards in the Context of Technical Communication and Verification Technology (freely adapted from [Voe93, Voe98, Nie03, Sri08, Kwa11, Har14])

Mechanisation and Proliferation The need for communicating technical ideas and the designer's intent of product geometry has led engineers to create and distribute engineering drawings for centuries and historic evidence suggests, that the first engineering drawings in the form of *sketches* containing projected views have been used around 2,000 BC [Boo63, Sri99]. Advancements in the fields of analytic geometry (e. g. by Descartes around 1640) and descriptive geometry (e. g. by Dürer in 1525: "Underweysung der messung mit dem zirckel und richtscheyt in Linien ebnen unnd gantzen corporen", and Monge in 1799: "Géométrie descriptive") led to the use of more sophisticated two-dimensional drawings by the end of the 18th century. During that time, also the measurement technology made progress and particularly the invention of the Vernier scale gave birth to a precise measurement instrument, that was comparably small regarding existing measurement instruments, easy to read and use, and simple to fabricate [Kwa11]. Such measurement devices and gauging technology enabled the first attempts of *interchangeable parts* during the 18th century[17], with particularly functional gauging being considered as the key technology behind this concept, that forms the basis of mass production [Voe93]. However, from its invention, it took almost 200 years to the mid of the 19th century, until the Vernier scale and other precise measurement instruments, such

[17] There exist different sources on when and by whom the concept of interchangeable parts was firstly achieved. Juran even states, that "Interchangeability as a concept has also existed in nature for millions of years before man came on the earth" [Jur62]. However, the first implementation of this concept in shop floors must have happened between 1720 and 1820 [Woo60, Voe93, MCB98, Voe98, Dan14].

as micrometers and callipers, could themselves be manufactured in mass production and were widespread in shop floors [Voe98]. Their availability triggered designers to add dimensions to their engineering drawings by approx. 1850. From that, it did not take a long time until the first dimensional tolerances, serving as a means to communicating the allowable limits of part dimensions from design to the shop floor, began to appear on engineering drawings by approx. 1880[18]. However, back then, engineering drawing and drafting, which comprises also the organisational and documentary efforts related to the technical product documentation [Boo63, Sri08], as well as dimensional tolerances and their indication on engineering drawings were based on company practices, but had not been standardised. However, at that time, i. a. the industrial revolution and increasing trade fuelled the need for a universal length standard [Sri08, Wen10], which, 90 years after the French had defined the metre based on the distance between the north pole and the equator [Wen10], led to the first definition of the international prototype metre as the distance between two lines on a prototype metre bar in 1889 [Swy01, Wen10]. Another important achievement related to verification technology during that time was the British patent No. 6900 from 1905 ("Improvements in gauges for screws"), in which, conscious of the fact, that dimensional tolerances and their verification by micrometers and callipers did not ensure part interchangeability, Taylor described the concept of full-form inspection and defined requirements for go and no-go gauges. From that, the underlying principle for dimensional tolerances to ensure part interchangeability is widely known as the Taylor or envelope principle, which is still the default tolerancing principle in the American GD&T standard ASME Y14.5, defined as rule #1. Shortly after that, the British standard 27 "Report on Standard Systems of Limit Gauges For Running Fits" [BS27] made recommendations for dimensional tolerances, which were defined as "a difference in dimensions prescribed in order to tolerate unavoidable imperfections of workmanship" [Hal13], regarding running fits and introduced three classes of workmanship.

Automation Between the world wars, increasing transnational trade and growing demand for external procurement (sometimes referred to as "outsourcing") required the standardisation of engineering drawings as the predominant means for the communication of workpiece specifications [Hoo93, Voe98]. In this regard, the British standard 308 "Engineering drawing office practice" [BS308], issued in 1927, was "one of the earliest national drawing standards" [Sri08]. However, tolerancing issues firstly appeared in such national standards at around 1935 [Voe93]. During the second world war, local "process callouts"[19], which had often been added to drawings in order to formulate implicit tolerances, complicated military procurement, since they inhibited process independence [Voe93, Voe98], i. e. for example the fabrication of armaments in formerly civil companies. As a consequence, such process callouts were prohibited in "postwar American tolerance standards" [Voe98], the first one issued by the American Department of Defence as the DOD DOC 30-1-7 in 1946 [Hon94, CF14], in order to strengthen

[18] Dimensional tolerancing, also called parametric tolerancing, is said to be already invented by Jean-Baptiste Vaquette de Gribeauval (* 1715, † 1789) [MCB98]. However, most sources state, that it was introduced in a larger extent not until the end of the 19th century.

[19] An example of such a local process callout comprising implicit tolerances is given by Voelcker as "Finish-mill then grind" in [Voe98].

the idea of process independence[20], which, from that time, has been a prevalent directive in tolerancing practice for several decades, but has been recently questioned in the context of integrated product and process development [Voe93, Voe98]. In order to counterbalance this development and to take account of the fact, that manufacturing inaccuracies regarding "dimensional tolerances had shrunk to a level where the form errors of typical manufacturing processes became significant" [Nie03], the concept of geometrical tolerancing as a possibility to add further geometrical specifications to drawings was introduced during the second world war [Voe93, Nie03]. In the further course, geometrical tolerancing allowed to "ameliorate some intrinsic weaknesses in parametric tolerancing" [Voe93].

The introduction of computers in industry then rapidly changed how physical artefacts were built, designed, and measured. In this regard, the first commercially used numerically controlled (NC) machines were presented in 1952 and the first computer-aided drafting systems took over design offices around the 1960s. At first, these computer-aided drafting systems slightly changed how drawings were created, but did not alter the concept itself. But with the advent of computer-aided design (CAD) tools[21] and the development from wireframe to solid, feature, and assembly models, the process of designing, modelling, and specifying product geometry evolved. However, a "dual role of computer-aided design and drafting (that is, creating three-dimensional nominal models and detailing their two-dimensional projections" [Sri08] still remains. As for engineering drawings, also computer-aided design required standardisation in the form of standardised file formats in order to allow the sharing of product data within and between companies. In this context, the Initial Graphics Exchange Specification (IGES) was issued in 1980 [NBK80] and the Standard for the Exchange of Product model data (STEP) was launched in 1994/95, to which the latest release is the application protocol 242 (ISO 10303-242:2014) from 2014, which is now capable of "handling tolerance information associated with product geometry" [FFS15].

Comparably to the advent of CAD tools, the introduction of coordinate-measuring machines (CMM) during the 1970s[22] entailed important changes regarding the measurement and verification of workpieces and led to the "metrology crisis" [Hoo93, Voe93, Voe98], as "early CMM algorithms produced results different from those obtained with traditional methods" [Voe98]. Moreover, after computed tomography had been used in manufacturing for non-destructive testing since the 1980s, its application in manufacturing metrology since 2005 [PS10] opened even new possibilities for the verification of workpieces [WK09, CCK+14]. With regard to measurement technology, it is also worth mentioning, that during this period, the definition of the metre as the basic length standard had been revised to a number of wavelengths in 1960 and to the distance travelled by light in the vacuum in one second in 1983, which "decreased the relative uncertainty attainable in realization of the meter by five orders of magnitude" [Swy01].

[20] As Voelcker pragmatically defines process independence: "Define the result you want, not how to get it" [Voe93].

[21] The term "computer-aided design" is said to be coined by Ross at the MIT in 1960 [Ros60]. Moreover, a definition of the term CAD can be found in [Lut14a].

[22] The first CMMs were already developed at the end of the 1950s, but, however, the first numerically controlled CMM, the Zeiss UMM 550, was introduced in 1973 [Sla16].

History and Evolution of GPS Standards As dimensional tolerances had been used in companies already since the end of the 19th century and geometrical tolerances were then introduced during the 1940s in the American defence sector, the upcoming geometrical dimensioning and tolerancing standards tried to capture and represent these best practices. In this regard, a first standard for dimensioning and tolerancing was issued by the American Department of Defence as the DOD DOC 30-1-7 in 1946 [CF14], which was followed by the MIL-STD 8 entitled "Military Dimensioning and Tolerancing" published in 1949. Some time later, the American Standards Association issued the American Standards Manual ASA 14.5-1957, which contained some notes on dimensioning and tolerancing and finally led to the USASI Y14.5-1966 "Dimensioning and Tolerancing for Engineers" published by the United States of America Standards Institute (USASI) [CF14]. The USASI was then renamed to the American National Standards Institute (ANSI) in 1969 and published the ANSI Y14.5-1973 "Dimensioning and Tolerancing" standard in 1973 as "an American National Standard for Engineering Drawing and Related Documentation Practices" [CF14]. This document is considered as a start for growing acceptance and wider use of geometric dimensioning and tolerancing in the United States industry [CF14]. Over the following years, it has been regularly revised, leading to the current ASME Y14.5-2009 as a part of the ASME Y14 "Engineering Product Definition and related Documentation Practices", where the history of the ASME Y14.5 dimensioning and tolerancing standard is briefly highlighted in [WS93] and the differences of some early American tolerancing standards are discussed in [Hon94].

With some delay to its American counterpart, the predecessor of the most commonly known international GPS standard ISO 1101:2012 ("Geometrical product specifications (GPS) – Geometrical tolerancing – Tolerances of form, orientation, location and run-out"), namely the ISO recommendation ISO/R 1101:1969 "Tolerances of form and of position" was published in 1969 and issued as a standard in a revised form in 1983 as the ISO 1101:1983 "Technical drawings – Geometrical tolerancing – Tolerancing of form, orientation, location and run-out – Generalities, definitions, symbols, indications on drawings". Only two years after this revision and motivated by reviews on drawings showing that the envelope principle as a reasonable restriction for the tolerancing of fits was only necessary in less than 10% of the toleranced dimensions, the independency principle was introduced as the default tolerancing principle in the ISO GPS standards in 1985 in the ISO 8015:1985 ("Technical drawings – Fundamental tolerancing principle") [Hen91]. To that time, the standards for the geometrical product specification were under responsibility of three independent and uncoordinated ISO technical committees (TC), namely the ISO TC 3 (Limits and Fits), the ISO TC 10 (Technical Drawings) and the ISO TC 57 (Metrology and Properties of Surfaces) [Ben98]. As it became obvious, that the standardisation efforts of these three TCs should be consolidated in order to enable a "a dialogue between those who specify geometry and those who measure it" [Nie13], the Joint Harmonization Group ISO/TC 3-10-57/JHG was launched in 1993 leading to the birth of the ISO/TC 213 "Dimensional and geometrical product specifications and verification" in 1996, which coined the term "geometrical product specification" [Sri15] and is since then in charge of all ISO standards related to the geometrical product specification.

Similar to the ASME GD&T standards, the first ISO tolerancing standards tried to capture best engineering practices and relied to a large extent on simple examples in order to explain and define the syntax and semantics of the GD&T language [Nie13]. However, the aforementioned developments in the fields of technical communication and verification technology, particularly the increasing use of computers and the evolving metrology crisis (also referred to as "method divergence" [Hoo93]) caused by the growing availability of CMMs, revealed severe ambiguities in these best practices [Voe93, Sri99]. Especially novel measurement technologies triggered efforts related to the "scientification" and "mathematization" of the standards for the geometrical product specification, aiming at providing a sound scientific, mathematical basis for the tolerancing language [Hoo93, Voe93, Voe98, Sri99, Nie13]. In this regard, the concept of GeoSpelling as developed by Ballu and Mathieu since the end of the 1980s [BM93, BM96, MCB98, BMD03, MB03, MB07, DBM08, ABM13, BMD15] can be seen as an important step towards this direction and serves as the basis of modern GPS standards. These efforts towards math- and rule-based standards have led to a high number of standards approvals, especially in the years of 2010 and 2011[23] [Nie13], and they are also expected to result in a revised version of the ISO 1101 soon [Nie13]. Furthermore, as the predominantly used form of technical communication slowly shifts from two-dimensional engineering drawings, that have been used for more than a century [VR77], to three-dimensional solid models [Sri91, QRP$^+$10], also the GPS standards are to answer this trend. In this regard, the latest revision of the ISO 1101:2012 [ISO1101] mainly aimed at making the "tolerances independent of the view plane, so [that] they are unambiguous when used on a three-dimensional [...] model in a computer-aided design [...] system" [Nie13].

Thus, until now, much work of the ISO TC 213 has dealt with "building a sound theoretical foundation for the GPS system" [Nie13] in order to answer the rapid changes in technical communication and verification technologies. This "had little impact on and created little interest from the end users of GPS standards" [Nie13], but "is now about to change" [Nie13] as revised versions of some GPS standards "have direct impact on what can be expressed on a technical drawing" [Nie13]. Consequently, endowed with a strong scientific basis, the tolerancing language is expected to change and further evolve during the next years. In the following, the fundamentals and basics of the current ISO standards for the geometrical product specification are highlighted. However, for details about the various concepts in the ISO GPS standards as well as application examples, the reader is referred to the standards themselves and further literature, such as [WH01, Hen06, Hen11, Kle11, Kle12, Cha13, Cha14, JS14, Sri15].

2.2.2 Fundamentals and Basic Concepts of modern GPS Standards

Structure of the ISO GPS Standards The structure of the ISO GPS standards is laid down in the ISO 14638:2015[24] [ISO14638], the ISO GPS "Masterplan", which defines the ISO GPS standards as a system for the description of geometrical characteristics of workpieces to be used in

[23] According to Nielsen, the ISO TC 213 approved nine standards between 2006 and 2009, whereas 35 standards have been approved in total during 2010 and 2011 [Nie13].

[24] It should be highlighted, that the revision of the ISO 14638:2015 introduced important changes regarding the chain links and the categories of geometrical characteristics in the matrix model of the ISO GPS standards compared to the former ISO 14638:1995.

Table 2.1: The Matrix Model for ISO GPS standards according to [ISO14638]: ∗ indicates the cells affected by the ISO 1101:2012 [ISO1101] and † the cells affected by the ISO 5459:2011 [ISO5459]

	Chain Links						
	A	B	C	D	E	F	G
Geometrical Characteristics	Symbols and Indications	Feature Requirements	Feature Characteristics	Conformance and Non-Conformance	Measurement	Measurement Equipment	Calibration
Size							
Distance							
Form	∗	∗					
Orientation	∗, †	∗, †	†				
Location	∗, †	∗, †	†				
Runout	∗, †	∗, †	†				
Surface Texture: Profile							
Surface Texture: Areal							
Surface Imperfection							
	Specification				*Verification*		

some stages of the life-cycle of a workpiece [ISO14638]. This system comprises three kinds of standards, namely **fundamental**, **general**, and **complementary** GPS standards, which are arranged in the matrix model of the ISO GPS standards (see Table 2.1). The columns of this matrix model are spanned by different chain links, which roughly follow the steps of the product origination process from the indication of geometrical specifications in the drawing to their verification by measurements [ISO14638, Cha13]. The rows of the matrix model are built by various categories of geometrical characteristics, such as characteristics of size, distance, form, orientation, and location [ISO14638], which have several sub-categories [ISO14638] and are often broadly classified in "size and dimensions", "geometrical tolerances", and "geometrical surface finishes" [WH01]. Each category of geometrical characteristics can be divided in different "chains of standards" [Ben93, MCB98] built by the different chain links. An exemplary chain of standards for the geometrical characteristic "size" can be found in the annex of the ISO 14638:2015 [ISO14638]. In this regard, **fundamental** ISO GPS standards describe rules and principles, that apply to all geometrical characteristics and all chain links, i. e. they affect all cells of the matrix model [ISO14638]. In contrast to that, **general** ISO GPS standards affect one or more cells of the matrix model, without being fundamental ISO GPS standards [ISO14638]. **Complementary** ISO GPS standards, in turn, add further definitions to one or more cells of the matrix model for specific manufacturing processes [ISO14638]. Which cells of the matrix model are affected by a specific GPS standard is indicated in the annex of the respective standard.

Fundamental Concepts of the ISO GPS Standards The basics and fundamental concepts of the GPS philosophy are defined in the ISO 17450-1:2011 [ISO17450-1] and the ISO 17450-2:2012 [ISO17450-2]. These fundamental concepts ground on four basic tenets, which are

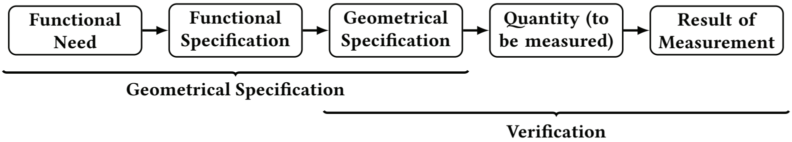

Figure 2.6: The Relationships between the Functional Need, the Geometrical Specification, and the Result of the Measurement according to [ISO17450-1, Cha13]

formulated in the ISO 17450-2:2012 [ISO17450-2]. In this context, the geometrical product specification is considered as a design step, in which the designer defines the allowable limits of a set of geometrical characteristics of the workpiece in such a manner that the workpiece conforms to its functional specifications [ISO17450-1, Cha13] (see Figure 2.6).

This is performed by firstly defining the workpiece in its ideal, nominal shape, leading to the **Nominal Model** [ISO17450-1]. Compared with this nominal model, the real, manufactured workpiece will always have geometrical deviations, which can impossibly be completely measured [ISO17450-1]. Thus, based on the nominal model, the designer develops an abstract model of the real workpiece surface, being the physical interface between the workpiece and its environment, in order to consider the deviations, that can be expected on the real workpiece [ISO17450-1]. With this abstract model, which is called the **Skin Model** (see Figure 2.7), the designer is enabled to adapt the allowable limits of certain geometrical characteristics, so that the functional specifications may be deteriorated but are still ensured [ISO17450-1]. These allowable limits define the tolerances of each geometrical characteristic of the workpiece [ISO17450-1]. The metrologist, in turn, defines the measurement operations for these tolerances based on the Skin Model in order to perform the comparison for conformance of the specification with the measurement result [ISO17450-1]. This manufacturing step is called the verification, which is independent of the specification process [ISO17450-1] (see also Figure 2.6).

Hence, the ISO GPS standards view **geometrical specifications** as **conditions** on **characteristics**, that are defined on one or more geometrical **features**, which are in turn created from the **Skin Model** by certain **operations** [ISO17450-1, ISO25378, DBM08] (see Figure 2.8).

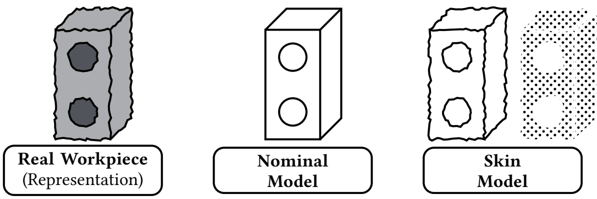

Figure 2.7: The Differences between the real Workpiece, the Nominal Model, and the Skin Model according to [ISO17450-1]

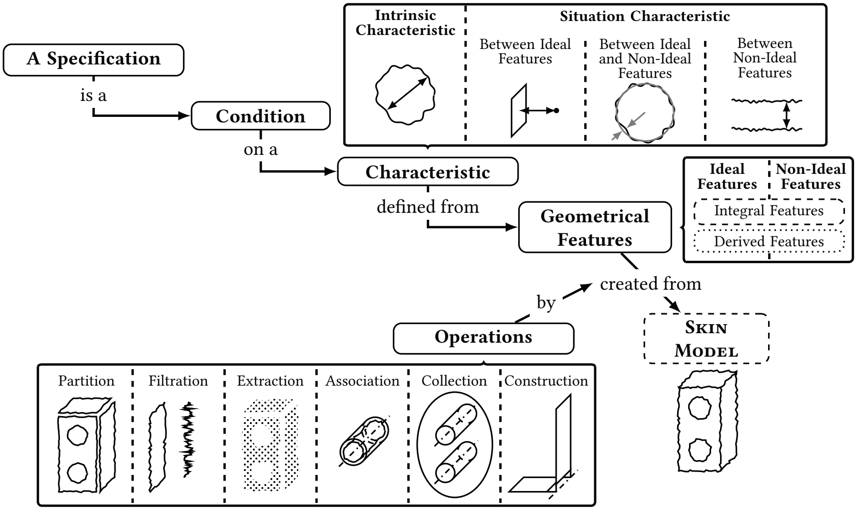

Figure 2.8: A Geometrical Specification according to ISO GPS Standards based on GeoSpelling [ISO17450-1, MB03, MB07, DBM08]

Accordingly, the ISO 25378:2011[25], which serves as a "road-map" for standardisation activities regarding geometrical characteristics, defines a specification as an "expression of a set of one or more conditions on one or more geometrical characteristics" [ISO25378], with a **condition** being defined as a "combination of a limit value [i. e. a tolerance limit] and a binary relational mathematical operator" [ISO25378]. In this regard, the ISO 17450-1:2011 [ISO17450-1] differentiates between two basic types of **characteristics** (see Figure 2.8), namely intrinsic and situation characteristics. Each of the different characteristics defined in the GPS matrix model (e. g. characteristics related to the surface texture as in ISO 4287:1997 [ISO4287] and ISO 25178-2:2012 [ISO25178-2], geometrical characteristics of form, orientation, location, and runout according to ISO 1101:2012 [ISO1101], and dimensional characteristics according to ISO 14405-1:2010 [ISO14405-1] and ISO 14405-2:2011 [ISO14405-2]) can be assigned to intrinsic or situation characteristics.

These characteristics are defined on geometrical **features**, which are understood as "point, line, surface, volume or a set of these previous items"[26] [ISO22432], are usually (but not always) separated by edges [ISO17450-1], and are obtained from the nominal model or the skin model. They can be classified as ideal and non-ideal features as well as integral and derived features according to ISO 17450-1:2011 [ISO17450-1] (see Figure 2.9). Beside this, the ISO 22432:2011 [ISO22432], also serving as a guideline for future standardisation activities and programmers,

[25] The ISO 25378:2011 [ISO25378] also introduces the concept of population specifications as limits on population characteristics, which can be considered as an extension of the "statistical tolerancing" modifier. It also allows to apply specifications on (moveable) assemblies [Nie13].

[26] As it has been mentioned, this definition does not consider any semantics in contrast to the feature definition by Shah [Sha91] or the concept of high grade semantic features by Wartzack [WM00].

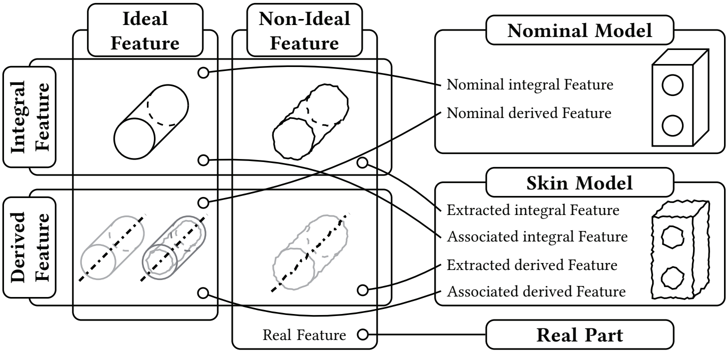

Figure 2.9: Different kinds of Features according to [ISO17450-1, ISO22432]

defines further terms and definitions related to features, such as associated features, discrete features, and sampled features. As can be seen from Figure 2.8, the various features are obtained from the nominal model or the skin model by different operations, such as extraction, partition, and filtration, which are highlighted in the ISO 17450-1:2011 [ISO17450-1] and are explained in separate standards[27].

The operations used to define certain characteristics on the Skin Model build the **specification operator**, whereas the operations used to measure these characteristics from the real workpiece form the **verification operator** [ISO17450-1]. In this regard, the verification operator and the specification operator are independent, with the idea of differentiating between the specification operator and the verification operator being introduced in the ISO 17450-1:2011 [ISO17450-1] and the ISO 8015:2011 [ISO8015] as the **duality principle** (see Figure 2.10).

Even though the verification operator should mirror the specification operator, there will always remain some differences, which can be quantified in terms of **uncertainties** [ISO17450-1, Nie13]. Based on these uncertainties, it is up to the user to decide, if a certain measuring process is suitable for the verification of a specification or not [ISO17450-1, Nie13]. In this regard, the specification and verification steps involve different *types* of uncertainties (see Figure 2.11), which are covered by the ISO 17450-2:2012 [ISO17450-2] (see also [MB03, Sri03, Nie06, LJLX08, DVGM10]):

- **correlation uncertainties**, which are due to the imperfect translation of functional needs to geometrical specifications,
- **specification uncertainties** arising from ambiguities in the GPS standards or inaccurate specifications made by the designer,
- **method uncertainties** due to the choice of the measurement processes, and
- **implementation uncertainties**, which may be inherent to the measurement equipment.

Thus, uncertainties are not considered as being only related to measurement, but concern all

[27] See e. g. ISO 14406:2010 for extraction and ISO 16610-1:2015 for filtration.

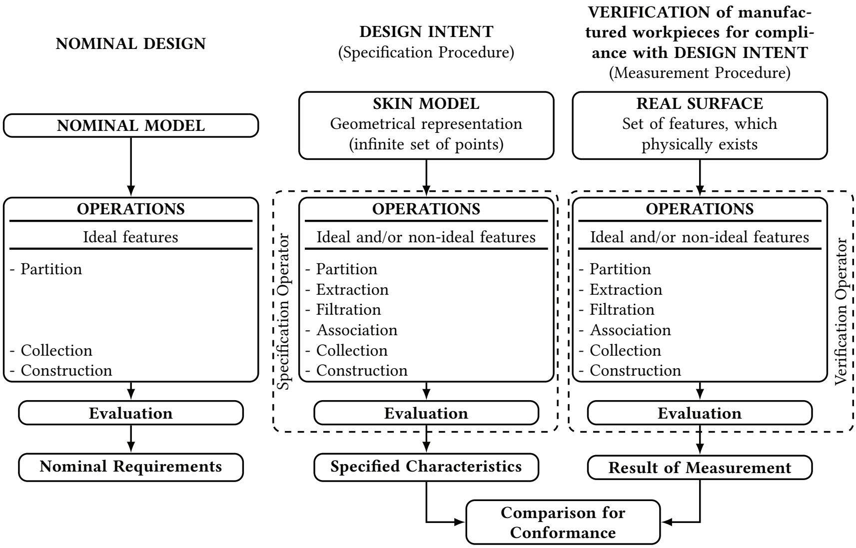

Figure 2.10: The Difference between the nominal Design and the Design Intent and the "Duality Principle" of Specification and Measurement Procedures according to [ISO17450-1, ISO8015]

stages of specification and verification and are therefore also to be taken into account in design when defining specifications [MB03, Nie03].

Fundamental Assumptions and Basic Principles of the ISO GPS Standards Beside the ISO 14638:2015 [ISO14638], which defines the overall structure of GPS standards, and the standards ISO 17450-1:2011 [ISO17450-1] and ISO 17450-2:2012 [ISO17450-2], which state fundamental concepts, such as the concepts of operators, operations, and uncertainties, the ISO 8015:2011 [ISO8015] is a further fundamental GPS standard and introduces fundamental assumptions regarding the reading of specifications on drawings or other kinds of technical product specifications as well as thirteen fundamental principles. These fundamental assumptions regarding the reading of specifications comprise, that the **functional limits** of a workpiece are known by experiment or theory without uncertainties, that the **tolerance limits** are equal to these functional limits, and that the workpiece will fully function inside the tolerance limits and will not function outside these limits (the tolerance limits themselves are part of the function region) [ISO8015]. Among the thirteen fundamental principles are the **duality principle** as shown in Figure 2.10, which highlights the differentiation between the specification and the verification operator, the **independency principle**[28], which states, that each specification has to be fulfilled independently from others, the **feature principle**, which clarifies, that by default each specification applies to one whole feature, and the principles of

[28]The independency principle has been introduced in the GPS standards already in 1985 with the ISO 8015:1985. However, the envelope principle was the default tolerancing principle in Germany until 2011, when the DIN 7167:1987 was finally withdrawn [Har14].

reference condition and **rigid workpiece**, which state, that each specification is defined under reference conditions (such as defined by the ISO 1:2002) and in an undeformed workpiece state without external loads[29] (such as gravity) [ISO8015]. Before the ISO 8015 had been issued in 1985, these thirteen principles had often been taken for granted, without being manifested in a standard [Nie13].

Tolerance Specifications according to the ISO GPS Standards The aforementioned ISO GPS standards aimed at providing the structure and foundations of the GPS framework without defining symbols or concepts, that are directly visible as tolerance specifications on engineering drawings or solid models [Nie13]. Thus, in the following, the ISO GPS standards for geometrical dimensioning and tolerancing are highlighted, which provide the designer with symbols and concepts to express geometrical characteristics as tolerance specifications on technical product specifications. In this regard, a focus is set on tolerances for geometrical and dimensional characteristics, whereas characteristics regarding the surface texture are only briefly mentioned. An overview of the most relevant standards for dimensional and geometrical characteristics and their indication on technical drawings is given in Figure 2.12.

The ISO 17450-1:2011 [ISO17450-1] generally distinguishes between two types of **specifications**, namely specifications by dimension and specifications by zone [ISO17450-1]. In this regard, a **specification by dimension** may be indicated on linear or angular dimensions, with both of them covering dimensions of size and dimensions of distance. Dimensions of size can only be applied to **features of size**, where there exist three features of size for linear dimensions, namely cylinder, sphere, and two parallel opposite planes[30], and two features of size for angular dimensions, namely cone and wedge [ISO17450-1, ISO14405-1, ISO22432, ISO5459]. The tolerances on linear dimensions of size are covered by the ISO 14405-1:2010 [ISO14405-1], which defines fourteen different types of linear sizes (such as the classical two-point size, the least-squares size, and the maximum size), that are grouped in four classes, namely local, global, calculated, and rank-order sizes. The different types of linear sizes with their corresponding modifiers "allow the designer to express requirements to linear sizes that go far beyond the old-fashioned and expensive envelope requirement" [Nie13] and are discussed

[29] See the ISO 10579:2010 [ISO10579] for the dimensioning and tolerancing of non-rigid parts.

[30] The ISO 17450-1:2011 [ISO17450-1] defines further features of linear size, namely a circle, two straight lines, and a torus.

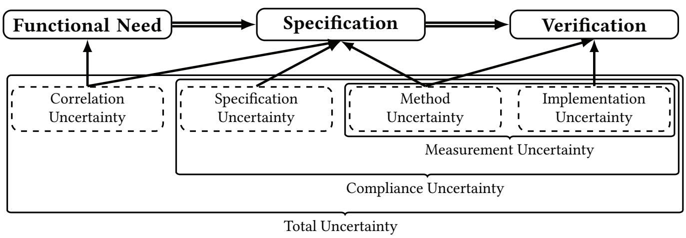

Figure 2.11: Different Uncertainties in the Context of Specification and Verification [ISO17450-1, MB03, LJLX08, Nie06]

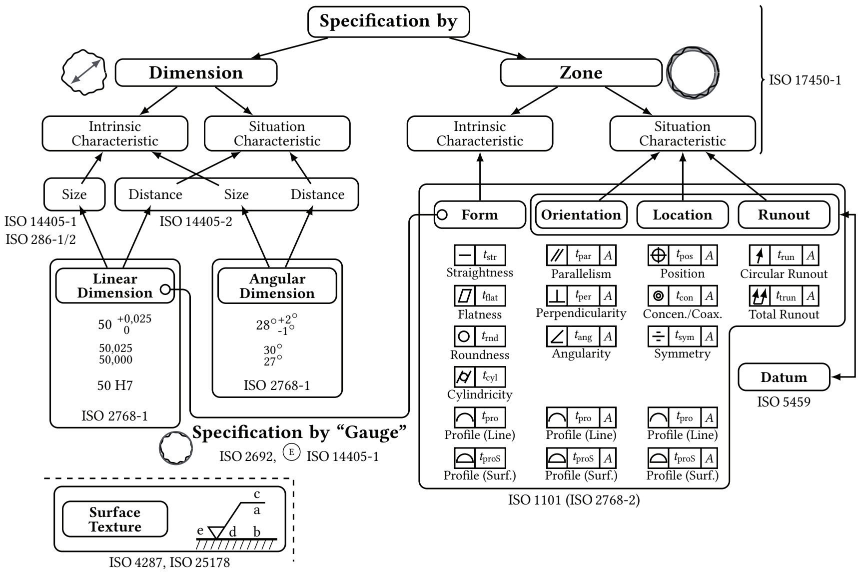

Figure 2.12: Overview of Dimensional and Geometrical Tolerance Specifications according to [ISO17450-1, ISO1101, ISO14405-1, ISO14405-2, ISO5459, ISO2692, ISO286-1, ISO286-2, ISO2768-1, ISO2768-2]

more in detail in [MS13b, Sri13]. In addition to this, the standards ISO 286-1:2010 [ISO286-1] and ISO 286-2:2010 [ISO286-2] provide the well-known ISO code system for tolerances on such linear sizes. Tolerances for all other kinds of dimensions, i. e. linear dimensions of distance and angular dimensions, are covered by the ISO 14405-2:2010 [ISO14405-2]. As Figure 2.12 highlights, dimensional tolerances may generally be indicated by ± tolerancing, e. g. as $50^{+0{,}025}_{0}$ or $28^{\circ}\,{}^{+2^{\circ}}_{-1^{\circ}}$, or by indicating the upper and/or lower dimensional limit. Moreover, tolerance specifications on linear dimensions of size can also be indicated using the ISO code system of the ISO 286-1/2 [ISO286-1, ISO286-2], e. g. 50 H7, and further possibilities for the indication of tolerances on angular dimensions of size are described in the ISO 2538 for wedges and in the ISO 3040 for cones. Beside this, the ISO 129-1:2004 [ISO129-1] regulates the indication of dimensions and tolerances on technical drawings. Another possibility for the indication of tolerances on linear and angular dimensions is the use of general tolerances[31], which are defined in the ISO 2768-1:1989 [ISO2768-1] for workpieces, that are manufactured by metal removal or sheet metal forming.

In contrast to that, a **specification by zone**[32] is in general indicated by symbols for geometrical tolerances, which are defined in the ISO 1101:2012 [ISO1101]. In this regard, fourteen

[31] General tolerances are also provided in the ISO 8062-3:2007 [ISO8062-3] for moulded parts and in the ISO 13920:1996 [ISO13920] for welded constructions.

[32] The **tolerance zone** is defined as the "space limited by one or several geometrically perfect lines or surfaces, and characterized by a linear dimension, called a tolerance" [ISO1101]. The toleranced non-ideal feature is to lie completely within this tolerance zone.

symbols for geometrical characteristics are covered by the ISO 1101:2012 [ISO1101], which describe tolerances of form, orientation, location, and run-out. Some of them are further defined in additional standards, such as the dimensioning and tolerancing of profiles in the ISO 1660:1987 [ISO1660], positional tolerancing in the ISO 5458:1998[ISO5458], the straightness tolerance in the ISO 12780-1:2011 [ISO12780-1] and ISO 12780-2:2011 [ISO12780-2], the flatness tolerance in the ISO 12781-1:2011 [ISO12781-1] and ISO 12781-2:2011 [ISO12781-2], the roundness tolerance in the ISO 12181-1:2011 [ISO12181-1] and ISO 12181-2:2011 [ISO12181-2], as well as the cylindricity tolerance in the ISO 12180-1:2011 [ISO12180-1] and ISO 12180-2:2011 [ISO12180-2]. Moreover, additional modifiers and symbols, such as CZ defining a common tolerance zone, Ⓟ for projected tolerance zones, Ⓕ indicating the free state condition for non-rigid parts, or ⟨//|B⟩ describing an orientation plane, are introduced [ISO1101]. Tolerances of form control the form deviations of a toleranced feature and hence build intrinsic tolerance zones, whereas tolerances of orientation, location, and run-out also control the feature's orientation or location deviations, respectively, with reference to a datum feature or a datum system and thus limit situation characteristics[33]. Such a **datum**, in turn, is defined as "one or more situation features of one or more features associated with one or more real integral features selected to define the location or orientation, or both, of a tolerance zone or an ideal feature representing for instance a virtual condition" [ISO5459] and a **datum system** as a "set of two or more situation features established in a specific order from two or more datum features" [ISO5459]. The ISO 5459:2011 [ISO5459] distinguishes between primary, secondary, and tertiary datums. While primary datums are "not influenced by constraints from other datums" [ISO5459], secondary datums are datums, that are "influenced by an orientation constraint from the primary datum in the datum system" [ISO5459], and tertiary datums are in analogy "influenced by constraints from the primary datum and the secondary datum in the datum system" [ISO5459]. Based on their definitions, there exist **interrelationships between geometrical tolerances**, meaning, that form tolerances control only the form deviations of a feature, whereas orientation tolerances control form and orientation deviations, and location tolerances control location, orientation, and form deviations [ISO1101].

Beside the specification by dimension or by zone, the standards also offer possibilities to locally suspend the independency principle and to expand specifications to various kinds of geometrical characteristics as well as to link certain tolerance specifications by modifiers. In this regard, the ISO 14405-1:2010 [ISO14405-1] provides the **envelope requirement** Ⓔ as the "simultaneous use of a combination of the two-point size as the specification operator applied for the least material limit of the size and either the minimum circumscribed size or the maximum inscribed size as the specification operator applied for the maximum material limit of the size" [ISO14405-1]. The use of the envelope requirement (formerly known as the Taylor principle) is often considered as a third type of specification, namely the **specification by "gauge"** [Cha13], which can be considered as jointly controlling the feature's deviations of dimension and form. Beside this, the ISO 2692:2014 [ISO2692] introduces the maximum material requirement, the least material requirement, and the reciprocity requirement as further modifiers.

[33]Position tolerances can also be indicated without datums [ISO1101].

In addition to the dimensional and geometrical tolerances, the ISO GPS standards also provide many possibilities for the indication of limits on characteristics regarding the surface texture. In this context, the ISO 4287:1997 [ISO4287] covers terms, definitions, and surface texture parameters for profile methods and the ISO 25178-2:2012 [ISO25178-2] for areal methods. Moreover, the ISO 8785:1998 [ISO8785] introduces terms and definitions for surface imperfections.

2.2.3 Recent Trends regarding the GPS Standards

As measurement technologies advance and the requirements on mechanical products continuously tighten, the ISO GPS standards are in steady change to provide an unambiguous language for the communication in geometrical variations management. In this regard, NIELSEN [Nie13] reports six initiatives covered by the strategic plan of the ISO TC 213 for the future of ISO GPS standards, such as:

- the conversion of the GPS standards towards **rule-based standards** in order to reduce required inter- and extrapolation by users and to enable a more uniform implementation of the tolerancing standards in CAD, CAM, and CMM systems,
- the definition of "**characteristics and actual values** for geometrical specifications and [...] a signed and global characteristic (actual value) for each workpiece" [Nie13], which will also allow the definition of **population specifications**,
- the establishing of new concepts for **form standards**, which has already been performed for straightness, flatness, roundness, and cylindricity, as well as
- the update of the standards for **general tolerances** and for the tolerancing of **edges**.

The strategic plan is divided in two stages, with the second aiming at converting the "ISO 1101 into a multipart standard to strengthen the ISO 1101 brand" [Nie13], which will imply the consolidation of several ISO GPS standards in the ISO 1101 [Nie13].

Beside this, current research works are i. a. dedicated to detailing the syntax of GeoSpelling, as the basis of modern GPS standards, based on programming languages employing function calls and control structures, such as conditions and loops [BMD15]. Moreover, different extensions and improvements for current GPS standards have been suggested, such as for the functional tolerancing of complex junctions in [CA12] and for the specification of complex surfaces in [PPA15]. Furthermore, possibilities for the specification of requirements on the kinematic behaviour of products in analogy to the ISO 230-1:2012 [ISO230-1] are investigated in [HK14, HK15], whereas the integration of GPS concepts in Product Life-cycle Management (PLM) tools is investigated in [RSBMG+13].

In contrast to the further development of the underlying GPS concepts and the possibilities for the specification of geometrical requirements on engineering drawings, the **education** of the ISO GPS language to engineers and metrologists is identified as a highly relevant challenge. In this regard, the question of how to integrate the GPS language for geometrical dimensioning and tolerancing and related topics in the curriculum has been a constant issue in the research communities [Gab93, BM99], where a course for technical universities has been issued in [WH01], a multimedia tolerancing course has been presented in [HB13, HB15], a blended learning course related to measurement uncertainty is described in [GGL+15], and numerous handbooks regarding geometrical dimensioning and tolerancing are available (such as [Hen06, Kle12, Cha13, JS14]). Moreover, a recently formed European project[34] is "to develop and implement a coherent learning system for higher-level vocational training concerning the GPS" [PJH+14].

2.2.4 Further Approaches for the Specification of Geometrical Requirements

It is worth highlighting, that there are also other approaches to establishing a framework for the expression of geometrical specifications beside the ISO GPS standards, with the most commonly known being the ASME Y14.5-2009 standards [ASM09]. Further approaches are for example vectorial tolerancing [Wir88, Wir91], fractal tolerancing [Sri94, SW95, SW97], and modal tolerancing [SF06, FS07], which are briefly highlighted in the following, as well as a formal dimensioning and tolerancing model described in [PG03] and continued in [LPG13].

ASME Y14.5-2009 The ASME Y14.5-2009 standard [ASM09] is similar to the ISO GPS standards, although it is said to be even more comprehensive and some differences between the ISO and the ASME GD&T standard have been reported in [Hen06, Kle12, JS14], with the difference in the default tolerancing principle being often regarded as the most important[35]. However, as there is a substantial consistency between the ASME Y14.5-2009 and the ISO GPS standards, the reader is referred e. g. to [Hen06, Kle12, JS14] for detailed comparisons.

Vectorial Tolerancing Following the vectorial tolerancing approach proposed by Wirtz [Wir88, Wir89, Wir91], geometrical specifications are expressed as tolerances on the mathematical parameters of basic geometry elements, such as planes, cylinders or spheres, or other types of surfaces [Mar93]. For example, a cylinder can be mathematically described by a three-dimensional position vector (x_0, y_0, z_0), a three-dimensional (unit) direction vector (e_x, e_y, e_z) and a size M_1. To each of these seven parameters $(x_0, y_0, z_0, e_x, e_y, e_z$ and $M_1)$, a plus-minus tolerance can be added in order to specify the geometrical requirements on the manufactured cylinder. Since the verification of vectorial tolerances is performed based on the substitute elements computed by the least-squares criterion, the orientation and location deviations are separated from the form deviations (in contrast to the GPS standards, where the form deviations are also controlled by the tolerance zones of orientation and location tolerances) [Hen93]. The main advantage of the vectorial tolerancing approach is said to be the straightforward process control for machined parts [Wir91], where the statistical process control using vectorial tolerancing has been implemented in [Mar96]. Furthermore, vectorial tolerancing may be advantageous for specific functional requirements [Hen93]. The successful application of this tolerancing approach in industry has been reported in [KM99]. Some research works aim at integrating vectorial tolerances (i. e. the possibility of specifying geometrical requirements by adding tolerances to the mathematical description of basic geometry elements) in computer-

[34] "Geometrical Product Specification and Verification as toolbox to meet up-to-date technical requirements", http://gpsvtoolbox.ath.eu

[35] The default tolerancing principle in the ISO GPS standards is the independency principle [ISO8015], whereas the envelope principle, known as rule #1, is the default tolerancing principle in the ASME Y14.5 standards [ASM09].

aided design tools [BW99, HOWG14, GHO+15] and to overcome the conversion problems between ISO GPS tolerances and vectorial tolerancing as reported in [BHK98].

Fractal Tolerancing Since the functionality of many mechanical systems depends on the form deviations of the constituting parts, a form tolerancing theory based on fractals and wavelets has been proposed in [Sri94, SW95, SW97]. It is based on the surface error abstraction by fractional Brownian motion and the form tolerancing based on the fractal parameters, which are computed by wavelets [SW97]. The method has been applied for the tolerance analysis of a slider bearing considering the pressure distribution and load capacity calculated by the Reynolds equation in [SW95] and for the analysis of bearing forces taking into account the roundness deviations of the bearing components (i. e. inner race, outer race, and ball) in ball bearings in [SW97]. The results show, that the idea of using fractals for form tolerancing seems suitable for certain applications as it allows a more detailed expression of form errors than the well-known concept of tolerance zones. Moreover, the measurement of surface errors using fractals has been successfully applied in other studies [Li10, SBD11]. However, the reported applications are limited to one-dimensional surface errors and do not cover other kinds of geometrical deviations, such as deviations of dimension, orientation, and location.

Modal Tolerancing A further approach for the expression of geometrical deviations and the definition of limits on these deviations is the modal tolerancing approach as proposed by Samper et al. in [SF06, FS07, ASP10, ASF10, GLS13]. It employs a modal decomposition of discretised surfaces using the finite element method for the expression of feature deviations [SF06]. The form tolerancing is then performed by defining limits on the modal coefficients, i. e. the eigenfrequencies, of the natural modes [SF06]. The modal decomposition of feature deviations for a disc-shaped feature has been compared to the use of Zernike polynomials in [FS07], where it has been shown, that the natural mode decomposition is more efficient. Moreover, the modal shape parametrisation has been used to study the effects of two- and three-dimensional form errors on the assembly behaviour in [SAFP09, ASF10] and the clearance domain of two-dimensional linkages in [ASF10]. Mechanical loads have also been integrated in these analysis in [SCT+12, GLS13, GLSF13]. Beside this, the modal decomposition of form defects has been combined with an inertial acceptance criterion in [ASP10] resulting in the inertial tolerancing approach, whereas a statistical modal analysis approach for variation characterisation has been proposed in [HLC+14]. The overall approach for the expression of form deviations by natural modes is very promising and comparably widely applied in research. However, similarly to the fractal tolerancing approach, modal tolerancing is limited to form deviations and does not provide a comprehensive language for geometrical variations management.

2.3 Tolerancing as an integral Part of Geometrical Variations Management

As geometrical part deviations distinctly affect the quality and function of physical products, companies are required to manage these geometrical variations throughout the product life-cycle. The language offered by the international standards for the geometrical product specification amplifies the concept of tolerances and geometrical specifications as a means of communication between the different actors in geometrical variations management. In this regard, tolerances are ubiquitous in geometrical variations management and have manifold repercussions on all stages of the product origination process [SWM96, HC02a]. Consequently, tolerancing is an highly important and integral part of geometrical variations management. It comprises many different sub-activities and affects all phases of the product realisation process. However, there exists a plethora of different terms regarding tolerancing, that are often insufficiently defined and sometimes used interchangeably. Thus, this section is to give an overview of relevant terms and their definitions in the context of tolerancing and to highlight the various tolerancing activities throughout the product life-cycle with a focus on product design. Moreover, it will describe the state of the art regarding computer-aided tolerancing with a special attention on the tolerance analysis.

2.3.1 Disambiguation and Definition

The management of geometrical deviations throughout the product life-cycle comprises many partially disrupted activities, which are performed by different departments and various actors. **Geometrical variations management** covers all these efforts and activities related to controlling geometrical deviations throughout the product life-cycle. In order to overcome the disruption of these activities, the concept of tolerances, which is used to specify and communicate the limits of acceptable geometrical part deviations, serves as a means of communication.

In this regard, **tolerancing** is defined as "the set of activities which manage the tolerances during the product development" [Dan14], with *product development* being understood in this context in a broad sense as "the set of activities beginning with the perception of a market opportunity and ending in the production, sale, and delivery of a product"[36] [UE12]. Based on this definition, the three central functions of product development are considered as marketing, *(product) design*, which includes engineering design as well as industrial design, and manufacturing [UE12]. Thus, tolerancing is an important sub-area of geometrical variations management covering the different activities during the product realisation, that deal with or are affected by tolerance information[37]. Consequently, **computer-aided tolerancing** covers all efforts aiming at supporting these tolerancing activities by computer technology. A term with similar meaning to tolerancing is *tolerance engineering*, which "can be seen as all those engineering activities which directly focus on tolerances" [KAV13].

Beside this, the term **dimensional management**, which is rarely used in scientific literature but often in industry, can be defined with ambiguities as "an engineering methodology combined with computer simulation tools used to improve quality and reduce cost through controlled variation and robust design" [Cra96]. However, divergent definitions for this term

[36] With some similarity to this, product development is also defined as "the *creation* of products with new or different characteristics that offer new or additional benefits to the customer" [Lut14b].

[37] However, although the majority of the different activities in geometrical variations management is connected and interrelated by tolerances, some of them do not directly generate, require or share tolerancing information.

as well as for **tolerance management** are summarized in Table 2.2. Based on these definitions, it can be found, that these terms often describe the industrial practice applied in a company or industry sector regarding tolerancing and geometrical variations management, but do not offer an unambiguous and comprehensive understanding or designation of certain tolerancing activities. Consequently, these terms are avoided in the following.

Table 2.2: Different Definitions of the Terms "Dimensional Management" and "Tolerance Management"

"Dimensional management is an engineering methodology combined with computer simulation tools used to improve quality and reduce cost through controlled variation and robust design. The objective of dimensional management is to create a design and process that "absorbs" as much variation as possible without affecting the function of the product. Dimensional management accomplishes this through optimal selection of datums, feature controls, assembly methods and assembly sequence." [Cra96]
"Dimensional management is a process by which the design, fabrication, and inspection of a product are systematically defined and monitored to meet predetermined dimensional quality goals. It is an engineering process that is combined with a set of tools that make it possible to understand and design for variation. Its purpose is to improve first-time quality, performance, service life, and associated costs." [Nic99]
"Dimensional management is a preventive quality assurance method that ensures the functionality and producibility of designs at an early stage. Dimensional management makes it possible to avoid potential problems before they occur. It enables engineers to fulfil required quality characteristics (joint scheme) and safeguard points of constriction and critical functions" [MS13a]. "Dimensional management is primarily comprised of three central components: *specifications – functional dimensions and joint scheme*, the *reference point system*, and *statistical tolerance analysis*." [MS13a]
"Integrated tolerance management is a systems approach for achieving global consistency of tolerances throughout an organization. The purpose is to facilitate harmonization of tolerances throughout an organization to achieve high quality functionality at low cost." [GB99]
"The term tolerance management comprises the activities in the product life-cycle, that are associated with the analysis and validation of functional and aesthetic key characteristics for the continuous optimization of the product definition and the manufacturing and assembly processes." (translated from German) [WMS+11]
"Tolerance management is a sub-process of the product development process with the aim to ensure the proper functioning of a product at lowest possible manufacturing cost by an optimal tolerance design using management methods." (translated from German) [BH13]

While tolerancing comprises all different tolerance-related activities throughout the product life-cycle, **functional tolerancing** (or tolerancing for function) can be found as the *design* activities, which aim at translating functional requirements in functional tolerances [FG86, WCH+88, CCD+89, CM89]. Particularly, "the purpose of functional tolerancing activity is to define the geometrical specifications of parts ensuring a certain level of quality defined by some product geometrical requirements"[38] [DBM08].

The functional tolerancing activities are often regarded as important elements of **robust design** (RD) and **variation risk management** [CBW05, SLD06, Sto10, HCBS13], considering robust design as "a framework for designing products and processes which perform con-

[38] A similar definition is given as: "The purpose behind functional tolerancing is to generate mechanical drawings of the parts of a mechanism, with such drawings serving to define acceptable component geometry" [Ans06].

sistently in spite of variations"[39] [KEH15] and variation risk management as "a process of continually identifying, assessing, and mitigating variation risk throughout the design process" [Tho99a]. **Robust design methodology** (RDM), in turn, "means systematic efforts to achieve insensitivity to noise factors [where] [...] these efforts are founded on an awareness of variation and can be applied in all stages of product design" [AG08]. Hence, functional tolerancing can be seen as a branch of robust design, that deals with noise factors, which are related to the product geometry.

Tolerance design is also broadly defined as "the engineering process for developing tolerances" [Cre97], whereas a **robust tolerance design** is "based on the balance between manufacture cost and quality loss expected" [WT98]. Thus, a robust tolerance design may be considered as the set of tolerances leading to minimal tolerance-related costs (i. e. manufacturing and inspection costs vs. costs of malfunction expressed by the quality loss due to decreased performance) [WT98, Jea99, JC02, CBW05, HZ10].

In summary, *geometrical variations management* is understood as the set of activities related to controlling geometrical deviations and their effects on the product quality throughout the product life-cycle, while *tolerancing* is a subset of geometrical variations management, which particularly comprises all of these tasks, that are linked to tolerance information. More specifically, *functional tolerancing* includes the tolerancing activities during design, which focus on the translation of functional requirements into functional tolerances. These functional tolerancing activities, in turn, can be seen as a subset of variation risk management and robust design, with *variation risk management* being a process aiming at controlling variation risk during the design stage and *robust design* being considered as a comprehensive framework for designing products, so that they are insensitive to noise factors. The qualitative relationships between these terms and concepts can be seen from Figure 2.13.

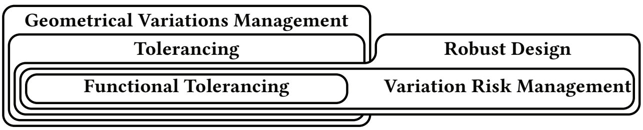

Figure 2.13: Qualitative Relationships between different Tolerancing-related Terms in the Context of this Work

2.3.2 Tolerancing Activities throughout the Product Life-Cycle

Tolerancing Process Models According to the provided definition, tolerancing covers all activities throughout the product life-cycle, that generate, require, or share tolerancing information. There exist manifold practices and proposed tolerancing processes for the practical implementation of these activities, with some of them considering different product development steps, while others merely focusing on the design stage. In this regard, [BH13] defines seven central activities in tolerancing, that are iteratively performed in different product design

[39] There are various definitions of robust design, which are not discussed in this work. However, these definitions as well as further readings on the topic can be found in [Tag86, Pha89, And96, Mat97, TDE00, MTA05, HAG09, UE12].

phases, such as the function clarification, the definition of assessment criteria, the development of the assembly sequence, as well as the optimization of the part design. A comparable process with eight steps, which particularly focus on the application of simulation models for the assessment of the effects of geometrical deviations on functional characteristics, is illustrated in [Man15], whereas nine steps are defined in the process proposal in [MS13a]. With a broader view, fourteen tolerancing steps, comprising the validation of measurement equipment and gauges and the statistical process control, are described in [Wei15a, Wei15b]. Moreover, a standardised comprehensive tolerancing process, issued by the German Association of the Automotive Industry (VDA), is illustrated in [VDA06]. Beside this, many companies define their own tolerancing process depending on their products, their culture, and their vertical range of manufacture. An overview of some of these, often company-specific, proposals is for example also given in [Sto10].

In addition to these industrial tolerancing process schemes, several research works aim at proposing adequate tolerancing processes. In this regard, particularly the integration of the tolerancing process into early design stages (based on the paradigms of concurrent engineering and front-loading) has been identified as an important trigger for cost savings and quality improvements [RLW91, Mil92, Isl04, HZX05, HP07, HZ08, ZLB+10]. For example, the "Integrated Tolerancing Process" (ITP), which is based on a multi-level architecture to collect functional requirements and to decompose and translate them into geometrical specifications, aims at integrating the tolerancing process in the conceptual design stage [DAM03]. Similarly to the ITP, Roy et al. integrate the tolerancing activities in a concurrent design approach and place tolerancing as one of fifteen steps in a function-to-form mapping approach for design synthesis [RPS+01]. Beside this, the authors also propose a "design for tolerancing" approach, which allows to perform the tolerancing activities during design incrementally [SR00]. Another approach to perform tolerancing in early design stages is based on the "geometry as soon as possible"-idea [BFCM06], which focuses on the geometrical modelling of parts and assemblies as well as the definition of geometrical specifications already in early design. The early completion of the geometrical product information during the design process is achieved by applying different models and tools, starting with skeleton models, through part interface design, to final part models, and is supported by assembly-nested graphs. A systematic way of translating functional requirements into geometrical specifications using functional requirements/dimensions matrices (FR/D), similar to design structure matrices (DSM) [Ste81, PE94, Bro01], as well as a software prototype supporting this approach is presented in [Isl04]. The axiomatic design perspective is picked up in [JS00], where a structure model and a matrix-based geometry design procedure are presented as a means to support robust geometry design during the different design stages. Furthermore, a concurrent design approach based on the principles of decomposition and reconstitution has been presented [ZCWY13]. Beside this, a geometry assurance process comprising different steps from conceptual design to production is presented in [SLC06b], which involves a rich set of different, partly virtually performed, tolerancing and geometrical variations management activities. In addition, a tolerance management system is detailed in [GB99], which is based on the quality management concepts of Shewart [She39] and Deming [Dem82], such as the plan-do-check-act cycle, and which

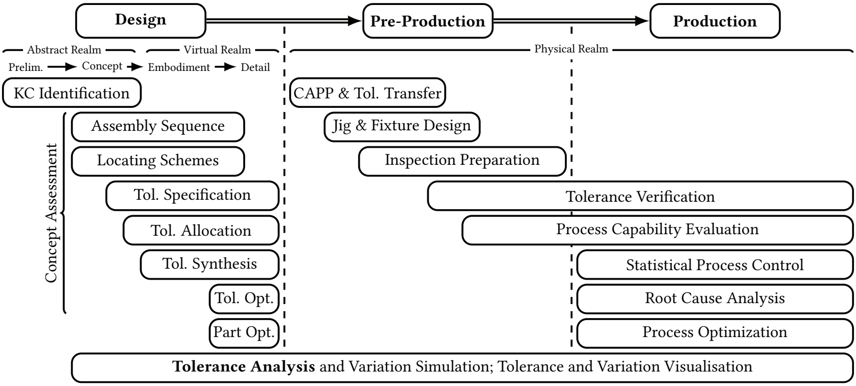

Figure 2.14: Main Activities in Tolerancing and Geometrical Variations Management according to [DAM03, SLC06b, VDA06, MB07, Sto10, KM12b, BH13, MS13a, Man15, Wei15b]

focuses on the communication and management issues related to tolerancing. Furthermore, the "closed-loop tolerance engineering" model (CLTE), which sorts the tolerancing activities in four basic groups, has been used to describe and improve the tolerancing process in various case studies [KA12, KM12b, KAV13, KMA14, KGA14, KUWA14]. Moreover, an approach for the design of kinematically constrained assemblies comprising two stages with different sub-activities is proposed in [WMAR99]. The importance of early decisions regarding the product structure and the assembly sequence is also emphasized by the integrated design method proposed in [MM01, MM03], which is based on the application of assembly graphs, propagation chains, and risk analysis.

Beside these tolerancing process models, various product models have been proposed, which are to support controlling tolerancing information throughout the product design and development process [BDT07, DLSM07] as well as enabling the traceability of functional requirements and geometrical specifications [JD08].

Overview of Tolerancing Activities Based on the review of these various tolerancing process models, several core activities in tolerancing and geometrical variations management can be identified, which are discussed in the following and a rough placement of them in the preliminary, conceptual, embodiment, and detail design stages according to Pahl/Beitz [FG13] as well as the pre-production[40] and the production stage is given in Figure 2.14.

KC Identification The first of these activities is the identification and decomposition of functional requirements and particularly their translation into suitable geometrical requirements as well as the definition of quality levels for these requirements. Since these geometrical requirements on the assembly or part level are often referred to as **key characteristics** (KCs), defined as "the product, sub-assembly, part, and process features that significantly im-

[40]In this stage, "the product and the production system is physically tested and verified" [SLC06b] in order to "prepare for full production" [SLC06b].

pact the final cost, performance, or safety of a product when the KCs vary from nominal" [Tho99b], this activity is called **KC identification**. Different approaches for this activity have been proposed, such as a mathematical framework for the KC process [Tho99b] as well as a function-to-form mapping approach [RPS+01] and a method supporting the identification of key parts in the decomposition of global KCs [MAM05]. Based on these identified key characteristics, an **assessment of product and process concepts** can be performed by iteratively repeating a set of analysis and synthesis steps for different product and process alternatives [SLC06b, Wei15a], that are explained in the following .

Assembly Sequence These steps involve firstly the **definition of the assembly sequence** for each concept. In this regard, the assembly sequence has distinct effects on the propagation of part deviations through assemblies and is therefore an important issue in geometrical variations management, particularly in automotive and aircraft industries [MM01]. Different methods and tools may be used to perform and to support this activity, with an integrated design approach to identifying the most suitable assembly sequences having been proposed in [MM01] and a theory for the design of mechanical assemblies considering different assembly sequences having been presented in [MW98, WMAR99]. Beside these methods, an approach for the determination of the influences of the assembly sequence considering compliant parts has been proposed in [MTB+11], whereas a method for the assembly sequence planning based on weighted assembly graphs has been presented in [WT15]. Moreover, the evaluation of the product assemblability considering different assembly sequences has been addressed in [LFW06] and tools for the analysis and control of the assembly precision for different assembly sequences is investigated in [ZQ15]. Furthermore, function-means modelling methods and matrix-based approaches supporting the design of robust assembly configurations, i. e. assembly configurations, that are less sensitive to geometrical part deviations, have been presented in [SJ99, SL99, JS00, SLD06, SLC06a].

Locating Schemes Once the assembly sequence is determined, the **part locating schemes** need to be decided. Locating schemes (sometimes also called positioning or fixture layouts) are required to position parts or sub-assemblies relatively to their surrounding [SJ99, SL99]. In industrial applications, 3-2-1 and 4-1-1 locating schemes are often used to locate parts and to lock their six degrees of freedom (dof) [SJ99, SLC06a, Wei15a]. The terms *3-2-1 positioning* and *4-1-1 positioning* emerge from the the number of part dofs, which are sequentially disabled by the assembly steps. In this regard, the translation in z-direction and the rotations around the x- and y-axes are locked by the first assembly step with three contact points between the part and the assembly surrounding according to the 3-2-1 positioning scheme. The translation in y-direction and the remaining rotation around the z-axis are then locked by the second assembly step with two contact points, whereas the last translation in x-direction is locked by the last assembly step with one contact point [SJ99]. In contrast to that, the first assembly step locks two translational and two rotational part dofs in the 4-1-1 positioning scheme, whereas the second assembly step locks the remaining translation and the third assembly step disables the remaining rotational dof. This is illustrated in Figure 2.15. Beside the 3-2-1 and the 4-1-1 locating schemes, over-constrained locating schemes, such 4-2-1 locating schemes, are used

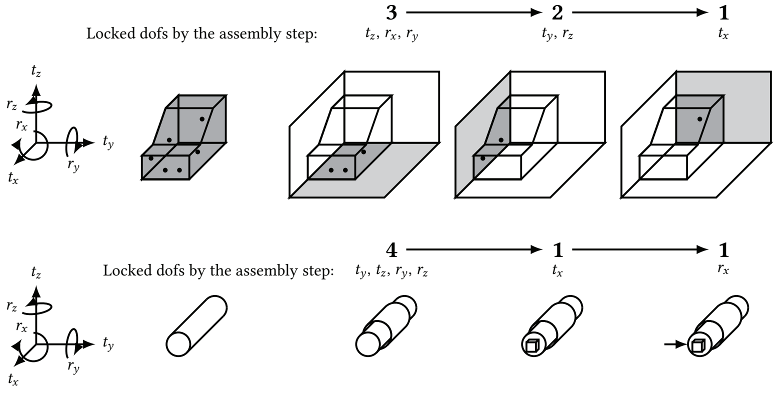

Figure 2.15: Commonly used Locating Schemes: 3-2-1 Locating Scheme of a planar Part (top) and 4-1-1 Locating Scheme of a cylindrical Part (bottom) according to [SJ99, Wei15b]

to fixate compliant parts in certain assembly processes, such as welding and other joining operations [CHC04, SLD06, LYHZ09, Sto10, WSL13, LCE+14]. In order to identify the most suitable locating scheme for a part or sub-assembly, stability analysis tools, which support the evaluation of the "geometrical robustness of a concept, i. e. how much variation, introduced to the components by the locators, propagate and affect critical features" [SLC06b], have been proposed for rigid parts in [SL99, JS00, SL03, SLC06a, SLC06b] as well as for compliant parts in [SLD06] and considering large part deformations in [HCBS13].

Tolerance Specification Given the assembly sequence and the part locating schemes, tolerance specifications for each part are to be defined in order to control the individual part deviations. In this regard, slightly varying guidelines of how to deduce the single part tolerances have been proposed e. g. in [Hen06, Kle12, JS14]. However, in general, five distinct sub-activities for the assignment of part tolerances can be distinguished, which can be seen from Figure 2.16. The first of them is the **tolerance specification**[41], which aims at identifying required tolerance types on features relevant for the function as well as suitable datum features (see Figure 2.16) [Arm13]. Various approaches have been proposed to support this activity, with a brief review being given for example in [Dan14]. Among them are tolerance specification methods based on the concept of technologically and topologically related surfaces (TTRS) [CCD+89, CDR91, DC94], such as in [SPH+96] and in QuickGPS [CA09, ACYA10], as well as approaches based on graphs [BM99, BFCM06]. Moreover, various works regarding the tolerance specification ground on reasoning algorithms [ZLGH11], ontologies [ZQH+13], description logics [ZQH+14], or on functional decomposition methods and the application of rules, such as the Excel-based tool CLIC described in [Ans06] and the works presented in [Arm13, HMK+15]. Furthermore, matrix-based approaches to the tolerance specification have been presented in [RPS+01, Isl09a, Isl09b]. Beside this, methods and tools for the automatic

[41] A definition of tolerance specification is given as follows: "tolerance specification: the types of tolerances on functional features and the datum reference frame are chosen for each part" [Arm13].

generation of first-order dimensioning and tolerancing schemes [HMK⁺15] and their validation have been presented [KSD01], as well as an approach for the semantic interpretation of such GD&T schemes for the tolerance analysis [SRR14].

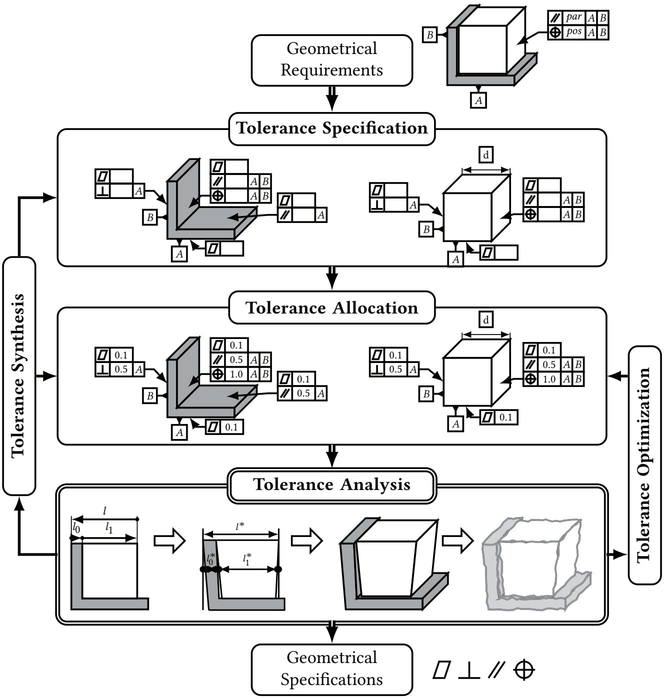

Figure 2.16: The Relationship between Tolerance Specification, Tolerance Allocation, Tolerance Analysis, Tolerance Synthesis, and Tolerance Optimization

Tolerance Allocation After the required tolerance types have been identified, values for these tolerances have to be assigned. This step is called **tolerance allocation** and is most often performed based on experience, rough empirical data, such as tables and databases of achievable manufacturing precisions or process capability maps [Tan83, Hol94, Kle12], or following general tolerance allocation strategies [Pet70, JLMC00]. In this context, typical strategies and rules of thumb for the distribution of tolerances are [JLMC00]:

- the same tolerance method, i. e. all tolerances t_i are equal ($t_1 = t_2 = \ldots = t_n$),
- the constant precision factor method, which "is based on the rule of thumb, that the tolerance of a part increases as the cubic root of the nominal size" [JLMC00], i. e. $t_i = P\sqrt[3]{d_i}$, where d_i is the nominal size corresponding to the ith tolerance t_i, $\mathcal{J}$ is the functional requirement on the assembly, and $P = \mathcal{J}/\left(\sum_{i=1}^{n} \sqrt[3]{d_i}\right)$ is the precision factor,

- the same influence method, which employs the linearity coefficient[42] ξ_i and leads to $t_1\xi_1 = t_2\xi_2 = \ldots = t_n\xi_n$ (tighter tolerances for dimensions with larger linearity coefficient),
- the proportional scaling method (each tolerance is proportional to its corresponding dimension), leading to $d_1/t_1 = d_2/t_2 = \ldots = d_n/t_n$,
- and the assignment of tolerance values according to the process capability of each manufactured dimension, i. e. looser tolerances are assigned to processes with larger variation, whereas tighter tolerances are assigned to processes with less variation [Pet70].

Tolerance Analysis and Variation Simulation As soon as some initial values for the specified tolerances are assigned, a **tolerance analysis** is performed to check if these tolerance types and their values ensure the quality levels defined on the key characteristics. Various approaches for the tolerance analysis and variation simulation have been proposed in research and quite a few proprietary tolerance analysis tools are available, which are used to establish a (analytical or numerical) relationship between the different (dimensional and/or geometrical) tolerances $\boldsymbol{t} = [t_1, \ldots, t_i, \ldots, t_n]$ and each key characteristic Y [NT95]:

$$Y = f(\boldsymbol{t}, \boldsymbol{\beta}), \tag{2.1}$$

where $\boldsymbol{\beta}$ is a vector that may contain further parameters depending on the model used and the analysed mechanism, such as the number of analysed points or the considered directions. In this regard, the **tolerance representation**, which "refers to how tolerances are represented computer-internally [...] for the description of the mechanism without and with geometric variations" [Dan14], is of great importance. However, a detailed overview of the different approaches and computer-aided tools for tolerance analysis and variation simulation based on various tolerance representation schemes is given in the following section 2.3.3.

Tolerance Synthesis If the results of the tolerance analysis reveal, that the specified tolerances and their values not ensure the required quality level regarding the key characteristics, then the tolerances have to be revised. In general, this step is called **tolerance synthesis**, which aims at adjusting the initial tolerancing or GD&T scheme (i. e. both tolerance types and values) by reasoning based on the tolerance analysis results to finally achieve the quality goals. To perform this, tolerance specification, tolerance allocation, and tolerance analysis are iteratively repeated, and coupled with a synthesis step to identify suitable part tolerances from given geometrical product requirements [WW00]. In this regard, the terms "tolerance allocation", "tolerance synthesis", and "tolerance optimization" are often used interchangeably in literature[43]. However, in the context of this work, these terms are understood as connected, but distinct activities, with tolerance allocation referring to the assignment of first, often

[42] The linearity coefficient can be regarded as the partial derivative of the functional relationship between the tolerances and the key characteristic with respect to the corresponding tolerance, i. e. $\xi_i = \partial f(t_i)/\partial t_i$.

[43] While tolerance synthesis "is regarded as a tolerance allocation and a tolerance optimization method taking into account manufacturing and inspection aspects" in [Dan14], it is broadly understood as "the process of taking some desired behaviour of the design function along with suitable models relating tolerances to manufacturing cost and computing a set of tolerances which minimize the cost" in [GT93a].

tentative, tolerance values, that are adjusted during tolerance synthesis, which in turn may be performed employing tolerance optimization methods and tools.

Tolerance Optimization Particularly, a **tolerance optimization** may be performed if the assigned tolerancing scheme, which comprises the specified tolerance types, seems sufficient and only the tolerance values are to be optimized regarding quality and cost. For this purpose, mathematical optimization algorithms are applied to compute the tolerance values, that balance the trade-off between loose tolerances, which may entail decreased quality, and tight tolerances requiring increased manufacturing and inspection costs. During the last decades, various approaches for the tolerance optimization have been proposed, with most of them aiming at minimizing the tolerance-related costs $C(\boldsymbol{t})$ on condition, that the mechanism under consideration fulfils its intended function [BG70b, WCT98, HC02a], i. e. that the (set of) key characteristic(s), which is computed using a given tolerance analysis model, is inside a functional domain spanned by upper (USL_Y) and lower (LSL_Y) specification limits [GS15]. Hence, the tolerance optimization problem is formulated as:

$$\min C(\boldsymbol{t}) \quad \text{subject to } USL_Y - \underbrace{f(\boldsymbol{t}, \boldsymbol{\beta})}_{=Y} \geq 0 \text{ and } \underbrace{f(\boldsymbol{t}, \boldsymbol{\beta})}_{=Y} - LSL_Y \geq 0. \tag{2.2}$$

The tolerance-related costs $C(\boldsymbol{t})$ are often expressed as the sum of the individual tolerance-related costs $c(t_i)$ for the n tolerances in the tolerancing scheme [BG70a], i. e. :

$$C(\boldsymbol{t}) = \sum_{i=1}^{n} c(t_i), \tag{2.3}$$

These individual tolerance-related costs $c(t_i)$ are modelled by tolerance-cost relations, with reviews of commonly used tolerance-cost models being e. g. given in [WEE88, CGLH90, DHX94, Cre97] and an approach for the automated cost modelling being presented in [DW98]. Figure 2.17 highlights an exemplary (multi-process) tolerance-cost function for a dimension, that can be manufactured by three different manufacturing processes depending on the required precision, with each process implying an own tolerance-cost characteristic. Although a variety of different tolerance-cost functions has been proposed in the literature, it has been shown, that most of them can be generalised by the following equation [ATLD14]:

$$c(t) = a + b \cdot e^{-m(t-t_{lim})} \cdot (t - t_{lim})^{-k}, \tag{2.4}$$

where $c(t)$ are the costs associated with a certain tolerance t and a, b, m, k, and t_{lim} are fixed parameters, which have to be identified based on tolerance-cost information gathered from production. A review of such tolerance-cost information is given in [BG70a], from which it can be found, that the disproportionate increase of cost with tightened tolerances as shown in Figure 2.17 has been confirmed only for certain machining processes, whereas other manufacturing processes, such as forming, show an almost linear trend. This can also be seen from the charts provided in [CM88] and has also been reported by companies according to [Kle12]. However, the individual tolerance-related costs are not only caused by fabrication, but may

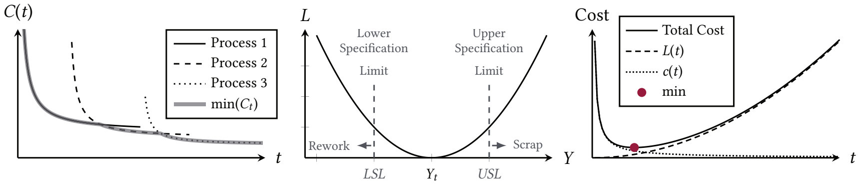

Figure 2.17: Exemplary Tolerance-Cost Relation (left), quadratic Quality Loss Function (middle), and Total Costs (right) according to [Tag86, CM88, DZ88, CP91, Hsi06, ATLD14]

also comprise costs related to inspection and assembly. The solution of the optimization problem formulated in eq. (2.2) is performed employing mathematical optimization algorithms, where early works on this issue can for example be found in [BG70a, BG70b, Pet70, Spe72, Spo73, Kum83] and reviews of such approaches are provided e. g. in [NO98, HC02a, KPB16]. Beside these early approaches to the tolerance optimization, various adoptions and extensions have been proposed, such as the consideration of correlated tolerances t_i in [GS09] and non-normal, non-independent variables in [GS15] as well as the extension of the optimization problem to systems in motion in [WW13, WSW15]. Moreover, the selection of alternative manufacturing processes is treated in [SBR11a, SBR11b], whereas measurement and adjustment activities in assembly have been considered in the optimization problem formulation in [GLLH15]. Also related to the adoption of the optimization problem is the consideration of a trade-off between cost and product sensitivity in a multi-objective optimization formulation for tolerance optimization applied to an automobile body structure assembly in [LIK⁺08] as well as of multi-constraints in an aircraft assembly model in [WYWSC16]. Furthermore, a trade-off between economic cost and environmental impact in a multi-objective tolerance optimization for automotive assemblies has been presented in [HDS13b, HDS14].

Whereas the typical tolerance optimization problem given in eq. (2.2) aims at minimizing the tolerance-related costs on condition that a certain quality level is ensured, there are also approaches, which follow the assumption, that the cost of missed key characteristics due to variations can be described by a quality loss function [DZ88, WCT98, WT98, CC01, HZX05, Hsi06, PRA07, Adr09, MDS09, SKC10, Cha15, JLW15, ZLW15]. In this regard, the quality loss L is usually described by Taguchi's (quadratic) quality loss function [Tag86], which expresses L as a function of the difference between the actual value Y of the KC from its target value Y_t and a cost coefficient K [DZ88] (see Figure 2.17):

$$L(Y) = K(Y - Y_t)^2. \tag{2.5}$$

Based on this assumption, the tolerance optimization problem is re-formulated as a straight cost minimization problem:

$$\min \underbrace{L(f(\boldsymbol{t}, \boldsymbol{\beta})) + C(\boldsymbol{t})}_{=\text{Total Cost}}, \tag{2.6}$$

where tolerances $\boldsymbol{t}$ are to be identified, that balance the sum of the quality loss due to loose tolerances and increased tolerance-related costs due to tight tolerances. The relationship between the tolerance-related costs, the quality loss, and the total cost can be seen from Figure 2.17.

Depending on the chosen optimization strategy and the available tolerance-cost relations (e. g. discrete tolerance grades vs. continuous tolerance values), different mathematical optimization algorithms, such as the Lagrange multiplier method [WCT98, KPB16], evolutionary algorithms (such as genetic algorithms) [SJJ05], meta-heuristic algorithms [MDS09], or particle-swarm optimization algorithms [For09, SBR11a, SBR11b], may be applied to solve the tolerance optimization problem. In this context, it should be mentioned, that the optimization strategy formulated in eq. (2.6) is an unconstrained optimization problem, focusing on the minimization of the total costs as the sum of tolerance-related costs and the quality loss, whereas the strategy in eq. (2.2) is a constrained optimization problem, which usually has its solution on the boundary of the search space spanned by the constraints (i. e. the functional specification limits). This is because the tolerance-cost relations $c(t)$ as well as the relations between the tolerances and the key characteristics $f(\boldsymbol{t}, \boldsymbol{\beta})$ are usually monotonic[44].

Despite the broad research interest in this topic during the last decades, tolerance optimization is not widely spread in industry. The reasons for this are a lack of information about the tolerance-cost relations, which hinders the identification of tolerance-cost model parameters, the limitation to dimensional tolerances, which holds for most of the presented tolerance optimization approaches, the difficulties in identifying suitable specification limits for the key characteristics, and the non-trivial formulation of adequate tolerance optimization strategies, that are in line with the company strategy. Furthermore, as can be seen from eqs. (2.2) and (2.6), the results obtained by tolerance optimization approaches totally depend on the tolerance analysis model used to predict the key characteristics from the set of tolerances $\boldsymbol{t}$. Thus, adequate tolerance analysis models are a prerequisite to produce reliable tolerance optimization results [WEE88, HC02a].

Part Optimization As it has been mentioned, the tolerance specification, the tolerance allocation, the tolerance analysis, the tolerance synthesis, and optionally the tolerance optimization are performed iteratively for different product and process concepts in order to assess the advantages and disadvantages of each concept and to bring about a decision for the further product development proceeding. Based on this decision, the most deviation-prone **parts** of the favoured concept are **optimized** to further reduce their sensitivity to noise factors, such as manufacturing-caused deviations as well as thermally or mechanically induced part deformations, and thus to decrease their introduced part deviations during operation.

Computer-Aided Process Planning and Tolerance Transfer Once the product definition, including all required tolerances, is specified, adequate manufacturing processes are to be selected, which is usually performed based on process capability charts, and the design tolerances are to be transferred to tolerances suitable for manufacturing, which is usually called

[44]Tolerance-cost relations are generally monotonically decreasing with increasing tolerances, since looser tolerances are cheaper to manufacture, whereas the relation between the tolerances and the key characteristics is usually monotonically increasing, as looser tolerances usually lead to decreased quality.

tolerance transfer [HC02a] or tolerancing in process planning[45] [FWB86, Wei88]. Various approaches have been proposed to support this activity, such as a software tool, which also helps to identify the minimal dimensions for the raw material, in [FWB86], and a module for the tolerance transfer of one-dimensional tolerances in [Wei88]. Moreover, an approach for the definition of the optimal part position in the machine tool workspace with regard to accuracy and cost is presented in [SDP95] and an automated tolerance analysis method for computer-aided process planning is highlighted in [ZM95]. Furthermore, the optimization of tolerances in the context of process plan simulation has been discussed in [HCLD06]. Beside this, the generation of manufacturing tolerances and process plans for ISO GPS specifications, particularly geometrical tolerances, is investigated based on the Small Displacement Torsor (SDT) in [AL05, RA16], based on the concept of technologically and topologically related surfaces (TTRS) [CCD+89, CDR91, DC94] in [JBL+11], and based on a vectorial representation of tolerance zones in [MB12]. Additionally, a review of further approaches for the tolerance transfer can be found in [HC02a].

Jig and Fixture Design Based on the part design and the decided process plan, the fixtures and jigs for the different manufacturing steps are to be designed in order to allow the physical manufacturing of the parts. In this regard, a fixture is considered as a "tool used for locating and firmly holding a workpiece in the proper position during a manufacturing operation" [Hen73], whereas a jig "is a type of fixture with means for positively guiding and supporting tools for drilling, boring, and related operations" [Hen73]. Since the fixture and jig layout has distinct effects on the accuracy of the manufacturing operations [CHC04], various computer-aided tools are used for their proper design, optimization, and verification [Cab90, RH05, NRFK14, DFC15]. Particularly, the assignment of locator tolerances has been identified as an important issue in fixture design [KRY03a, KRY03b, KRY03c] and different models have been proposed to study the effects of locator tolerances on the product key characteristics in single or multi-stage machining [LZC07] or assembly processes [HLB+07, HLKC07, LIK+08, QLMW16, WCS16]. In this regard, the allocation of locator tolerances has been investigated under the term "process-oriented tolerancing" [DJCS00, DJCS05] to emphasize the fact, that process-related tolerances are analysed and allocated instead of product tolerances. In order to model the relationship between locator tolerances and the product characteristics, these process-oriented tolerancing approaches also considered fixture maintenance policies, cutting tool wear, and the thermal state of the machine tools [CDJC06, ANLS13].

Inspection Preparation and Tolerance Verification When parts are manufactured, they need to be verified against the specified tolerances in order to prove their fitness for purpose. This activity is called **tolerance verification** or tolerance evaluation [HC02a], which aims at defining "inspection planning and metrological procedures for functional requirements, func-

[45] "Process planning, in the manufacturing context, is the determination of processes and resources needed for completing any of the manufacturing processes required for converting raw materials into a final product to satisfy the design requirements and intent and respect the geometric and technological constraints" [EN14]. Computer-aided process planning is considered as the "missing link between computer-aided design and computer-aided manufacturing" [Wei88].

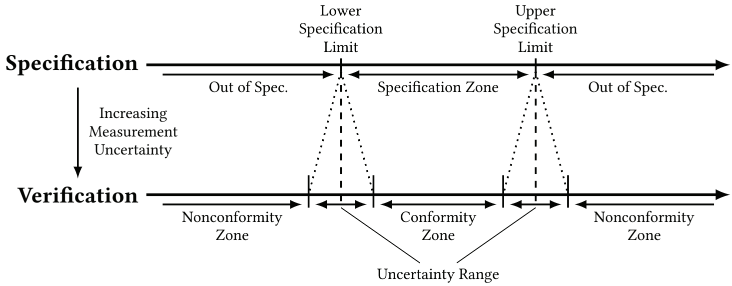

Figure 2.18: Conformity and Nonconformity Zone as well as Uncertainty Range of a Specification according to [ISO14253-1]

tional specifications and manufacturing specifications" [MB07] and "permits to close the process loop, to check the product conformity and to verify assumptions made by the designer" [MB07]. The tolerance verification is nowadays usually performed by assessing "the geometric deviations of a part using the data obtained from the coordinate measuring machines (CMM)" [HC02a], whereas the set of inspection points on the single parts and the final assembly is decided during **inspection preparation** [SLC06b]. In this context, particularly, the processing of measured point sets obtained from CMMs in conformance to the standards for the geometrical product specification and verification has been identified as a critical research issue [BBM91], which led to the term *computational metrology* [Sri91, Hop93, Sri05, Sri06], that broadly covers all computational problems and their solutions related to the verification of manufactured parts [Sri91] and is defined in a narrower sense as "fitting and filtering of discrete geometric data" [Sri06]. In this regard, an approach for the verification of location tolerances with degrees of freedom has been presented in [BLM94] and a least-squares approach for the evaluation of geometrical deviations has been proposed in [YM96]. Moreover, the tolerance evaluation for vectorial tolerances has been discussed in [Yau97]. However, an overview of different approaches for the verification of geometrical deviations from point clouds is given in section 5.2. Beside this, the interaction between dimensioning, tolerancing, and metrology has been highlighted in [Hoo93], whereas the representation of geometrical tolerances in measurement processes has been studied in [ZPW06].

The tolerance verification inevitably introduces measurement uncertainties, which decrease the conformity zone of each specified tolerance [ISO14253-1], with the specification zone, the conformity zone, as well as the uncertainty range being qualitatively illustrated in Figure 2.18. Thus, the tolerance verification should be considered "early in the design activities to be able to evaluate uncertainties" [MB07], where for example the effects of measurement errors on the form deviation estimation have been investigated in [LZW01] and their influences on the process capability estimation are discussed in [FKM11]. In this regard, it can be found, that the measurement uncertainties have distinct effects on the observed process variation, since the "measurement inaccuracy leads to the measurement results being distributed wider than the actual process values" [FKM11] (see also Figure 2.19). In order to consider these effects in the process capability estimation, a model for the calculation of escape and overkill rates has been presented in [FKM11]. Moreover, various approaches for the measurement uncertainty evaluation have been proposed, such as the "Guide to the Expression of Uncertainty in Measurement" (GUM) [JCG08], and a procedure for the validation of measuring systems and measurement processes has been standardized in ISO 22514-7:2012 [ISO22514-7]. Additionally, early cost estimation approaches for the tolerance verification [MPT11] and methods for the optimal inspection strategy planning [MP14] should be applied already during the specification stage to assess the influences of the tolerance verification on the conformity decision and hence on the product quality and cost.

Process Capability Evaluation and Statistical Process Control In series production, the measurement results of the different product specifications are often used to compute **process capability indices**, which serve as measures "to compare the requirements of specification with the capability of the manufacturing process" [PK06]. These indices are widely used to communicate the relationship between the specification limits and the actual process performance as well as to establish a feedback-loop to the specification stage from manufacturing [Cre97, KM12b]. This may be performed by building process capability databases for different manufacturing processes from manufacturing data and the provision of these databases to design and process planning teams [Cre97, KA12, ORE+14]. However, "the interpretation of these indices depends on assumptions that are often not made explicit" [PK06] and that "may not necessarily hold true for a specific process" [PK06]. Among these assumptions are that the considered process is in statistical control, that the specification is one-dimensional, and that it follows an univariate Gaussian distribution [PK06]. There exists a wide variety of different process capability indices, with the most prominent being the precision index c_p, which firstly appeared in the literature, the process accuracy c_a, and the well-known c_{pk} index [PK06, Cre97]:

$$c_p = \frac{\overbrace{USL - LSL}^{\text{Allowed Design Variability}}}{\underbrace{6\sigma}_{\text{Manufacturing Variability}}}, \quad c_a = 1 - \frac{\left|\mu - \frac{USL+LSL}{2}\right|}{\frac{USL-LSL}{2}}, \quad c_{pk} = \min\left\{\frac{USL-\mu}{3\sigma}, \frac{\mu - LSL}{3\sigma}\right\}, \tag{2.7}$$

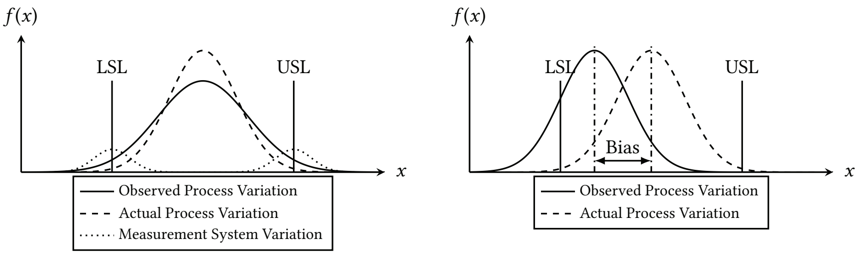

Figure 2.19: Effects of Measurement Uncertainties on the observed Process Variation according to [FKM11]: Influence of Measurement System Variation on the observed Process Variation (left) and Effect of Measurement Bias on the observed Measurement Average (right)

where μ is the sample mean and σ the sample standard deviation of a measure X:

$$\mu = \frac{1}{n}\sum_{i=1}^{n} X_i, \qquad \sigma^2 = \frac{1}{n-1}\sum_{i=1}^{n} (X_i - \mu)^2 . \tag{2.8}$$

Beside these basic indices, the c_{pm} index, which is often called TAGUCHI index and is based on the squared quality loss function (eq. 2.5), is gaining increasing attention in the automotive industry recently, since it "concentrates on measuring the ability of the process to cluster around the target" [PK06], whereas the aforementioned indices rather focus on the process variability and do not take into account the cost of missing requirements [PK06]. It is defined as [PK06]:

$$c_{pm} = \frac{USL - LSL}{6 \cdot \sqrt{\sigma^2 + \left(\mu - \frac{USL+LSL}{2}\right)^2}} . \tag{2.9}$$

All these process capability indices are constructed in such a way, that a value of greater or equal to 1 indicates a well-balanced relation between the design specifications and the manufacturing variability, whereas a value below 1 implies increased scrap or rework [PK06]. Beside these basic process capability indices, which are predominantly used for dimensional tolerances with univariate Gaussian distributions, various other indices have been proposed, such as for position tolerances in [TL09], for geometrical tolerances with material modifiers in [TC12], and for multivariate distributions in [GG16]. Moreover, the relationship between the process capability and the geometrical complexity of a part has been investigated in [LT15].

Though process capability indices capture some basic information about the manufacturing process, they also imply significant intrinsic weaknesses and limitations, which can be traced back to their underlying assumptions. However, their use in industry to define certain quality levels related to geometrical specifications is widely used. Moreover, they have also been used for the process-related tolerance allocation in [Hol93], for the tolerance synthesis based on a surrogate model of the process capability in [HPC09], for the tolerance optimization considering the manufacturing context in [MCLY09], for the process-based tolerance assessment in [SRSB16], as well as for the assessment of the assembly quality employing a fuzzy-based analysis in [KM12a] and the maximization of process tolerances in [Con13]. Further details about process capability indices and their estimation can be found in [PK06] and the standards ISO 22514-1:2014 and ISO 22514-2:2013 [ISO22514-1, ISO22514-2].

Moreover, permanent measurements of dimensional and geometrical tolerances during manufacturing are widely used for the **statistical process control**, which has been proposed by SHEWART [She30, She31] and employs (quality) control charts for the steady assessment of the process stability. In this regard, the statistical process control based on vectorial tolerancing has been highlighted in [Mar96] and the geometrical dimensioning and tolerancing for quality control has been discussed in [HG92]. However, further details on different control charts and the statistical process control can be found e. g. in [She30, She31, GS13] and the standards ISO 7870-1:2014, ISO 11462-1:2001, and ISO 11462-2:2010 [ISO7870-1, ISO11462-1, ISO11462-2].

Root Cause Analysis and Process Optimization During full production, various errors and problems in the manufacturing and assembly processes may occur, which need to be detected and adjusted [SLC06b]. In order to perform this, **root cause analysis** can be applied, which aims at identifying the root causes of such errors and their removal [WDA93]. In the context of geometrical variations management and tolerancing, e. g. an approach for the root cause analysis based on the stream of variation analysis method has been proposed in [CHZ+04] and a method for the root cause analysis in assembly processes aiming at reducing the dimensional variation in assemblies has been highlighted in [CS03]. Moreover, based on steady measurements of process and product data, manufacturing and assembly **processes** may be **optimized**. In this context, e. g. the optimization of manufacturing processes for machined parts regarding their geometrical quality has been investigated in [MSD05, LABH06]. Furthermore, a method for the setting of optimal process means has been discussed in [DSMW15] and the optimization of sheet forming processes has been investigated in [LLDM15] and of deep drawing processes in [ABW14].

However, due to the increasing complexity of modern manufacturing and assembly processes, the root cause analysis as well as the (statistical) process optimization are demanding research issues, where further details on these issues can be found e. g. in [WDA93, SM16].

Tolerance Analysis and Tolerance Visualization The assessment of the effects of different assembly sequences, geometrical deviations of single parts, and other design and process parameters on product key characteristics during the product and process development process is nowadays widely performed by the use of tolerance analysis and variation simulation tools. Moreover, the visualization of geometrical deviations on the part, assembly, or product level strongly supports decision making in the design, pre-production, and production stages. Thus, an overview of the different approaches for the tolerance analysis and variation simulation as well as of means for the tolerance and variation visualization is given in the next section.

2.3.3 Computer-Aided Tolerance Analysis

Tolerance analysis, sometimes also called variation simulation [LH97, SLC06b, LLS07, HCBS13, WSL13, LCE+14], can be considered as a “key element in industry for improving product quality and decreasing the manufacturing cost” [DGD+12] as well as for reducing scrap and customer returns [DGD+12, QDS+12], which “affects not only the performance of products but also the cost” [CJLL14]. This is because it prevents the need for cost- and time-expensive physical mock-ups and part prototypes during product design and is thus a means for improving the product development performance. Moreover, it is an inevitable tolerancing activity, since “any tolerance allocation guidelines to be offered to designers must be based on tolerance analysis investigations” [WEE88]. Beside its wide applicability in design, it can be used in the pre-production stage to support process planning activities and the tolerance verification and it can be used in the production stage to support the root cause analysis and the process optimization.

Due to its high importance, tolerance analysis is quite a prominent research topic [HC02a, GAMQ14, CMJ15] and enjoys strong acceptance in industry. This section is to give an introduction to this issue as well as to provide an overview of different approaches for the computer-aided tolerance analysis.

What is Tolerance Analysis? Various answers to this question have been given during the last decades, with a set of slightly differing definitions of the term "tolerance analysis" being collected in Table 2.3. Based on the review of these definitions, tolerance analysis can be found as an activity aiming at virtually predicting the effects of geometrical specifications on assembly or product key characteristics by building, evaluating, and interpreting adequate mathematical models for the representation of geometrical specifications as well as for their accumulation.

Table 2.3: Different Definitions of "Tolerance Analysis"

"Tolerance analysis is the process of taking known tolerances and computing their effect on a particular design function." [GT93a]
"After specifying the variation of the individual components in an assembly, the propagation of the variations in the assembly must be determined. This is frequently referred as tolerance analysis." [CGMS96]
"Tolerance analysis is a method to verify the proper functioning of the assembly after tolerances have been specified." [SHP$^+$96]
"In variation analysis, statistical data [...] for the total population are calculated for the specified critical assembly dimensions." [JS00]
"It [tolerance analysis] is a method to verify the proper functionality of a design, taking into account the variability of the individual parts. While the methods of analysis can be either deterministic or statistical, the design models to be analysed can be of 1D, 2D or 3D." [HC02a]
"The objective of tolerance analysis is to check the extent and nature of the variation of an analyzed dimension or geometric feature of interest for a given GD&T scheme. The variation of the analyzed dimension arises from the accumulation of dimensional and/or geometric variations in the tolerance chain." [SASD05]
"The purpose of tolerance analysis is to study the accumulation of variations on a geometric attribute of interest (dimension, location, orientation, etc,[...]). The need for this arises because the analyzed dimension is not explicitly specified. The most common case is analysis of clearances in assemblies." [SASD07]
"The aim of the tolerance analysis is to study the accumulation of dimensional and/or geometric variations resulting from a stack of dimensions and tolerances. The results of the analysis are meaningfully conditioned by the mathematical model adopted." [BYWC13]
"Tolerance analysis: the stackup of errors allowed by selected tolerance values is evaluated and compared to design requirements (possibly more than once during the allocation procedure)." [Arm13]
"The objective of tolerance analysis is to check the feasibility and quality of assemblies or parts for a given GD&T scheme. The results of tolerance analysis include worst case variations and statistical distribution of functional requirement, acceptance rates, contributors and their percent contributions, and the sensitivity coefficients with respect to each contributor." [CJLL14]
"Tolerance analysis: it concerns the verification of the value of functional requirements after tolerance has been specified on each isolated part. This verification is totally dependent on the models chosen before. A lot of tools are also generally provided to the designer to understand the results. " [Dan14]

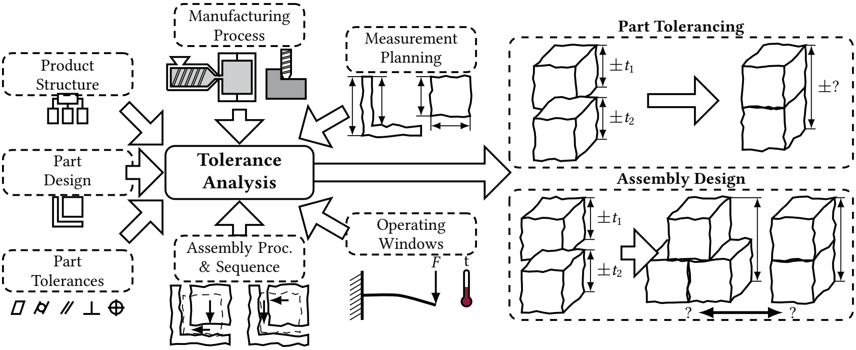

Figure 2.20: Task Settings for the Tolerance Analysis in Geometrical Variations Management

In this regard, it can be found, that the task setting for the tolerance analysis can be roughly divided into part tolerancing, i. e. answering the question "How much part variation is admissible given a specific product and assembly design to ensure the required product quality level?", and in assembly design and process tolerancing, i. e. identifying adequate solutions to the problem "How should the parts be assembled given an irreducible amount of part variation in order to achieve the required quality level?" (see Figure 2.20). Beside this, various other issues may require or can be supported by tolerance analysis, such as the specification of admissible operating windows ("Which operating conditions are admissible considering thermal expansion or elastic deformations of parts given a specific product and assembly design to ensure the required product quality level?") [AS13], or process-oriented tolerancing ("Which fixture tolerances are required to ensure the geometrical part requirements in multi-station manufacturing and assembly processes?") [ANLS13], which can be classified as part tolerancing problems.

Main Issues in Tolerance Analysis All of these aforementioned questions require a quantitative relationship between the different part tolerances $\boldsymbol{t} = [t_1, \ldots, t_i, \ldots, t_n]$ in the tolerancing scheme as well as all other parameters in geometrical variations management and the key characteristic Y of the assembly. This analytical or numerical relationship is sometimes called "stack-up function" [Pol12] or "assembly response function" [DGD+12] and is generally formulated as $Y = f(\boldsymbol{t}, \ldots)$ (see also equation (2.1)). In order to establish and evaluate this relationship, mainly three mathematical issues in tolerance analysis can be distinguished according to Dantan et al. [DGD+12, QDS+12, DDG15], namely (see Figure 2.21):

- **tolerance representation**, i. e. establishing mathematical models for the expression of geometrical deviations, gaps, specifications, and requirements,
- **tolerance propagation**, i. e. modelling the effects of these geometrical deviations and gaps on the assembly and system behaviour, and
- **evaluation techniques**, i. e. providing solution approaches for these models based on assumptions about the tolerances and assembly gaps, such as worst-case or statistical evaluation approaches.

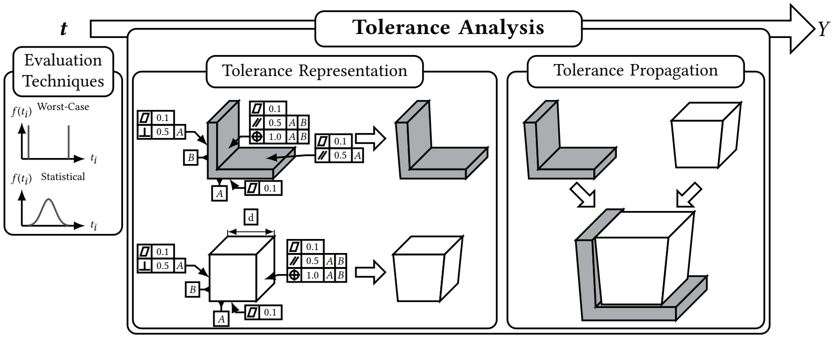

Figure 2.21: Mathematical Issues in Tolerance Analysis [DGD⁺12, QDS⁺12, DDG15]

In this regard, the first and probably most important aspect[46] of tolerance analysis is the **tolerance representation**, which "refers to how tolerances are represented computer-internally" [Dan14]. It is required to map the different tolerance specifications as input parameters to model-internal parameters, which are used to express the allowable geometrical part deviations. This mapping generally requires the formulation of implicit or explicit inequations between the tolerances and such model parameters, which is comparably straightforward for dimensional tolerances, but not for tolerances with three-dimensional tolerance zones. In this context, computer-aided design tools and solid modellers employ various methods for modelling the three-dimensional *nominal* part geometry, which can be broadly classified as wireframe models, surface models, solid models[47], and voxel models [VWB⁺09]. Initial attempts to the computer-aided tolerance representation aimed at creating *variational* solid models using nominal parametric solid models for the construction of tolerance zones by adding variations, i. e. inequations, to the model parameters [ASG11], see e. g. [HB78, TW87, GZS88, Tur88, GT93a]. The limitations of these approaches regarding parts with many features and multiple tolerance zones led to the idea of solid offsets [Req83, RR86], which were then extended to variational surfaces [BS91, GT93b, GT93a, RL98, RL99] and tolerance envelopes [OBJ05, OBJ07]. Overviews of such approaches for the construction of tolerance zones based on solid modelling are for example given in [KPMW03, ASG11]. In contrast to these efforts, most of the established tolerance analysis approaches employ kinematic formulations[48], such as (linearised) homogeneous matrix transforms [WGJ94] or the small displacement torsor (SDT) [BC76, BMLB96], other kinematic approaches [LZC07], or vector loops [GCM98, WCH04] to model geometrical deviations within defined tolerance zones [DGD⁺12, DDG15]. Moreover, further approaches for the tolerance representation are for example reviewed in [HC02a, SASD05, SASD07, CJLL14].

[46] As Mathieu and Ballu state: "The representation of deviations and tolerances, on parts or assembly, is the key problem of tolerancing" [MB07].

[47] Solid models can be further classified as boundary representations (BRep), constructive solid geometry (CSG), hybrid, and further models [VWB⁺09].

[48] Beside these methods, further approaches for the formulation of translations and rotations exist [WS08], such as rotation matrices, Euler angles, quaternions, screw transformations, screw axis, and Plücker coordinates. Moreover, a rich survey on kinematic modelling is provided in [DS10].

The geometrical part deviations are then accumulated employing **tolerance propagation** (also called **tolerance accumulation**) models in order to calculate the key characteristic [DGD+12, Pol12]. Depending on the accumulation input, these tolerance propagation approaches can be classified as [DQ09, DGD+12, Pol12, QDS+12, DDG15, HTB15]:

- **deviation accumulation** approaches, in which the key characteristic is expressed as a function of the geometrical part deviations, which often employs kinematic approaches for the accumulation of geometrical deviations as well as of part displacements and gaps, and
- **tolerance accumulation** approaches, in which the tolerance zones to be analysed are expressed as subsets of multidimensional spaces, accumulated using operations on these subsets, such as Minkowski sum and intersection, and compared to the functional subset in the multidimensional space.

Typical deviation accumulation approaches are parametric ones, which "formalize the relative position of any two surfaces of a mechanism at a specific point by a simple relation (linear or non-linear) between parameters of position (translation and/or rotation)" [HTB15] (see also [SASD05]), assembly functions of solid modellers used for the tolerance propagation of variational solid models, and kinematic approaches used for the accumulation of deviations, displacements, and gaps based on matrix transforms, vector loops or Jacobian matrices [SASD05, Pol12, HTB15]. Regarding the tolerance accumulation, most used multidimensional spaces for the tolerance representation are the SDT and Tolerance-Maps® (T-Maps®), which represent "a hypothetical Euclidean point-space, the size and shape of which reflects all variational possibilities for a target feature" [ASG11], as well as the gap space approach [ZM04]. The various deviation and tolerance accumulation approaches, which build the relationship between the model parameters and the key characteristic, can be classified as analytical and numerical functions depending on the respective tolerance representation scheme [DGD+12].

These functions, that establish a quantitative relationship between the tolerances and the key characteristic, may be **evaluated** considering different assumptions about the input tolerances. In this context, mainly worst-case and statistical approaches for the tolerance analysis have been discussed in the literature, with worst-case approaches being for example presented in [DQ09, MGH11, MGH13] and reviews of statistical methods being found e. g. in [Eva74, NT95, Mor98, HC02a]. However, also other evaluation techniques to the tolerance analysis have been proposed, such as fuzzy logic and fuzzy sets [JLMC00, KM11, KMF11, KM12a, KM16] as well as the non-probabilistic set theory [ZZL16].

Overview of Tolerance Analysis Approaches Based on the different solutions for the aforementioned issues in tolerance analysis, a wide variety of tolerance analysis approaches has been presented in the literature. Moreover, a considerable number of review papers is available, such as [CP91, Tur93, NT95, NO98, SvHK98, HC02a, PG02, SASD05, SASD07, MP09, ASG11, MP11b, MP11a, DGD+12, Pol12, BYWC13, CJLL14], which propose various classification criteria for tolerance analysis approaches. In this context, the tolerance analysis approaches are classified according to their tolerance accumulation input as displacement accumulation and tolerance accumulation approaches in [DQ09, DGD+12, QDS+12, DDG15]. In contrast to this, a taxonomy based on seven criteria is proposed in [Pol12], in which these criteria are the considered tolerance types, the consideration of the envelope and independency principle, of tolerance zone interactions, of datum precedence, and of material modifiers, the model parametrization (e. g. for statistical tolerancing), the considered joint types, and the considered functional requirements (only characteristics for points on features or also characteristics defined on the features themselves). Moreover, five categories for distinguishing tolerance analysis approaches are highlighted in [CJLL14], namely the dimensionality (1D, 2D, 3D; see also [CP91]), the objective (rigid vs. flexible assemblies), the level (part vs. assembly level), the device (computer-aided vs. manual), and the phase (design, process planning, manufacturing, inspection). However, in order to provide an overview of the most common tolerance analysis approaches in Table 2.4, the classification according to their tolerance representation and tolerance propagation methods is adopted. Furthermore, these approaches will be briefly discussed in the following and are schematically illustrated in Figure 2.22.

Probably the oldest and most commonly used tolerance analysis approach in industry are one-dimensional **tolerance stacks**, which offer a simple and straightforward approach to model the effects of part deviations on distances between different part features in an assembly [Eva74, SASD05, SASD07]. In this regard, tolerance stacks include most often only dimensional tolerances, though modern modifications of this method also consider geometrical tolerances [SASD05]. The procedure of performing the tolerance analysis based on tolerance stacks comprises firstly the definition of a stack coordinate system, secondly the identification of the stack path and the formulation of the stack equation (or tolerance chain), and finally the evaluation of the stack equation using worst-case or Monte-Carlo methods [SASD05], where the worst-case evaluation can be supported by **tolerance charts**, being “spreadsheets, where each row represents the variations of a contributor” [SASD05]. Further details on this method can e. g. be found in [Man04, Man05c, SASD05, SASD07].

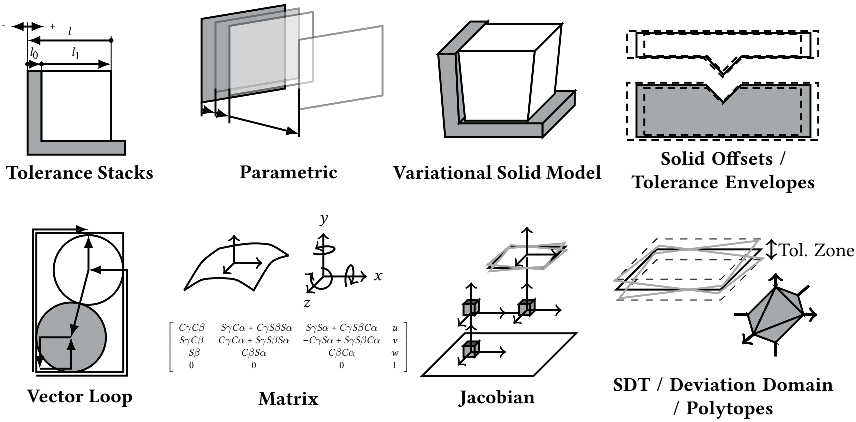

Figure 2.22: Schematic Visualization of Tolerance Analysis Approaches according to [TW87, IMK95, LL99a, SASD05, MP09, ASG11]

Table 2.4: Overview of common Tolerance Analysis Approaches

Tolerance Analysis Approach	**Tolerance Representation**	**Tolerance Propagation** Variation vs. Tolerance Accumulation	**Sources**
Tolerance Stack / Charts	Dimensions and Distances	Var. Acc. (Stack Equation)	[Sch95, Man04, Man05c, SASD05, SASD07]
Parametric / Variational	Parametric (Translation and/or Rotation)	Var. Acc. (Algebraic Function)	[BS91, GT93b, ABC+99, SASD05, SASD07, MP11a, Pol12, HTB15]
Variational Solid Models	Parametric (CAD)	Var. Acc. (Solid Modeller)	[Req83, RR86, TW87, Tur88, BS91, GT93b, GT93a, RFM94, RL98, RL99]
Tolerance Envelopes	Tolerance Envelopes	Tol. Acc. (Configuration Space)	[IMK95, JSS97, SJ97, SJ98b, SJ98a, OBJ05, OBJ06]
Vector Loop & DLM	Vectors	Var. Acc. (Rotational Transformation and Translation Matrices)	[CGMS96, GCM98, RHK+01, PPC04, WCH04, SASD05, IP09, MP09, Pol11, BYWC13]
Matrix	Matrix Transforms	Var. Acc. (Matrix Transforms)	[VW86, LH94, WGJ94, DR97, LZ01, MP09, Pol11]
Torsor	SDT	Tol. Acc. (SDT Propagation)	[BC76, BMLB96, BB98, LAS02, LABH06, Asa09, SBF+10, MP11b, BYWC13, LZLH14, JCLL15]
Deviation Domains	SDT	Tol. Acc. (Set operations)	[GSP07, ASG11, MGH13, MGD13, ZW15a]
Polytopes	SDT	Tol. Acc. (Set operations)	[TCD99, TD11, PTN14, DT15a, DT15b, HTB15]
Tolerance-Maps®	Areal Coordinates	Tol. Acc. (Set operations)	[WSD03, SASD05, SASD07, ASG11, Jai12, MGD13, JDLS14, RHSD14, ZW15b, ZW15a, HDKS16]
Jacobian	Translations and Rotations	Var. Acc. (Jacobian)	[SC86, PL97, LY98a, LL99a, LL99b, MP11b, Pol11, BYWC13]
Jacobian-Torsor	SDT	Var. Acc. (Jacobian)	[LGD02, Des07, GLD07, GLD10, Ghi10, CJLL15b, CJLL15a, SPL+15]
Analysis Line	Distances and Dimensions, SDT	Var. Acc. (Linear Transfer Relations for Analysis Points along the Directions of Analysis Lines)	[SPH+96, SHP+96, Ans06, CA09, ACYA10, Ans10, PA15]
Constraint Solving	Dimensions, Matrix Transforms, SDT	Solving of Constraints by Numerical Optimization	[AKC96, MA98, SRW99, DMBM05, DQ09, FGP10, QDS+12, BGDD13]

In contrast to that, most commercial tolerance analysis tools are based on **parametric** tolerance analysis approaches (sometimes also called variational approaches), which “represent the variability of an assembly, due to the tolerances and the assembly conditions, through a set of parameters of a mathematical model” [MP11a]. Thus, in such parametric approaches, “the analysed dimension is expressed as an algebraic function (an equation, or a set of equations) that relates the analysed dimension to those on which it depends” [SASD05]. Sometimes, these equations are linearised using the Taylor series expansion, leading to “linearised tolerance analysis”, whereas the direct use of these parametric functions is called “non-linear tolerance analysis” [SASD05]. Moreover, the parametric models can be directly built on the parameters used in computer-aided design tools to describe the nominal geometry or based on abstracted feature models, which usually involves the expression of features by few points and is the more common approach [SASD05, SASD07, ZW15a]. Beside this, it can be distinguished between vertex-based and feature-based approaches as well as between models involving only translational parameters and models considering rotational and translational parameters [MP11a]. The parametric or variational tolerance analysis approach is discussed more in detail in [SvHK98, PG02, SASD05, SASD07, MP11a, Pol12].

A particular means of parametric models are **variational solid models**, which employ the possibilities of solid modellers for the tolerance representation as well as for the tolerance propagation by built-in assembly functions. Most of these approaches are based on the idea of solid offsets by Requicha [Req83], in which variational solid models are designed using feature offset boundaries. In this regard, Turner and Wozny [TW87] use the vector space representation for tolerance zones, which limit geometrical deviations (translations and rotations) for nominal part features, and use a linear programming approach for the generation of variational models as well as for the tolerance analysis. Beside this, Roy and Li [RL98] use algebraic constraints for the representation of form tolerance zones in variational solid models. The obtained admissible surface points (points at the boundary of the form tolerance zone) are then used as control points for modelling form deviations with NURBS and Splines. In [RL99], they model size, location, and orientation tolerance zones by algebraic inequalities, in which the deviation parameters are sequentially varied in order to keep the feature within the tolerance zone (without considering form tolerances). Moreover, approaches for the tolerance propagation of solid offsets models (sometimes also called **tolerance envelopes**) employing the configuration space have been presented in [IMK95, JSS97, SJ97, SJ98b, SJ98a, OBJ05, OBJ06].

A further, quite established tolerance analysis model, is the **vector loop** approach. It employs vector loops to model the assembly considering dimensional variations of the part features and kinematic variations between mating part features [CGMS96, GCM98]. Furthermore, the direct linearisation method (DLM) has been introduced, which employs the linearised Taylor expansion of such vector loops for assembly tolerance analysis [CGMS96, GCM98, WCH04, IP09]. However, similar to the vector loop approach, only dimensional part deviations are considered, which is not conform to tolerancing standards. More information about these models can be found in [CGMS96, GCM98, PPC04, WCH04, SASD05, IP09, MP09, Pol11, BYWC13].

The tolerance representation for assemblies based on homogeneous **matrix transforms** has been proposed in [WGJ94] based on the fundamentals presented in [VW86], with the matrix transforms describing feature deviations of orientation and location based on the six rigid body degrees of freedom (dof). The advantage of this approach is the consistent representation of nominal and variant features. However, no form deviations are considered. Similarly, DESROCHERS and RIVIÈRE [DR97] employ homogeneous matrix transforms to represent tolerance zones, feature deviations, and clearances. Furthermore, homogeneous matrix transforms are used to model situation deviations of features whereas a parametric vector representation is employed to model intrinsic feature deviations in [CZM⁺11].

In contrast to the aforementioned approaches, which translate tolerance zones into variational part models or abstract mathematical deviation representations and use them for the displacement accumulation, the following methods aim at representing tolerance zones as subsets in the space of the **Small Displacement Torsor** (SDT) [BC76, BMLB96]. Based on the assumptions of small rotations, it describes the displacement of a geometrical element by a translation vector and a linearised rotation matrix written as a three-element rotation vector [BC76, BMLB96]. Thus, the SDT $\boldsymbol{\tau}$ is given as $\boldsymbol{\tau} = \langle \boldsymbol{t} \quad \boldsymbol{\omega} \rangle$ with $\boldsymbol{t}, \boldsymbol{\omega} \in \mathbb{R}^{3\times 1}$. By doing so, the displacement Δp of a point p is expressed as:

$$\Delta p = \boldsymbol{t} + \boldsymbol{\omega} \times p \tag{2.10}$$

where $\boldsymbol{t}$ is the vector of translations, i. e. $t = \left[t_x \; t_y \; t_z\right]$, and $\boldsymbol{\omega}$ is the vector of rotations, i. e. $\boldsymbol{\omega} = [\alpha \; \beta \; \gamma]$. Hence, the SDT can be used to express the displacement of each part in an assembly, leading to the *part SDT*, the displacement of points on a toleranced feature compared to a substitute surface, leading to the *deviation SDT*, and the relative displacement between two parts, leading to the *gap SDT* [BMLB96]. As the allowable displacements of each point on a toleranced feature are constrained by the respective tolerance zone(s), inequations between the entries of the deviation SDT and the respective tolerances can be formulated, which leads to the concept of **deviation domains** as subsets in the SDT space representing respective tolerance zones (this concept is also linked to the configuration space) [GSP07]. These constraints and consequently the boundaries of the deviation domains are in general not linear [HTB15]. However, there are approaches to express the deviation domains by **polytopes** and thus to replace the non-linear constraints by sets of linear constraints [GSP07, HTB15]. The tolerance analysis employing the SDT concept is performed by propagating the different SDTs, the deviation domains, or polytopes using set operations, such as Minkowski sums and intersections, to obtain the possible deviations of a feature or point of interest [TD11, LZLH14, HTB15]. **Tolerance-Maps**® (T-Maps®) are based on a similar concept, though areal coordinates are used as the multidimensional parameter space for the expression of deviations [DMS02, GSP07, ASG11]. In this regard, a T-Map® "is a hypothetical Euclidean point-space, the size and shape of which reflects all variational possibilities for a target feature" [ASG11]. The tolerance analysis is then also performed using Minkowski sums to accumulate the tolerance zones, which have been expressed as individual T-Maps® [ASG11].

A further tolerance analysis approach is the **Jacobian** method, which models the effects of small variations of toleranced functional elements (FE) on a key characteristic by Jacobian computations [LL99a]. In this regard, the nominal spatial relationships between pairs of functional elements (internal and kinematic pairs) are expressed as matrix transforms, which are used to build the tolerance chain [LL99a, MP11b]. Small translational and rotational variations of an internal FE are then propagated employing the Jacobian matrix associated with the respective FE, which is computed from the tolerance chain [LL99a]. However, further details can e. g. be found in [LY98a, LL99a, LL99b, MP11b, Pol11, BYWC13].

The **Jacobian-Torsor** model combines the benefits of the SDT for the tolerance representation and the advantages of the Jacobian matrix for the tolerance propagation [CJLL15a]. More information about this model can be found in [LGD02, Des07, GLD07, GLD10, Ghi10, CJLL15b, CJLL15a].

Beside this, the **analysis line** method has been proposed by Anselmetti [Ans06] with some similarity to an approach presented by Salomons [SPH+96, SHP+96]. It is “based on transfer relations that have been established for ten classical junctions” [PA15]. These linear transfer relations are used to calculate the influences of the feature defects at certain *analysis points* on the key characteristic along defined *analysis directions*. Further details are given in [SPH+96, SHP+96, Ans06, CA09, ACYA10, Ans10, PA15].

Furthermore, the tolerance analysis based on the formulation of **constraints** (compatibility equations and interface constraints) and the subsequent **solving** of assembly or functional objective functions considering the set of constraints employing numerical optimization algorithms has been applied [SRW99, DMBM05, DQ09, FGP10, QDS+12]. In this context, particularly approaches, which integrate the quantifier notion ($\exists$: “there exists”, $\forall$: “for all”) in the mathematical formulation of the tolerance analysis problem and employ Quantified Constraint Satisfaction Problem solvers and Monte-Carlo simulation for its solution, have been proposed recently in [DMBM05, DQ09, QDS+12, BGDD13].

Tolerance Analysis Software Nowadays, computer-aided design (CAD) tools allow the solid modelling of the nominal product geometry and the model-based definition of geometrical tolerances by annotating geometrical specifications on the two-dimensional engineering drawing as well as on the three-dimensional[49] solid part model [QRP+10], but though they provide basic functionalities for the analysis of dimensional variations on key characteristics, they are not capable of performing three-dimensional tolerance analysis. Hence, in order to allow this, various computer-aided *tolerancing* tools have been proposed during the last decades, which ground on the aforementioned tolerance analysis approaches and are widely used in industry. In this context, an overview of some of these tools is given in Table 2.5 and reviews of the most common tolerance analysis software tools can e. g. be found in [Tur93, PG02, SvHK98, SASD05, Sto10]. Beside the tolerance analysis, some of these tools offer additional functionalities, such as a GD&T check, which assists and supports the user in the tolerance specification by checking the consistency of the entered tolerancing scheme (see for example the “GD&T Advisor” by Sigmetrix, LLC).

Regarding the underlying mathematical models, most of the proprietary tools use parametric tolerance analysis methods, whereas some tools perform spreadsheet analysis of tolerance

[49] Annotations on the three-dimensional solid model have also been discussed as a means for the communication of the design intent in [CCJC14].

Table 2.5: Overview of common commercial Tolerance Analysis Software Tools

Name	Software Vendor	Tolerance Representation
Variation Analysis®	Siemens PLM Software, Inc.	Parametric
	Formerly VSA®; Application: [WG98]	
Tecnomatix em-TolMate®	Siemens PLM Software, Inc.	Parametric
	Further Info: moved to Variation Analysis®; Applications: [CG03, GFV12]	
CETol6σ®	Sigmetrix, LLC	Parametric
	Further Info: used formerly Vector Loop	
3DCS®	Dimensional Control Systems, Inc.	Parametric
	Application: [HLKC07]	
MecaMaster®	MECAmaster Sarl.	SDT
	Further Info: [CLR12]	
Sigmund	Varatech, Inc.	Parametric
Enventive®	Enventive Engineering, Inc.	Parametric
	Further Info: Also Functional Equations, Spreadsheet-based	
TolAnalyst™	Dassault Systèmes, SE	Parametric
RD&T®	RD&T Technology	Parametric
	Further Info: [SLC06b]	
ASU GD&T Testbed	Arizona State University	T-Maps®
	Design Automation Lab, Arizona State University, Tempe Further Info: [DMS02, ASG11, MGD13, JDLS14, RHSD14]	
PolitoCAT	I2M, Bordeaux	Polytopes (SDT)
	Institute of Mechanics and Engineering (I2M), Bordeaux; Open Source	
Tolerance Stackup Software Toolset	Advanced Dimensional Management, LLC	Tolerance Stacks
	Further Info: Spreadsheet-based	
VarTran®	Taylor Enterprises, Inc.	Tolerance Stacks
	Further Info: Also Functional Equations, Spreadsheet-based	
simTOL®	Casim GmbH & Co. KG	Tolerance Stacks

stacks, that are automatically created or have to be entered manually by the user. Though, it has to be emphasized, that in general "the models used within the systems are not clearly presented because it is very difficult to obtain information from CAT system vendors" [MB07]. Moreover, as Mathieu and Ballu highlight, "the actual solutions are very specific and are described to the users as black boxes" [MB07], which leads to the fact, that "it is very difficult to understand the models implemented and the results provided" [MB07]. Consequently, though commercial tolerance simulation software tools are widely applied in industry, "the user has a great difficulty to understand what happens when he uses commercial packages for tolerance analysis" [MB07].

Applications and Adoptions of Tolerance Analysis Approaches The various tolerance analysis methods have been applied to many applications and have also been extended to allow the consideration of different sources of geometrical deviations. In the following, some of these applications and extensions are briefly highlighted in order to provide an overview of the broadness of research directions in tolerance analysis (see also Figure 2.23).

In the past, the different tolerance analysis approaches have mainly been used for the **"tolerancing for assembly"**, i. e. analysing the effects of tolerances on clearances in assemblies or on the product assemblability, as this has been the main concern in tolerancing for

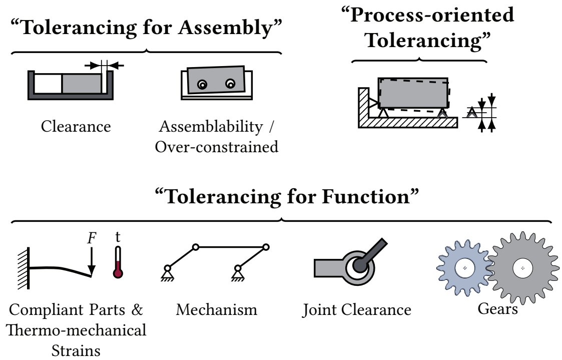

Figure 2.23: Selected Tolerance Analysis Applications and Extensions

many years [Voe98]. In this regard, a system for the tolerance analysis of mechanical assemblies based on the vector loop approach has been discussed in [CMG98] and a method for determining the fitting conditions in assemblies using a gap-space approach has been proposed in [ZM04]. Moreover, a framework for assembly tolerancing employing the SDT is highlighted in [LZZ+16] and an algorithm for the generation of assembly configurations based on the SDT and its integration in CAD has been discussed in [LTBT15]. Additionally, assemblies with interrelated dimension chains for multiple key characteristics have been the focus in [SJJ05] and particularly automotive body assemblies have been examined using variation propagation models and stability analysis in [HW92, CS95, HK97, SL02, CZC+06, CDJC06, HLB+07, HLKC07, Cai08]. Furthermore, stability analysis for assemblies without [MBKR95] and with friction [MBK96] have been performed to identify part orientations, that leave the assembly motionless under the effect of gravity. Beside this, approaches to the **assemblability** analysis have been presented in [LY95, LY98b, LY98a, San99, LFW06] and the tolerance analysis for **over-constrained** assemblies has been addressed for example in [QDS+12, BGDD13, DDG15, DGDS15, LSRC15].

These aforementioned works focus on the effects of part deviations on *assembly* requirements, which is considered as a straightforward geometrical task [Voe98] and which is justified by the assumption, that an assembly, that fits well, will also function properly. However, due to steadily increasing requirements on the quality of technical products, there exists a growing interest in considering the functional behaviour and operating conditions in computer-aided tolerancing for ensuring the product function during *use*, which is referred to as **"tolerancing for function"** [Voe98]. In this context, e. g. critical operating conditions, such as temperature and pressure, are determined for assemblies with parameter-dependent dimensions and admissible operating windows based on a tolerance stack-up are evaluated in [AS13]. Particularly, the effects of **thermo-mechanical strains**, which have been determined analytically or by finite-element analysis, on the behaviour of assemblies have been considered in [JHC02, JST11] using dimension chains, in [WSW15] by vector loops, in [PTN09b, PTN09a, PTN14] based on polytopes, and in [BA11] employing the analysis line approach. Beside this, four methods for the consideration of part deformations of **compliant parts** and the integration of elastic displacements in tolerance analysis are proposed in [SG98] based on kinematic loops, whereas compliant parts are considered in [CTBF07] based on the SDT, in [SPG07] employing elastic clearance and deviation domains, and in [VHD13] using dynamic splines. In this context, the modelling and analysis of compliant sheet metal assemblies and automotive body structures, sometimes also taking into account the place, clamp, fasten, and release (PCFR) cycle, is a constant research issue [CG97, LH97, SACS03, SLD06, FGP11, GFP15]. Moreover, the impact of geometrical deviations on the long-life fatigue of mechanical components has been investigated in [GS12] and the effects of initial fit tolerances on the residual stresses in a joint have been analysed using a finite-element analysis in [ZLT15].

Furthermore, various approaches for the tolerance analysis of **mechanism**[50] have been proposed. For example, a tolerance analysis framework for planar and spatial mechanism based on the screw theory is presented in [KSS13], a parametric tolerance analysis approach for planar mechanism is proposed in [SJ97], the force analysis method has been introduced as a means for the tolerance analysis of planar linkages in [Arm15], and the tolerance zone approach has been used for the computation of the envelope of rotating parts in [LLS07]. Based on the vector loop approach, the Direct Linearization Method has been employed for the tolerance analysis of mechanism considering position errors in kinematic linkages [WCH04] and taking into account part flexibility in [IP09]. Moreover, vector loops have been employed for the tolerance analysis of mechanism with lower kinematic pairs considering different kinds of geometrical deviations, such as manufacturing deviations, deviations caused by elastic deformations and thermal expansion, and clearance in linkages [SM09]. The approach has been extended with regard to the consideration of interactions between these deviations [WSW13] and has also been used for the tolerance-cost optimization of systems in motion [WW13]. In this regard, the consideration of **joint clearances** is a quite prominent research issue in the context of tolerance analysis for mechanism. For example, cardan joints considering tolerances have been optimized in [HC00], the effects of joint clearances in linkages and manipulators have been analysed in [TZW00], the kinematic sensitivity of linkages with joint clearances has been investigated in [TL04], a robust tolerance design considering joint clearances is performed in [HZ10], and the position accuracy in planar and spatial parallel manipulators is estimated in [FSPB11, CWL13]. Apart from this, a rich survey on multi-body systems with imperfect kinematic joints can be found in [MKI11], a comparison of clearance models for revolute joints is given in [SMM02], and a joint clearance model for the tolerance analysis is presented in [Pol14]. In contrast to that, the tolerance analysis for mechanism with higher kinematic pairs is treated in [CW09] for a cam disk mechanism based on a parametric contact analysis model and in [BDBM07, DBVB08] for bevel **gears** utilizing the combination of the vector loop approach and a numerical contact analysis approach. Additionally, the kinematic accuracy of gear mechanism is analysed in [HHZX15] and different approaches for the tolerance analysis of gears are compared in [Dan15].

In contrast to the aforementioned methods, **"process-oriented tolerancing"**, which aims at allocating tolerances to *process* variables instead of product variables, has been used to analyse the effects of fixture errors on part deviations [DJCS02, DJCS05]. In this regard, allowable

[50] The relationship between "assembly" and "mechanism" is for example studied in [DS10].

deviations of locator positions in assembly [DJCS02, CHC04, QLMW16, WCS16] and machining fixtures [DJCS00, HS03, HYS03, Asa09, ANLS13] have been derived, where also different fixture designs and maintenance strategies have been taken into account [CDJC06, ANLS13]. Most of these approaches use the stream-of-variation-analysis (SOVA) method for the variation propagation in multi-station machining and assembly processes [CHZ+04], which is based on a state-transition model [MW99], that uses a model similar to the SDT for the tolerance representation and matrix transforms for the tolerance propagation [VW86]. Beside this, also the effects of the assembly sequence on the assembly precision have been investigated considering rigid [ZQ15] as well as compliant parts [CHC03, CHM04, MTB+11, LJZ+14] and tolerance analysis by solid offsets has been used for the assembly sequencing [LWG97]. Furthermore, an integrated approach for the parallel allocation of product and process tolerances has been proposed in [LIK+08].

However, it should be noted, that the term "process-oriented tolerancing" as coined by Ding, Jin, and Ceglarek [DJCS00, DJCS02, DJCS05, CDJC06] is understood as an approach to "explicitly include process variables, such as the locator dimension and tolerance [...] in the tolerancing scheme" [DJCS02] and should be clearly differentiated from the method of assigning tolerance values according to process capabilities, which is also often translated to "process-oriented tolerancing" [Man05a, Man05b], and ongoing research projects dedicated to the integration of virtual validation activities in geometrical variations management [WSH16].

Sensitivity Analysis in the Context of Tolerance Analysis Sensitivity analysis[51] aims at studying the relationship between the different sources of uncertainty in the model input and uncertainty in the model output [SRA+08]. These relationships are most often quantified by sensitivity indices (or sensitivity measures), that express the relative importance of the model inputs to the output. In the context of tolerance analysis, sensitivity analysis is used to estimate the influences of the different tolerances in the tolerancing scheme on the key characteristic in order to improve the tolerance design [Wu97, SM09, ZW15b]. Beside this, it may also "provide insights with respect to the correctness of the analysis (i.e. analysis verification), which input uncertainties dominate the output uncertainties, and how to appropriately invest resources to reduce uncertainty in analysis results" [HO04].

In this regard, various approaches to sensitivity analysis exist, such as graphical or index-based methods, which have been classified and used for the evaluation of solution variants in conceptual design in [EME+11]. In particular, different sensitivity analysis approaches have been applied in the context of geometrical variations management and tolerance analysis, such as the arithmetical contributor analysis, the statistical contributor analysis, and the high-low-median sensitivity analysis [SM09], which are *local* methods, as well as a *global* variance-based sensitivity analysis framework [ZW15b, ZW15a]. The arithmetical contributor index for a tolerance t_i is based on the linearity coefficient ξ_i of the corresponding tolerance, which is defined as the partial derivative of the functional relationship with respect to t_i, i. e. $\xi_i = \partial f(\boldsymbol{t})/\partial t_i$, the specification limits of t_i, and the arithmetical range of the key characteristic obtained from worst-case evaluations [Man05a, Man05b]. In order to consider also the statistical distribution

[51] Sensitivity analysis is sometimes also called *contributor* analysis in the context of tolerancing [SM09].

of each tolerance, the statistical contributor index also considers the statistical tolerance range of t_i and the statistical range of the key characteristic (obtained by statistical evaluations[52]), both expressed as quantile differences [Man05a, Man05b]. In contrast to that, the high-low-median analysis employs one-at-a-time (OAT) samplings and varies each tolerance between a high and a low value while keeping all other tolerances at the median [SRA⁺08, SM09]. These local sensitivity analysis approaches are typically implemented in commercial computer-aided tolerancing packages and have been applied to the uncertainty analysis for a crank-slider and a disk cam mechanism in [GD07] and for the sensitivity analysis of parallel manipulators in [TCG14]. Their advantage is that they can be computed very efficiently and as they partially rely on linearity coefficients, their formulation is close to partial derivatives, which can be "thought of as a mathematical definition of the sensitivity" [SRA⁺08].

However, the information offered by these local sensitivity approaches is quite limited, as they are "only informative at the base point where they are computed" [SRA⁺08], which is particularly unfavourable for non-linear analysis models [SRA⁺08]. Indeed, as many commercial CAT software packages employ linearised tolerance analysis models anyway, this disadvantage has no effect on the obtained results. Nevertheless, since tolerance analysis problems are in general not linear, global sensitivity analysis approaches have been used to study tolerancing problems e. g. in [ZW15b, ZW15a], where *variance*-based sensitivity analysis methods [Sob01, SRA⁺08] have been employed. These variance-based methods ground "on a decomposition of the variance in the model output into components each depending on just one input variable, components each depending on two variables and so forth" [Pli10]. Thus, they "provide a factor-based decomposition of the output variance" [Sal02] and overcome the shortcomings of local sensitivity analysis methods. Different approaches for the estimation of variance-based sensitivity analysis indices (based on the computation of the (conditional) output variances) have been proposed, such as specific sampling methods (e. g. [KH06]), the (extended) Fourier amplitude sensitivity test ((E)FAST), random balance design, or the Sobol algorithm, which require the model to be evaluated at specific points in the input space [Pli10]. Moreover, a method for the estimation of these indices from given data has been presented in [Pli10].

However, these variance-based methods "implicitly assume that this moment [the variance] is sufficient to describe output variability" [Sal02]. Hence, current approaches to sensitivity analysis employ moment-independent sensitivity indices [Bor07, LH09], which overcome the limitations of variance-based methods and "unveil statistical dependencies that would not be captured using variance-based statistics" [PBS13]. They ground on the estimation of conditional probability densities and are therefore called *density*-based sensitivity indices, with details being described e. g. in [Bor07]. Moreover, some toolboxes for the sensitivity analysis and uncertainty quantification have been proposed recently, such as the GSAT [Can12], the SAFE [PSW15, PW15], and the UQLab toolbox [CoRUQ16]. Additionally, a review of recent developments in the context of sensitivity analysis can be found in [BP16].

[52] The statistical evaluations may be performed by analytical approaches for the convolution of input distributions (or for the estimation of moments of the output distribution) or based on the Monte-Carlo simulation [NT95].

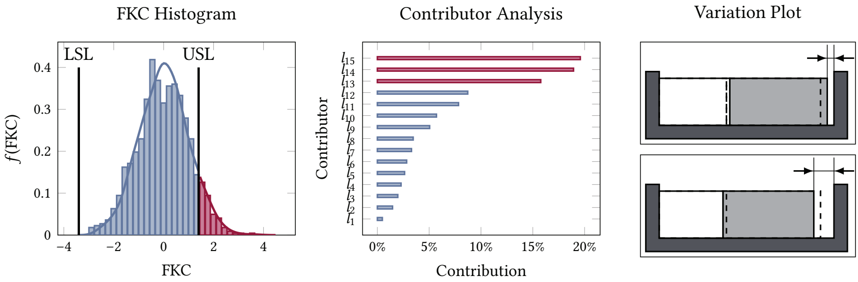

Figure 2.24: Tolerance Analysis Result Visualisation in commercial CAT packages

Visualisation in the Context of Tolerance Analysis The comprehensibility and interpretation of tolerance analysis results largely depends on their adequate visualisation. Moreover, the sound preparation and documentation of tolerance analysis results may support the reuse of knowledge in the context of tolerance engineering [KUWA14]. In this context, most commercial tolerance analysis software packages typically employ simple statistical data visualisation techniques, more particularly histograms and probability density plots, for the visualisation of population key characteristics as well as bar plots for visualising sensitivity analysis results (see Figure 2.24). Some of these tools also allow the animated visualisation of the assembly process considering part deviations. As the consideration of perceived quality and aesthetic key characteristics, such as gap and flush in car body assemblies, interior, or smart-phones, is gaining increased relevance in the automotive and consumer goods industry[53] [FS10, FKS13, QKFS13, HDS15], approaches for the visualisation of component and assembly variation have also been proposed in scientific literature for rigid [SLC06b, SSW11] and flexible parts [HCBS13], with some of these approaches having also been integrated in virtual reality environments [WS04, WS07, SMW09]. Furthermore, a method for the visualisation of part variations considering different tolerance types has been proposed in [Koc06] and a convex hull approach for the variation simulation of parts and assemblies, which is particularly applicable in early design stages, is proposed in [LSL06]. Beside this, volume visualisation methods have been investigated in [WS06, WSP07, PWW08], that aim at visualising a set of variational parts in a single scene instead of focusing on one variational part per scene.

Consideration of Form Deviations and Form Tolerances in the Tolerance Analysis
Though the aforementioned tolerance analysis approaches are based on different tolerance representation schemes and employ various mathematical methods for the tolerance propagation, they all have in common, that they inherently neglect form deviations of toleranced features. In order to overcome this shortcoming, few works aimed at considering form defects in the tolerance analysis. While some of these works focus on the consideration of form deviations employing established tolerance analysis approaches, the majority of them make use of discrete geometry representations, such as point clouds and surface meshes.

In this context, virtual transformations of single points have been introduced in the vector

[53] Gap and flush are also important issues from a functional perspective in the aircraft industry.

loop approach to consider form defects in [CGMS96]. Beside this, form deviations are considered in the tolerance analysis using deviation domains by simply cutting subdomains of the initial deviation domains according to the form tolerances in [CBA14a, CBA14b]. However, both approaches do not reflect the real assembly behaviour considering form deviations of mating features, since they do not take into account part displacements due to irregular contact points.

In contrast to that, several works focused on the consideration of form deviations in the tolerance analysis by representing deviated workpiece geometry employing point-based models, such as point clouds and surface meshes. In this regard, e. g. Samper et al. investigated the effects of form defects on two-dimensional [AFSP08, ASF10] as well as three-dimensional assemblies [SAFP09, GLS11, GLSF13] (also considering part deformations in [GLS13]). They employ the modal tolerancing approach (see section 2.2.4) for the expression of part defects and the generation of deviated workpiece representatives [SF06, FS07, SBF+10] and make use of the difference surface, which is computed by subtracting the modal coefficients of mating surfaces, for the contact determination between two features [SAFP09]. Due to this modal surface decomposition for the difference surface computation, each two mating features have to share the same discretization, which is a strong drawback in many situations. Beside this, an approach for the integration of form defects by node displacement has been presented, which employs quadratic functions for modelling the form defects and optimisation approaches for the assembly modelling [MMLS10]. With some similarity to this, the modelling of form defects is performed using morphing approaches and the assembly simulation is conducted by finite-element solvers in [FGP11]. Moreover, Stoll and Wittmann use offset functions for the generation of deviated surface mesh representations in [Sto06, SWM09, Wit11]. Furthermore, influenced by approaches of Pierce and Rosen [PR07b, PR07a], they present registration methods for simulating the position of these variant surface meshes in their assembly surrounding [SWHP07, SLMW10, SWM09, GWHK09, SWM+10a]. These approaches can be used to generate workpiece representatives with elementary form deviations and to simulate their assembly behaviour for particular assembly processes. However, they do not allow the generation of part deviations according to specified tolerances, particularly when taking into account multiply toleranced features. In addition, the proposed registration approaches require a great deal of know-how and are not applicable for arbitrary assembly processes. In addition, Wittmann et al. proposed an adapted path-planning approach for non-ideal workpieces in [WWP09] and focused on the visualization of deviated part representatives using volume visualization approaches [WS06, WSP07], while Stoll et al. also treated the visualization of gap and flush situations in virtual reality surroundings [SMW09, SSW11, Sto12]. Beside these works, approaches for the consideration of manufacturing signatures in tolerance analysis based on point clouds of deviated workpieces have been presented recently, which use decomposition methods for the identification of manufacturing errors and the generation of deviated workpiece representatives as well as registration methods for the simulation of two-dimensional mechanical assemblies [PM15b]. With some similarity to this, a method for the consideration of form errors in planar datum features has been proposed in [Arm16], which is limited to assemblies with single three-point assembly moves, and a tolerance analysis approach considering cylindrical joints also using modal decompositions and registration approaches has been presented in [HDL16]. Additionally, Zhang et al. proposed methods for the generation of deviated workpieces using second order shapes and Gaussian sampling as well as employing approaches known from statistical shape analysis [ZAMZ11, Zha11, ZAS+13], while methods for the feature-wise generation of workpiece representatives with form errors are presented in [YB16]. However, these works focus on the generation of single parts with form defects, but do not study the effects of these form defects on the assembly behaviour.

In conclusion, it can be found, that, though some works are focusing on the adaptation of established tolerance analysis approaches, particularly the application of discrete geometry representations seems promising regarding the consideration of form deviations and form tolerances in the tolerance analysis. However, in fact, current works on this issue allow to quantify the effects of form *deviations* on the assembly behaviour of simple mechanical assemblies, but they are not capable of evaluating the effects of form *tolerances* on key characteristics of more complex mechanical products. This is because these approaches lack of methods for the tolerance representation, that are conform to international tolerancing standards and allow establishing a relation between the introduced part deviations and the specified part tolerances, particularly when considering multiply toleranced features. Consequently, these works do not provide a comprehensive framework for the tolerance analysis considering form deviations. Additionally, in order to enable the prediction of the effects of form tolerances on the behaviour of complex assemblies, enhanced approaches for the relative positioning and assembly simulation of point-based models are required. Beside this, the consideration of form tolerances in the tolerance analysis of systems in motion is not sufficiently addressed yet. Thus, though there is an increased need and research interest in considering form tolerances in the tolerance analysis by employing discrete geometry representation schemes, fundamental issues are still to be investigated.

3 Identification of Need for Research

The aim of this chapter is to clearly identify the need for a comprehensive tolerance analysis theory, that is capable of holistically considering form deviations and which is conform to international standards for the geometrical product specification. In this regard, firstly a brief discussion of the state of the art is provided, before the research gap is deduced. Thereafter, the outline of the further work is briefly presented.

3.1 Discussion of the State of the Art

As it has been argued, geometrical deviations are observable on every manufactured artefact and have distinct effects on the quality and function of mechanical products. Thus, these geometrical variations have to be managed throughout the whole product life-cycle in order to control their effects on the product behaviour. As it has been shown, this requires many activities, that are nowadays performed by various departments and actors. Modern international standards for the geometrical product specification and verification offer a language for the unambiguous communication between these different actors and provide a sound scientific basis for the specification of the allowable workpiece deviations as well as for their verification based on few basic concepts and fundamental principles. These standards for the geometrical product specification are used as a toolbox during design to define the allowable geometrical workpiece boundaries by dimensional and geometrical tolerances. Since these tolerances express the required workpiece precision, they have manifold repercussions on all other stages of the product life-cycle, such as manufacturing and inspection. Consequently, the tolerance specification during design is accompanied by a high cost responsibility, as tight tolerances require cost-intensive manufacturing and measurement processes, whereas loose tolerances probably lead to increased scrap and rework as well as deteriorated product quality. Thus, in order to perform the tolerance specification activities during design efficiently, tolerance analyses are employed to predict the effects of geometrical part deviations on assembly and product characteristics. In this regard, "any tolerance allocation guidelines to be offered to designers must be based on tolerance analysis investigations" [WEE88]. Hence, tolerance analysis is "key element in industry for improving product quality and decreasing the manufacturing cost" [DGD$^+$12], since many tolerancing decisions rely on tolerance analysis results. Due to its importance, manifold tolerance analysis approaches have been proposed during the last decades, which have been applied to various problems and which have also been reviewed and compared in a considerable number of review papers [CP91, Tur93, NT95, NO98, SvHK98, HC02a, PG02, SASD05, SASD07, MP09, ASG11, MP11b, MP11a, DGD$^+$12, Pol12, BYWC13, CJLL14]. Based on these works and a critical assessment of the underlying mathematical approaches for the tolerance representation and tolerance propagation employed by the various tolerance analysis methods, it can be found, that the established tolerance analysis theories are not capable of holistically considering form deviations, imply shortcomings regarding the combination of three-dimensional tolerance zones, envelope and independency principle, material modifiers, and datum precedence, and are consequently not fully conform to the standards for

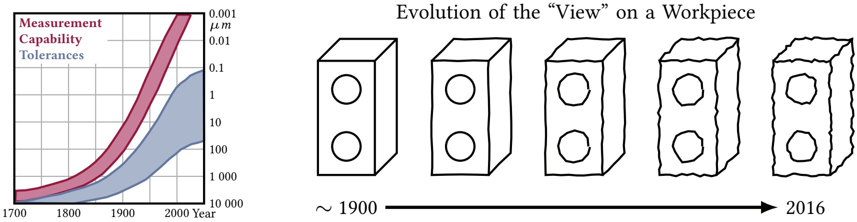

Figure 3.1: Observed geometrical Workpiece Deviations according to [Nie12]: as the Manufacturing Accuracy regarding Form Deviations increases far less than regarding Dimensional Tolerances, the relative Importance of Form Deviations increases.

the geometrical product specification. These issues also apply to commercial computer-aided tolerancing packages, since they are based on the established tolerance analysis models and "the tolerance representation and the analysis algorithms are chosen for the convenience of the developers rather than the user" [MB07]. Thus, "none of the models proposed in the literature provide a complete and clear mechanism for handling all the requirements included in the tolerancing standards, and this limitation is reflected also in the available commercial CAT software" [Pol11].

3.2 Research Gap and Scientific Challenge

In times of ever tightening requirements on the function and quality of products, particularly, the lacking consideration of form deviations by existing tolerance analysis approaches is a critical shortcoming. This is because the functionality of mechanical products is increasingly affected by form deviations of the single parts, since the manufacturing accuracy regarding form tolerances is far less affected by the progress in manufacturing technology than regarding dimensional tolerances. In this context, "it is important to realize that different tolerance attributes and different manufacturing inaccuracies have been shrinking at different rates" [Nie03], considering that "dimensional tolerances and inaccuracies have been shrinking the fastest" [Nie03], while "form, such as roundness, cylindricity, and flatness shrink at a much lower rate" [Nie03] (see Figure 3.1). This has led to the situation, in which form deviations, "which occur through normal machining processes, are sometimes greater than small dimensional tolerances"[54] [Hen91] and in which the general tolerances for form tolerances are already at approximately half the size of the dimensional tolerances [ISO2768-1, ISO2768-2]. Thus, the common and widespread assumption in tolerance analysis, that form deviations have only minor effects on assembly and functional requirements and could consequently be neglected, becomes more and more inappropriate with ongoing technological progress and may lead to bad tolerancing decisions with serious consequences.

Beside this, also the lacking conformance to international standards for the geometrical product specification is an important drawback of most tolerance representation schemes.

[54] These results have been obtained from 9,500 measurements from Swiss companies, in which the straightness deviation was greater than the dimensional deviation in 19%, and similar results have been obtained from measurements in Germany, Japan, and the United Kingdom [Hen91].

In this regard, the standards for the geometrical product specification are closely linked to available verification methods, i. e. measurement and inspection technologies. Whereas verification processes were predominantly based on the measurement of two-point measures by callipers and micrometers until the 1950s, coordinate measurement machines and optical inspection systems are nowadays widely spread in the industry and allow the fast collection of large measurement point sets on the workpiece surface and their processing for the verification of geometrical as well as of form tolerances at high precision. In contrast to that, the established tolerance analysis approaches employ functional relationships either between single points on the workpiece surface or between ideal substitute geometry elements. Thus, they do not respect the established practice for the verification of tolerances and the obtained tolerance analysis results consequently imply uncertainties regarding the real assembly characteristics and discrepancies between the virtual models and the observed reality. In this context, as Hong states, "a promising research direction would be the development of a 3D tolerance analysis theory that models and handles the three-dimensional geometric tolerances *per se*" [HC02a].

Moreover, as it has been shown, many departments and actors are involved in the geometrical variations management process, who employ various tools for the prediction of physical effects, such as manufacturing errors, part deformations, or thermal expansion. In this regard, for example manufacturing process simulations are widely used to obtain information about the expected part deviations and finite element methods are frequently employed for the structural analysis and the calculation of thermo-mechanical strains. In order to reduce analysis uncertainties, there exist a "continuing need to resolve differences between these different modelling and analysis techniques" [Wil03]. However, due to the limitations of the underlying tolerance representation approaches, existing tolerance analysis methods hardly allow the complete integration of results obtained by the different computer-aided engineering tools. Consequently, they do not provide a holistic image of the product behaviour considering the influences of various physical phenomena.

In order to overcome these illustrated shortcomings (see Figure 3.2), a novel approach to the modelling of geometrical deviations is required, which enables the virtual consideration of all different kinds of geometrical defects in geometrical variations management. Moreover, a paradigm shift for the tolerance analysis is necessary to allow the realistic prediction of the effects of geometrical specifications and part defects on the key characteristics of mechanical products.

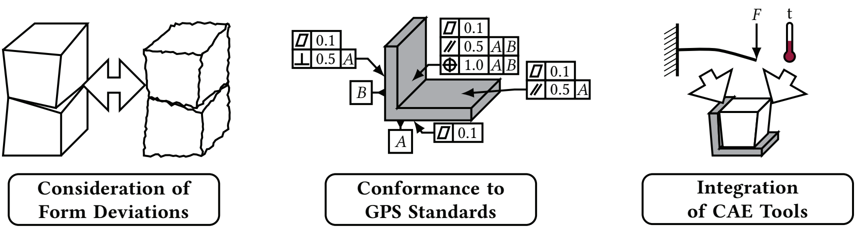

Figure 3.2: Main Limitations of established Tolerance Analysis Approaches

3.3 Further Outline of the Work

As a response to the highlighted issues, the concept of Skin Model Shapes as a novel paradigm for the modelling of geometrical deviations in mechanical engineering is introduced and a tolerance analysis approach based on this concept is highlighted in the following. In this regard, the subsequent chapters are organised as follows (see Figure 3.3). In chapter 4, the concept of Skin Model Shapes is conceptualised, approaches for its representation and visualisation are illustrated, a framework for the generation of Skin Model Shapes is provided, and possible applications and perspectives in mechanical engineering are carved out. Thereafter, a comprehensive framework for the tolerance analysis based on Skin Model Shapes is introduced and the necessary computational algorithms are detailed in chapter 5. In chapter 6, the prototype implementation of a tolerance analysis tool based on Skin Model Shapes, which grounds on the proposed framework and the required algorithms, is illustrated. After that, in chapter 7, the Skin Model Shape based tolerance analysis approach is applied to various study cases and the obtained results are compared to theoretical values as well as to results obtained from established tolerance analysis methods and they are critically discussed. Finally, a conclusion is given and perspectives for future research are presented in chapter 8.

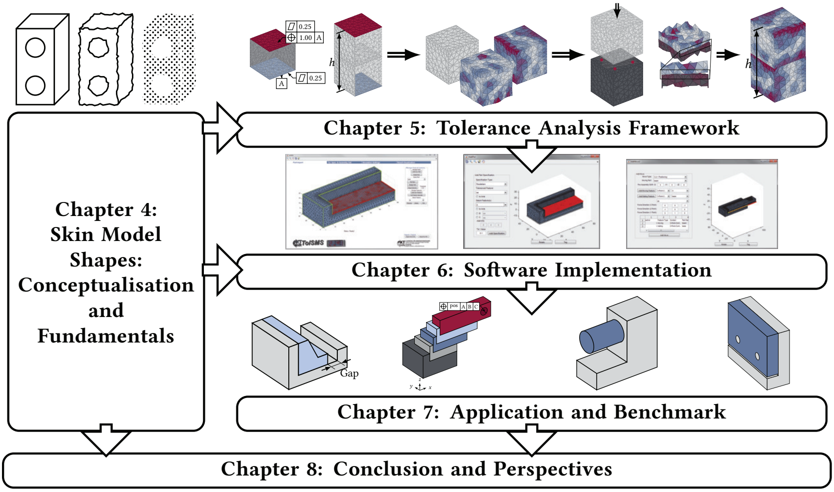

Figure 3.3: Further Outline of the Work

4 The Concept of Skin Model Shapes as a new Paradigm for the Modelling of Geometrical Variations

The aim of this chapter is to provide a fundamental understanding of the concept of Skin Model Shapes as a novel paradigm for the virtual modelling and representation of geometrical variations throughout the product life-cycle. In this regard, firstly, the idea behind Skin Model Shapes is conceptualised, before approaches for the virtual representation, the visualisation, and the generation of Skin Model Shapes are discussed. After that, applications for the concept of Skin Model Shapes in geometrical variations management and mechanical engineering are illustrated.

4.1 Motivation and Model Conceptualisation

Many tasks in product design, manufacturing, and inspection have to be performed in order to manage and control geometrical variations and their consequences on the product quality. Thus, a coherent and univocal language for geometrical specifications is required, which enables the unambiguous communication between the various actors and thereby ensures a coherent and complete tolerancing process [MB07]. GeoSpelling, as proposed by Mathieu and Ballu [MB03] and adopted by the standards for the geometrical product specification [ISO17450-1], is a response to these needs. It is based on few basic concepts [BDM10] and offers a clear definition of a geometrical specification (see Figure 2.8): "A specification is a condition on a characteristic" [BMD03], with the characteristic being defined from one or between more geometrical features [BDM10, ISO17450-1].

Various operations such as partition, extraction, filtration, association, collection and construction are required to obtain these ideal or non-ideal geometrical features [ISO17450-1]. These operations are also described and defined in GeoSpelling [BDM10] and may be applied to the nominal model as well as to the non-ideal surface model. This non-ideal surface model (**Skin Model**) comprises the deviations brought in by manufacturing and assembly processes [BDM10] and is defined as a "model of the physical interface of the workpiece with its environment" [ISO17450-1].

However, there exist different viewpoints on the Skin Model. On the one hand, coming from the workpiece itself, the Skin Model is a model of the physical workpiece surface. Therefore, there is a clear distinction between the workpiece surface in the physical world and its model in the abstract world. On the other hand, coming from the engineering design perspective, the Skin Model is a model of the physical workpiece surface in contrast to the nominal model which is a "simple" model of the intended workpiece not taking into account inevitable geometrical deviations. From a technical view, the Skin Model is an infinite model and does not allow its identification or simulation since the theoretical workpiece surface comprises an infinite number of points [CBP12]. In this regard, the infinite description is required to be able to consider all kinds of geometrical deviations from a macro to a nano scale and to capture these different variations. It is not possible to clearly define geometrical specifications and to

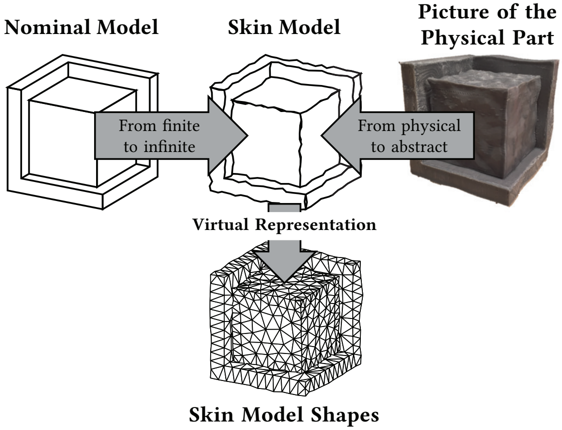

Figure 4.1: Differentiation between the Nominal Model, the Skin Model, the physical Part, and the Concept of Skin Model Shapes

enable an unambiguous product development process at a conceptual level without the infinite description. However, a finite description has to be available in order to compute and to process the Skin Model [ABM13]. This leads to the idea of Skin Model Shapes, which are particular finite Skin Model representatives comprising a finite number of geometry parameters or points. Thus, a Skin Model Shape is a specific finite Skin Model outcome and comprises deviations from manufacturing and assembly. Due to the random nature of geometrical deviations, there may exist an infinite number of possible Skin Model Shapes. If these Skin Model Shapes are sufficiently precise, then all relevant kinds of geometrical variations can be captured. Figure 4.1 shows the Skin Model Concept from these different perspectives.

At a conceptual level, Skin Model Shapes are not related to a specific geometry representation scheme, such as discrete or parametric. Furthermore, they allow the consideration of geometrical deviations at different scales from macro to nano. Therefore, the concept of Skin Model Shapes allows a holistic and persistent geometrical variations management process, in contrast to other established variation modelling and tolerance representation models (see Figure 4.2).

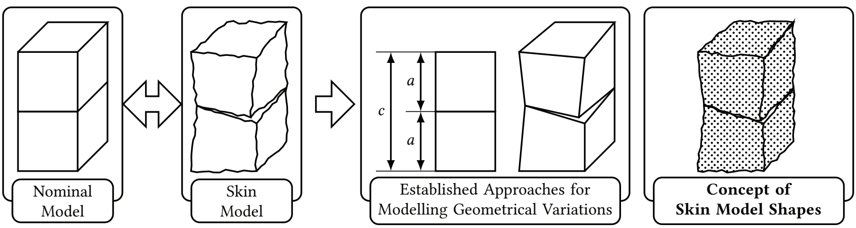

Figure 4.2: Established digital Representations of physical Artefacts for Variations Modelling and Computer-Aided Tolerancing

In synthesis, the Skin Model is a conceptual tool useful for all actors involved in engineering design, manufacturing, and inspection to imagine the allowable deviations of a part's shape with respect to geometrical specifications. However, since the Skin Model itself is an infinite model, an operationalisation is required to obtain a finite model ready for simulation [ABM13]. Therefore, particular Skin Model Shapes are generated, which represent the Skin Model and allow the assessment of the effects of part deviations on product characteristics. The geometry representation scheme and shape modelling as well as the procedure for obtaining these Skin Model Shapes is explained in the following sections.

4.2 Representation and Visualisation of Skin Model Shapes

Skin Model Shape Representation Modern computer-aided simulation tools in engineering applications are highly based on the representation of physical objects and solid modelling [Req80, RV83]. Common representation schemes for three-dimensional models are wire frames, surface models, volume models, and cell models [VWB+09]. Discrete geometry representation schemes such as point clouds and surface meshes can be understood as surface models. These discrete geometry representations allow an integrated computer-aided geometrical variations management process, since they are available throughout the product life-cycle from design, where they can be obtained from the CAD model by tessellation techniques, to manufacturing, inspection, and reverse engineering, where they are gathered from tactile or optical measurement systems [ASMW14]. Furthermore, surface models comprising discrete geometry elements, such as triangles and points, enjoy increasing attention in the computer graphics and the CAD community [AS05]. Though point clouds only approximate the surface of the object, the level of approximation can be adjusted by the point density. Moreover, a surface mesh of the object can be created from a point cloud by triangulation approaches, such as the well-known Delaunay triangulation method [Kle05]. This offers possibilities to approximate the surface of the object for visualization and further processing. Moreover, other surface models can be processed from the point cloud through surface reconstruction methods.

Due to their broad availability throughout the product life-cycle and their simple and efficient exchange and conversion to various computer-aided engineering tools, the representation of the concept of Skin Model Shapes is implemented by discrete geometry representations, such as point clouds and, based thereon, surface meshes. Thus, in the following, a Skin Model Shape $\boldsymbol{X}$ is represented as a point cloud consisting of N points x_i with $i = 1, \ldots, N$ in $\mathbb{R}^3$ (i. e. $\boldsymbol{X} \in \mathbb{R}^{N \times 3}$), where the corresponding point cloud of the nominal part is denoted by $\boldsymbol{X}_{\text{nom}} \in \mathbb{R}^{N \times 3}$.

Moreover, particular features of the Skin Model Shape are denoted by $\boldsymbol{X}^{\text{f}} \subset \boldsymbol{X}$, consist of M points $x_i^{\text{f}}, i = 1, \ldots, M$ (with $M \ll N$), and are obtained from the Skin Model Shape by GeoSpelling partition operations [DBM08, ISO17450-1, ISO17450-2] (see Figure 4.3), which may be implemented by geometrical segmentation techniques [LDB05, LX08, ZAB13, DD15]. In analogy, the nominal features are defined as $\boldsymbol{X}^{\text{f}}_{\text{nom}}$. Furthermore, the center $\hat{x}$ of a Skin Model Shape is defined as $\hat{x} = 0.5 \cdot (\max \boldsymbol{X} + \min \boldsymbol{X})$ and the center of a feature is defined in analogy as $\hat{x}^{\text{f}}$.

Moreover, the vertex normal of each specific point x_i in the Skin Model Shape is denoted by n_i and the vertex normals of the points in the nominal model are denoted by $n_{\text{nom},i}$. These vertex normals of the points in a point cloud or a surface mesh may be estimated from the point set using various approaches [HXMP05, Zha10, Zha11], but, however, in the following, the surface mesh representation is used to estimate the vertex normals as “the average of the normals to each polygon [triangles] associated with this particular vertex” [Gou71] (see Figure 4.4).

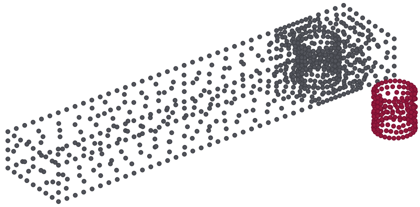

Figure 4.3: Partition of a Skin Model Shape (Beam, gray) and resulting Feature of the Skin Model Shape (Cylinder, red)

Skin Model Shape Visualization Skin Model Shapes are Skin Model representatives, which comprise various kinds of geometrical deviations. However, in order to extract valuable information from these Skin Model Shapes in engineering design, visualization techniques have to be employed, which illustrate geometrical deviations and make them visible.

Coming from a point-based geometry representation, a straightforward idea for the visualization of geometrical deviations of Skin Model Shapes is to determine the distances between the points of the nominal model and the Skin Model Shape, which are then mapped to a color scale. Furthermore, projected distances between the nominal model and the Skin Model Shape may be used according to defined spatial directions, for example the direction of the vertex normals. For this purpose, the point distances between the nominal model and the Skin Model Shape are only computed in the local vertex normal direction. These local vertex normals can also be used to determine a deviation volume, which is composed by the vertex normals of the nominal model and those of the Skin Model Shape. Indeed, this approach should not be confused with other volume visualization methods, which are e. g. based on a voxelization [WSP07].

The aforementioned visualization approaches build on a point-based representation of Skin Model Shapes. However, mesh-based representations are common in many engineering applications. In order to visualize geometrical deviations employing such representations, a suit-

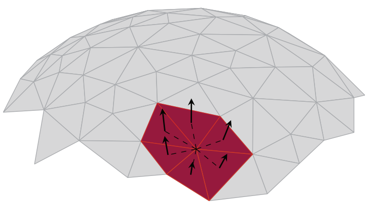

(a) Normals of adjacent Triangles

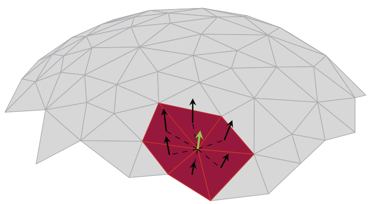

(b) Vertex Normal as the Average of the Triangle Normals

Figure 4.4: Vertex Normal Estimation by Averaging the Normals of each adjacent Triangle

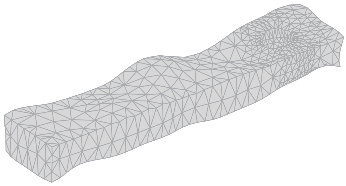

(a) Beam with exaggerated geometrical Deviations

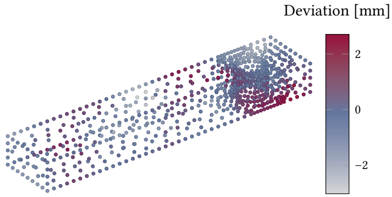

(b) Vertex Normal Projection of Point Distances

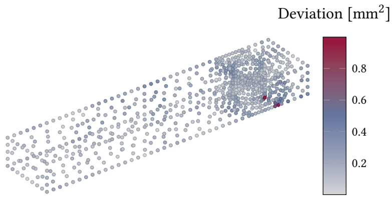

(c) Deviation Volume Visualization

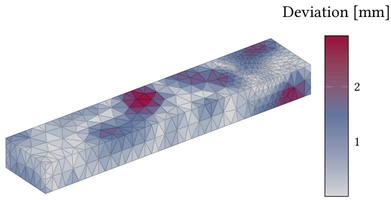

(d) Mesh-based Visualization

Figure 4.5: Visualization techniques for Skin Model Shapes

able approach is the computation of the distances between the center of gravity of the mesh elements (triangles or polygons) of the nominal model and the Skin Model Shape. These center of gravity distances are then also mapped to a color scale and the mesh elements are filled according to these colours. Figure 4.5 shows an identical Skin Model Shape of a beam where the geometrical deviations are visualized by a vertex normal technique, by a deviation volume approach, and a mesh-based visualization.

4.3 Generation of Skin Model Shapes

The concept of Skin Model Shapes is a novel paradigm for the modelling of geometrical deviations throughout the geometrical variations management process employing point-based models. However, in order to fully exploit the benefits of this innovative concept, versatile approaches for the generation of such virtual part representatives are required. Thus, a general framework for the generation of Skin Model Shapes, which comprises two different strategies, is highlighted in the following. However, before this framework is detailed, some related works are briefly reviewed in order to provide an adequate background.

4.3.1 Related Work

The Skin Model is a surface model, which comprises the geometrical deviations of manufactured parts. These geometrical imperfections of surfaces can be roughly classified into lay, waviness, and roughness (see Figure 2.1) [DIN4760, Wec14]. These classes of geometrical deviations differ in terms of the relationship between distance and depth of the imperfections [DIN4760, Wec14], though this classification is not disjunct.

The described geometrical deviations can furthermore be distinguished between systematic and random deviations [HSB+99, SHB+02, DFO03, DD04]. This classification is based on the experience, that in many manufacturing processes, similar geometrical deviations can be observed on every part whereas some geometrical deviations can be observed only on a few workpieces. The systematic deviations are deterministic, predictable, and reproducible [Zha11] and may be depending on the manufacturing process, such as products of clamping errors or the machine dynamical behaviour. In contrast to that, random deviations arise from fluctuations of the production process such as tool wear, varying material properties, or fluctuations in environmental parameters.

Due to these different characteristics, systematic and random geometrical deviations should be modelled employing different methods even if they can be classified as the same kind of geometrical deviation (e. g. lay or waviness). Therefore, various mathematical approaches for generating and reproducing observable geometrical deviations have been proposed (see Figure 4.6), which can be roughly distinguished as mesh morphing methods and decomposition approaches. The mesh morphing methods use deformations of nominal surface models to generate form deviations and surface errors [FGP11]. These deformations may be based on mere geometrical considerations or may follow physical laws, such as elastic deformations or spring-mass systems. In this regard, some approaches employ basic functionalities of parametric computer-aided design (CAD) systems [GT93b, LTBT15], Bézier curves, Splines and NURBS [SWM10b], or generate systematic deviations by second order shapes [ZAMZ11, ZAS+13]. For the generation and modelling of random geometrical deviations, sampling methods based on autoregressive stochastic processes [DD04], the Gibbs sampling [ZAMZ11, ZAS+13], or random fields have been employed [CGC07, Buc09, SWW+12, SW13a]. Furthermore, the concept of fractals is often considered for describing the roughness of surfaces [Li10, SBD11], which, however, plays only a minor role in most tolerancing considerations. Regarding the deformation of nominal models based on physical phenomena, mesh deformation and morphing methods have been developed for non-rigid part tolerance analysis using free form deformation approaches [FGP11] and FEA methods [LH97, CS97]. In contrast to the mesh morphing approaches, decomposition methods use signal processing theories and spectral methods, such as Direct Cosine Transfom, Discrete Fourier Transform, and Discrete Modal Decomposition to represent form deviations and errors as the respective variation modes [Tau95, HC02b, SF06, FS07, VL08, HLC+14].

Beside these two classes of approaches for modelling geometrical deviations, variability analysis and reduction techniques such as the Principal Component Analysis (PCA) have been used to establish descriptive models and to express and generate surface errors and form deviations [HW92, CHM04, CP07, LLAS13]. In this regard, Statistical Shape Analysis (SSA) techniques have been used to represent different kinds of geometrical deviations from observations and measurements of manufacturing processes and simulations [MCHR10, dC11].

These approaches for shape and deviation modelling can be applied to a single part feature or to a group of part features. Furthermore, after the approaches for deviation modelling have been applied to all relevant part features, Skin Model Shapes can be obtained by collecting these features. By employing this procedure to several workpieces, also whole assembly

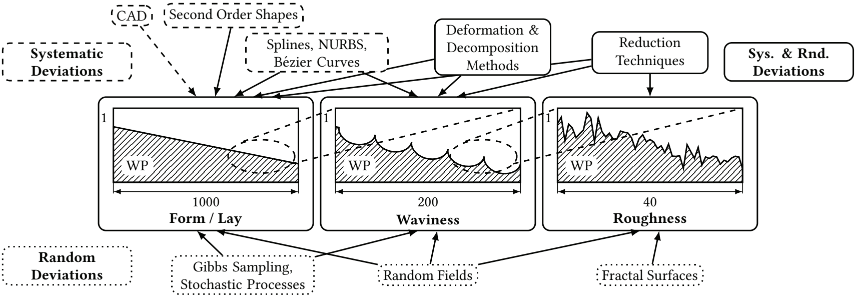

Figure 4.6: Overview of Methods for the Modelling of Geometrical Surface Errors and Form Deviations

groups can be modelled. In this regard, the scalability is an important property of Skin Model Shapes. Different shape and deviation modelling approaches can be applied to the whole Skin Model Shape or just to local features. In this manner, various kinds of geometrical deviations can be captured. However, depending on the shape or deviation modelling approach, points on the edges have to be smoothed in order to limit their deviations when collecting the independently modelled features. For this purpose, for example Laplacian Smoothing can be employed [OBB01].

4.3.2 Overall Framework

As mentioned above, the operationalisation of the Skin Model concept by Skin Model Shapes employing a discrete geometry representation is highly based on the generation of realistic representatives of the workpieces considering observable geometrical deviations. These generated Skin Model Shapes can then be used in various engineering simulations, such as assembly analysis or tolerance simulations, for predicting the later product behaviour. Hence, approaches for the generation of Skin Model Shapes should incorporate all available information about the actual shape and dimensions as well as the expectable geometrical deviations of the workpiece. Thus, it is appropriate to split the process of generating Skin Model Shapes in two phases depending on the current status in product development and to develop a Skin Model Shape simulation approach for each of these two stages:

- In early stages of product design, geometrical deviations of the relevant parts and their features are not yet observed. Therefore, assumptions on systematic and random deviations need to be considered for predicting Skin Model Shapes. Consequently, this stage is referred to as the **prediction stage**.
- During later design stages, manufacturing process simulations and even physical part prototypes are available. Thus, these observations should be taken into account and possible outcomes of the production process based on few sample parts should be simulated. This stage is hence referred to as the **observation stage**.

The required information for both Skin Model Shape generation approaches during the prediction and the observation stage can be seen from Figure 4.7.

4.3.3 Skin Model Shape Generation in the Prediction Stage

In general, the generation of Skin Model Shapes in early design stages builds up on the nominal model (e. g. modelled in solid modellers and CAD systems) and is based on the deviation of each point in the nominal model along the direction of the corresponding vertex normal in order to avoid shape discontinuities. The nominal model is firstly enhanced with information about the systematic deviations, which are likely to occur as a consequence of a certain manufacturing processes. Following that, random deviations are added to the Skin Model Shapes. The highlighted shape modelling techniques from subsection 4.3.1 are employed for modelling both systematic and random deviations. The Skin Model Shape generation approach in the prediction stage is illustrated in Figure 4.8.

In this regard, similarities and differences between the Skin Model Shape generation approach during the prediction stage and the generation of reference data sets for acceptance and reverification tests of coordinate measurement machine software as standardized in the ASME and ISO standards [ASM00, ISO10360-6] can be observed. These standards propose the generation of reference data sets by adding form deviations to the nominal range of a reference feature using Fourier series with random parameters. Thereafter, nominal points within the nominal feature range are sampled and projected onto the deformed feature. Finally, the resulting form deviations are scaled according to reference values and Gaussian white noise is added to the sample points in order to consider scanning errors. As can be seen, similarly to the Skin Model Shape generation approach during the prediction stage, geometrical deviations are added to the nominal model even if this is performed by continuous Fourier series methods and not employing shape modelling approaches for discrete geometry representations. However, no differentiation is made between systematic deviations and random deviations, since only random deviations are considered for the acceptance and reverification tests. Furthermore, the measurement uncertainties due to scanning errors are respected by Gaussian white noise, but are not considered in the Skin Model Shape generation.

Modelling Systematic Deviations Among the highlighted approaches for modelling systematic deviations in subsection 4.3.1, quadric shapes (also depicted as quadrics or second

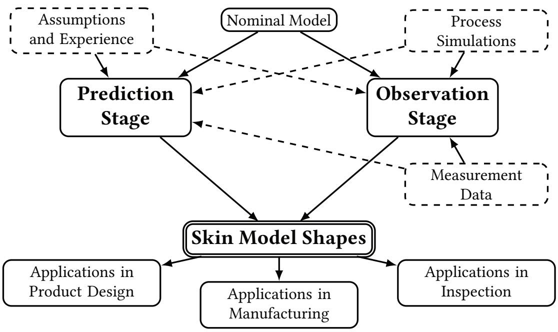

Figure 4.7: Comprehensive Framework for the Generation of Skin Model Shapes

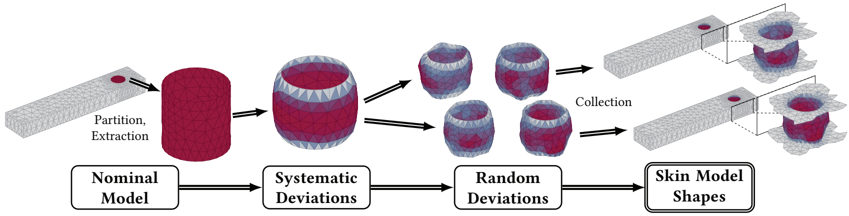

Figure 4.8: The Skin Model Shape Simulation Process in the Prediction Stage

order shapes) seem adequate. This is because most observable systematic deviations can be explained by a combination of quadric surfaces [ZAMZ11]. Second-order algebraic surfaces are described by the following general equation [Zwi11]:

$$0 = ax^2 + by^2 + cz^2 + 2fyz + 2gzx + 2hxy + 2px + 2qy + 2rz + d. \tag{4.1}$$

Beside this, also Fourier series can be used to express systematic deviations of certain manufacturing processes, which leave periodic manufacturing errors on the workpiece surface [HSB+99, Bau15]. However, the procedure of describing systematic deviations by second order shapes for the generation of Skin Model Shapes is as follows:

- Choose a second order shape, an interference of second order shapes, an adequate Fourier series, or an analytical expression, that represent the expected systematic deviations.
- Based on this expression, the systematic deviation h_i needs to be computed for every point x_i of the Skin Model Shape or a specific feature. This may be performed by reformulating the general equation for quadric surfaces or by evaluating the Fourier series or analytical expression.
- The point coordinates of the Skin Model Shape with systematic deviations $\tilde{x}_i$ are then obtained by adding the point-wise systematic deviations h_i to the nominal coordinates along the direction of the vertex normal $n_{\text{nom},i}$:

$$\tilde{x}_i = x_{\text{nom},i} + h_i \cdot n_{\text{nom},i}. \tag{4.2}$$

In order to illustrate this approach, several different systematic deviations for a plane feature and a cylindrical feature can be seen from Figure 4.9.

However, in early product design stages, the manufacturing process may not even be known or decided. In such cases, no sufficient and solid assumptions about the expected systematic deviations can be made. Thus, the step of modelling systematic geometrical deviations has to be skipped in the procedure of Skin Model Shape generation, which results in Skin Model Shapes, that only comprise random deviations, which in turn may be generated employing the following approaches.

Modelling Random Deviations Different approaches for modelling random deviations can be found in the literature, such as the 1D and the Multi-Gaussian method [ZAS+13] as

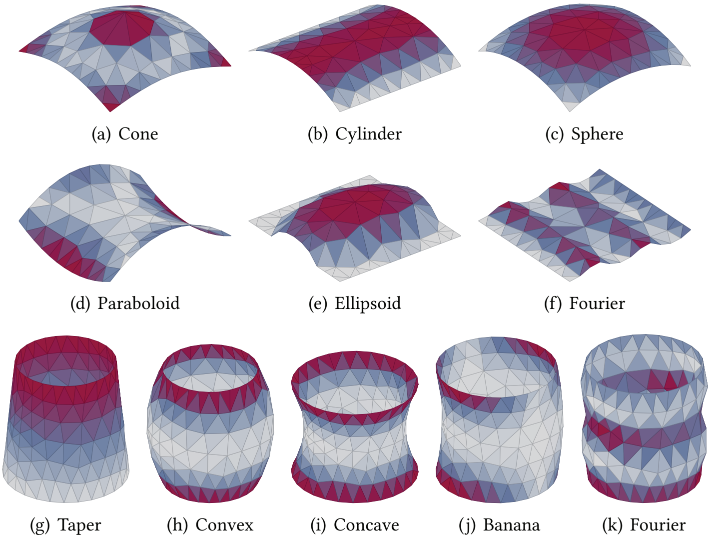

Figure 4.9: Different systematic Deviations for Planar and Cylindrical Features

well as random fields [SK00, CGC07, Buc09]. In this regard, particularly the random field theory has become increasingly popular in many research areas over the past decades [AT07, Buc09, MZ11], because it offers a framework for the expression and representation of spatial random processes. In this context, random fields are for example used in structural mechanics for the modelling of environmental loads and random geometrical deviations [Buc09]. Adler [AT07] defines a random field as follows. Given a parameter space T, a stochastic (or random) process f over T is a collection of random variables

$$\{f(t) : t \in T\}. \tag{4.3}$$

If T is a set of dimension N, and the random variables $f(t)$ are all vector valued of dimension d, then the vector valued random field f is called a (N, d) random field. Thus, a random field is a generalization of a stochastic process in this spirit, that the input variables are not unidimensional (e. g. over time) but multidimensional (e. g. point coordinates in the three-dimensional space).

Random fields can be described by their finite-dimensional distributions [AT07]. In particular, Gaussian random fields are determined by their mean $\mu(t)$ and covariance $C(s, t)$ functions and are called isotropic if their covariance function is a function of the Euclidean distance $\zeta_{s,t}$ of s and t only [AT07]. In general, the covariance function can be expressed as:

$$C(i, j) = \rho(i, j) \cdot sd(i) \cdot sd(j), \tag{4.4}$$

where $\rho(i, j)$ is the correlation function and $sd(i)$ and $sd(j)$ are the standard deviations of two points $t_i \in T$ and $t_j \in T$, respectively. Frequently used correlation functions for isotropic random fields are the exponential correlation function ($\rho^{\exp}$) and the squared exponential correlation function ($\rho^{\exp^2}$) [SK00]::

$$\rho^{\exp}(\zeta_{i,j}) = \exp\left(-\frac{\zeta_{i,j}}{l_\rho}\right); \qquad \rho^{\exp^2}(\zeta_{i,j}) = \exp\left(-\frac{\zeta_{i,j}^2}{l_\rho^2}\right). \tag{4.5}$$

The correlation length l_ρ is a characteristic parameter, that varies the impact of one random variable on the neighbouring random variables [SK00] and can be generally expressed by [Buc09]:

$$l_\rho = \frac{\int_0^\infty \zeta \cdot |\rho(\zeta)| \mathrm{d}\zeta}{\int_0^\infty |\rho(\zeta)| \mathrm{d}\zeta}. \tag{4.6}$$

Therefore, when employing Gaussian random fields, spatially correlated random variables can be generated by defining a mean function $\mu(i)$, a correlation function $\rho(\zeta_{i,j})$ with correlation length l_ρ, and standard deviations $sd(i)$ for all $t_i \in T$.

In many applications, a discretisation, i. e. a transformation of a continuous to a discrete model, of the random field has to be performed. Hence, the continuous function of the random field $f(t)$ needs to be approximated by a vector $\boldsymbol{f}(t)$ at certain discrete points in T. A straightforward approach to perform this is to employ the Cholesky decomposition of the covariance matrix to convert a set of uncorrelated random variables into a set of correlated random variables, which requires a random variable for each discrete point in T. In contrast to that, various other discretisation methods for random fields can be found, such as point discretisation methods, average discretisation methods, and the series expansion method, which exactly represents the random field as a series involving random variables and deterministic spatial functions and approximates the random field by a truncation of the series [SK00]. The series expansion method is an efficient method for the discretisation of random fields, since only a comparative small number of random variables is required. However, solving the arising eigenvalue problem can be problematic and can not be performed analytically for all autocorrelation functions. Indeed, there are approaches to convert the underlying eigenvalue problem in a matrix eigenvalue problem, in which the eigenvalues and eigenvectors of the autocorrelation matrix $\boldsymbol{\rho}$ are determined and the largest eigenvalues are used for the approximation of the random field [LK93, CGC07].

Consequently, based on the theory of random fields, the procedure for the generation of Skin Model Shapes with random geometrical deviations is based on a deviation of the points in the Skin Model Shape along the direction of their vertex normals, with the amount of deviation for the points being defined by a collection of spatially correlated random variables $\chi(t)$, $t \in T$, which are in turn defined by a spatial random process. It can be summarized as follows:

- Calculate a covariance matrix $\boldsymbol{C}$ following equation (4.4) based on an assumed correlation function ρ and correlation length l_ρ, which is a parameter that varies the impact of one random variable on its neighbouring random variables, as well as based on estimated point standard deviations $sd(i)$.

- Determine the vector of random deviations $\boldsymbol{\chi}$, where χ_i is the random deviation for a specific point in the Skin Model Shape x_i. This may either be performed by a Cholesky decomposition, i. e.:

$$\boldsymbol{\chi} = \boldsymbol{\mu} + \sqrt{\boldsymbol{C}} \cdot \boldsymbol{\psi}, \tag{4.7}$$

  where $\boldsymbol{\mu}$ is the mean vector of the random field (i. e. μ_i is the mean deviation of point x_i, which is usually assumed zero), $\boldsymbol{C}$ is the covariance matrix (i. e. the (i, j)th element of $\boldsymbol{C}$ is the covariance between the deviation of point x_i and point x_j), and $\boldsymbol{\psi}$ is a vector, which contains standard normally distributed random variables for each point in the Skin Model Shape ($\sim \mathcal{N}(\mu = 0, \sigma = 1)$), or by employing a series expansion of the random field:

$$\boldsymbol{\chi} = \boldsymbol{\mu} + \boldsymbol{A}\boldsymbol{\xi}, \tag{4.8}$$

  where $\boldsymbol{\mu}$ is again the mean vector of the random field, $\boldsymbol{A} = \boldsymbol{V}\sqrt{\boldsymbol{D}}$ with $\boldsymbol{D}$ is a diagonal matrix with the M largest eigenvalues of $\boldsymbol{C}$ on the principal diagonal and $\boldsymbol{V}$ a matrix containing the corresponding eigenvectors, and $\boldsymbol{\xi}$ is a vector of M independent Gaussian random variables.
- Add the random deviations to the model with systematic deviations along the directions of the vertex normals to obtain the point coordinates of the Skin Model Shape with systematic and random deviations $\check{x}_i$:

$$\check{x}_i = \tilde{x}_i + \chi_i \cdot n_{\mathrm{nom},i}. \tag{4.9}$$

In the following, a mean of $\mu(i) = 0$ is chosen for all points x_i in the Skin Model Shape, since the mean deviation of each point x_i is expected to be zero. Furthermore, ρ is supposed to follow the squared exponential correlation function with correlation length $l_\rho = 2\text{cm}$, and $sd(i) = 0.01\text{cm}$. Both the correlation length and the standard deviation are characteristic parameters of manufacturing processes. For the industrial application, these parameter values can be estimated from part measurements or can be chosen based on experience.

Exemplary realizations of random fields and Skin Model Shapes with random deviations with different correlation lengths are illustrated in Figure 4.10.

4.3.4 Skin Model Shape Generation in the Observation Stage

In contrast to early design stages, at least few observations of part deviations from manufacturing process simulations or even measurement data of physical part prototypes are available in later design stages. Thus, the information about such systematic and random geometrical part deviations is to be used for the generation of Skin Model Shapes. Consequently, the approach for the generation of Skin Model Shapes in such later observation stages aims at exploiting such available data.

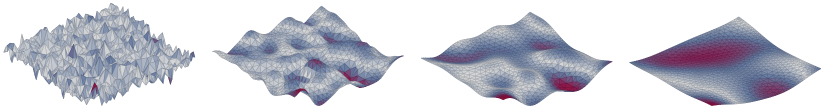

(a) $l_\rho = 1$ (b) $l_\rho = 5$ (c) $l_\rho = 10$ (d) $l_\rho = 20$

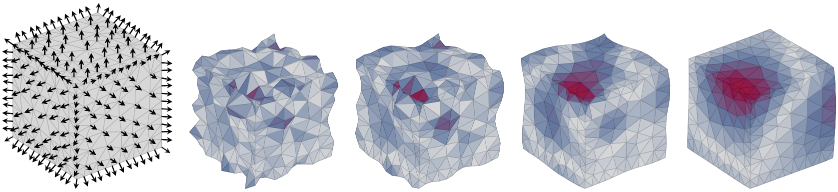

(e) Nominal Cube with Vertex Normals (f) $l_\rho = 5$ (g) $l_\rho = 10$ (h) $l_\rho = 20$ (i) $l_\rho = 50$

Figure 4.10: Illustrative Realizations of Random Fields and Skin Model Shapes with random Deviations and different Correlation Lengths

General Procedure The main idea behind the Skin Model Shape generation approach during the observation stage is to reproduce Skin Model Shapes based on a limited training set of observations gathered from manufacturing process simulations or measurement data. These observations comprise systematic and random geometrical deviations, which are likely to occur through certain manufacturing or assembly processes. For this purpose, methods of Statistical Shape Analysis (SSA) known from computer vision and image interpretation are applied, which are based on adoptions of the Point Distribution Model (PDM) [CTCG95] such as the Kernel Density Estimate/Point Distribution Model (KDE/PDM) [Mat08, MCHR10]. Generating new Skin Model Shapes by employing these approaches is based on the procedure of the Statistical Shape Analysis and comprises the following steps [SG02]:

- Acquire a training set of observations from manufacturing process simulations or measurement data.
- Determine the correspondence between the training set [DM98, CT04, NLS07].
- Align the training set and correct differences in terms of rotation, scale, and location if necessary. For this purpose, e. g. Procrustes Analysis, Generalized Procrustes Analysis, and Tangent Space Projection are suitable methods [SG02].
- Establish a Statistical Shape Model as for example the point distribution model or an extension of the PDM such as the Kernel Density Estimate/Point Distribution Model [MCHR10].
- Generate Skin Model Shapes based on the employed statistical shape model.

In this context, the basic idea behind the PDM is to express each shape $\boldsymbol{X}_i$ in the training set as a combination of the mean shape $\overline{\boldsymbol{X}}$, which can be computed easily by:

$$\overline{\boldsymbol{X}} = \frac{1}{n}\sum_{i=1}^{n}\boldsymbol{X}_i \tag{4.10}$$

and the variation of the shape around the mean shape along the main modes of variation:

$$\boldsymbol{X}_i \approx \overline{\boldsymbol{X}} + \boldsymbol{\Phi}\boldsymbol{b}_i. \tag{4.11}$$

The main modes of variation $\boldsymbol{\Phi}$ are identified by applying a Principal Component Analysis (PCA) or a non-linear extension of the PCA such as the Kernel PCA (KPCA) or approaches employing autoassiociative neural networks to the training set. The scores $\boldsymbol{b}$ can then be found as random variables, which distributions can be estimated by a multivariate Gaussian or using the kernel density estimation (KDE) [CT04, MCHR10]. Skin Model Shapes can then be generated by sampling new scores $\tilde{\boldsymbol{b}}$ from these score distributions via the inverse transform sampling. For this purpose, uniformly distributed random values in the interval $[0; 1]$ are generated and set into the inverse cumulative distribution functions (ICDFs) of the estimated score distributions. The Skin Model Shapes themselves can be obtained by transforming these random score values $\tilde{\boldsymbol{b}}$ by employing equation (4.11):

$$\tilde{\boldsymbol{X}} = \overline{\boldsymbol{X}} + \boldsymbol{\Phi}\tilde{\boldsymbol{b}}. \tag{4.12}$$

The procedure of the Skin Model Shape generation by Statistical Shape Analysis is illustrated in Figure 4.11. It should be mentioned, that this procedure also reflects systematic and random geometrical deviations of shapes, since the systematic deviations are implicitly included in the mean shape $\overline{\boldsymbol{X}}$ and the random deviations are expressed by the main modes of variation $\boldsymbol{\Phi}$. Furthermore, the representation of the training set in equation (4.11) is related to the series expansion representation of random fields. The overall procedure for the Skin Model Shape Simulation during the observation stage is illustrated in Figure 4.12.

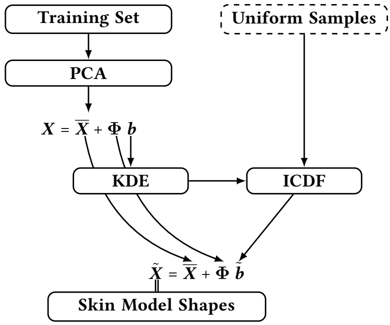

Figure 4.11: Statistical Shape Analysis for the Generation of Skin Model Shapes

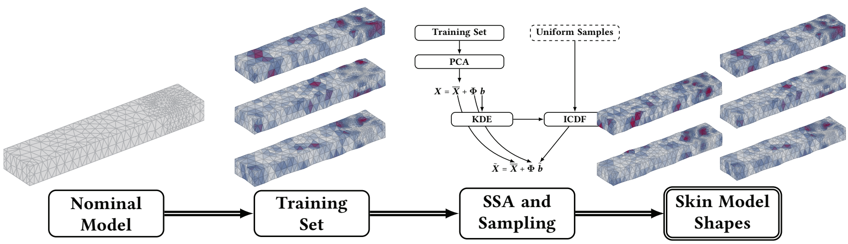

Figure 4.12: Skin Model Shape Simulation Process in the Observation Stage

Parameter Estimation for the Prediction Phase Information about the random and systematic deviations within the training set can also be extracted to help creating future Skin Model Shapes in early design stages, in which predictions and assumptions about the systematic deviations and the correlation structure of the random deviations have to be made. In this regard, the systematic deviations can be approximated by fitting quadratic surfaces to the mean shape $\overline{\boldsymbol{X}}$ employing various approaches, such as least squares fitting [YWLY12] or type-specific fitting methods [AS14]. With respect to random deviations, several parameters have to be identified, such as the correlation length l_ρ, the mean μ and the standard deviation σ of the random field. These parameters can also be identified by different approaches for the fitting of random fields to spatial data, such as presented in [RT02, CV08].

Required Sample Shapes in the Training Set The results of the Skin Model Shape generation approach during the observation phase depend on the ability of the training set to reflect the variability of part deviations in the population. However, few research works deal with the question of finding an "optimal" training set size, which balances the trade-off between closeness to reality on the one hand and the costs for the training set acquisition on the other hand.

However, as mentioned earlier, in most cases the training set consists either of measurement data or manufacturing process simulation results. In the first case, it is helpful to know when the adding of new training set samples is no longer expected to increase the captured variability as every new training set sample requires additional measurement costs. In the latter case, the training set size is usually determined by an experimental design, which depends on the considered factors of the manufacturing process. Even so, the size of the used training set may be increased if it is assumed that the available training samples lead to insufficient results.

However, when performing the PCA as a part of the Skin Model Shape generation process in the observation stage, the sum of all eigenvalues of the covariance matrix is a measure for the variability comprised in the training set. For every new training shape, the growth of variability can therefore be computed. If the growth of variability is expected to lie below a certain threshold for every new training shape, then the training set seems to be adequate and no further training shape has to be added.

4.3.5 Comparison of the Approaches for the Generation of Skin Model Shapes

The highlighted approaches for the generation of non-ideal workpiece representatives employing discrete geometry representation schemes in both the prediction and the observation stage enable design teams to generate plausible Skin Model Shapes based on assumptions, manufacturing process simulations, or measurement data. However, the methods in the prediction and the observation stage differ in terms of applicability and required previous knowledge.

For the analysis of methodical similarities and differences of the introduced approaches, firstly the basic equations for both methods, (4.9) and (4.12), are given:

- The equation for the Skin Model Shape generation approach in the prediction phase is

(4.9):

$$\breve{x}_i = \underbrace{x_{\mathrm{nom},i} + h_i \cdot n_{\mathrm{nom},i}}_{\tilde{x}_i} + \chi_i \cdot n_{\mathrm{nom},i}. \tag{4.13}$$

It can be seen, that this approach adds random geometrical deviations to the nominal point coordinates with systematic deviations. These expected systematic deviations apply to every workpiece. Hence, the nominal model with systematic deviations can be referred to as a mean model $\overline{\boldsymbol{X}_i}$.

- For the generation of Skin Model Shapes in the observation phase, the basic equation is (4.12):

$$\tilde{\boldsymbol{X}}_i = \overline{\boldsymbol{X}} + \boldsymbol{\Phi}\boldsymbol{b}_i. \tag{4.14}$$

This method also adds random geometrical deviations to a mean model based on given observations. Hence, the mean model of the prediction approach $\tilde{x}_i$ should reproduce the mean model gathered from observations $\overline{\boldsymbol{X}}$.

However, the modus operandi differs in both approaches. During the prediction phase, assumptions about the expected systematic and random deviations have to be made. Furthermore, parameter values for the geometrical deviations have to be chosen. Though these deviations can be estimated from earlier observations of similar parts and workpieces, these estimates may be uncertain and hence it is not always easy to make realistic assumptions about the deviations that can be observed later during manufacturing. Thus, this approach requires good knowledge of the underlying mathematical methods, the workpiece itself, and the manufacturing processes.

In contrast to that, the procedure of the observation phase approach is straightforward. Based on the observations gathered from manufacturing process simulations or measurement data, the Skin Model Shapes can be generated without further assumptions or parameter settings. Hence, no deeper expertise or knowledge of the mathematical background of this approach is necessary. Thus, this approach may be referred to as more robust, since the obtained results do not depend on the user or the designer and their knowledge. However, the quality of the results highly depends on the training set. If the training set is gathered from a poor manufacturing process simulation or from bad measurement data, then, though the general procedure is quite robust, this approach may lead to implausible results.

Both approaches for the Skin Model Shape generation can be applied to uniformly or non-uniformly distributed shape discretisations. Even the results of the Skin Model Shape generation approach in the observation stage do not depend on the mesh density and are not adulterated by an inhomogeneous point distribution. Furthermore, the obtained Skin Model Shapes do not depend on the grid size of the nominal model or the training shapes. Thus, different restrictions on the point distribution and the grid size from engineering design, manufacturing, and inspection can be considered. For example, in virtual metrology, the obtainable results for different dimension and form deviation measurements depend on the point sampling strategy and measurement point distribution. These aspects can be considered in the prediction stage by employing adequate tessellation techniques on the nominal model and in the observation stage by following these restrictions when acquiring the training set. Therefore, both approaches for the generation of Skin Model Shapes allow a coherent geometrical variations management process.

4.4 Applications and Perspectives for Skin Model Shapes in Mechanical Engineering

Many activities in geometrical variations management are supported by computer-aided tools. To avoid uncertainties due to lacking variation integration and suboptimal data exchange between these tools, a product geometry representation is required, which is conform to a coherent and complete language for the geometrical product specification.

In this regard, the concept of Skin Model Shapes enables a versatile geometrical product representation, which considers all kinds of geometrical variations and accompanies all stages and relations in the product life-cycle, since it is based on the Skin Model as a basic concept in GeoSpelling, which serves as an univocal language for all activities in geometrical variations management. Furthermore, this concept supports the relations between all different activities related to controlling geometrical variations. Thus, in the following, main applications of the concept of Skin Model Shapes in geometrical variations management, particularly in the areas of engineering design, manufacturing, and inspection, are highlighted.

Applications in Engineering Design and Computer-Aided Tolerancing In order to ensure the product function during use, limits for geometrical deviations of workpieces and assembly groups have to be specified during product design. However, this task is not trivial and requires a lot of knowledge and experience. In this regard, the operationalisation of the Skin Model by the concept of Skin Model Shapes supports product design teams by visualizing geometrical deviations and their effects on product key characteristics. The Skin Model Shape visualisation helps to understand and to appraise possible effects of geometrical variations on the product quality, which may lead to more suitable functional requirements as well as geometrical specifications. For instance, the application of virtual and augmented reality systems in design reviews can be enhanced by considering geometrical workpiece deviations [SSW11], which facilitates the definition of functional requirements as well as geometrical specifications. Moreover, the interpretation of geometrical specifications recorded in technical drawings can be supported by software tools for the visualisation on the basis of Skin Model Shapes. This can be performed even in early design stages by feature-based Skin Model Shapes obtained from skeleton models.

Furthermore, a tolerance analysis framework based on Skin Model Shapes offers vast potentials for the realistic prediction of the effects of geometrical part deviations on product key characteristics considering the various issues in geometrical variations management. Since tolerancing decisions are highly based on tolerance analysis results, the application of a Skin Model Shape based tolerance analysis framework bears great opportunities for cost savings. Thus, a tolerance analysis theory employing the concept of Skin Model Shapes is proposed in the following.

Applications in Manufacturing and Assembly The number of rejected parts, i. e. parts out of specification, is of high interest in the context of manufacturing process design. In this regard, e. g. the process capability index c_{pk} is a valuable measure for the extent in which a process meets its specification [ISO22514-2]. The determination of the process capability index based on manufacturing process simulations or measurement data can be performed by Skin Model Shapes, that have been generated in the observation stage. For this purpose, the Skin Model Shapes can be analysed with respect to specified tolerance requirements. Based on the gathered results, manufacturing engineers can gain valuable information and insights about the effects of process parameter variations on geometrical deviations as well as about the expected process capability. Furthermore, based on the early information about the impact of manufacturing process parameter variation on geometrical deviations, the tolerance values can be revised, the manufacturing process can be optimized, and manufacturing costs can be saved.

Applications in Inspection Tight tolerance requirements lead to increasing costs not only because of cost-intensive manufacturing but also due to additional inspection routines. The optimization of measuring processes is therefore yet another trigger for costs reductions. In this regard, the concept of Skin Model Shapes supports the identification of critical workpiece features, for which the inspection should be intensified, as well as features, which are minor relevant for the product function and quality. For this purpose, the Skin Model Shapes created during the observation stage can be used to identify workpiece features with a high variability by analysing the statistics of observed geometrical deviations. Moreover, the results gained from measurements can be returned to product design to adjust the parameters for the Skin Model Shape generation in the prediction stage and to validate the tolerance analysis and other computer-aided engineering tools.

5 A comprehensive Framework for the Computer-Aided Tolerance Analysis based on Skin Model Shapes

The concept of Skin Model Shapes is a response to the shortcomings of established computer-aided models and representations of non-ideal part geometry considering inevitable geometrical deviations. It is based on the Skin Model, which is a fundamental concept of modern standards for the geometrical product specification and which can be regarded as a model of the physical interface between a part and its environment. Since the Skin Model is an infinite model in order to allow the consideration of all different kinds of geometrical deviations at an abstract level, it can neither be identified nor simulated. In contrast to that, Skin Model Shapes are specific outcomes of the Skin Model employing discrete geometry representation schemes, such as point clouds and surface meshes, which can hence serve as part representatives in simulations and virtual mock-ups. Thus, the concept of Skin Model Shapes is a novel paradigm for modelling geometrical variations throughout the product life-cycle and enables the representation of various kinds of geometrical deviations, that are inevitably introduced in manufacturing, assembly, and use. Since it enables the representation of parts and assemblies considering deviations at different levels, such as macro, micro, or nano, it can be used for many applications in the context of virtual product realisation. However, as tolerance analysis is a key tool for supporting the tolerancing activities in design, the following sections are dedicated to providing a comprehensive tolerance analysis theory based on the concept of Skin Model Shapes. In the following, the main procedure for the tolerance analysis based on Skin Model Shapes is highlighted and every stage of this procedure is detailed.

5.1 Framework for the Tolerance Analysis based on Skin Model Shapes

The general framework for the tolerance analysis based on Skin Model Shapes reflects the designers native view on the product origination process and enables the consideration of all sources of geometrical deviations. It can be divided in a pre-processing, a processing, and a post-processing stage as can be seen from Figure 5.1. In the pre-processing stage, Skin Model Shapes of single parts are generated employing the approaches highlighted in section 4.3 and they are scaled to conform to the pre-defined tolerancing scheme. The Skin Model Shapes at the part level are then processed to compute the assembly positions and the motion behaviour in the processing stage. For this purpose, approaches for the assembly simulation as well as for the contact and mobility simulation are used. Finally, in the post-processing stage, the functional key characteristics are measured from the resulting assemblies in order to perform a comparison for conformance. Moreover, the assemblies are evaluated regarding the contact quality, and the results are visualised and interpreted. Thus, the tolerance analysis procedure employing Skin Model Shapes reflects the reality in this sense that possible outcomes of the workpieces are successively generated, inspected, and assembled. Thereafter, a functional check is performed whether or not the product fulfils the requirements. By ad-

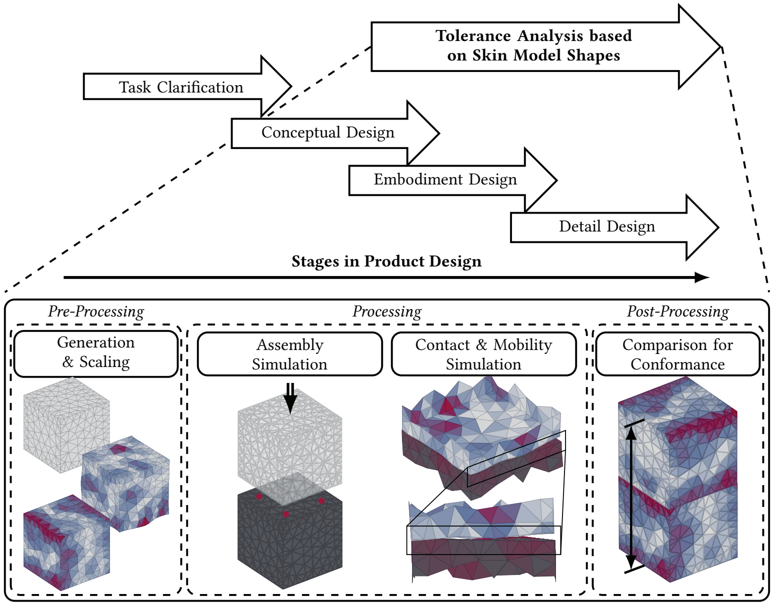

Figure 5.1: Procedure for the Tolerance Analysis based on Skin Model Shapes

justing the tolerances, the functional behaviour and the quality of the product can hence be virtually influenced.

In the following, the different steps of this general procedure are explained in detail and highlighted by applying it on a tolerance analysis case study, which has been presented by the author in [SAMW16]. The case study comprises three parts as can be seen from Figure 5.2, in which a beam is positioned on a base part according to a 3-2-1 positioning scheme (three-point move in negative z-direction, two-point move in negative x-direction, and one-point move in positive y-direction), and a pin is assembled to the beam with "best-fit" condition. The single parts are specified by different tolerances, while the functional key characteristic of the assembly is the position deviation *pos* of the pin with reference to the datum system spanned by the base part.

5.2 Scaling of Skin Model Shapes

The concept of Skin Model Shapes allows the representation of part geometry considering all different kinds of geometrical deviations. The approaches for the generation of Skin Model Shapes highlighted in section 4.3 allow the modelling and reproduction of such different kinds of part defects, with mathematical approaches for the modelling of geometrical deviations being used in early design stages, whereas results of manufacturing process simulations or measurement data from part prototypes being employed in later design stages. However, these approaches do not allow the generation of Skin Model Shapes, which fit pre-defined tolerance specifications.

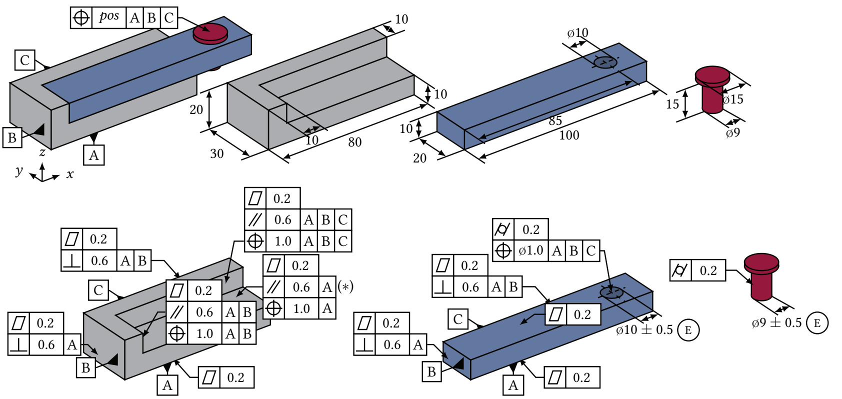

Figure 5.2: Accompanying Example for the Tolerance Analysis based on Skin Model Shapes

The aim of the following section is thus to provide a comprehensive approach for the generation of variational part representatives with pre-defined tolerance values in discrete geometry for the use in computer-aided tolerance analysis (see Figure 5.3). For this purpose, algorithms for the evaluation of geometrical tolerances are developed, which are then used for the *scaling* of discrete geometry workpiece representatives to fit user-defined tolerance specifications. These approaches have also been discussed by the author in [SW15b].

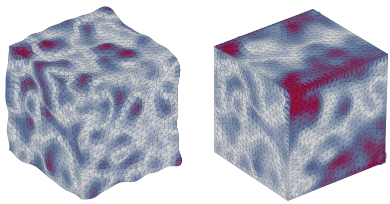

Figure 5.3: Initial Skin Model Shape (left) and Skin Model Shape after Scaling with reduced Form and introduced Orientation Defects (right)

The section is structured as follows. Firstly, a brief overview of related work regarding the tolerance verification based on algorithms for the computational metrology is provided. Thereafter, algorithms for the evaluation of geometrical tolerances from point clouds are developed, which are subsequently used for the adjustment of variational part representatives in discrete geometry to fit pre-defined tolerance specifications. Thereafter, the approaches are applied to the accompanying case study.

5.2.1 Related Work

The tolerance verification of physical workpieces is nowadays widely performed by algorithms for the computational metrology, that evaluate point sets, which have been obtained from the workpiece by optical and tactile measuring systems [BBM91]. In this regard, various works dealing with the verification of different kinds of dimensional and geometrical tolerances have been proposed, that allow the computation of minimum zone elements or the establishment of datums and datum systems by fitting operations. For example, tests for computational metrology algorithms used in coordinate measurement machines have been discussed in [Dia95], reference algorithms for Chebyshev and one-sided data fitting have been presented in [SC04], and a library of feature fitting algorithms for the tolerance verification has been presented in [MHSD15]. Furthermore, a review on mathematics for modern precision engineering is given in [SF12]. More specifically, the least-squares paradigm has been used in [YM96] for the best-fit of geometrical features and the assessment of dimensional part deviations and its role in coordinate metrology has been discussed in [SSM11]. Beside this, methods for the computation of minimum circumscribed circles [XJ14], for the identification of minimum zones for circles and cylinders [LC96], as well as for the determination of minimum zones in general [MP08] have been proposed. Furthermore, the straightness and flatness tolerance verification based on minimum zone elements has been investigated in [ZD02, Lee09, CK12], whereas the roundness evaluation has been discussed in [Gad10] based on convex hull methods, in [RABL11] based on genetic optimization algorithms, in [SZ12] using four different methods for the roundness assessment, and in [NB14] based on the small displacement screw. Moreover, Gaussian processes have been used for the form error assessment in [XDW08], form errors of spheres, cylinders, and cones have been treated in [ZJF+13], the evaluation of geometrical deviations for sculptured surfaces and other kinds of free-form surfaces have been proposed in [BEK07, PW10, FZW+13, HZS15], and the form assessment in coordinate metrology has been discussed in [FM11]. The accurate size evaluation for cylinders has furthermore been discussed in [RA10] and constraint substitute elements for the geometrical tolerance verification have been derived in [ITK97]. Moreover, the tolerance verification of orientation tolerances has been performed based on constrained optimization in [GCWL98]. Beside this, also the evaluation of geometrical deviations for sculptured surfaces [BEK07] and other kinds of free-form surfaces have been proposed [PW10, FZW+13, HZS15]. In contrast to that, approaches for the identification of systematic geometrical deviations for cylinders have been proposed in [HSB+99] and optimal point sample sets for such systematic deviations of cylinders have been derived in [SHB+02]. Additionally, systematic errors in layered manufacturing have been identified and assessed in [LLK98a, LLK98b] and methods for the identification and compensation of errors in additive manufacturing have been presented in [GFLH13]. Beside this, the geometrical error measurement and compensation for machines has been investigated in [SKH+08]. Regarding surface errors, the surface roughness has been evaluated based on fractal theory in [Li10] and a surface texture information system has been proposed in [QSJL14].

Thus, a wide variety of algorithms and approaches for the assessment of point sets regarding the verification of dimensional and geometrical tolerances has been proposed. However, none of these approaches allows the generation or scaling of deviated workpiece representatives, so that they conform to pre-defined tolerance values. Nevertheless, these algorithms serve as a basis for the development of such scaling algorithms in the following.

5.2.2 Scaling Sequence based on the Relationship between different Tolerances

Different geometrical tolerances limit different kinds of geometrical feature characteristics, such as form tolerances, which limit intrinsic characteristics (e. g. the flatness of a plane), whereas orientation tolerances and location tolerances limit situation characteristics (e. g. the parallelism or the position of a plane with reference to a datum plane) [DBM08]. In this con-

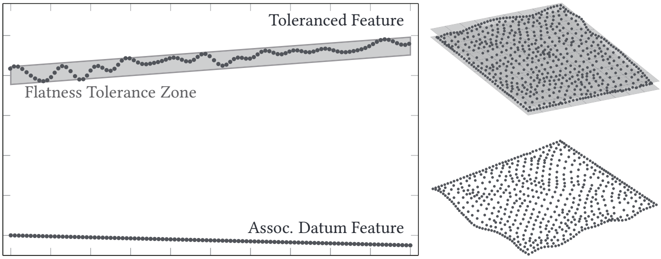

(a) The Flatness Tolerance Zone limits feature-intrinsic Characteristics

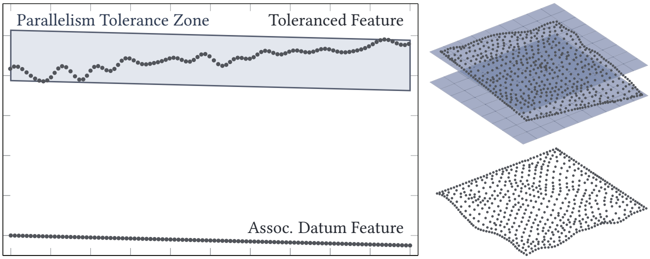

(b) The Parallelism Tolerance Zone limits situation Characteristics considering rotational Feature Defects

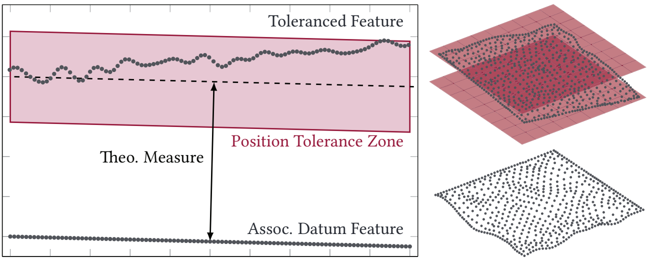

(c) The Position Tolerance Zone limits situation Characteristics considering rotational and translational Feature Defects

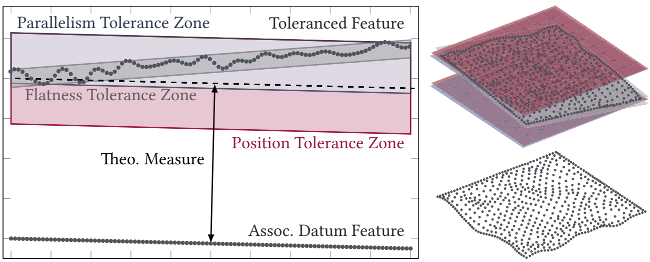

(d) All Tolerance Zones combined

Figure 5.4: Tolerance Zones implied by different Tolerance Specifications

text, the concept of tolerance zones is often used to express and to illustrate the geometrical "boundaries" for toleranced features, which are implied by certain tolerance specifications. Based on this concept, it can be seen, that form tolerances build tolerances zones, which are not limited regarding their orientation and location. In contrast to this, the tolerance zones of orientation tolerances, such as parallelism and perpendicularity, are limited regarding their orientation with reference to datum features. Location tolerance zones are furthermore limited with regard to their absolute location by datum features or datum systems in combination with theoretical measures. As a consequence, form tolerance zones are in general covered by orientation tolerance zones, which are in turn covered by location tolerance zones. Moreover, it can be found, that form tolerance zones limit only feature-intrinsic parameters, whereas orientation tolerances limit additional *rotational* feature defects and location tolerances limit intrinsic, *rotational*, and *translational* feature defects with reference to datum features. These relationships between form, orientation, and location tolerances are also covered by international standards for the geometrical product specification [ISO1101] and are illustrated in Figure 5.4. Beside this, depending on the tolerancing principle, there exist also relationships between dimensional and form tolerances, in case when the envelope requirement or material modifiers are added to dimensional tolerances.

As a consequence, these relationships are to be respected by the evaluation and scaling sequence. Thus, firstly the dimensional tolerances without envelope requirement or material modifier have to be considered, thereafter the form tolerances, then dimensional tolerances with envelope requirement or material modifier, followed by the orientation tolerances, and finally the location tolerances are evaluated and scaled. Regarding the orientation and location tolerances, additionally the datum precedence has to be considered in the scaling sequence. After the scaling, depending on the scaling methods, smoothing operations can be performed to ensure the topological continuity of the resulting (scaled) Skin Model Shapes [OBB01]. Consequently, the order of the following subsections, which cover dimensional, form, orientation, location, and run-out tolerances, takes this into account.

5.2.3 Dimensional Tolerances

5.2.3.1 Definition and Computation of Dimensional Tolerances

Dimensional tolerances or fits are specified in order to ensure, that the actual size of a feature of size or the distance between two part features is within two limiting dimensions. The need for defining limiting sizes and fits has emerged from the requirement of part interchangeability conjoined with the axiom of manufacturing imprecision [ISO14405-1]. Whereas past standards for the geometrical product specification used the envelope requirement for the definition of sizes, current standards employ two-point-sizes as the default specification criterion [ISO14405-1]. In the

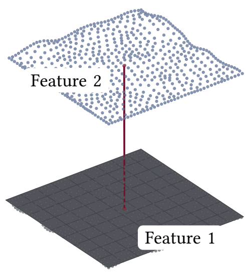

Figure 5.5: Computation of the linear size between two planar Features

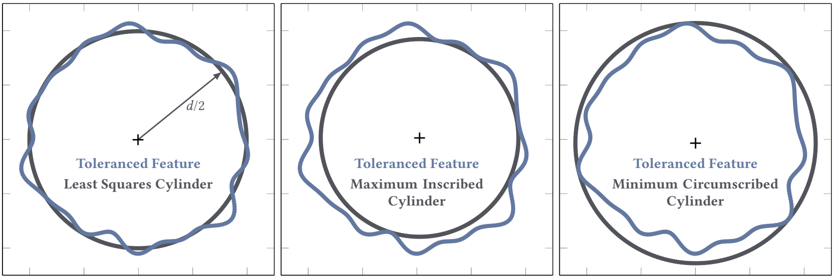

Figure 5.6: The size of a cylindrical Feature is computed as the diameter of its associated Least-Squares Cylinder (left) or the maximum inscribed (middle) or minimum circumscribed Cylinder (right) in Case of Material Modifiers.

following, the least-squares size as a global linear dimension following [ISO14405-1] is used for the computation of linear sizes. In this regard, the dimension between two planar features $d^{\mathrm{p}}_{\mathrm{dim}}$ is defined as the mean of the distances between the associated least-squares plane of one planar feature and the corresponding second planar feature in the default case, whereas one-sided fitting operations have to be employed to obtain the associated planes when the envelope requirement or material modifier are added to the dimensional tolerance specification (see Figure 5.5). Obviously, this reflects only one viewpoint on the definition of "size" [MS13b]. The size of a cylindrical feature $d^{\mathrm{c}}_{\mathrm{dim}}$ is defined as the diameter of its associated least-squares cylinder (LSC) in the default case. In contrast to that, the size of the cylindrical feature is defined as the diameter of the associated maximum inscribed (MIC) or minimum circumscribed cylinder (MCC) when the envelope requirement or material modifier are added to the dimensional tolerance. This can be seen from Figure 5.6.

5.2.3.2 Scaling of Dimensional Tolerance Specifications

In order to ensure, that two planar features of a given Skin Model Shape comply to a specified dimension, the second feature is shifted along the normal of the associated least-squares plane of the first feature until the specified dimension is reached. Regarding a cylindrical feature, the points of the initial feature are firstly mapped onto the axis of the associated least-squares cylinder (or the maximum inscribed or minimum circumscribed cylinder, respectively).

For this purpose, the radial distances d_i^r between the cylinder axis and the points are determined:

$$d_i^r = \frac{|(x_i^{\mathrm{f}} - a) \times \boldsymbol{b}|}{|\boldsymbol{b}|}, \tag{5.1}$$

where a is a point on the axis of the associated cylinder (LSC, MIC, or MCC) and $\boldsymbol{b}$ is the direction of the cylinder axis. The footpoints $\underline{x}_i$ of the feature points on the axis of the associated

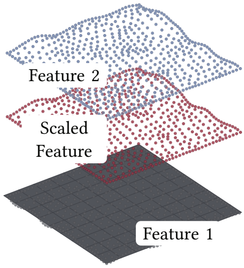

(a) Planar Features

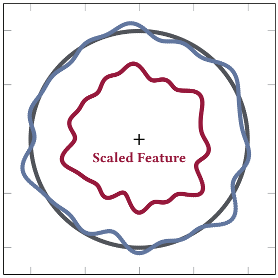

(b) Cylindrical Feature

Figure 5.7: Results of the Scaling of Dimensional Tolerances

cylinder result to:

$$\underline{x}_i^{\mathrm{f}} = a + \sqrt{\left|a - x_i^{\mathrm{f}}\right|^2 - (d_i^r)^2} \cdot \boldsymbol{b}. \tag{5.2}$$

Thereafter, the scaling is performed by weighting the initial distances between the cylinder axis and the feature points considering the specified cylinder size, with the new point coordinates $\tilde{x}^{\mathrm{f}}$ of the scaled feature $\tilde{\boldsymbol{X}}^{\mathrm{f}}$ resulting with the specified cylinder size $t_{\mathrm{dim}}^{\mathrm{spec}}$ to:

$$\tilde{x}_i^{\mathrm{f}} = \underline{x}_i^{\mathrm{f}} + \left(t_{\mathrm{dim}}^{\mathrm{spec}} + (d_i^r - r)\right) \cdot \frac{(x_i^{\mathrm{f}} - \underline{x}_i^{\mathrm{f}})}{\left|x_i^{\mathrm{f}} - \underline{x}_i^{\mathrm{f}}\right|}, \tag{5.3}$$

where r is the radius of the associated cylinder. By doing so, the cylindricity deviation of the initial cylindrical feature stays unaffected. However, the scaling for dimensional tolerances with envelope requirement or material modifier has to be performed after the form tolerance scaling, since the diameter of the MIC and MCC obviously depends on the magnitude of the form deviations. The result of the scaling procedure for the dimensions can be seen from Figure 5.7.

5.2.4 Form Tolerances

5.2.4.1 Flatness Tolerance

Definition and Computation of Flatness Tolerance Specifications The flatness tolerance limits deviations of surface planes or center planes as well as the straightness of lines on even planes [ISO1101]. The definition of the tolerance zone can be seen from Figure 5.8 and is given as follows:

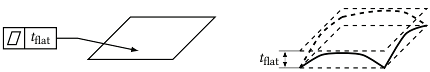

Figure 5.8: Flatness Tolerance Specification and corresponding Tolerance Zone

Definition 1– Flatness Tolerance [ISO1101]
The tolerance zone is limited by two parallel planes with distance t_{flat}. The measured surface is to lie between these two parallel planes with distance t_{flat}.

The orientation of these parallel planes has to be chosen in such a manner that their distance is at a minimum. In order to compute the flatness tolerance zone for a plane feature, the convex hull of the plane is computed [Roy95], e. g. employing the QuickHull algorithm [BDH96]. Following that, the maximum distance between the feature points and the facet are computed for each facet of the convex hull. Finally, the facet of the convex hull with the minimum greatest distance leads to the tolerance zone and the corresponding distance can be interpreted as the flatness deviation [Roy95]. This is illustrated in Figure 5.9. Thus, the flatness deviation d_{flat} can be found as:

$$d_{\text{flat}} = \min_j \left(\max_i d(x_i^{\text{f}}, f_j) \right), \text{ with } i = 1, \dots, n;\ j = 1, \dots, F, \tag{5.4}$$

where F is the number of facets of the convex hull around $\boldsymbol{X}^{\text{f}}$ and $d(x_i^{\text{f}}, f_j)$ is the (normal) distance between the plane spanned by the facet f_j and the point x_i^{f} of the feature. The corresponding facet of the convex hull, which defines the direction of the flatness tolerance zone, can be found as f_{j^*}, where:

$$j^* = \arg\min_j \left(\max_i d(x_i^{\text{f}}, f_j) \right), \text{ with } i = 1, \dots, n;\ j = 1, \dots, F, \tag{5.5}$$

and its normal vector is denoted by $\boldsymbol{n}^{f_{j^*}}$. In contrast to other approaches for the flatness tolerance zone computation, which employ associated plane features, the proposed method evaluates the minimum flatness deviation and is thus conform to international GD&T standards.

Scaling of Flatness Tolerance Specifications The scaling of flatness tolerance specifications is performed by a scalar weighting of the point-wise deviations $\epsilon^{\text{f}} \in \mathbb{R}^{n \times 3}$ of the feature compared to the nominal points, which can be found as:

$$\epsilon^{\text{f}} = \boldsymbol{X}^{\text{f}} - \boldsymbol{X}^{\text{f}}_{\text{nom}}, \tag{5.6}$$

in the direction of the relevant facet for the flatness computation f_{j^*}. Thus, the new point coordinates of the scaled feature $\tilde{\boldsymbol{X}}^{\text{f}}$ result with the specified flatness tolerance value t_{flat} to:

$$\tilde{\boldsymbol{X}}^{\text{f}} = \boldsymbol{X}^{\text{f}}_{\text{nom}} + \frac{t_{\text{flat}}}{d_{\text{flat}}} \cdot \boldsymbol{n}^{f_{j^*}} \cdot \epsilon^{\text{f}}. \tag{5.7}$$

By doing so, the characteristic of the initial form deviations is not modified, only their amplitude with respect to the flatness tolerance zone is adjusted. The procedure can be seen from Figure 5.10.

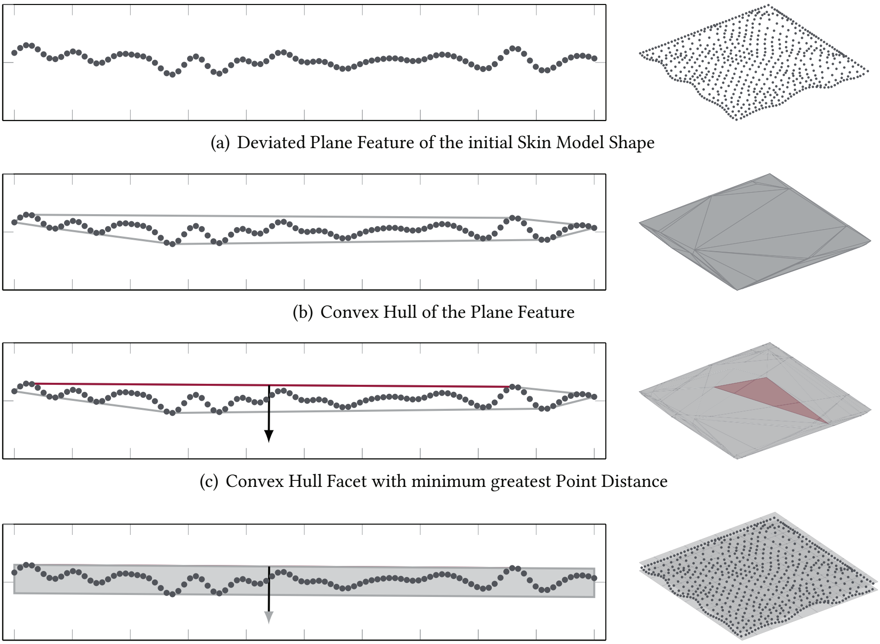

(a) Deviated Plane Feature of the initial Skin Model Shape

(b) Convex Hull of the Plane Feature

(c) Convex Hull Facet with minimum greatest Point Distance

(d) Flatness Tolerance Zone

Figure 5.9: Flatness Tolerance Zone Computation for a Plane Feature: the Flatness Deviation can be found as the minimum of the maximal Distances between the Feature Points and the Facets of the Feature Convex Hull

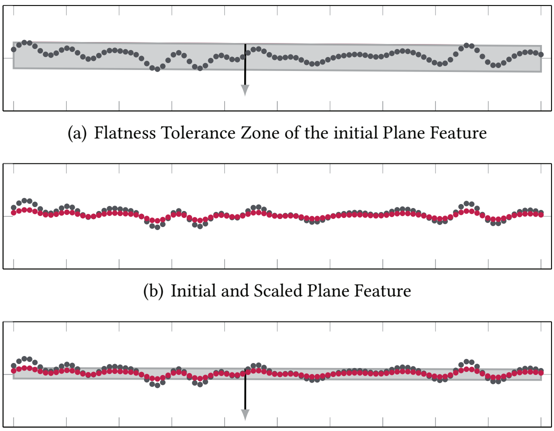

(a) Flatness Tolerance Zone of the initial Plane Feature

(b) Initial and Scaled Plane Feature

(c) Flatness Tolerance Zone of the scaled Plane Feature

Figure 5.10: Flatness Tolerance Scaling of a Plane Feature

5.2.4.2 Cylindricity Tolerance

Definition and Computation of Cylindricity Tolerance Specifications The cylindricity tolerance limits form deviations of cylinder surfaces and the corresponding tolerance zone can be described as follows (see also Figure 5.11):

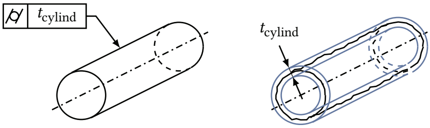

Figure 5.11: Cylindricity Tolerance Specification and corresponding Tolerance Zone

Definition 2– Cylindricity Tolerance [ISO1101]
The tolerance zone is limited by two coaxial cylinders with radial distance t_{cylind}. The measured cylinder surface is to lie between these two coaxial cylinders with radial distance t_{cylind}.

All points of the toleranced cylinder feature are to lie between these two coaxial cylinders with radial distance t_{cylind}, with the orientation of the coaxial cylinders not being limited by the cylindricity tolerance. In order to compute the cylindricity tolerance zone, a minimum zone cylinder (MZC) is associated to the cylindrical Skin Model Shape feature. Thereafter, the radial distance between each point of the feature and the axis of the associated cylinder is evaluated. The cylindricity deviation can then be found as the difference between the maximum radial distance and the minimum radial distance between any point of the feature and the MZC axis:

$$d_{\text{cylind}} = \left(\max_i d_r(x_i^{\text{f}}, C_{\text{ls}})\right) - \left(\min_i d_r(x_i^{\text{f}}, C_{\text{ls}})\right), \text{ with } i = 1, \ldots, n, \tag{5.8}$$

where $d_r(x_i^{\text{f}}, C_{\text{ls}})$ is the radial distance between the point x_i^{f} of the feature and the axis of the MZC C_{ls} of the feature. This is illustrated in Figure 5.12 (a).

Scaling of Cylindricity Tolerance Specifications The scaling of cylindricity tolerances is performed by a scalar weighting of the radial distances between the feature points and the axis of the associated minimum zone cylinder of the cylindrical feature similarly to the size scaling for cylindrical features.

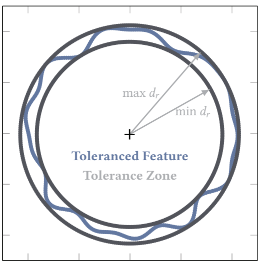

(a) Toleranced Feature and Tolerance Zone

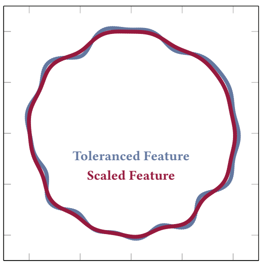

(b) Toleranced Feature and Scaled Feature

Figure 5.12: Cylindricity Tolerance Computation: the Cylindricity Tolerance can be found as the difference between the minimum and maximum radial Distance between the Feature Points and the Center of the Associated Minimum Zone Cylinder

In this regard, firstly the feature points are mapped on the axis of the MZC. Thereafter, the points are shifted back considering a scalar weighting. The new point coordinates $\tilde{x}^{\mathrm{f}}$ of the scaled feature $\tilde{\boldsymbol{X}}^{\mathrm{f}}$ result with the specified cylindricity tolerance value t_{cylind} to:

$$\tilde{x}_i^{\mathrm{f}} = \underline{x}_i^{\mathrm{f}} + \left(r + \left(\frac{t_{\mathrm{cylind}}}{d_{\mathrm{cylind}}} \cdot (d_i^r - r) \right) \right) \cdot \frac{(x_i^{\mathrm{f}} - \underline{x}_i^{\mathrm{f}})}{|x_i^{\mathrm{f}} - \underline{x}_i^{\mathrm{f}}|}, \tag{5.9}$$

where r is the radius of the associated cylinder. The result of the scaling procedure for the cylindricity tolerance can be seen from Figure 5.12 (b).

5.2.5 Orientation Tolerances

5.2.5.1 Parallelism Tolerance

Definition and Computation of Parallelism Tolerance Specifications Parallelism tolerances apply to straight lines or planes and are defined with reference to straight lines, planes or datum frames [ISO1101]. In the context of this work, the parallelism tolerance of two planes is of interest. Therefore, the tolerance zone can be described as follows and is illustrated in Figure 5.13:

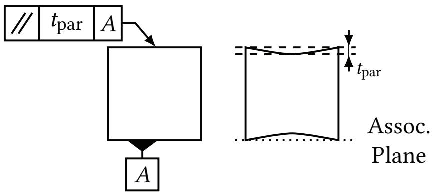

Figure 5.13: Parallelism Tolerance Specification and corresponding Tolerance Zone

Definition 3– Parallelism Tolerance of a Plane to a Datum Plane [ISO1101]
The tolerance zone is limited by two planes with distance t_{par} both parallel to the datum plane. The measured surface is to lie between these two parallel planes with distance t_{par}.

The computation of the parallelism tolerance zone starts with the determination of an associated plane for the datum point cloud. According to [ISO5459], the associated features, which are used to establish the datum or datum systems, simulate the contact with the real integral features in a way ensuring that the associated feature is outside the material of the non-ideal feature. If this procedure is ambiguous, then the associated feature has to be used, which minimizes the orthogonal maximal distance to the non-ideal feature. In order to respect this, the plane spanned by f_{j^*}, which is the relevant facet of the flatness tolerance zone of the datum feature, is used for the associated datum plane, since it minimizes the maximal distance to the non-ideal feature. However, in some cases this plane may lie inside the part material. In this case, the plane is shifted in the direction of its normal vector $\boldsymbol{n}^{f_{j^*}}$ along the flatness value. By doing so, a plane is identified, which ensures contact with the real integral feature and minimizes the orthogonal maximal distance to the non-ideal feature even for convex datums. However, an alternative approach for the association of the datum plane is highlighted in section 5.2.8.1, which identifies the contact plane with a measurement fixture and thus leads to a plane, which also simulates the contact with the real integral feature, but does not minimize the orthogonal maximal distance.

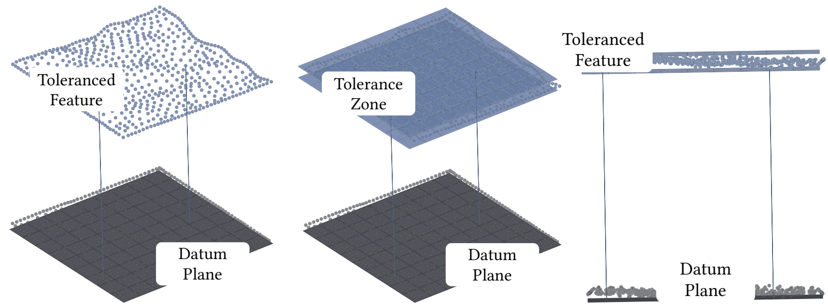

(a) Toleranced Feature, associated Datum Plane and extremal Distances

(b) Tolerance Zone (shifted Datum Planes)

Figure 5.14: Computation of the Parallelism Tolerance Zone: The Parallelism Deviation can be found as the Difference of the maximal and minimal Distance between the toleranced Feature and the associated Plane of the Datum Feature.

After the association of the datum plane, the minimum and maximum distance of the toleranced point cloud to the associated datum plane are determined. The minimum distance is then subtracted from the maximum distance. The result is the parallelism deviation of the point cloud with reference to the datum point cloud. Thus, the parallelism deviation d_{par} can be found as:

$$d_{\text{par}} = \max_i d(x_i^{\text{f}}, p^{\text{f-ref}}) - \min_i d(x_i^{\text{f}}, p^{\text{f-ref}}), \text{ with } i = 1, \dots, n, \tag{5.10}$$

where $p^{\text{f-ref}}$ is the associated plane of the datum feature and $d(x_i^{\text{f}}, p^{\text{f-ref}})$ is the (normal) distance between this associated plane of the datum feature and the point x_i^{f} of the toleranced feature. The procedure can be seen from Figure 5.14.

From the tolerance definition, it can be found, that feature form deviations are implicitly covered by the parallelism tolerance. Thus, the parallelism tolerance zone is of the same size as the flatness tolerance zone only if the normal vector of the flatness tolerance zone $\boldsymbol{n}^{f_j*}$ is equal to the normal of the associated plane of the datum feature. In this case, the form deviations are oriented according to the datum feature. In any other case, in which orientation defects of the toleranced feature are observed, the parallelism deviation is greater than the flatness deviation.

Furthermore, for a toleranced feature with form deviations, there is a piece-wise linear relationship between the orientation defects (rotations) of the toleranced feature and the size of the parallelism tolerance zone. This piece-wise linear relationship converges to a straight linear relationship as soon as the parallelism tolerance is solely influenced by the relative position of the feature edges. This can be seen from Figure 5.15 (a), where the resulting parallelism tolerance zones for different rotations of the toleranced feature are shown. It can be seen, that the parallelism tolerance zone is spanned by different feature points for different rotations, which are denoted to as control points [RL99], since they “control” the size of the tolerance

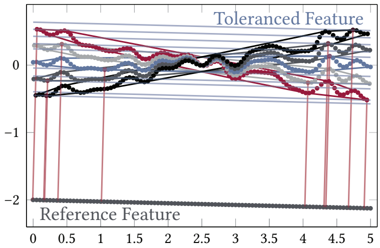

(a) Resulting Parallelism Tolerance Zones for rotated Features and corresponding Control Points

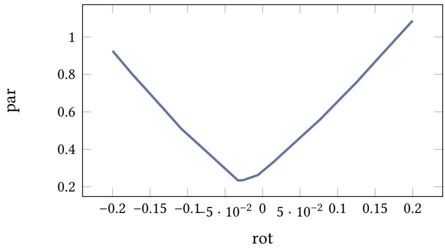

(b) Piece-Wise linear Relationship between the Feature Rotations and the Parallelism Tolerance

Figure 5.15: Effects of Feature Rotations on the Parallelism Tolerance

zone. It can be found, that these control points are the edges of the feature convex hull. This results in a piece-wise linear relationship between the feature rotation rot and the parallelism deviation par in Figure 5.15 (b), since a linear relationship between the rotation and the parallelism deviation can be observed for each control point, until the next control point is reached due to the increased feature rotation. In general, the control points move from feature-intrinsic points to the "edges" of the toleranced plane feature with increasing rotation and consequently increasing parallelism tolerance.

Scaling of Parallelism Tolerance Specifications The parallelism tolerance limits *orientation* defects of the toleranced feature with reference to the datum feature. However, the location of the tolerance zone is not restricted. Therefore, two rotational degrees of freedom are limited by the parallelism tolerance in case of a toleranced plane feature. However, since the parallelism tolerance implicitly also covers form deviations, there is only a piece-wise linear relationship between the parallelism deviation and the orientation of the toleranced feature. Therefore, an optimization approach is used to evaluate the admissible rotations for a specified parallelism tolerance:

$$r^* = \arg\min_{r} \left| d_{\text{par}}(\boldsymbol{X}^{\text{f}}, r) - t_{\text{par}} \right|, \tag{5.11}$$

where $d_{\text{par}}(\boldsymbol{X}^{\text{f}}, r)$ returns the parallelism tolerance of the rotated feature as defined in eq. (5.10). For the expression of the rotations r, instantaneous kinematics are employed as can be found in [PLH02, PLH04]. In doing so, the rigid body motion $\boldsymbol{\alpha}$ is expressed as $\boldsymbol{\alpha}(\boldsymbol{X}^{\text{f}}) \approx \boldsymbol{m}(\boldsymbol{X}^{\text{f}}) = \boldsymbol{X}^{\text{f}} + \boldsymbol{v}(\boldsymbol{X}^{\text{f}})$, where:

$$\boldsymbol{v}(\boldsymbol{X}^{\text{f}}) = t + r \times \boldsymbol{X}^{\text{f}}. \tag{5.12}$$

In this context, t represents the velocity vector of the origin and r is the vector of angular velocity (Darboux vector) [PLH02]. Since this linearization results in an affine transformation, but not necessarily in a rigid body transformation, the resulting velocity vector field is projected to the corresponding helical motion (see [PLH02, PLH04] for further detail). After the optimization, the helical motion of the resulting rotations r^* is applied to the Skin Model

Shape feature. It should be mentioned, that the Skin Model Shape feature is centred at the coordinate origin prior to the optimization, i. e. the following translation is performed:

$$\boldsymbol{X}^{\mathrm{f}} = \boldsymbol{X}^{\mathrm{f}} - \hat{x}. \tag{5.13}$$

After the helical motion has been applied to the feature, it is translated to its initial position.

For plane features, two rotations are limited by the parallelism tolerance and hence $r \in \mathbb{R}^2$. As a consequence, the optimization problem is of dimension two and solved employing an active-set algorithm. However, since the approaches for the scaling of Skin Model Shapes are to be used in statistical tolerance simulations, it must be ensured that the results of the optimization problem as given in eq. (5.11) do not lead to systematic effects with regard to the rotations r^*. To ensure this, random values are used as starting points for the optimization.

Some exemplary results for the resulting rotations for a given parallelism tolerance $t_{\mathrm{par}}^{\mathrm{spec}}$ are shown in Figure 5.16. It can be seen, that the rotations form a deviation domain [GSP07] as expected. Each point on the rhombus or circle (see Figure 5.16 (a) and (b), respectively) is a possible combination of rotations for a specified parallelism tolerance, whereas points on the inside correspond to combinations for smaller parallelism deviation values. Furthermore, it can be found, that the deviation domains for the nominal feature build a regular rhombus (or circle), whereas the edges of the deviation domain for a plane feature with form deviations are cropped. This can be explained by the fact, that the control points for a feature with form deviations not necessarily lie on the edges of the feature but on the inside, similarly to the 2D case explained in Figure 5.15. Furthermore, the resulting deviation domains for features with form deviations are smaller than for the nominal features, since the parallelism tolerance zone is party filled by the form deviations and thus the allowable feature rotations are limited by the form deviations (see Figure 5.4). Another finding is, that the facets of the deviation domain are evenly filled and therefore no systematic effects of the parallelism scaling approach can be observed. Thus, the approach is suitable for worst-case and statistical tolerance analyses.

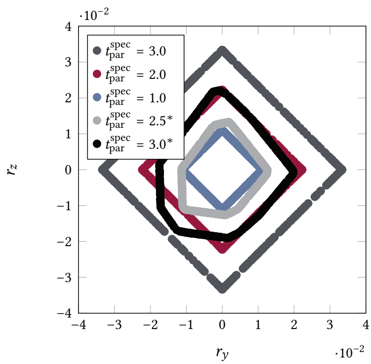

(a) Rotations for a quadratic Feature

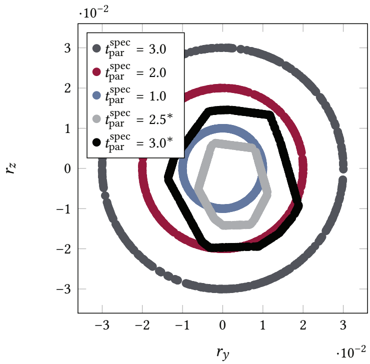

(b) Rotations for a cylindrical Feature

Figure 5.16: Rotations for given Parallelism Tolerance Specifications of Plane Features (* indicates a Feature with Form Deviations)

5.2.5.2 Perpendicularity Tolerance

Definition and Computation of Perpendicularity Tolerance Specifications Perpendicularity tolerances also apply to straight lines or planes and are defined with reference to straight lines, planes, or datum frames [ISO1101]. The corresponding tolerance zone of perpendicularity tolerances on plane features is illustrated in Figure 5.17 and defined as follows:

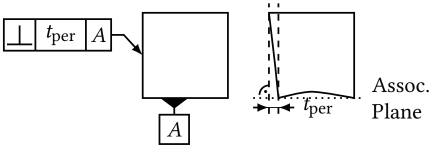

Figure 5.17: Perpendicularity Tolerance Zone

Definition 4– Perpendicularity Tolerance of a Plane to a Datum Plane [ISO1101]
The tolerance zone is limited by two parallel planes, which are perpendicular to the datum plane and have the distance t_{per}. The measured surface is to lie between these two parallel planes with distance t_{per}.

For the computation of the perpendicularity tolerance zone, first of all, the associated plane of the datum feature according to the procedure explained in section 5.2.5.1 is performed. Thereafter, the points of the toleranced feature are (orthogonally) projected onto this associated datum plane. Then, the convex hull of these projections is computed and, similar to the flatness deviation computation, the perpendicularity deviation d_{per} can be found as:

$$d_{per} = \min_{j} \left(\max_{i} d(\tilde{x}_i^f, f_j) \right), \text{ with } i = 1, \ldots, n;\ j = 1, \ldots, F, \tag{5.14}$$

where F is the number of facets of the convex hull around the projections of $\boldsymbol{X}^f$ onto the associated datum feature and $d(\tilde{x}_i^f, f_j)$ is the (normal) distance between the plane spanned by the facet f_j and the projected point $\tilde{x}_i^f$ of the toleranced feature. The procedure can be seen from Figure 5.18.

Scaling of Perpendicularity Tolerance Specifications The perpendicularity tolerance limits *orientation* defects of the toleranced feature with reference to the datum feature. Similar to the parallelism tolerance, the *location* of the tolerance zone is not limited. However, for the perpendicularity tolerance of plane features, only one rotational degree of freedom is relevant and limited. An optimization approach is used to evaluate the admissible rotation for a perpendicularity specification similarly to the parallelism tolerance:

$$r^* = \arg\min_{r} \left| d_{per}(\boldsymbol{X}^f, r) - t_{per} \right|, \tag{5.15}$$

where $d_{per}(\boldsymbol{X}^f, r)$ returns the perpendicularity tolerance of the rotated feature as defined in eq. (5.14).

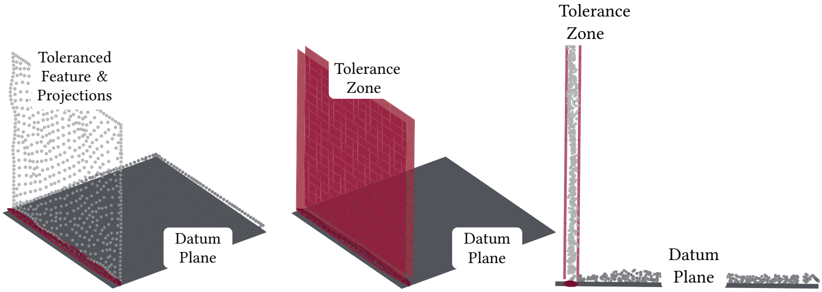

(a) Toleranced Feature, associated Datum Plane, and Convex Hull of the Projections

(b) Tolerance Zone (shifted Perpendicular Planes)

Figure 5.18: Computation of the Perpendicularity Tolerance Zone: The Perpendicularity Deviation can be found as the minimum of the maximal Distances between the projected Feature Points onto the associated Datum Feature and the Facets of their Convex Hull.

5.2.5.3 Angularity Tolerance

Definition and Computation of Angularity Tolerance Specifications Angularity tolerances apply to straight lines or planes and are defined with reference to straight lines, planes or datum frames [ISO1101]. The corresponding tolerance zone of angularity tolerances on plane features is defined as follows and illustrated in Figure 5.19:

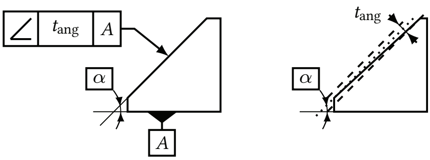

Figure 5.19: Angularity Tolerance Zone

Definition 5– Angularity Tolerance of a Plane to a Datum Plane [ISO1101]
The tolerance zone is limited by two by the specified angle with reference to the datum plane inclined planes with distance t_{ang}. The measured surface is to lie between these two parallel planes with distance t_{ang}, which are inclined by the theoretical angle with reference to the datum plane.

For the computation of the angularity tolerance zone, a procedure analogue to the parallelism deviation computation is employed. For this purpose, firstly the associated datum plane is computed. Thereafter, the associated datum plane is inclined by the specified theoretical angle. Finally, the (normal) distances between the points of the toleranced feature and the inclined associated datum plane are computed. The angularity deviation d_{ang} can then be found as:

$$d_{\text{ang}} = \max_i d(x_i^{\text{f}}, \tilde{p}^{\text{f-ref}}) - \min_i d(x_i^{\text{f}}, \tilde{p}^{\text{f-ref}}), \text{ with } i = 1, \ldots, n, \tag{5.16}$$

where $\tilde{p}^{\text{f-ref}}$ is the inclined associated plane of the datum feature and $d(x_i^{\text{f}}, \tilde{p}^{\text{f-ref}})$ is the (normal) distance between this inclined associated plane of the datum feature and the point x_i^{f} of the toleranced feature. The procedure can be seen from Figure 5.20.

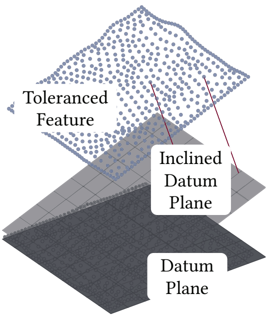

(a) Toleranced Feature, associated Datum Plane, and inclined Datum Plane with extremal Distances

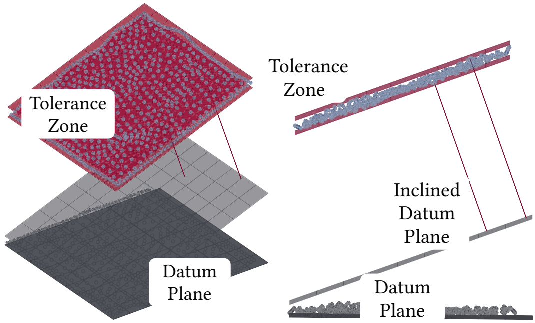

(b) Tolerance Zone (shifted inclined Datum Planes)

Figure 5.20: Computation of the Angularity Tolerance Zone: The Angularity Deviation can be found as the Difference of the maximal and minimal Distance between the toleranced Feature and the inclined associated Plane of the Datum Feature.

Scaling of Angularity Tolerance Specifications Similar to the parallelism and perpendicularity tolerance, the angularity tolerance limits *orientation* defects, whereas the *location* of the tolerance zone is not limited. Thus, similarly to these tolerances, an optimization approach is used to evaluate the admissible rotation for an angularity specification t_{ang}:

$$r^* = \arg\min_r \left| d_{\text{ang}}(\boldsymbol{X}^{\text{f}}, r) - t_{\text{ang}} \right| , \tag{5.17}$$

where $d_{\text{ang}}(\boldsymbol{X}^{\text{f}}, r)$ returns the angularity tolerance of the rotated feature as defined in eq. (5.16).

5.2.6 Location Tolerances

5.2.6.1 Coaxiality Tolerance

Definition and Computation of Coaxiality Tolerance Specifications The coaxiality tolerance limits deviations of axes with reference to datum axes and the tolerance zone is defined as follows and can be seen from Figure 5.21:

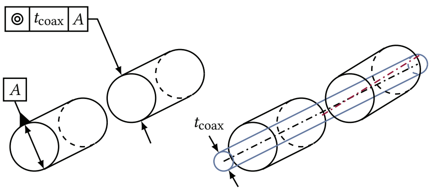

Figure 5.21: Coaxiality Tolerance Zone

Definition 6– Coaxiality Tolerance [ISO1101]
The tolerance zone is a cylinder with diameter t_{coax}, which axis is given by the axis of the datum cylinder. The axis of the measured cylinder is to lie within this cylinder with diameter t_{coax}.

The computation of the coaxiality deviation is performed by firstly mapping all points of the toleranced Skin Model Shape feature x_i^{f} on the axis of its least squares cylinder $x_i^{\text{f-a}}$:

$$x_i^{\text{f-a}} = a + \sqrt{\left|a - x_i^{\text{f}}\right|^2 - (d_i^r)^2} \cdot \boldsymbol{b}, \tag{5.18}$$

where a is a point on the axis of the least squares cylinder, $\boldsymbol{b}$ is the direction of the least squares cylinder, and d_i^r is the radial distance of the point x_i^{f} to the cylinder axis. In this context, according to [ISO5459], the associated datum cylinder has to be chosen in a manner, so that it is outside the material of the non-ideal cylindrical datum feature, i. e. maximum inscribed or minimum circumscribed cylinders have to be identified. Thereafter, the distances between these points and the axis of the associated cylinder of the datum feature are determined, with the coaxiality deviation resulting as the maximum radial distance:

$$d_{\text{coax}} = \max_i \left| d_r(x_i^{\text{f-a}}, A_{\text{ls-ref}}) \right|, \quad i = 1, \ldots, n, \tag{5.19}$$

where $d_r(x_i^{\text{f-a}}, A_{\text{ls-ref}})$ is the (radial) distance between the mapped points on the toleranced cylinder axis $x_i^{\text{f-a}}$ and the axis of the associated cylinder of the datum feature $A_{\text{ls-ref}}$. The procedure can be seen from Figure 5.22.

Scaling of Coaxiality Tolerance Specifications Since the coaxiality tolerance limits the location of the toleranced axis with reference to the datum axis, the scaling of the coaxiality tolerance has to consider not only rotational degrees of freedom, but also translational degrees of freedom. Thus, the optimization formulation for the scaling can be found as:

$$r^*, t^* = \arg\min_{r,t} \left| d_{\text{coax}}(\boldsymbol{X}^{\text{f}}, r, t) - t_{\text{coax}} \right|, \tag{5.20}$$

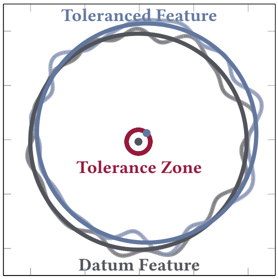

Figure 5.22: Coaxiality Tolerance Computation

where $d_{\text{coax}}(\boldsymbol{X}^{\text{f}}, r, t)$ returns the coaxiality tolerance of the rotated and translated feature.

5.2.6.2 Position Tolerance

Definition and Computation of Position Tolerance Specifications Position tolerances are specified to control the location of features with reference to datum features employing theoretical measures. In this work, the position tolerance of a line (such as an axis) as well as the position tolerance of a plane are considered, with the position tolerance zone of a line being defined as follows and can be seen from Figure 5.23:

Definition 7– Position Tolerance of a Line [ISO1101]
The tolerance zone is limited by a cylinder with diameter t_{pos}, if the ⌀-symbol is prefixed. The axis of the tolerance zone cylinder is defined by theoretical measures to the datums. The associated axis is to lie within this cylinder with diameter t_{pos}.

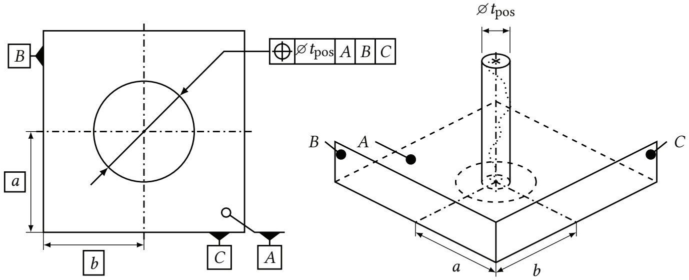

Figure 5.23: Position Tolerance Zone for an Axis

Similarly to the coaxiality tolerance, the tolerance zone is defined by a cylinder as illustrated in Figure 5.23, which is to contain the associated axis of the toleranced cylinder. Therefore, the procedure of the coaxiality tolerance evaluation and scaling can be applied (see section 5.2.6.1), with the datum axis being set as the axis defined by the theoretical measures and datums.

In contrast to this, the position tolerance zone for a plane feature is defined as follows (see Figure 5.24):

Definition 8– Position Tolerance of an even Plane or a Center Plane [ISO1101]
The tolerance zone is limited by two parallel planes, which lie symmetrically around the theoretical exact position and have the distance t_{pos}. The theoretical exact position is defined by theoretical measures and datums. The measured plane is to lie between these two parallel planes with distance t_{pos}.

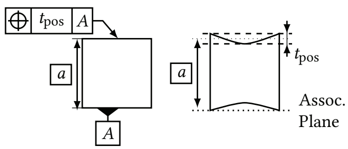

Figure 5.24: Position Tolerance Zone for a Plane Feature

The position tolerance zone for a plane feature is limited by two parallel planes, which are positioned symmetrically around the theoretically exact position of the plane feature. This theoretically exact position is in turn defined by datum features and theoretical measures. In this section, a focus is laid upon the position tolerance for one datum feature, whereas multiple datum features are discussed in section 5.2.8.2. For the computation of the position tolerance zone of a plane feature with reference to a datum plane feature, the theoretically exact position of the toleranced plane feature is determined by a translation of the associated datum plane by the theoretical measure. The position tolerance zone is then limited by two planes, which lie symmetrically around the translated associated datum plane. Their distance is determined by calculating the maximum point distance for each point of the Skin Model Shape feature and the symmetry plane. Thus, the position deviation is defined as:

$$d_{\text{pos}} = 2 \cdot \max_{i} \left| d(x_i^{\text{f}}, p^{\text{f-ref}}) - d_{\text{theo}} \right|, \; i = 1, \ldots, n, \tag{5.21}$$

where $p^{\text{f-ref}}$ is the associated plane of the datum feature, $d(x_i^{\text{f}}, p^{\text{f-ref}})$ is the (normal) distance between this associated plane of the datum feature and the point x_i^{f} of the toleranced fea-

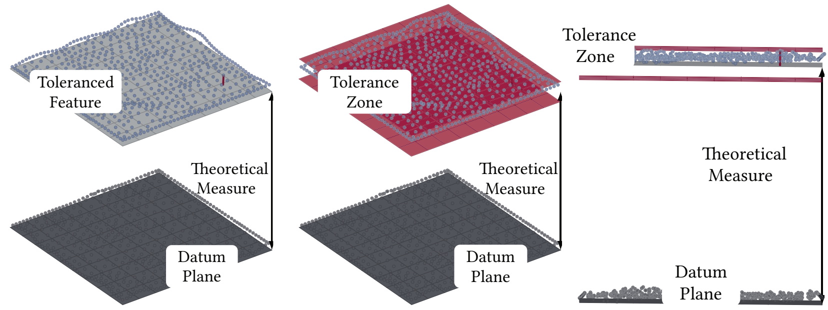

(a) Toleranced Feature, associated Datum Plane, and Shifted Datum Plane along the theo. Measure

(b) Tolerance Zone (shifted Datum Planes)

Figure 5.25: Evaluation of the Position Tolerance Zone: The Position Deviation with one Datum can be found as twice the maximal Distance between the toleranced Feature and the Plane parallel to the associated Plane of the Datum Feature and shifted along the theoretical Measure.

ture, and d_{theo} is the theoretical measure. The procedure for the computation of the position tolerance zone is illustrated in Figure 5.25.

From the definitions of the parallelism tolerance and the position tolerance, it can be seen, that the position deviation is always greater or equal to the parallelism deviation, since its tolerance zone is dependent on the theoretical exact position of the toleranced feature in contrast to the parallelism deviation. Furthermore, the position tolerance zone lies symmetrically around the shifted associated datum plane and is not “fitted” to the toleranced plane feature as for the parallelism tolerance zone.

Scaling of Position Tolerance Specifications The position tolerance limits *location* defects of the toleranced feature with reference to one or multiple datum features. Therefore, the scaling of position tolerances considers not only rotational degrees of freedom, but also additional translational degrees of freedom. Thus, the optimization is formulated as follows:

$$r^*, t^* = \arg\min_{r,t} \left| d_{\text{pos}}(\boldsymbol{X}^{\text{f}}, r, t) - t_{\text{pos}} \right|, \tag{5.22}$$

where $d_{\text{pos}}(\boldsymbol{X}^{\text{f}}, r, t)$ returns the position tolerance of the rotated and translated feature. The optimization problem is formulated in analogy to the parallelism tolerance scaling. However, if the feature rotations r are already limited by orientation tolerances (e. g. by a parallelism tolerance), lower lb and upper bounds ub for the rotations as $lb = ub = 0$ are specified as constraints in the optimization. Similarly to the optimization problem given in eq. (5.11), random values are used as initial starting points for the active-set algorithm.

Some exemplary results for the resulting rotations and translations for a given position tolerance are shown in Figure 5.26. It can be seen, that the deviation domain of the rotations

r_y and r_z is filled in contrast to the deviation domain for the parallelism tolerance scaling in Figure 5.16, since this space is covered by an additional translation t_z.

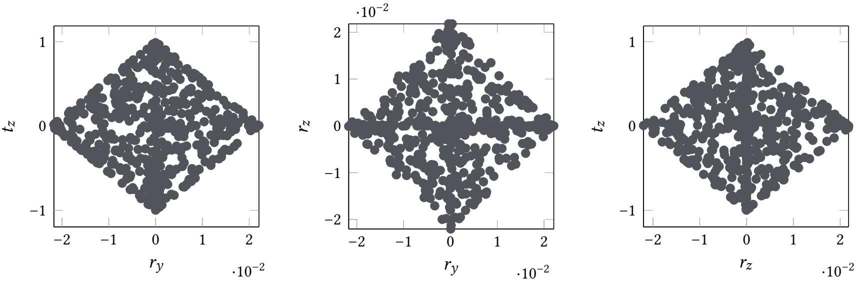

Figure 5.26: Resulting Rotations and Translations for a given Position Tolerance of a Plane Feature with one Datum

5.2.6.3 Runout Tolerance

Definition and Computation of Runout Tolerance Specifications Runout tolerances limit location defects of cylinder surfaces and the tolerance zone can be found as (see also Figure 5.27):

Definition 9– Runout Tolerance [ISO1101]
The tolerance zone is limited by two coaxial cylinders with radial distance t_{run}, which axis is identical to the datum axis. The measured cylinder surface is to lie between these two coaxial cylinders with radial distance t_{run}.

The computation of the total runout tolerance deviation can be performed similar to the cylindricity tolerance, with the axis of the least-squares cylinder being replaced by the datum axis. Thus, the radial distances between the datum axis and the points of the toleranced Skin Model Shape feature have to be evaluated and eq. (5.8) can be applied, with C_{ls} being replaced by the datum axis.

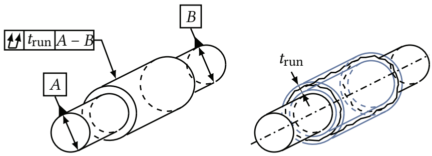

Figure 5.27: Total Runout Tolerance Zone

Scaling of Runout Tolerance Specifications The scaling of runout tolerances is also performed in analogy to the scaling of cylindricity tolerance specifications. Thus, eq. (5.9) can be applied, with the axis of the associated cylinder C_{ls} being replaced by the datum axis.

5.2.7 Profile and Runout Tolerances

Profile tolerances limit line or surface profiles, where the real part surface is to lie between two surfaces with identical distance, which enfold spheres with diameter t_{profile} and which centres lie on the surface with theoretically exact form [ISO1101]. In this regard, the projection of measured points onto the vertex normals of the nominal surface is current practice e. g. for the measurement of flank profile deviations of gears [Gue11]. An approach for the profile tolerance measurement based on vertex normal projections is proposed in [SW14]. In analogy to this, the scaling of profile tolerances can be performed by shifting the points of the toleranced Skin Model Shape feature in the direction of their corresponding vertex normals along the weighted profile deviation.

5.2.8 Alternative Tolerance Specifications

5.2.8.1 Parallelism Tolerance revisited

In section 5.2.5.1, the parallelism deviation evaluation based on an associated datum plane was highlighted. However, an alternative measurement approach of the parallelism tolerance can be seen from Figure 5.28, where the toleranced part is placed on a measurement fixture, which also serves as the datum feature. Therefore, the plane of the measurement fixture serves as the datum plane $p^{\text{f-ref}}$ in the parallelism tolerance computation as given in eq. (5.10). In order to evaluate the parallelism tolerance of the toleranced plane feature, the part is to be placed on a measurement fixture, which is performed employing relative positioning approaches (see Figure 5.29 and section 5.3). However, the determination of the parallelism deviation as well as the scaling approach stay unaffected.

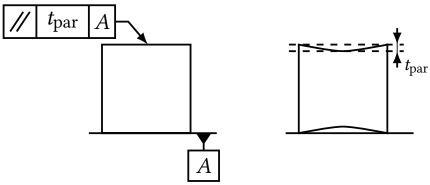

Figure 5.28: Alternative Parallelism Tolerance Measurement and corresponding Tolerance Zone

In order to illustrate possible differences regarding the resulting rotations between the parallelism deviation evaluated based on the associated datum plane and the datum plane of the measurement fixture, respectively, a parallelism tolerance is specified on the top plane of a cube with reference to the cube's bottom plane as illustrated in Figure 5.13 and Figure 5.28. For the parallelism deviation evaluation based on the associated datum plane, the procedure as illustrated in Figure 5.14 is pursued, whereas the cube is assembled on a measurement fixture employing relative positioning approaches for the parallelism deviation evaluation based on the fixture datum plane as can be seen from Figure 5.29.

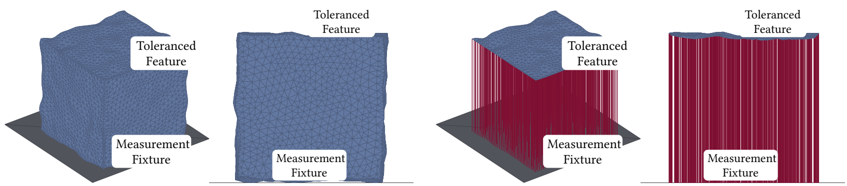

(a) Part positioned in the Measurement Fixture employing Relative Positioning Approaches

(b) Distances between the Toleranced Feature and the Measurement Fixture

Figure 5.29: Tolerance Zone Evaluation for a Parallelism Tolerance employing Relative Positioning Approaches: The Parallelism Deviation can be found as the Difference of the maximal and minimal Distance between the toleranced Feature and the Measurement Fixture.

The differences for the resulting rotations for the scaling of parallelism specifications between the two approaches for the parallelism tolerance evaluation are shown for a single Skin Model Shape in Figure 5.30. It can be seen that there is a shift of the deviation domain, which results from the different orientations of the measurement fixture plane and the associated plane of the datum feature. This effect is highlighted in Figure 5.31, where the relevant facet f_{j^*} for the association of the datum plane as explained in section 5.2.5.1 as well as the resulting facet f_{RelPos} of the relative positioning on the measurement fixture are shown. It can be seen, that both approaches lead to planes, which ensure the contact with the integral non-ideal feature. However, the associated plane based on f_{j^*} minimizes the orthogonal maximal distance to the non-ideal feature and can be computed even for convex non-ideal features, whereas the plane f_{RelPos} ensures the contact with the measurement fixture, but does not minimize the orthogonal distance. In this context, it should be mentioned, that the alternative computation of associated datums for planar features employing relative positioning approaches is also possible for other tolerances of orientation and location.

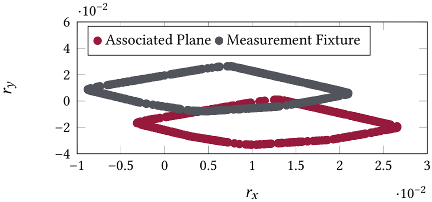

Figure 5.30: Resulting Rotations for the Parallelism Tolerance Scaling

5.2.8.2 Position Tolerances with multiple Datum Features

In many applications, the location of features is to be specified with reference not only to a single but to multiple other part features. In such cases, the datum features build a datum system, which comprises the order of features to be respected for the measurement of the specified location tolerance. As a typical example, the position tolerance for a plane feature with reference to two datum features and the corresponding tolerance zone is shown in Figure 5.32. It can be found, that the measurement of the position deviation requires the consideration of measurement fixtures. In order to consider the datum system, the toleranced part is placed in a measurement fixture employing relative positioning approaches, with the part being positioned is such a manner, that there result three contact points between the part and the first datum A and two contact points between the part and the datum B, i. e. the first two steps of a 3-2-1 positioning scheme [JS00] are simulated.

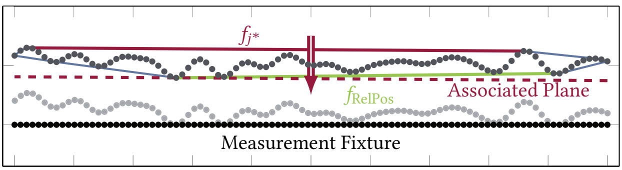

Figure 5.31: Difference between the associated Plane based on f_{j^*} and based on the relative Positioning on a Measurement Fixture f_{RelPos}: The associated Plane (dashed Line) is computed based on the relevant facet of the flatness tolerance zone f_{j^*}, whereas the positioning on the measurement fixture leads to a different contact facet f_{RelPos}.

The evaluation of the position deviation is then performed according to equation (5.21), with the required reference plane $p^{\text{f-ref}}$ being given by the datum B plane of the measurement fixture. The procedure can be seen from Figure 5.33. However, similarly to the scaling of the parallelism tolerance, the general approach for the position deviation evaluation and scaling is not influenced by the change of the relevant datum planes.

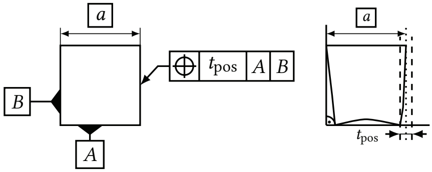

Figure 5.32: Tolerance Zone for a Position Tolerance with two Datums measured employing a Measurement Fixture

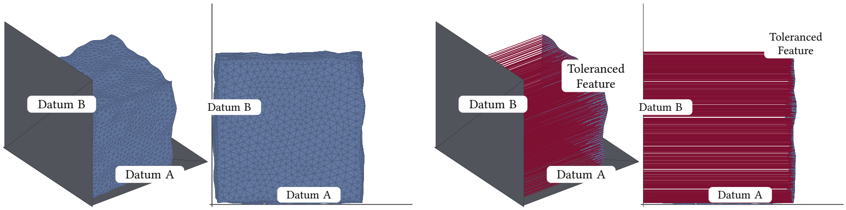

(a) Part positioned in the Measurement Fixture

(b) Distances between the Toleranced Feature and the Measurement Fixture

Figure 5.33: Tolerance Zone Evaluation for a Position Tolerance with two Datums: The Position Deviation can be found as double the maximum absolute Difference of the theoretical Measure and the Distances between the Measurement Fixture and the toleranced Feature.

5.2.9 Results for the Example Case Study

In order to perform a tolerance analysis for the example case study illustrated in Figure 5.2, firstly Skin Model Shapes have to be generated. This has been performed by modelling random geometrical deviations using the random field approach as described in section 4.3.

However, as this approach for the generation of Skin Model Shapes does not necessarily lead to part representatives, which conform to specified tolerances, the obtained Skin Model Shapes have to be "scaled". This has been performed using the presented algorithms for the scaling of Skin Model Shapes, which allow the manipulation of the single Skin Model Shapes, so that they conform to pre-defined tolerance specifications. In this regard, worst-case and statistical tolerance analyses for the case study have been conducted with and without consideration of form tolerances, respectively. For the worst-case analyses, the parts conform to the (maximum) specified tolerances but are randomly as-

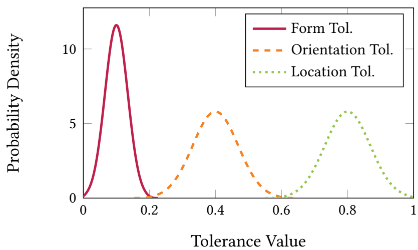

Figure 5.34: Input Probability Densities of the different Tolerances for the Statistical Analysis

sembled, whereas Gaussian input probability densities for the tolerances as can be seen from Figure 5.34 have been assumed for the statistical analyses.

In order to illustrate the results of the part scaling, the parallelism tolerance of the base part ($*$) in Figure 5.2 is considered. Figure 5.35 shows the introduced orientation defects around the x- and y-axis as components of the Small Displacement Torsor r_x and r_y for the toleranced plane feature. It can be seen, that a regular rhombus is obtained for the worst-case when the form deviations of the feature are nil, whereas an irregular rhombus results when form deviations are considered. This is because the parallelism tolerance zone comprises the form deviations according to GPS standards. Thus, the allowed orientation defects (i. e. feature rotations) are decreased by the form deviations of the plane feature. Furthermore, irregular rhombi are obtained when considering Gaussian input probabilities for the tolerances for the analysis with as well as without form tolerance considerations, respectively. Again, it can be seen, that the rhombus for the case when form deviations are considered is slightly smaller than for the case when the form deviations are nil, since the form deviations decrease the allowed orientation defects.

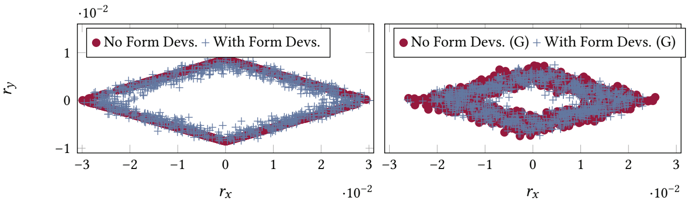

Figure 5.35: Introduced Orientation Defects for the Parallelism Tolerance ($*$) with and without consideration of Form Tolerances (left shows the Worst-Case, right the Statistical Analysis).

5.3 Relative Positioning and Assembly Simulation of Skin Model Shapes

Assembly modelling as one of the most important steps in the product development process relies more and more on the extensive use of CAD systems. Digital mock-ups enable virtual assembly and testing without building physical artefacts while reducing time and costs in product development and increasing product quality. The modelling of geometrical interfaces between the components of the assembly is of central importance in the simulation of mechanical assemblies. Over the past decades, many researchers have devoted their efforts to establish theories and systems covering assembly modelling. Although the product form or shape have been extensively investigated considering the nominal CAD geometry, inevitable limitations can be reported. Computer-aided tolerancing systems provide simulation tools for modelling the effects of tolerances on the assembly and product function and also allow the integration of manufacturing simulations and physical modelling into tolerance analysis, but still lack of form deviation considerations.

The concept of Skin Model Shapes aims at overcoming these shortcomings, but, however, the application of the concept of Skin Model Shapes to the computer-aided tolerance analysis requires models for the simulation of their relative positioning and assembly considering different kinds of geometrical part deviations. In this context, the term "relative positioning" describes the positioning[55] of a digital part representative relative to others in an assembly [LR01]. The need for such models gives rise for this section, which introduces approaches for the relative positioning and assembly simulation of Skin Model Shapes. These methods have a strong geometrical component and are therefore closely linked to the subject of *Industrial Geometry* [PLH+05].

It is structured as follows. In the following section, existing approaches for the assembly simulation of non-ideal workpiece representatives are briefly reviewed. Following this, a framework for the assembly simulation of Skin Model Shapes is proposed and then applied to the example case study. This framework has been discussed by the author in [SW15a].

5.3.1 Related Work

Various models for the assembly simulation in computer-aided tolerancing tools have been proposed, from simple 1D and 2D tolerance stack-ups [She30, FG86] to vectorial tolerancing and the DLM method [Wir88, GCM98] and to approaches for the assembly constraint modelling and solving for variational part geometry [LR01, OBJ06, FGP10]. It can be found, that these approaches differ in the formulation and derivation of assembly constraints and the proposed solution techniques. However, a main similarity is that they hardly allow the consideration of form deviations and are not capable of dealing with discrete geometry part representatives.

In contrast to that, local registration techniques, such as the Iterative Closest Point (ICP) framework [BM92] and adaptions of it [RL01], are widely used for the registration of 3D data point clouds to model shapes. Furthermore, alternative concepts, such as constrained registration approaches, have been developed to match broken objects [HFG+06] and to fit point clouds to surfaces in the presence of obstacles [Flö09, FH10]. In these works, the constraint modelling is mainly based on local vertex normal distance computations, whereas Pierce and Rosen [PR07b] convert the constrained optimization to an unconstrained optimization problem employing penalty functions. A similar approach for the relative positioning of surface meshes is presented in [SWM+10a, SWHP07, SWM09], where the objective function for the optimization is defined as the sum of projected point-to-point distances and the non-penetration requirement is checked by collision detection algorithms, which also trigger penalty terms in the objective function. However, these registration-based approaches for the matching and relative positioning of point clouds seldom allow the consideration of assembly process characteristics, such as multiple assembly steps with different assembly directions, assembly forces, gravitational forces, or assembly constraints. This hinders their application to computer-aided tolerance analysis.

Unlike these methods, Samper et al. [SAFP09] present an approach for the assembly modelling, which is based on the difference surface computation of mating surfaces by modal analysis. Due to this modal surface decomposition for the difference surface computation em-

[55] Positioning can be defined as "the act of putting a part in a certain place with the right orientation; placing or aligning in the appropriate location one component relatively to another" [Pag14]. It can be performed "manually or automatically by a manipulation system, e. g. linear or rotation axis, robot, and pick-and-place system" [Pag14].

ploying the finite-element analysis (FEA), each two mating features have to share the same discretization, which is a strong drawback in many situations. Though, the algorithm allows the computation of the "deterministic" contact points between each two discretized variant part representations.

Hence, it can be found, that none of these approaches allows the assembly simulation of Skin Model Shapes with arbitrary geometrical deviations for the tolerance analysis considering different positioning schemes. In order to overcome this shortcoming, two classes of approaches for the relative positioning of discrete geometry Skin Model Shapes for the application in computer-aided tolerance analysis are introduced, discussed, and compared in the following, namely adapted registration techniques and an algorithm based on the feature difference surface. These approaches are introduced and discussed, as well as applied to two case studies in the field of computer-aided tolerance analysis.

5.3.2 Relative Positioning of Skin Model Shapes

In order to analyse the effects of geometrical part deviations on product requirements, the resulting assembly positions of parts with deviations in the assembly have to be investigated. Since the resulting assembly configurations for deviated parts are far more complicated than for nominal assemblies [LR01], the computation of the resulting part positions requires algorithms, with [PR07b] defining three requirements for such an algorithm:

- R1: The algorithm should minimize the distances between any point on one feature and the corresponding closest point of the other feature.
- R2: The algorithm should avoid interference of parts.
- R3: In the case when the form deviations are nil, the algorithm should converge to the nominal assembly position.

The second requirement R2 is related to the physical properties of rigid mechanical parts, which not tend to interfere in real assembly processes, whereas the third requirement R3 is somehow related to robustness issues of the algorithm (a robust algorithm is expected to converge to the nominal assembly position for nominal parts). In contrast to that, the first requirement R1 is not primarily a general requirement for any algorithm but rather expresses *one* approach to the relative positioning problem. As it will be shown, there exist algorithms, which fulfil R2 and R3, though they not minimize point-to-point distances. However, these three requirements may serve as first indications for the choice of adequate relative positioning algorithms in the following.

5.3.2.1 Constrained Registration

Introduction and Formulation of the Optimization Problem An intensively discussed registration problem is the "fitting" of a 3D data point cloud to a given model shape. The idea of the Iterative Closest Point (ICP) framework as a well-known approach to this registration problem is the minimization of an error metric, that is defined on pairs of points each one consisting of a point from the model shape, which stays unaffected, and a corresponding point from a data shape, which is translated and rotated to fit the reference shape [BM92, RL01].

In the context of relative positioning, a slightly different registration problem occurs, since a 3D data point cloud of a part feature (plane, cylinder, etc.) has to be "fitted" to the 3D point cloud of another parts' feature. For this purpose, the ICP framework has been generalized in this regard, that the objective function for the minimization is not necessarily defined between pairs of points, but allows more general formulations [SWHP07]. This generalized framework can be employed for the contact simulation of Skin Model Shapes and is extended to the assembly simulation considering multiple assembly steps in the following. However, firstly, the mathematical foundation is introduced.

Let $\boldsymbol{Y} = \{\boldsymbol{y}_i \in \mathbb{R}^3 : i = 1, ..., M\}$ be the point cloud of the data shape feature and $\boldsymbol{X} = \{\boldsymbol{x}_i \in \mathbb{R}^3 : i = 1, ..., N\}$ the point cloud of the reference shape feature. Then, the adjusted position of the data shape feature $\boldsymbol{Y}$ can be obtained by minimizing an objective function $f(\cdot)$, which is a function of both point clouds $\boldsymbol{X}$ and $\boldsymbol{Y}$ and the rigid body transformation of the data shape $\boldsymbol{\alpha}$:

$$\min f(\boldsymbol{\alpha}; \boldsymbol{X}, \boldsymbol{Y}). \tag{5.23}$$

Thus, the unknown rigid body transformation $\boldsymbol{\alpha}$ of $\boldsymbol{Y}$ is identified by minimizing an objective function $f(\boldsymbol{\alpha}; \boldsymbol{X}, \boldsymbol{Y})$. Similarly to alternative solutions to this generalised registration problem [HFG+06, FH10, PLH02, PLH04] and the approaches for the part scaling considering orientation and location tolerances, instantaneous kinematics are employed for the expression of the rigid body motion $\boldsymbol{\alpha}$ with $\boldsymbol{\alpha}(\boldsymbol{Y}) \approx \boldsymbol{m}(\boldsymbol{Y}) = \boldsymbol{Y} + \boldsymbol{v}(\boldsymbol{Y})$ in the following, where:

$$\boldsymbol{v}(\boldsymbol{Y}) = \boldsymbol{t} + \boldsymbol{r} \times \boldsymbol{Y}. \tag{5.24}$$

In this regard, $\boldsymbol{t}$ represents the velocity vector of the origin and $\boldsymbol{r}$ is the vector of angular velocity [PLH02]. Since this linearization results in an affine transformation, but not necessarily in a rigid body transformation, the resulting velocity vector field is projected to the corresponding helical motion after the optimization (see [PLH02, PLH04] for further detail). With $\boldsymbol{t}, \boldsymbol{r} \in \mathbb{R}^3$, the optimization problem is of dimension six [FH10]:

$$\min_{\boldsymbol{t},\boldsymbol{r}} f(\boldsymbol{m}; \boldsymbol{X}, \boldsymbol{Y}). \tag{5.25}$$

5.3.2.2 Objective Functions for the Optimization

Many objective functions for the optimization problem given in eq. 5.25 have been proposed, e. g. the sum of squared distances and the Hausdorff distance in [SWHP07], approximations of the unsigned distance function (l_1-norm) in [Flö10], and projected distances and the convex hull volume in [SAMW15]. Some of these functions are phrased as least-squares problems and are theoretically backed by the Gauss-Markov theorem [Flö10], some of them may result in non-smooth optimization problems. However, as a result of trials and systematic experiments, a focus is set on signed and absolute projected distance functions as well as convex hull volume computations in the following.

Since assembly processes are usually performed along predominant directions, the distance-based objective functions should consider these directions $\boldsymbol{w}$ in the evaluation of part feature distances. Thus, the vector $\boldsymbol{w} \in \mathbb{R}^3$ is defined as the assembly direction, being the main direction for the assembly step in the global coordinate system. It is typically determined by the invariant translations of the contact features and can be obtained from CAD by exporting

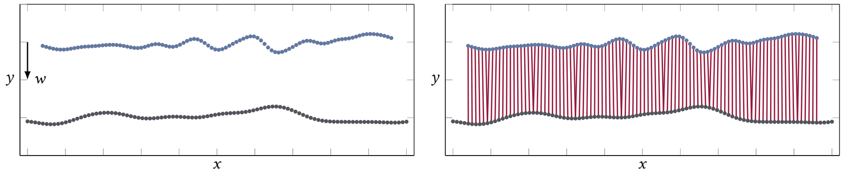

(a) Pre-Assembly Position of two Plane Features with Assembly Direction $\boldsymbol{w} = (0 \ -1)$

(b) Determination of Point Correspondences

Figure 5.36: Determination of the Point Correspondences

the assembly constraints. For example, if we consider a contact of two x-y-planes, then the feature assembly is performed in z-direction and $\boldsymbol{w}$ yields to $\boldsymbol{w} = (0 \ 0 \ 1)$. Furthermore, the distance functions are determined for every point of the moving part $\boldsymbol{Y}$ and its corresponding point in the fixed part $\boldsymbol{X}$ similarly to the ICP algorithm. For this purpose, the nearest neighbour (sometimes called *foot-point*) $\boldsymbol{x}_{y_i}$ for every point of the data shape feature $\boldsymbol{y}_i$ in $\boldsymbol{X}$ is computed by maximizing an adapted projected point-to-point distance a_j, which will be discussed in eq. (5.36) [AS05]:

$$\boldsymbol{x}_{y_i} = \boldsymbol{x}_{j^*}, \quad \text{where} \quad j^* = \arg\max_j \left(a_j\right). \tag{5.26}$$

In contrast to the ICP approach, these correspondences are not determined iteratively, but based on a pre-assembly position. Therefore, we deal with a registration problem for known point correspondences. The determination of the point correspondences is illustrated in Figure 5.36 for two plane features (without loss of generality, the 3D problem is reduced to 2D for the sake of improved comprehensibility).

The discussed objective functions for the optimization problem in eq. (5.25) are illustrated in Figure 5.37 for the assembly of two plane features in 2D:

- *Signed projected distance:* The distances between the adjusted points $\boldsymbol{m}(\boldsymbol{y}_i)$ and their correspondences $\boldsymbol{x}_{y_i}$ are projected along the assembly direction $\boldsymbol{w}$. Hence, the projected distance is defined as:

$$d_{\mathrm{PS}}\left(\boldsymbol{m}(\boldsymbol{y}_i), \boldsymbol{x}_{y_i}, \boldsymbol{w}\right) = \left(\boldsymbol{m}(\boldsymbol{y}_i) - \boldsymbol{x}_{y_i}\right) \cdot \boldsymbol{w}'. \tag{5.27}$$

  The objective function is then the *sum* of these *absolute* projected distances:

$$f_{\mathrm{PS}}(\cdot) = \sum_{i=1}^{M} \left| d_{\mathrm{PS}}\left(\boldsymbol{m}(\boldsymbol{y}_i), \boldsymbol{x}_{y_i}, \boldsymbol{w}\right) \right|. \tag{5.28}$$

  Due to the formulation of the optimization problem as a minimization task, the use of the absolute values $|d_{\mathrm{PS}}|$ is required to avoid negative values of the objective function, which may lead to implausible part positions.

- *Signed Normal Distance:* With some similarity to Flöry et al. [FH10], the directions for

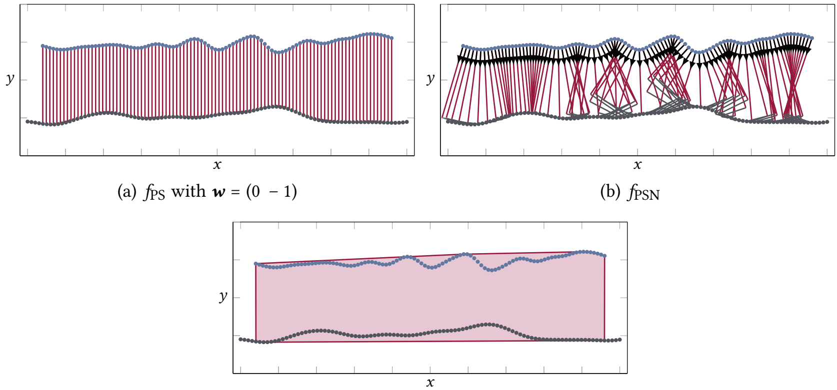

(a) f_{PS} with $\boldsymbol{w} = (0 \ -1)$

(b) f_{PSN}

(c) f_{Hull}

Figure 5.37: The Objective Functions for the Constrained Optimization

the signed projected distance can also be defined individually for every point pair as the vertex normals of the data points $\boldsymbol{w}_i := \boldsymbol{n}_{\boldsymbol{y}_i}$, which results in a distance-to-tangent measure:

$$d_{\mathrm{PSN}}\left(\boldsymbol{m}(\boldsymbol{y}_i), \boldsymbol{x}_{y_i}, \boldsymbol{n}_{\boldsymbol{x}_{y_i}}\right) = \left(\boldsymbol{m}(\boldsymbol{y}_i) - \boldsymbol{x}_{y_i}\right) \cdot \boldsymbol{n}'_{\boldsymbol{y}_i}. \tag{5.29}$$

For the objective function, again the absolute value of the projected distance metric is used:

$$f_{\mathrm{PSN}}(\cdot) = \sum_{i=1}^{M} \left| d_{\mathrm{PSN}}\left(\boldsymbol{m}(\boldsymbol{y}_i), \boldsymbol{x}_{y_i}, \boldsymbol{n}_{\boldsymbol{y}_i}\right)\right|. \tag{5.30}$$

- *Convex Hull Volume:* In contrast to the previous ones, the idea behind this objective function is the minimization of the volume between the part features. For this purpose, the volume of the convex hull of the data shape feature points and their correspondences in $\boldsymbol{X}$, being $\boldsymbol{X}_{\boldsymbol{Y}}$, is computed, e. g. employing the QuickHull algorithm [BDH96], and minimized. In this regard, the objective functions yields to:

$$f_{\mathrm{Hull}}(\cdot) = CV(\boldsymbol{X}_{\boldsymbol{Y}} \cup \boldsymbol{m}(\boldsymbol{Y})), \tag{5.31}$$

where $CV(\cdot)$ returns the volume of the convex hull. It is worth mentioning, that the results of this objective function are not influenced by inhomogeneous point cloud densities in contrast to the previously introduced point-distance based objective functions.

In real assembly processes, certain degrees of freedom are kept invariant by assembly fixtures. In order to consider this issue, constraints for specific components of $\boldsymbol{t}$ and $\boldsymbol{r}$ can be added in the formulation of the optimization problem, e. g. for a straight plane-to-plane assembly in z-direction with three degrees of freedom (t_z, r_x, r_y), the remaining translations along the x- and y- direction as well as the rotation around the z-direction are constrained:

$$\begin{aligned} &\min_{\boldsymbol{t},\boldsymbol{r}} f(\boldsymbol{m}; \boldsymbol{X}, \boldsymbol{Y}), \\ &\text{subject to } t_x = 0, t_y = 0, r_z = 0. \end{aligned} \tag{5.32}$$

Moreover, the adding of non-linear constraints has been used to respect the non-interference requirement R2 [Flö09, PR07b]. For example, the signed normal distance function can be added to constrain the minimization problem. Expressively spoken, the signed normal distance between any of the reference points and their correspondences is not to take a negative value, since this indicates interfering part positions. In this regard, the minimization problem in eq. (5.25) yields to:

$$\begin{aligned} &\min_{\boldsymbol{t},\boldsymbol{r}} f_{<\cdot>}(\cdot) \\ &\text{subject to } d_{\mathrm{PSN}}\left(\boldsymbol{m}(\boldsymbol{y}_i), \boldsymbol{x}_{y_i}, \boldsymbol{w}\right) \leq 0, \quad \forall_{\boldsymbol{y}_i \in \boldsymbol{Y}}. \end{aligned} \tag{5.33}$$

In analogy, the signed projected distances d_{PS} can be added as constraints, though signed normal distances d_{PSN} are more representative for part interference. However, d_{PS} does not require the computation of point normals. These point-based constraints can also be used in combination with the convex hull volume based objective function f_{Hull}.

The numerical solution of this constrained optimization problem is performed employing active set methods. Illustrative results for the relative positioning of two plane features and various objective functions with non-linear constraints are shown in Figure 5.38. It can be seen, that the adding of constraints based on signed projected distances and signed normal distances leads to realistic part positions.

It is worth mentioning, that there are approaches to discard the non-linear constraints and to convert the constrained optimization problem to an unconstrained optimization problem by adding penalty functions in case of part interference to the objective functions (i. e. in the case of $\boldsymbol{d}_{\mathrm{PSN}}\left(\boldsymbol{m}(\boldsymbol{y}_i), \boldsymbol{x}_{y_i}, \boldsymbol{w}\right) > 0$, $\forall_{\boldsymbol{y}_i \in \boldsymbol{Y}}$) [PR07b, SWHP07]. However, no instructions for the choice of the required penalty terms in case of constraint violations is given, which hinders the application of this adoption to the constrained registration in the context of computer-aided tolerancing.

5.3.2.3 Positioning based on the Difference Surface

In contrast to approaches for the registration of point clouds, Samper et al. [SAFP09] present a method for the assembly modelling based on the computation of the difference surface. The difference surface is defined to comprise the deviations between the model and the data shape. In doing so, the relative positioning problem between the model and the data shape is converted to a relative positioning problem between the difference surface and a perfect surface.

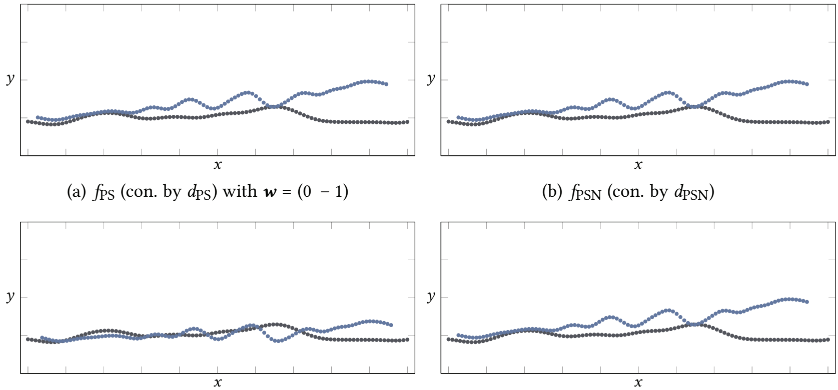

(a) f_{PS} (con. by d_{PS}) with $\boldsymbol{w} = (0 \ -1)$

(b) f_{PSN} (con. by d_{PSN})

(c) f_{Hull} (unconstrained)

(d) f_{Hull} (con. by d_{PS} with $\boldsymbol{w} = (0 \ -1)$)

Figure 5.38: Exemplary Results of the Relative Positioning with various Objective Functions

Since the approach of Samper et al. [SAFP09] is part of a modal tolerancing approach [FS07], the difference surface is computed based on a modal decomposition of both shapes in their work. For this purpose, both mating surfaces are identically discretized to compute their eigenshapes (modes) employing the Finite Element Analysis (FEA). Thereafter, the modes are fitted to measured surfaces based on a projection operator to obtain the modal spectrum of both mating surfaces. The difference surface between these mating surfaces is then easily computed as the difference between their modal spectra. Once the difference surface is computed, the contact points between the mating surfaces can be found as the intersection of the mating force vector (e. g. assembly or inertial force) and the convex hull of the difference surface. A detailed explanation is given in the following. However, as can be seen, a main drawback of this procedure is the computation of the difference surface based on modal shapes, since it does not allow for different discretizations of the mating surfaces. In the context of virtual product development, where the available surface discretization for each part is often dependent on precision requirements in structural analysis or manufacturing process simulations, this hinders the application of the approach to the integrated computer-aided tolerance analysis. Therefore, in the following, the approach is expanded to overcome this shortcoming and to allow the positioning of parts with different surface discretizations by applying and integrating ray tracing approaches for both point cloud- and surface mesh-based models.

As mentioned before, assembly processes are usually performed along predefined assembly directions and under the presence of inertial forces. In the last preceding subsection, registration techniques have been adapted in order to fit the data shape to the model shape along these directions by using projected distance functions. According to the difference surface approach for the relative positioning, the point-related distances between the data shape and the model shape along the assembly direction $\boldsymbol{w} \in \mathbb{R}^3$ are computed employing a ray trace algorithm for point clouds, which has been introduced as the *directed projection* algorithm [AS05, Aza04, LPY+06]. The algorithm finds the directed projection $\boldsymbol{y}_i' = \boldsymbol{y}_i + d_i\boldsymbol{w},\ d_i \in \mathbb{R}$ of a point $\boldsymbol{y}_i$ of the data shape onto the reference shape $\boldsymbol{X}$ in a predefined direction $\boldsymbol{w}$ by minimizing the sum of projected squared point-to-point distances [AS05, Aza04]: $\min \sum_{j=1}^{N} a_j||\boldsymbol{y}'_i - \boldsymbol{x}_j||^2$. It has been shown, that the solution to this problem can be given as [AS05]:

$$d_i = \frac{\lambda - \boldsymbol{y}_i \cdot \boldsymbol{w}}{||\boldsymbol{w}||^2}, \tag{5.34}$$

where:

$$\lambda = \frac{c_1 w_x + c_2 w_y + c_3 w_z}{c_0}, \tag{5.35}$$

with $c_0 = \sum_{j=1}^{N} a_j$, $c_1 = \sum_{j=1}^{N} a_j \boldsymbol{x}_j^x$, $c_2 = \sum_{j=1}^{N} a_j \boldsymbol{x}_j^y$, and $c_3 = \sum_{j=1}^{N} a_j \boldsymbol{x}_j^z$. As it has been pointed out by [AS05], the definition of the weights a_j has huge effects on the computation of the projection $\boldsymbol{y}'_i$. In the following, the weight function of [AS05] is slightly adapted as follows:

$$a_j = \frac{1}{||\boldsymbol{x}_j - \boldsymbol{y}_i||^2||(\boldsymbol{x}_j - \boldsymbol{y}_i) \times \boldsymbol{w}||^2}. \tag{5.36}$$

In order to increase the accuracy of the projection, insignificant points in $\boldsymbol{X}$ are gradually removed by an iterative procedure. Further detail of this algorithm can be found in [AS05].

Alternatively, when employing a surface mesh representation of deviated workpiece representatives, ray-triangle intersection algorithms as for example presented in [HH10] are used to compute the point-related distances d_i. In order to establish the difference surface for the general case when $\boldsymbol{w} = \boldsymbol{w}_z = (0\ 0\ 1)$, these distances d_i are used to replace the point z-coordinates of the data shape. Moreover, also the distances d_i^* between model shape and the data shape in the negative assembly direction $\boldsymbol{x}'_i = \boldsymbol{x}_i - d_i^* \boldsymbol{w}$, $d_i^* \in \mathbb{R}$ can be added to the difference surface in order to avoid inadequate part positions. For any case, when $\boldsymbol{w} \neq \boldsymbol{w}_z$, a coordinate transformation is performed prior to the relative positioning leading to $\boldsymbol{w} = \boldsymbol{w}_z$, i. e. the part positions are adapted so that the assembly is performed in z-direction. Consequently, the difference surface $\boldsymbol{S} = \{\boldsymbol{s}_i \in \mathbb{R}^3 : i = 1, ..., M\}$ is obtained as the x- and y-coordinates of the data shape ($\boldsymbol{Y}_x$ and $\boldsymbol{Y}_y$, respectively) and the distances $\boldsymbol{d}$ in the z-coordinate direction:

$$\boldsymbol{S} = (\boldsymbol{Y}_x \quad \boldsymbol{Y}_y \quad \boldsymbol{d}). \tag{5.37}$$

Thereafter, the convex hull of the difference surface is computed using e. g. the QuickHull algorithm [BDH96] and intersected with the force slope $\boldsymbol{F} = \boldsymbol{P} + \lambda\boldsymbol{w}, \lambda \in \mathbb{R}$ consisting of the force application point $\boldsymbol{P}$ and the assembly direction $\boldsymbol{w}$ as illustrated in Figure 5.39 (b). Since this usually results in two intersecting points, the minimal of both with regard to the distances d_i is chosen and marks the relevant segment (2D) or triangle (3D) of the convex hull. The vertices of the relevant segment or triangle in $\boldsymbol{Y}$ are then fitted to their projections on the model shape $\boldsymbol{Y}' = \{\boldsymbol{y}'_i \in \mathbb{R}^3 : i = 1, ..., M\}$, with $\boldsymbol{y}'_i = \boldsymbol{y}_i - d_i \cdot \boldsymbol{w}$, to obtain the final part position (see Figure 5.39 (c)). For this purpose, for example the absolute orientation approach [Hor87] can be used.

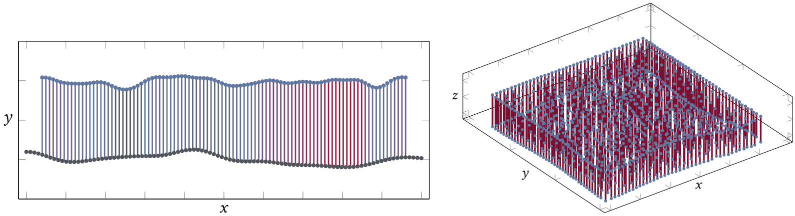

(a) Computation of the point-to-surface distances by Ray Tracing

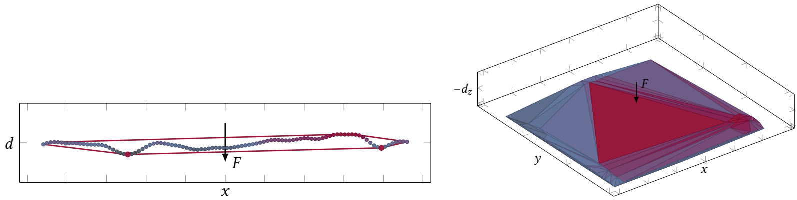

(b) Convex Hull Computation of the Difference Surface and Intersection with the Force Vector

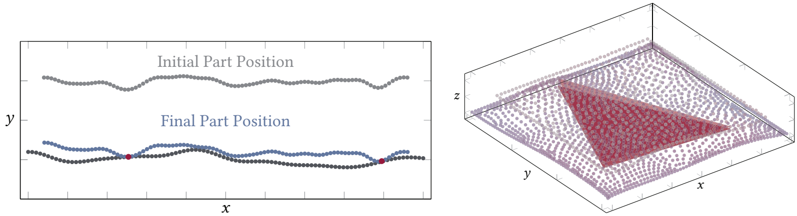

(c) Final Assembly Position and Contact Points/Contact Triangle

Figure 5.39: Procedure for the Relative Positioning based on the Difference Surface

In this context, the force application point $\boldsymbol{P}$ of the assembly force has a huge effect on the resulting part position as can be seen from Figure 5.40, where the shifting of the force application point in x-direction leads to a lifting of the data shape. In order to consider inertial forces, the force application point is set to the center of gravity in the following.

5.3.3 Assembly Simulation for Skin Model Shapes

In the previous section, two kinds of approaches for the relative positioning of discrete geometry workpiece representatives have been proposed, namely constrained registration approaches and an algorithm based on the computation of the difference surface between mating part features. Furthermore, they have been applied to the part positioning in consideration of *single* mating features. In this section, these approaches are applied to the relative positioning considering *multiple* features, as a primary problem in assembly simulations in the context of computer-aided design and computer-aided tolerancing.

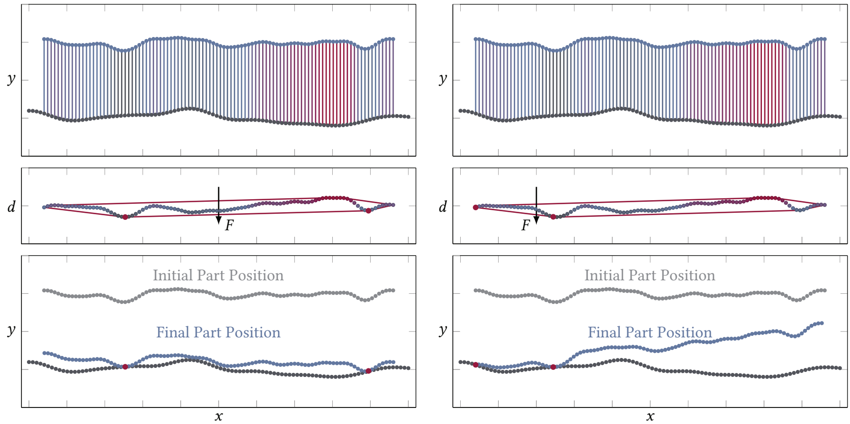

(a) Standard Force Application Point (b) Shifted Force Application Point

Figure 5.40: Influence of the Force Application Point on the resulting Part Position

5.3.3.1 3-2-1 Positioning of Planar Parts

In industrial applications, 3-2-1 locating schemes (sometimes also called positioning or fixture layouts), as can be seen from Figure 2.15, are often used to locate parts in assemblies and consequently to lock their six degrees of freedom (dof) [SJ99, SLC06a]. In the following, the simulation of such a 3-2-1 positioning of planar parts with form deviations is performed *simultaneously* employing the constrained registration and, in contrast to that, *sequentially* with the difference surface approach. For this purpose, a cube is assembled with a block as illustrated in Figure 5.41. As a pre-processing step, the relevant plane features of both the cube and the block are obtained employing GeoSpelling partition operations [DBM08] as can be seen from Figure 5.41 (b).

Registration for 3-2-1 Positioning The assembly simulation of a 3-2-1 positioning considering form deviations is a non-trivial task and an ongoing challenge for research in the fields of tolerancing, CAD, and computational geometry, since every single assembly step has an effect on the part's assembly environment. This is illustrated in Figure 5.42, where the 2-1 assembly of two rectangular plane features with form deviations is shown. It can be seen, that the first assembly step w_2 (see Figure 5.42 (b)) leads to two contact points in y-direction between the blue and the grey part, whereas the sequential execution of the second assembly step w_1 in Figure 5.42 (c) leads to one contact point in x-direction and the dissolving of the two contact points in y-direction (only one contact point remains). However, the expected final part position is illustrated in Figure 5.42 (d) with two contact points in y-direction and one in x-direction.

A straightforward idea to solve the assembly simulation problem for a 3-2-1 locating scheme employing constrained registration methods is to perform the assembly steps iteratively.

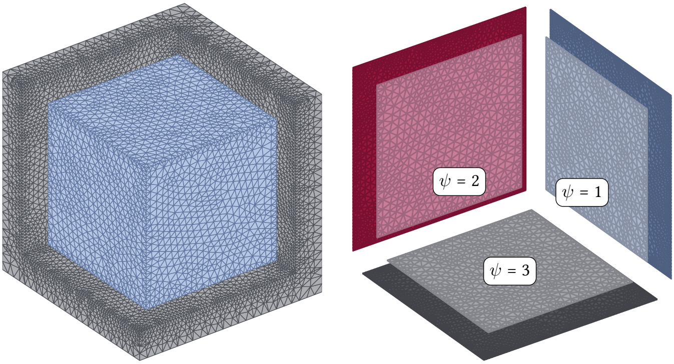

(a) Nominal Parts of the Example (b) Partition of the relevant Plane Features

Figure 5.41: Illustrative Example for the 3-2-1 Positioning of Planar Parts (Surface Mesh Representation)

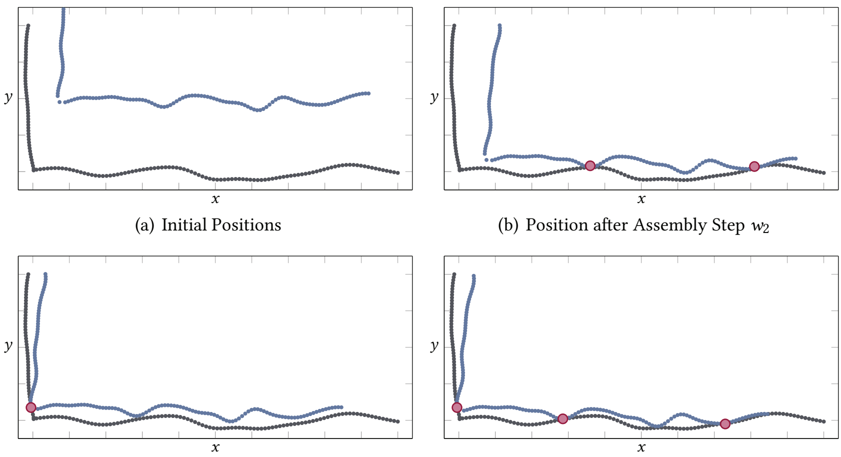

(a) Initial Positions (b) Position after Assembly Step w_2

(c) Position after Assembly Step w_1 (d) Final Position for the 2-1 Positioning

Figure 5.42: Dependence of the Part Position on the Assembly Step for a 2-1 Positioning

Table 5.1: Objective Function for the Constrained Registration of a 3-2-1 Positioning

$f_\Sigma = 0$; $\boldsymbol{Y} = \alpha(\boldsymbol{Y})$;
for $\psi = \{3; 2; 1\}$ **do**
  $\boldsymbol{Y}_\psi = \text{Partition}(\boldsymbol{Y}, \psi)$;
  $\boldsymbol{X}_\psi = \text{Partition}(\boldsymbol{X}, \psi)$;
  $\boldsymbol{X}_{\boldsymbol{Y}_\psi} = \text{DetermineFootPoints}(\boldsymbol{X}_\psi, \boldsymbol{Y}_\psi, \boldsymbol{w}_\psi)$;
  $d_\psi = \frac{\omega_\psi}{M_\psi} f_W(\boldsymbol{Y}_\psi, \boldsymbol{X}_{\boldsymbol{Y}_\psi}, \boldsymbol{w}_\psi)$;
  $f_\Sigma = f_\Sigma + \omega_\psi \cdot d_\psi$;
end for

Though, since the constrained registration approaches result in best-fit positions for every assembly step, the part position of the preceding assembly step is dissolved. Therefore, a combined formulation of the optimization problem is required and the constrained registration approach based on the absolute projected distance is adapted as follows, with the assembly steps being subscripted according to the number of locked dofs in the following (i. e. the first assembly step of a 3-2-1 positioning is depicted as $\psi = 3$):

- The part features for the assembly steps ($\boldsymbol{Y}_\psi$ and $\boldsymbol{X}_\psi$, $\psi = 1, 2, 3$) are obtained by partition operations, where $\boldsymbol{Y}_\psi \subseteq \boldsymbol{Y}$, $\boldsymbol{X}_\psi \subseteq \boldsymbol{X}$ and $M_\psi = |Y_\psi|$ (alternatively $M_\psi = \#Y_\psi$) for $\psi = 1, 2, 3$.
- The objective function is the sum of weighted *average* absolute projected distances:

$$f_\Sigma = \sum_{\psi=1}^{3} \frac{\omega_\psi}{M_\psi} f_{\text{PS}}(\boldsymbol{Y}_\psi, \boldsymbol{X}_\psi, \boldsymbol{w}_\psi), \tag{5.38}$$

  where $\boldsymbol{w}_\psi$ is the assembly direction of the respective assembly step, e. g. $\boldsymbol{w}_3 = (0\ 0\ -1)$. In this regard, the weights for the average point distances are chosen to respect the assembly steps as $\omega = \{3; 2; 1\}$ in analogy to [SWM⁺10a], where non-averaged objective functions are employed for unconstrained optimization formulations. This means, that the point-to-point distances, which are relevant for the first assembly step, are weighted three-times the point-to-point distances of the last assembly step. However, an adaptive weighting of the assembly steps could also be performed to consider different form deviations of the contact surfaces. The point-wise averaging of the unsigned projected distance function is used to avoid influences of different cardinal numbers M_i (otherwise features with many points would have a stronger contribution to f_Σ than features with less points).

The registration itself is performed by minimizing the objective function f_Σ, where a pseudo-code of the objective function f_Σ for the 3-2-1 positioning is given in Table 5.1. In this context, non-linear constraints based on the signed projected distance d_{PS} are added for every part feature $\boldsymbol{Y}_\psi$ according to the respective assembly directions $\boldsymbol{w}_\psi$ in order to avoid part interference.

Difference Surface Computation for 3-2-1 Positioning In contrast to the constrained registration approach, which solves the 3-2-1 positioning problem simultaneously, the dif-

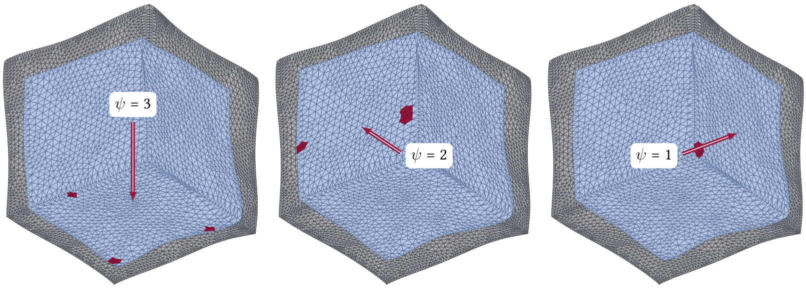

(a) 3-Point Move in z-Direction (b) 2-Point Move in y-Direction (c) 1-Point Move in x-Direction

Figure 5.43: 3-2-1 Positioning employing the Difference Surface Approach

ference surface method is employed to solve the three assembly steps sequentially. For this purpose, the part position after the first assembly step is computed based on the 3D difference surface approach for the translation in z-direction as can be seen from Figure 5.43 (a). Thereafter, the second assembly step is performed employing the 2D adaption of the difference surface algorithm (Figure 5.43 (b)). The last assembly step is then a simple translation along the x-direction (Figure 5.43 (c)), in which the amount of translation d_x is given by:

$$d_x = \min(d_i), \quad i = 1, \ldots, M. \tag{5.39}$$

For perfectly planar parts, the sequential execution of the three assembly steps seems admissible, since the data shape can be freely moved along the mating planes of the model shape. However, this does not hold when considering form deviations, since they prevent free movements along the remaining coordinate directions, which may lead to improper part positions after the positioning. This can be seen from Figure 5.44 (a), where intersections (red areas) of the part surface meshes are computed employing a mesh generator (tetgen) for illustration after the sequential execution of the three assembly steps. In order to solve this problem, similarly to the ICP, an iterative execution of the three assembly steps is performed until the change of the part position falls below a critical value *crit* or the algorithm reaches a predefined number of iterations i_{max}. A pseudo-code of this procedure is given in Table 5.2. The change of the part position can for example be computed as the Euclidean distance between a reference point in the data shape before and after the positioning iteration. The iterative procedure avoids inadmissible part positions and ensures, that the relative positioning represents the part behaviour according to the given assembly sequence (see Figure 5.44 (b)).

Results of the Approaches for the 3-2-1 Positioning The final assembly position for the two different approaches for the 3-2-1 positioning of planar parts are shown in Figure 5.45, in which part interferences are highlighted in red. As can be seen, both approaches lead to slight interference in the contact points as expected, with the part interference at the bottom features being more distinct for the constrained registration than for the difference surface approach. Though, both approaches conform to requirement R2. Furthermore, both methods

Table 5.2: Algorithm of the Relative Positioning with multiple Assembly Steps

dev = Inf; $i = 0$; $\boldsymbol{Y}_0^* = \boldsymbol{Y}$;
while $dev > crit$ **and** $i < i_{\max}$ **do**
  $\boldsymbol{Y}_{i+1}^* = \text{3DdiffSurf}(\boldsymbol{Y}_i^*)$;
  $\boldsymbol{Y}_{i+1}^* = \text{2DdiffSurf}(\boldsymbol{Y}_{i+1}^*)$;
  $\boldsymbol{Y}_{i+1}^* = \text{1DdiffSurf}(\boldsymbol{Y}_{i+1}^*)$;
  $dev = \text{getPartDev}(\boldsymbol{Y}_{i+1}^*, \boldsymbol{Y}_i^*)$;
  $i = i + 1$;
end while

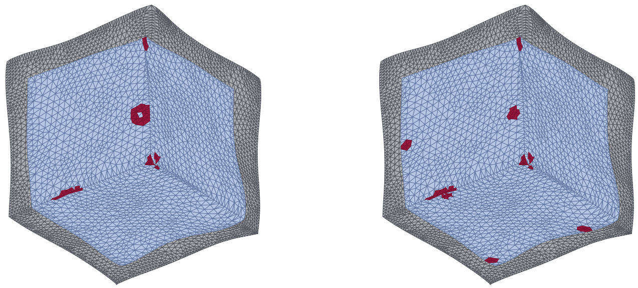

(a) Part Position after one Iteration (b) Part Position after fifteen Iterations

Figure 5.44: Part Positions of planar Parts with Form Deviations for the Difference Surface Approach: Inadmissible Part Interferences (red Areas) can be observed after one Iteration, whereas corresponding Contact Points result after fifteen Iterations.

converge to the nominal assembly position for nominal parts and therefore fulfil requirement R3.

However, in order to compare the resulting part positions of both approaches, the point projections of $\boldsymbol{Y}$ in $\boldsymbol{X}$ according to eq. (5.34) of the relevant part features are compared. The directed distances d_i between each mating features $\boldsymbol{y}_i$ and $\boldsymbol{y}_i^*$ for each of the three assembly steps can be seen from Figure 5.46, where it can be found, that both approaches lead to comparable results for this example. However, it can be seen from the histograms of d_i that the distances for the side features ($\psi = 1, 2$) differ considerably between the methods. This is influenced by the weighting vector ω in the constrained registration approach. Though, the choice of adequate weights ω is a non-trivial problem and a drawback of this method for the 3-2-1 positioning of planar features.

5.3.3.2 Positioning of Cylindrical Features

Beside planar features, the positioning of cylindrical fits, such as pin-and-hole connections, is of high importance in the assembly of mechanical products. In this context, a typical classification of such pin-and-hole connections is based on the clearance between the parts after the positioning. In this regard, it can generally be distinguished between *loose* and *tight* fits. The assembly processes of these fits differ in terms of the exerted assembly force, since tight fits require a higher mating force due to small elastic part deformations. As a consequence, these

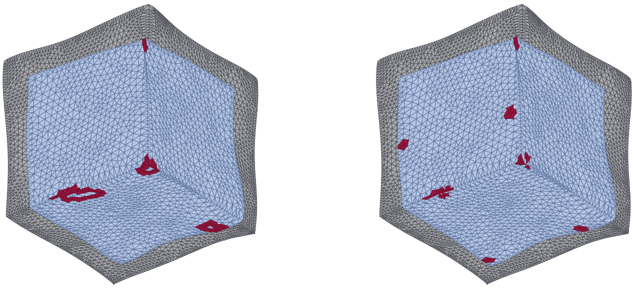

(a) Constrained Registration for deviated Parts (b) Difference Surface for deviated Parts

Figure 5.45: Exemplary Results of the 3-2-1 Positioning

types of fit require different strategies from a computational point of view:

- Mating forces introduce small elastic part deformations in the assembly of *tight fits*. Therefore, slight part interference is allowed in the relative positioning of rigid parts and requirement R2 is dropped. Thus, the ICP or unconstrained registration approaches can be used to simulate the behaviour of tight fits.
- Clearances between the parts result in the assembly of parts with *loose fit*. Consequently, no part interference should occur, which is conform to R2. Hence, constrained registration approaches or the difference surface approach should be used for the relative positioning of loose fits.

In the following, the positioning of cylindrical features with loose fit is illustrated by a pin-hole assembly as illustrated in Figure 5.47 and a two-pin-two-hole assembly as can be seen from Figure 5.51, which refer to typical study cases in the context of computer aided tolerancing [DQ09].

Constrained Registration for Cylindrical Feature Positioning The general formulation of the constrained registration problem allows the distinction between relevant part features for the minimization and for the constraint formulation. In this regard, the contacting plane of the pin head (Opt. Feature in Figure 5.47) is used for the minimization of the objective function, whereas a feature composed of the optimization feature, two cylinders, and the back of the cylinder (Con. Feature in Figure 5.47) is used for the constraint formulation as can also be seen from Figure 5.48. In doing so, the pin is positioned to obtain a minimal gap between the pin head and the hole considering the non-interference requirement for the whole pin.

Difference Surface Computation for Cylindrical Feature Positioning The assembly simulation based on the difference surface approach requires the definition of an assembly direction. For the presented example, a straightforward idea is to choose this direction according to the predominant direction of the pin. However, this may lead to implausible part positions in the final assembly depending on the part deviations of the pin head and the hole opening, since part interference may occur between the pin body and the hole as can be seen from Figure 5.49.

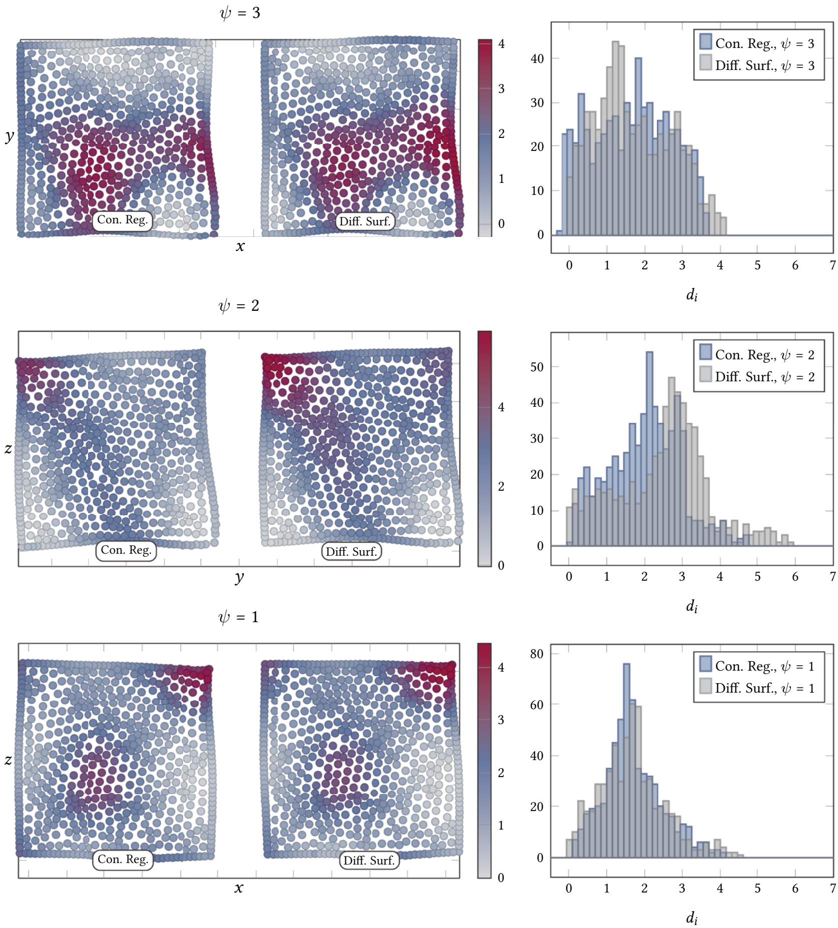

Figure 5.46: Distances between the Points of $\boldsymbol{Y}$ and their Projections in $\boldsymbol{X}$ after the Positioning

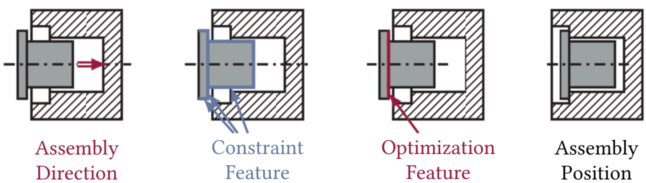

Figure 5.47: Pin-Hole Example for the Positioning of Cylindrical Features

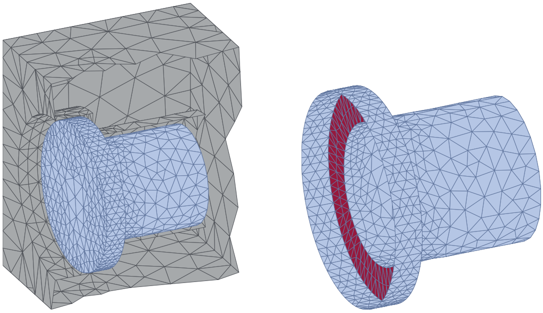

Figure 5.48: Pin in the Hole (left) as well as Optimization Feature (red) and Constraint Feature (blue) of the Pin (right)

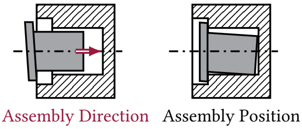

Figure 5.49: Deviated Pin in the Hole: The nominal Assembly Direction may lead to implausible Part Positions

In order to solve this issue, the assembly direction should be adjusted. Though, so far, there is no adequate algorithm to perform this efficiently. Thus, the choice of the "optimal" assembly direction holds some difficulties. Therefore, this approach may lead to implausible assembly positions, which can be regarded as a drawback of the difference surface approach in the positioning of cylindrical features.

Results of the Approaches for the Positioning of Cylindrical Features In analogy to the result presentation for the 3-2-1 positioning, the assembly positions as well as the point distances between the optimization feature are shown in Figure 5.50 for both relative positioning approaches. It can be seen, that the difference surface approach leads to a slightly tighter assembly position than the constrained registration method. However, it does not necessarily ensure the non-interference requirement for the complete pin, since only the planar contact between the pin head and the hole is considered.

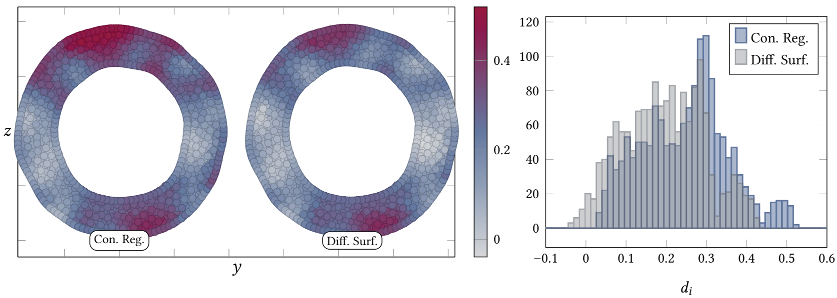

Figure 5.50: Distances between the Points of $\boldsymbol{Y}$ and their Projections in $\boldsymbol{X}$ after the Positioning for Cylindrical Features

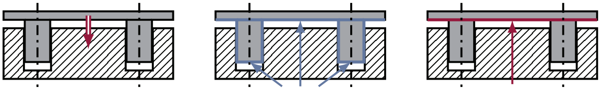

Figure 5.51: Over-constrained Assembly for the second Case Study

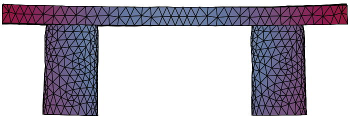

(a) Skin Model Shape obtained from an Injection Molding Simulation with magnified Deviations

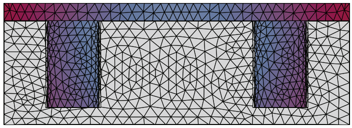

(b) Result of the Assembly Simulation

Figure 5.52: Skin Model Shape and resulting Assembly

Over-constrained Assemblies Particularly, the constrained registration approach for the assembly simulation of Skin Model Shapes can also be applied to the simulation of the part behaviour in over-constrained assemblies. In this regard, an over-constrained assembly similarly to the examples studied in [BPM08, DBM08, BGDD13] is analysed. It consists of a part with two tied cylinders and their corresponding holes in the second part as shown in Figure 5.51. The relevant constraint and optimization features are chosen in analogy to the example presented in section 5.3.3.2. For this example, a focus is set on the assemblability evaluation based on Skin Model Shapes, which are gathered from an injection molding simulation as can be seen from Figure 5.52 (a) with magnified deviations. For the assembly simulation, the constrained registration approach based on the absolute projected distance function f_{PS} with the assembly direction as projection vector and the signed normal distances d_{PSN} as constraints are employed. Regarding the part assemblability, it can be found, that the assembly is feasible, if the constrained optimization converges and results in an adequate part position. The results of the assembly simulation based on the constrained optimization approach for the case study can be seen from Figure 5.52 (b), where it can be found that the assembly is feasible though the presence of part deviations as a consequence of shrinkage and warpage.

5.3.3.3 Discussion of the Approaches for the Relative Positioning

Both presented approaches for the relative positioning of point-based Skin Model Shapes enable the assembly simulation of non-ideal part representatives. Main similarities between these approaches can be found in the fact, that they require the specification of assembly characteristics, that they converge to the nominal part position for nominal parts (R3) and that they prevent assembly positions causing part interference (R2). However, major differences between both approaches can be found as follows:

- In contrast to the constrained registration method, the difference surface approach aims not at minimizing the distances between any point pair of the features employing optimization algorithms, but computes deterministic contact points based on point-wise feature distances. Therefore, it does not fulfil R1 in a strict sense. However, as mentioned before, this requirement is not relevant for realistic assemblies.

- The constrained registration approach with (point) distance based objective functions is prone to inhomogeneous point densities, i. e. feature areas with a high point density contribute more to the objective function than sparely occupied areas. This may lead to implausible assembly positions. In order to avoid this, volume based objective functions combined with point based constraints can be employed. However, these problems do not arise in the difference surface approach.

Based on these similarities and differences as well as on the presented studies, it can be found, that the difference surface approach is well suited for simulating the assembly of parts along predominant assembly directions, such as for example planar contacts, whereas the constrained registration method should be considered for assembly processes with "best-fit" requirements, such as cylindrical joints and complex mating surfaces. However, it can be concluded, that a careful choice of relative positioning algorithms is required for different assembly processes.

5.3.4 Application to the Example Case Study

After the Skin Model Shapes for the example case study have been generated and scaled, they have to be assembled according to the positioning scheme. In order to perform this, two approaches have been developed, with the first one formulating the relative positioning problem as a constrained registration problem, which is solved using mathematical optimization approaches, whereas the second approach employing the difference surface between two mating parts to calculate the contact points in a specified assembly direction.

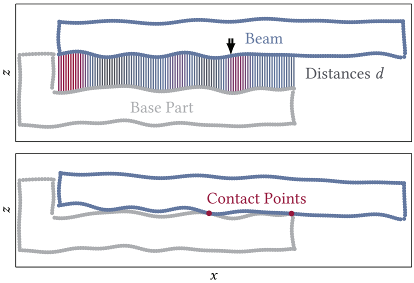

Figure 5.53: Relative Positioning for the Example Case Study: Positioning of the Beam employing the Difference Surface Approach

The relative positioning approach based on the difference surface identifies the contact points between two parts from their difference surface (see Figure 5.53) and enables the assembly simulation for a 3-2-1 positioning scheme by iteratively repeating the single assembly steps.

In contrast to that, the constrained registration approach uses mathematical optimization methods to minimize the sum of projected (signed) distances between the set of points in the moving part and their correspondences in the mating part (see Figure 5.54), such that these projected distances do not take negative values.

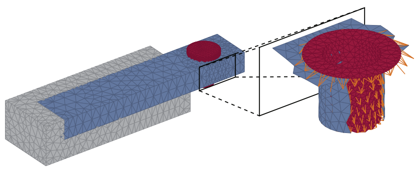

Figure 5.54: Relative Positioning for the Example Case Study: Correspondences of the Pin in the Beam for the Constrained Registration

This approach is well suited for the assembly simulation of best-fit conditions, as for example loose fits. In the studied example, the 3-2-1 positioning of the beam onto the base part is simulated using the difference surface approach, whereas the assembly of the pin in the beam is performed employing the constrained registration approach. A resulting assembly of the case study considering form tolerances can be seen from Figure 5.55.

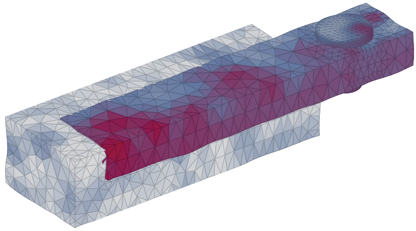

Figure 5.55: Resulting Assembly of the Case Study with magnified Form Deviations.

The proposed approaches for the assembly simulation of Skin Model Shapes can be applied for the tolerance analysis of static assemblies, but can also be used for the motion tolerancing by quasi-statically repeating the assembly simulation with varying initial part positions, which will be discussed in the next but one section.

5.4 Gap Hull Estimation for Skin Model Shapes

The embodiment of mechanical joints is both a highly demanding as well as responsible activity in the design of physical artefacts. In this regard, clearances play an important role in the behaviour of mechanical joints and thus influence the behaviour of the final product during use [RA96]. In order to predict these effects, models for the estimation of the gap hull, which is the domain of physically feasible rigid body transformations of a mechanical joint with clearance, are required. In the following section, an approach for the estimation of the gap hull, i. e. the set of all physically feasible positions of a part in a mechanical joint with clearance, by means of difference surface computations is highlighted and illustrated in two case studies.

5.4.1 Related Work

The consideration of joint clearance in the design and dimensioning of mechanical interfaces is a steady research issue. In this context, for example the effects of joint clearances on the position and orientation deviation of linkages have been studied in [TZW00, FSPB11], a kinematic sensitivity analysis of linkages with joint clearance has been performed in [TL04], and a clearance influence analysis is described in [PCV05]. Moreover, a comparison of revolute joint clearance models is provided in [SMM02], whereas computer models for the dynamic analysis of multibody systems with joint clearance is presented in [FA04], and a robust tolerance design for mechanism with joint clearance is presented in [HZ10]. Beside this, the concept of the clearance space [GDTA92] has been proposed to describe and represent clearances in mechanical assemblies.

Indeed, few works consider form deviations of the mating parts in the analysis of joint clearance. However, form defects of a single pair of mating surfaces in a planar joint have been analysed in [LLB14] employing the concepts of the gap hull and the difference surface [SAFP09]. Moreover, a bijective relationship between these concepts has been derived. Though, these

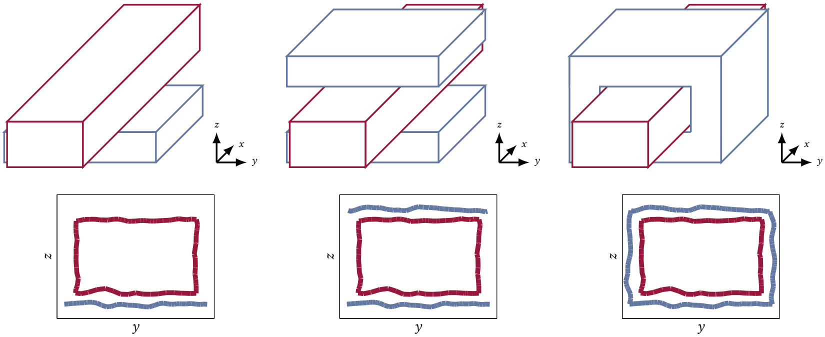

Figure 5.56: Considered Joint Configurations (top) and corresponding Cross-Sections

works only allow the consideration of a single pair of surfaces in the analysis of a mechanical joint with clearance. In order to allow the consideration of all joint surfaces, that may possibly be in contact, in the analysis of mechanical joints, a method for the estimation of the gap hull based on the concept of the difference surface is presented in the following.

5.4.2 Problem Description and General Approach

Due to clearance, a part under consideration in a mechanical joint may take various different positions during use. The gap hull can be considered as the domain of all physically feasible rigid body transformations (space of relative displacements) of a relevant part in a mechanical joint with clearance (perfect or imperfect geometry) [LLB14]. An approach for the estimation of the gap hull by means of difference surface computations is explained in the following starting from a joint with a single pair of mating surfaces, which is then extended to multiple pairs of mating surfaces, which constrain multiple degrees of freedom (see Figure 5.56). This approach is based on a bijective relationship between the gap hull and the difference surface as developed and exploited in [LLB14] and can be summarized as follows:

- *Difference Surface Computation:* calculate the difference surfaces for every pair of mating surfaces to obtain all possible part positions for each pair of mating surfaces.
- *Constrained Difference Surfaces:* perform the collision detection by line-line or plane-triangle intersections to obtain all feasible direct contact positions.
- *Extension of constrained Difference Surfaces:* connect the free edges of the resulting difference surfaces to obtain the part positions with maximal part rotations.
- *Estimating the Gap Hull:* estimate the gap hull as the convex hull of the single part positions.

Difference Surface Computation The concept of the difference surface has been used for the relative positioning and assembly simulation of Skin Model Shapes in section 5.3.2.3. It is an approach to simplify the positioning problem of a variant part in a variant assembly surrounding to a geometrical perfect part in a variant surrounding by projecting the part deviations onto the assembly surrounding. The projection is performed along predefined assembly directions or inertial forces. The difference surface of the first considered joint configuration

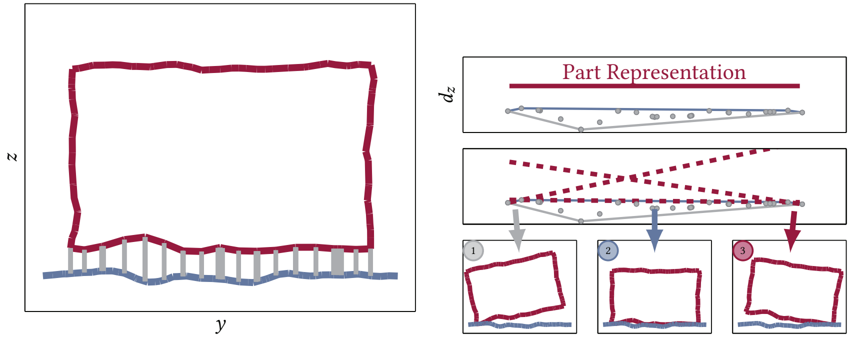

(a) Computation of the Difference Surface by Point Projections along the negative z-Direction

(b) Difference Surface and possible Part Positions

Figure 5.57: Analysis of the first Joint Configuration: The Difference Surface ((b), top) is obtained by projecting the mating surface of the Bar onto the Surface of the Base Part (a).

can be seen from Figure 5.57 and is obtained in analogy to Figure 5.39. From the difference surface, the possible part positions of the bar can be obtained.

Constrained Difference Surfaces However, as can be seen from Figure 5.58, which shows the second considered joint configuration, the convex difference surface of one pair of mating surfaces may lead to part positions, which result in part collisions on other pairs of mating surfaces. Therefore, the difference surfaces have to be constrained in order to obtain the physically feasible part positions, which do not lead to part interferences.

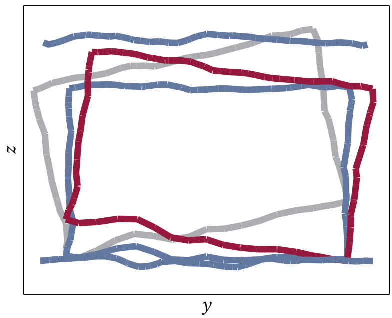

Figure 5.58: Positions of the first Configuration lead to Collisions in the second Configuration

In order to perform this, potential part collisions need to be detected. In the difference surface space, this can be performed by intersecting the resulting contact lines (2D) or planes (3D) of a pair of mating surfaces with the section-wise defined lines (2D) or triangles (3D) of all other relevant pairs of mating surfaces (see Figure 5.59). In the three-dimensional case, the intersection of contact planes and difference surface triangles can for example be performed employing a tetrahedral mesh slicer [FB09]. The intersection for mating surfaces, which do not lie in the same axis direction, is performed by applying a coordinate transformation of the difference surface prior to the intersection as can be seen from Figure 5.60. By doing so, the feasible part positions of the difference surfaces for all mating surface pairs can be identified.

Every facet of a convex difference surface, that leads to part collisions at other pairs of mating surfaces, is removed from the difference surface. Thus, the difference surfaces from all pairs of mating surfaces are constrained in order to respect the non-interference requirement.

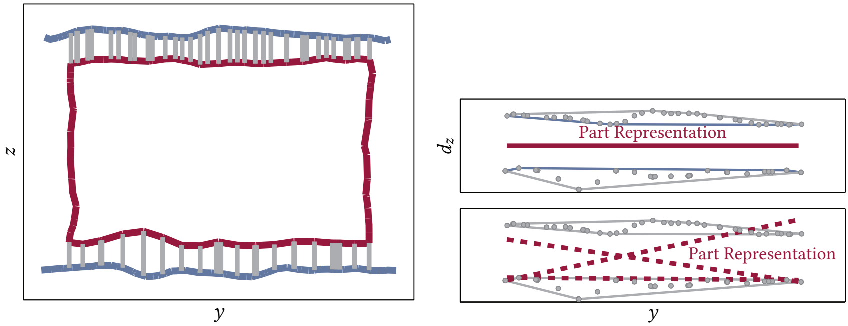

(a) Difference Surface Computation (b) "Collision Detection" by Plane/Triangle Intersection

Figure 5.59: Difference Surface Computation and Detection of non-feasible Part Positions for the second considered Joint Configuration

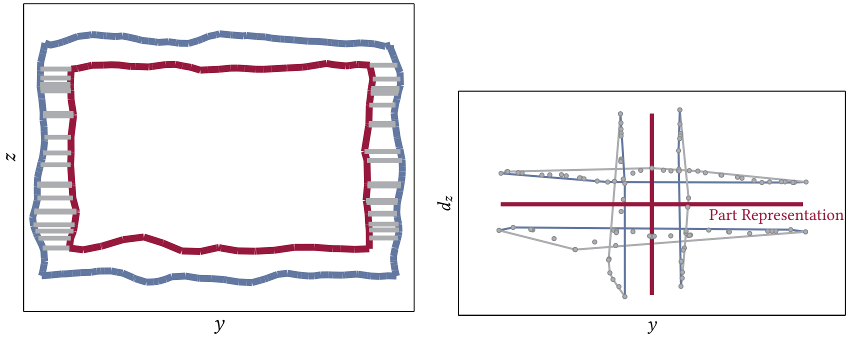

(a) Difference Surface Computation (b) Part Representation in the Difference Surface Space for the third considered Joint Configuration

Figure 5.60: Difference Surface Computation and Detection of non-feasible Part Positions for the third considered Joint Configuration

Extension of Constrained Difference Surfaces In order to consider not only the contact positions of parts between single mating surface pairs but also the extremal positions, which result from contacts between mating surfaces of *different* mating surface pairs, the extremal points of the difference surfaces in similar axis directions are connected (see Figure 5.61 (a)). These connecting lines or triangles can be regarded as new, constructed difference surfaces. The resulting part positions for these constructed difference surfaces are then also checked for part collisions in all mating surface pairs and non-feasible connections between the constrained difference surfaces are deleted. As a result, all relevant facets of the difference

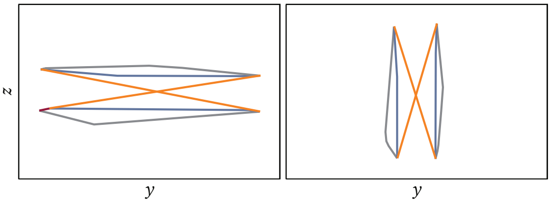

(a) Free Edges of Difference Surfaces with similar Directions are connected to obtain the extended Difference Surfaces

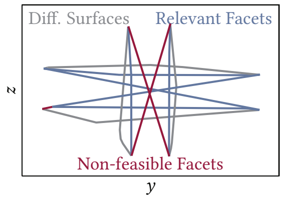

(b) Final Difference Surfaces

Figure 5.61: Extension of constrained Difference Surfaces and Final Difference Surfaces

surfaces, which refer to the extremal part positions in the joint, are obtained (see Figure 5.61 (b)).

Estimating the Gap Hull Each part position, that has been determined based on the constrained and extended difference surfaces, refers to a point in the six-dimensional space of rigid body transformations (see Figure 5.63).

In order to finally estimate the gap hull of the joint with clearance, the convex hull of these different points in the clearance space is calculated (see Figures 5.62 and 5.63). Each point inside the estimated gap hull refers to a part position, that is physically feasible, whereas each point on the outside is considered as a non-feasible part position, that may lead to part collisions. However, as the estimation of the gap hull is based on single difference surface computations and the assumption, that there is a linear relation between the single part positions, there may also exist feasible part positions on the outside of the gap hull. Thus, the approach for the gap hull estimation offers a pessimistic prediction of the feasible part positions.

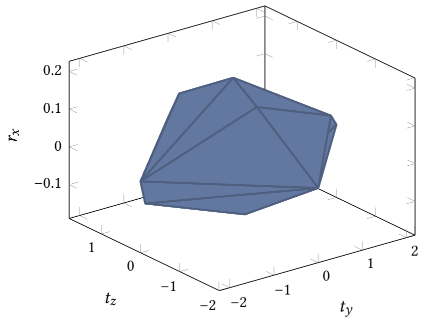

Figure 5.62: Final Gap Hull of the third considered Joint Configuration

5.4.3 Exemplary Application

Prismatic Joint The first application example is the third considered joint configuration of Figure 5.56 in the three-dimensional case (see Figure 5.64 (left)). It is a prismatic joint consisting of a bar, which can be translated along the x-direction inside a base part. In order to allow the relative movement of the bar in the prismatic joint, a gap between both parts is intended. This gap leads to a set of possible part positions of the bar, which shall be analysed for two given parts. In order to perform this, the proposed procedure for the estimation of the gap hull is applied, with the difference surfaces for the joint in the y- and z-directions being shown in

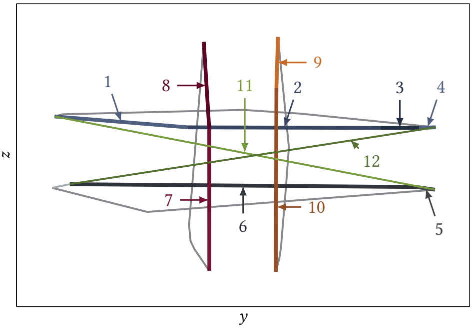

(a) Feasible Facets of the extended and constrained Difference Surfaces with respective Indices

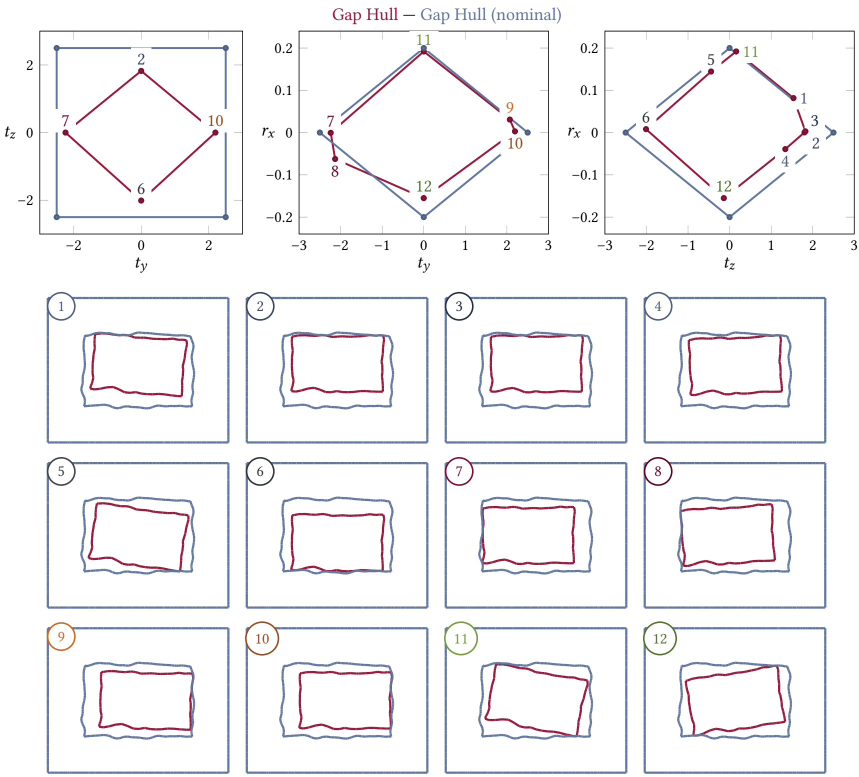

(b) Final Gap Hull (red) compared to the Nominal Gap Hull (blue) in different Views and feasible Part Positions

Figure 5.63: Each feasible Facet of the Difference Surfaces (top) corresponds to a point in Space of Rigid Body Transformations (middle), which results in a certain Part Position (bottom, the numbers indicate the respective part positions). The final Gap Hull (middle, red) is obtained by calculating the Convex Hull of these Points in the Space of Rigid Body Transformations.

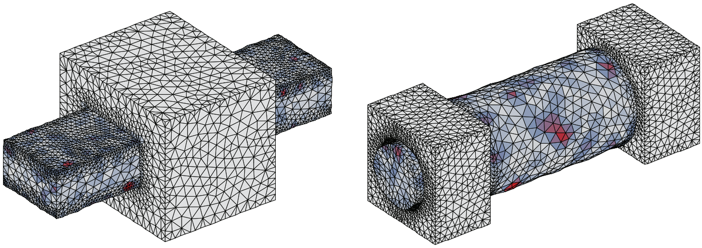

Figure 5.64: Application Examples: Prismatic Joint (left) and Cylindrical Joint (right)

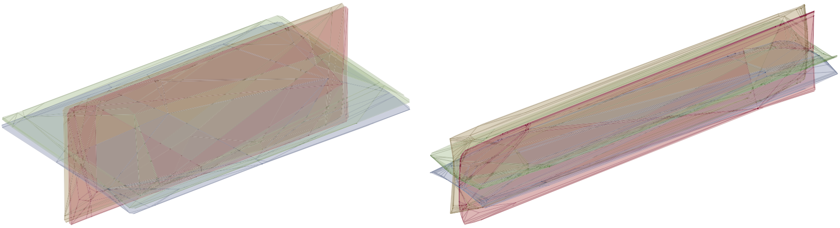

Figure 5.65: Initial Difference Surfaces: Prismatic Joint (left) and Cylindrical Joint (right)

Figure 5.65 (left). Finally, the estimated gap hull regarding the translations along the y- and z-direction as well as the rotation around the x-axis is illustrated in Figure 5.66 (left). It can be seen, that the form deviations of the parts lead to various different possible part positions.

Cylindrical Joint The second considered example is a cylindrical joint as can be seen from Figure 5.64 (right). It consists of a shaft, which is supported by two hubs. Similarly to the first example, a gap between the hubs and the shaft is intended, which leads to possible translations and rotations of the shaft. Again, the procedure for the gap hull estimation is applied, with the initial difference surfaces in the y- and z-directions being shown in Figure 5.65 (right). The final gap hull regarding the y- and z-translations as well as the rotation around the z-axis can be seen from Figure 5.66 (right). This example shows, that the procedure for the gap hull estimation also is applicable for cylindrical joints with multiple pairs of contact surfaces.

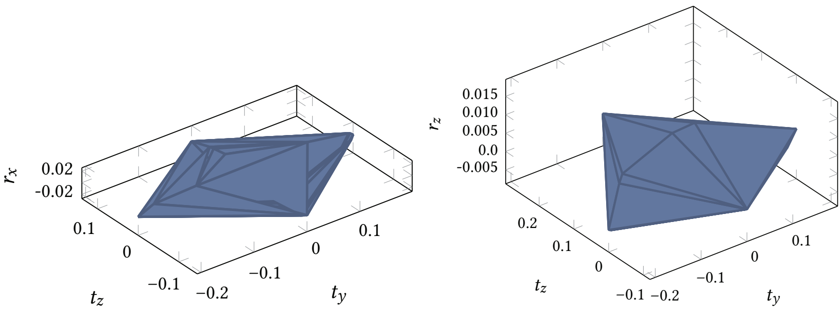

Figure 5.66: Final Gap Hulls: Prismatic Joint (left) and Cylindrical Joint (right)

5.5 Contact and Mobility Simulation for Gears and Rotating Mechanism

Manufacturing imprecisions lead to geometrical part deviations, which decrease the function and quality not only of static assemblies but also of mechanism and systems in motion. Thus, these deviations have to be controlled and managed throughout the product life-cycle and particularly the need for the design and manufacturing of high performance mechanism to moderate costs leads to an inevitable need for geometrical variations management and the increasing application of computer-aided tolerancing tools. However, up to now, such tools have mainly been used for assembly-oriented tolerance analysis, but due to steadily increasing requirements on the quality of technical products, there exists a growing interest in considering the functional behaviour and operating conditions in such tools to ensure the product function during use. Moreover, the ability to specify motion tolerances is gaining growing research interest [HK14, HK15].

In order to answer this trend, approaches for the contact and mobility simulation of Skin Model Shapes are presented in the following, which allow the tolerance analysis and motion tolerancing of mechanism with lower and higher kinematic pairs. Before these approaches are introduced and applied to two case studies, a brief state of the art with regard to tolerance analysis of mechanism is provided.

5.5.1 Related Work

During the last decades, various approaches for the tolerance analysis of mechanism based on established tolerance representation schemes have been proposed. For example, the vector loop approach has been employed for the dynamic analysis of linkages considering clearances and cracks in [DB10] as well as for the tolerance analysis of mechanism with lower kinematic pairs considering different kinds of geometrical deviations, such as manufacturing-inherent deviations, deviations caused by elastic deformations and thermal expansion, and clearance in linkages [SM09]. The approach has been extended with regard to the consideration of interactions between these deviations [WSW13] and has also been used for the tolerance-cost optimization of systems in motion [WW13]. Furthermore, vector loops have been employed for the tolerance analysis of mechanism with higher kinematic pairs (bevel gears) utilizing a numerical contact analysis approach [BDBM07] as well as for the tolerance allocation based on discrete optimization [DBVB08]. This vector loop approach is based on a geometrical specification model for gears [DBBM07] and a Tooth Contact Analysis (TCA) approach as illustrated in [LDP+00, LF04]. Moreover, a methodology for the tolerance specification of bevel gear based on proprietary software tools is developed in [WBvdL13].

In contrast to that, a parametric tolerance analysis approach for planar mechanism is proposed in [SJ97], an algorithm for worst-case kinematic tolerance analysis of general planar mechanical systems in generalized configuration space, which can be used to study kinematic variation, is introduced in [SJ98a], and the tolerance zone approach has been used for the computation of the envelope of rotating parts in [LLS07]. The Direct Linearization Method has been employed for the tolerance analysis of mechanism considering position errors in kinematic linkages [WCH04] and taking into account part flexibility in [IP09]. Apart from this, a rich survey on multi-body systems with imperfect kinematic joints can be found in [MKI11].

Though, when dealing with various sources of geometrical deviations, which are to be considered in tolerance analysis, a drawback of most of the established models for geometrical tolerance representation employed in the highlighted approaches for tolerance analysis of mechanism becomes obvious. These models make severe assumptions about geometrical deviations as they only consider rotational and translational feature defects and often somehow parametrize the geometrical deviations, which hinders their identification e. g. based on part measurements. As a consequence, it is difficult to consider results obtained from manufacturing process simulations (see e. g. [VNA06]) and measurements [Goc03] in these models. Thus, approaches for the tolerance analysis of mechanism based on discrete geometry representations of non-ideal parts are proposed. Since many computer-aided engineering tools employ a discretization of workpieces, results obtained from such tools, such as manufacturing process simulations or structural simulations based on the finite element method, can be considered in the highlighted approaches. Hence, they enable the functional kinematic tolerance analysis of mechanism considering various sources and kinds of geometrical deviations.

5.5.2 Approaches for the Contact and Mobility Simulation of Skin Model Shapes

In the following, approaches for the contact and mobility simulation of Skin Model Shapes with lower and higher kinematic pairs are highlighted, with a focus being set on the simulation models for the contact evaluation. For the sake of comprehension, these approaches are applied to a study case of a disk cam mechanism, which is to transmit a circular motion into a longitudinal motion, and a gear transmission of spur gears (see Figure 5.67). While the disk cam mechanism has been discussed by the author in [SW15d], the tolerance analysis for spur gears has been presented by the author in [SW14].

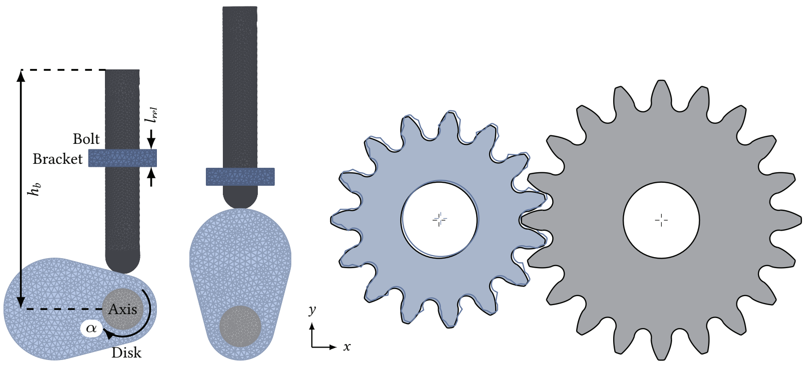

(a) Disk Cam Mechanism for a Cam Disk rotation of $\alpha = 0°$ (left) and $\alpha = 90°$ (right)

(b) Gear Transmission

Figure 5.67: Application Examples for the Contact and Mobility Simulation Approaches

5.5.2.1 Overall Procedure

The overall procedure for the contact and mobility simulation of Skin Model Shapes can be seen from Figure 5.68. In this regard, firstly, the contact simulation model has to be established. With the help of the contact simulation model, the parts of the mechanism are then positioned relatively to each other to obtain their final positions in contact.

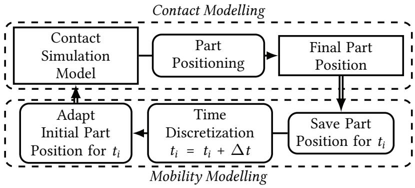

Figure 5.68: Overall Procedure for the Contact and Mobility Simulation of Skin Model Shapes

The mobility modelling is treated as a sequence of contact simulations for different initial part positions. Hence, a time discretization is performed, i. e. the initial part positions for every time step $t_i + \Delta t$ are adapted based on the previous time step t_i, with the distance between these time steps Δt depending on the discretization level. Thus, the contact simulation is performed for each relevant time step t_i of the motion cycle. As a result, the part positions for each of the time steps t_i are obtained. These part positions are stored and can then be used to determine the relevant functional key characteristics for each motion step t_i.

In the following, contact simulation models considering *translational* movements of mating parts in the mechanism as well as for *rotational* motions are discussed and the contact and mobility simulation is applied to the two case studies.

5.5.2.2 Motion Tolerance Analysis for a Disk Cam Mechanism

The first case study is a disk cam mechanism as an an irregular transmission, which is to transmit a circular motion into a longitudinal motion (see Figure 5.67 (a)). It consists of a disk, which is assembled on an axis, and a bolt, which is guided in a bracket. The key characteristic of the mechanism is the altitude of the bolt h_b. In the following, the tolerance analysis for the disk cam mechanism based on Skin Model Shapes is highlighted, with a particular focus being set on the contact simulation model between the axis and the disk as well as between the disk and the bolt.

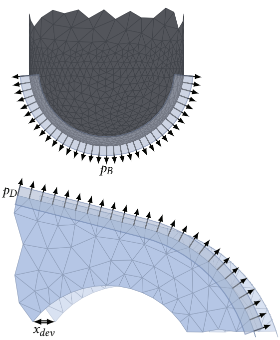

Figure 5.69: Considered Deviations of the Disk Cam Mechanism

Generation and Measurement of Skin Model Shapes As it has been highlighted in section 4.3, several approaches for the generation of Skin Model Shapes exist, such as modelling of systematic and random deviations as well as employing results from manufacturing process simulations or real-life measurements of part prototypes. These approaches allow the generation of Skin Model Shapes with different geometrical deviations, which have to be measured in

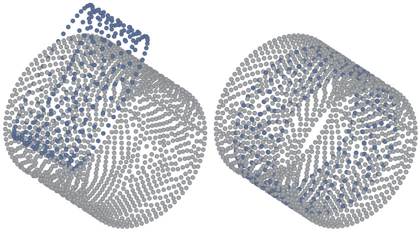

(a) ICP-based Assembly for Cylindrical Features

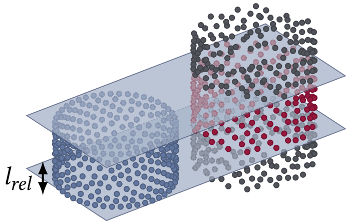

(b) Modification for the Bolt Assembly

Figure 5.70: Assembly of the Cylinders by Registration

order to build a relationship between the different part deviations and the key characteristic. For the sake of comprehension, geometrical form deviations of the cam disk and the bolt as well as position deviations between the disk axis and the disk are evaluated. Since the projection of nominal points along their corresponding vertex normals onto the measured points is common practice in the context of topography evaluations, this procedure is applied for the form deviation determination of the bolt p_B and the disk p_D. The respective tolerance zones can be seen from Figure 5.69. Furthermore, the position deviation of the disk in x-direction is considered as x_{dev}.

Contact Simulation Model In order to determine the relationship between the geometrical part deviations and the key characteristic of the mechanism, a contact simulation model for the Skin Model Shapes has to be evaluated. For the accompanying example, this requires firstly the simulation of tight cylindrical fits between the disk and its axis as well as the bolt and its bracket, respectively. For this purpose, the Iterative Closest Point algorithm (ICP) [BM92] is used to fit the cylinder of the disk and its axis as can be seen from Figure 5.70 (a). This procedure is adapted for the fit between the bolt and its bracket, with the relevant points of the bolt for the registration by the ICP being selected by GeoSpelling extraction operations according to the nominal bolt altitude l_{rel} as illustrated in Figure 5.70 (b). Since the ICP minimizes the sum of squared Euclidean distances between the selected vertices of the bolt and the bracket, the selection of the relevant bolt vertices is required in order to avoid adulterated results for the assembly fit.

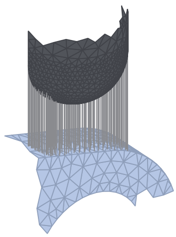

(a) Raytracing Approach

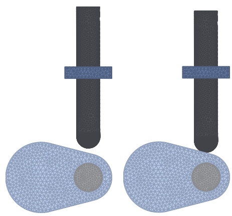

(b) Positions before (left) and after (right) the Ray Tracing

Figure 5.71: Raytracing for the Contact Analysis

Secondly, a simulation model for the contact between the disk and the bolt is required. This is performed by a ray trace algorithm [HH10], which is employed to determine the height between the pre-assembled bolt and the disk as illustrated in Figure 5.71 (a). In this regard, the vertices of the bolt are traced along the direction given by the cylinder axis of the bracket. The shortest distance between any of these vertices and the surface of the disk can then be found as the contact constraint and is used to adapt the altitude of the bolt as can be seen from Figure 5.71 (b).

Model for the System Behaviour The model for the contact simulation of the mechanism can be used to evaluate the system behaviour for selected positions of interest, for example for a disk rotation angle of $\alpha = 0^\circ$ or $\alpha = 90^\circ$. However, in order to determine the behaviour of the mechanism in motion, a time-discretization is performed, i. e. the rotation of the disk is apportioned in discrete angle steps α_i with distance $\Delta\alpha$. For each of these motion steps, the system behaviour of the disk cam mechanism is analysed based on the assembly and contact simulation models. For this purpose, the initial assembly positions of the parts are adapted taking into account the disk rotation as well as the bolt revolution. Thus, the model for the system behaviour is a sequence of contact simulation steps, with varying initial part positions. In this regard, the simulation of the different motion steps can be performed by parallel computing, which decreases the required computing time.

Post-Processing: Result Visualization and Interpretation The interpretation of tolerance analysis results is an important step to finally derive proper tolerancing decisions. Particularly for systems in motion considering not only dimensional but also form deviations, this task can become complex and requires user experience. Thus, in order to enable the result interpretation and to ease the decision making process, adequate visualization methods have to be employed. These methods are to visualize and to reveal relationships between the geometrical part deviations and the functional key characteristics. For this purpose, the parallel coordinates plot [Ins09] is a suitable approach for the visualization of tolerance analysis results for time invariant key characteristics, in which all input and output parameters are shown in one plot and highlighted as a connecting line. Such a parallel coordinates plot for the accompanying example of the disk cam can be seen from Figure 5.72 (a), where the functional key characteristic is the maximum bolt altitude h_b over the motion cycle. Based on the parallel coordinates plot, also the effects of geometrical part specifications on the key characteristic can be analysed. In this regard, Figure 5.72 (b) shows the effects of part tolerances of $p_D = 5$, $p_B = 2.5$, and $x_{dev} = [0; 2.5]$ on the KC. It can be seen, that these requirements lead to values of the FKC from 788.86 to 798.10.

The parallel coordinates plot aims at revealing the relationship between the geometrical deviations and one or more functional key characteristics. However, time variant key characteristics can hardly be visualized by this approach. In order to overcome this problem, a straightforward solution is to plot the KC over the motion cycle. This can be seen from Figure 5.72 (c), where the bolt altitude is plotted against the motion steps t_i for a disk revolution angle α from 0° to 360°. The red line highlights the bolt altitude for nominal parts, whereas the dark lines highlight the results for Skin Model Shapes, which conform to the tolerance requirements as specified ($p_D = 5$, $p_B = 2.5$, $x_{dev} = [0; 2.5]$). It can be seen, that the specification of part tolerances results in a less volatile developing of the bolt altitude over the motion cycle, which can be traced back to the profile tolerances.

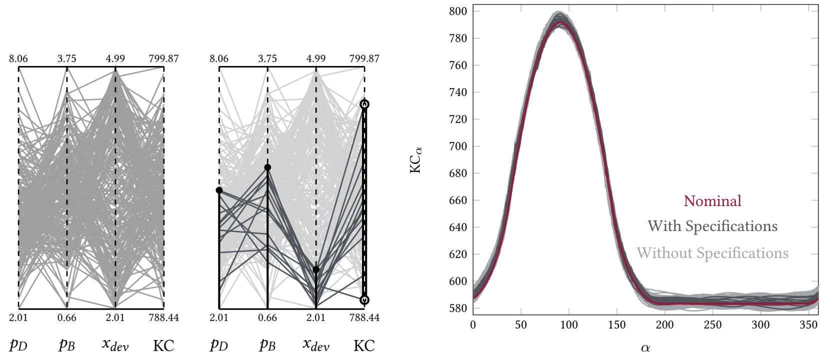

(a) Parallel Coordinates Plot without Tolerance Specifications

(b) Parallel Coordinates Plot with Tolerance Specifications

(c) Trajectories of the KC with and without Tolerance Specifications

Figure 5.72: Result Visualization for the Tolerance Analysis of the Disk Cam Mechanism

Table 5.3: Gear Parameters of the Example

Parameter	Pinion	Gear
Number of Teeth	$z_1 = 15$	$z_2 = 20$
Module	$m_1 = 2cm$	$m_2 = 2cm$
Headheight	$h_1^h = m_1 = 2cm$	$h_2^h = m_2 = 2cm$
Footheight	$h_2^f = 1.25m_1 = 2.5cm$	$h_2^f = 1.25m_2 = 2.5cm$
Pitch Circle Diameter	$d_1 = z_1 m_1 = 30cm$	$d_2 = z_2 m_2 = 40cm$
Profile Shift Coefficient	0	0
Center Distance	$(z_1 + z_2)\frac{m}{2} = 35cm$	
Pressure Angle	20°	

5.5.2.3 Tolerance Analysis for a Gear Transmission

The second example for the contact and mobility simulation for Skin Model Shapes is the tolerance analysis for a gear transmission of spur gears as illustrated in Figure 5.67 (b). The data of the accompanying illustrative example are given in Table 5.3.

Measurement of Skin Model Shapes and Evaluation of Gear Tolerances Similarly to the first example of the disk cam mechanism, the geometrical deviations of the single Skin Model Shapes, that have been generated using the approaches presented in section 4.3, have to be measured in order to evaluate the effects of the modelled or observed geometrical part deviations on the functional behaviour of the transmission. In this regard, various gear-specific tolerances can be specified, such as profile tolerances, pitch tolerances, and runout tolerances [DBBM07, Goc03, Gue11]. The measurement of these tolerances require algorithms for the virtual metrology and measurement, which in turn are based on contact simulation models as it will be shown in the following.

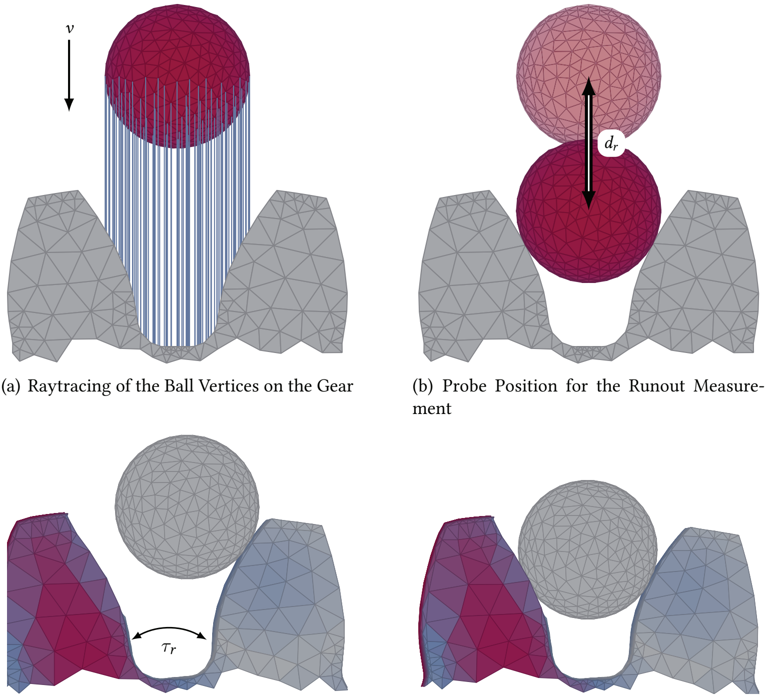

(a) Raytracing of the Ball Vertices on the Gear

(b) Probe Position for the Runout Measurement

(c) Runout Measurement of a non-ideal Gear without consideration of Clamping Rotation

(d) Final Position of the Probe for the Runout Measurement of a non-ideal Gear

Figure 5.73: The Runout Measurement for Skin Model Shapes of Gears

Runout Tolerance The runout measurement is defined in [VDI2613] as the radial location error of a specified probe, which is successively placed in all the tooth spaces in such a manner, that simultaneous contact is made with both flanks of each tooth space. F_r is designated as the greatest difference between the measured values for the radial probe position. As a consequence, the measurement of the runout error for Skin Model Shapes of gears aims at reproducing this measurement routine. For this purpose, similarly to the contact simulation model of the disk cam mechanism, a raytrace algorithm is employed [HH10], which allows the computation of the radial distance d_r between the ball in the initial measurement position and the tooth space (see Figure 5.73 (a, b)) along a predefined direction v. For this purpose, the distances d_j between the vertices of the probe ball mesh $j \in \mathcal{J}$ and the gear tooth space are computed by the raytrace algorithm. Based thereon, the radial distance between the probe ball and the tooth space can be found as the minimal distance between a vertex of the probe ball mesh and the gear: $d_r = \min d_j$. Since this algorithm disregards possible rotations of the gear in the measurement position (see Figure 5.73 (c)), which is usually a centric clamping, the raytrace algorithm is embedded in an optimization loop. Thus, the runout distance $r_{d,i}$ for each tooth space i is computed as the greatest radial distance between the probe ball in the initial measurement position with respect to the gear rotation τ_r:

$$r_{d,i} = \max d_r \text{ with respect to } \tau_r$$

For computational reasons, a constrained optimization procedure is employed, since the permitted gear rotation is constrained by the number of teeth z as $\tau_r \pm 360°/4z$. In this manner, it is ensured, that the probe ball is in contact with both tooth flanks (see Figure 5.73 (d)).

The runout error F_r is then calculated as the difference between the maximum and minimum runout distance of all tooth spaces:

$$F_r = \max r_d - \min r_d \tag{5.40}$$

Pitch Tolerance The pitch is defined as the arc length between all successive right or left flanks on a reference circle, which is typically a circle with the pitch diameter d_p [VDI2613].

The measurement of the pitch deviation of Skin Model Shapes of gears is performed based on their mesh representation as follows and as illustrated in Figure 5.74. Firstly, the surface mesh is cut employing a mesh cross-section algorithm [FB09] at the predefined measurement level. This can be seen from Figure 5.76. As a result, a set of sectionwise defined straight lines is obtained, which describe the gear surface at the predefined measurement level (in Figure 5.76 the z-direction). With the help of equation (5.48), the points of intersection between these straight lines and the pitch circle are computed, which result in the measurement points of the pitch measurement. The evaluation of the pitch measurement points can then be performed following the measurement guidelines and with the help of algorithms implemented in coordinate measurement machines. For this example, a straightforward approach is implemented, with the measurement points being used to calculate the arc lengths p_i on the pitch circle:

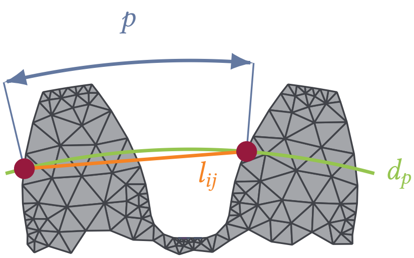

Figure 5.74: The Pitch Measurement for Skin Model Shapes of Gears

$$p_i = d_p \cdot \arcsin(l_{ij}/d_p), \tag{5.41}$$

where l_{ij} is the distance between the measurement points i and j.

Profile Tolerance Similarly to [DBBM07], flank topography specifications are used to define the profile tolerance. In this regard, the flank form tolerance t_f is evaluated by calculating the maximum difference between the nominal flank vertex coordinates and the flank vertex coordinates of the deviated gear in the vertex normal direction. In this context, the projection of the measured point onto the normal direction of the corresponding nominal point is a common

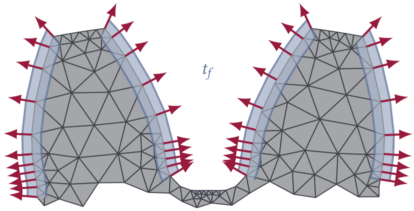

Figure 5.75: The Profile Tolerance Zone for Skin Model Shapes of Gears

method to calculate geometrical deviations of gears [Gue11]. Thus, the flank form tolerance t_f can be written as:

$$t_f = \max\left(\zeta^n(v_i, \tilde{v}_i)\right) - \min\left(\zeta^n(v_j, \tilde{v}_j)\right), \quad i, j = 1, \dots, N; \tag{5.42}$$

where $\zeta^n(v_i, \tilde{v}_i)$ is the vertex normal distance between the nominal vertex coordinates v_i and the deviated vertex coordinates $\tilde{v}_i$ of vertex i:

$$\zeta^n(v_i, \tilde{v}_i) = \sqrt{\zeta(\tilde{v}_i, v_i)^2 - \zeta(\tilde{v}_i, \boldsymbol{n}_i)^2}. \tag{5.43}$$

with $\zeta(\tilde{v}_i, v_i)$ is the distance from $\tilde{v}_i$ to v_i and $\zeta(\tilde{v}_i, \boldsymbol{n}_i)$ is the distance between $\tilde{v}_i$ and the vertex normal $\boldsymbol{n}_i$ of vertex i:

$$\zeta(\tilde{v}_i, \boldsymbol{n}_i) = \frac{\|(\tilde{v}_i - v_i) \times \boldsymbol{n}_i\|}{\|\boldsymbol{n}_i\|}. \tag{5.44}$$

Hence, the resulting tolerance zone is an envelope between the nominal gear flank and the gear flank deviated along the vertex normals of the nominal points as can be seen from Figure 5.75.

In the following, these gear tolerances (runout, pitch, profile) as well as radial positioning errors of the gear and pinion are considered in the illustrative example (see Figure 5.67 (b)).

Tooth Contact Analysis Approach In order to determine the behaviour of the gear transmission considering geometrical part deviations, a simulation model for processing the non-ideal part representatives and reproducing their characteristics in use is necessary. Thus, a model for the Tooth Contact Analysis (TCA) is required to evaluate the gear behaviour in use. The aim of the TCA is to determine the contact points and based thereon the contact paths on gear surfaces, the transmission errors as a source of vibrations and noise and the bearing contact [LF04]. In the past, the well-known approach for the TCA [LDP+00, LF04] has been extended and applied e. g. to investigate the undercutting and contact characteristics of cylindrical gears under different assembly conditions [TT04, TT05], to study the effects of misalignments on isostatic planetary gear trains [Vec06], to simulate mismatched spiral bevel gears [Sim07], and to analyse face-hobbed hypoid gears [Vim07].

However, the established TCA approach is based on the continuous tangency of a pair of

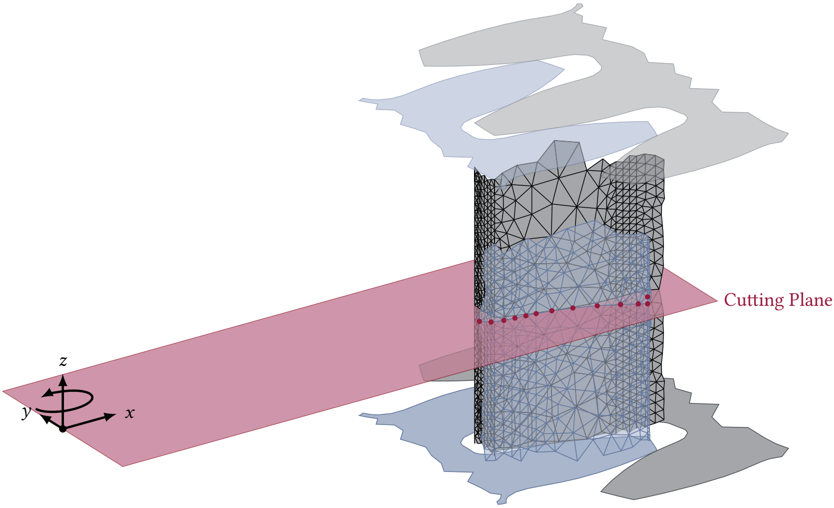

Figure 5.76: Intersection of the Driven Gear Surface Mesh

surfaces, which usually rotate around one axis [Vec06]. In discrete geometry, these surfaces are not expressed analytically but as a set of triangles. Thus, the established TCA cannot be applied to determine the behaviour of the given gear representatives. Therefore, a TCA-approach is proposed, which is based on the surface mesh representation of non-ideal gear wheels. The underlying idea is to compute the contact points between the gears in discrete motion angle steps. These contact points are evaluated as follows. For every vertex of the drive gear flank, the surface mesh of the driven gear flank is intersected with the plane orthogonal to the drive axis at the relevant vertex coordinates (see Figure 5.76) by employing a mesh cross-section algorithm [FB09].

As a result, the edges of the driven gears surface mesh at the level of the relevant drive gear vertex are obtained, which result to a set of sectionwise defined straight lines. Based thereon, the contact point $\overline{v}_i$ between each vertex v_i of the drive gear with coordinates (x_i, y_i) and the driven gear can be computed. For this purpose, the intersection between the surface mesh edges and the circular path of the drive gear vertex has to be found. The contact point at the driven gear $\overline{v}_i$ referring to vertex v_i can be calculated as follows. For every straight line n of the driven gear's surface mesh, the intersection between the circular path of the vertex v_i around the gear axis (x_m, y_m):

$$y_{v_i} = y_m + \sqrt{r_i^2 - (x - x_m)^2} \tag{5.45}$$

and the sectionwise defined straight line n given by:

$$y_n = m_n \cdot x + t_n, \quad \text{for } x \in [x_n^{\min}, x_n^{\max}] \tag{5.46}$$

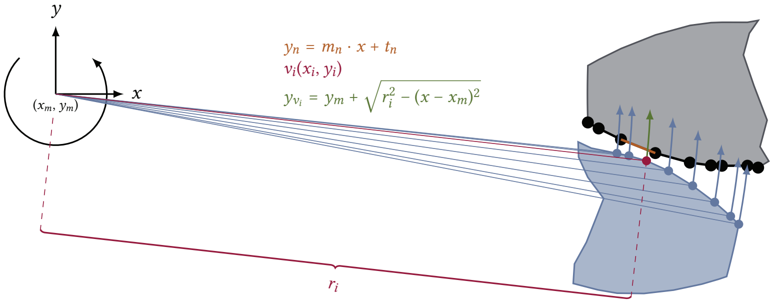

Figure 5.77: Evaluation of possible Contact Points

has to be found:

$$y_{v_i} \stackrel{!}{=} y_n. \tag{5.47}$$

This results in two real-valued solutions depending on the relevant segment of the circular path. In the following, the corresponding solution is given:

$$\rightsquigarrow x_s = \frac{1}{m_n^2 + 1} \left[\left[-x_m^2 m_n^2 + 2 x_m y_m m_n - 2 x_m m_n t - y_m^2 + 2 y_m t + m_n^2 r^2 + r^2 - t^2 \right]^{\frac{1}{2}} + x_m + y_m m_n - m_n t \right]. \tag{5.48}$$

Since the straight line is section-wise defined, x_s has to satisfy $x_n^{\min} \leq x_s \leq x_n^{\max}$. If this holds, then the corresponding y-coordinate of the contact point for vertex v_i results to:

$$y_s = m_n \cdot x_s + t_n. \tag{5.49}$$

Otherwise, the circular path of v_i does not intersect the straight line in the relevant section $[x_n^{\min}, x_n^{\max}]$. Therefore, there exists at most one contact point $\overline{v}_i$ with coordinates (x_s, y_s) for each vertex v_i with coordinates (x_i, y_i). This is illustrated in Figure 5.77.

The resulting contact angle α_i can then be computed based on the vertex coordinates and the contact point coordinates as illustrated in Figure 5.78 (a):

$$\alpha_i = \arcsin\left(\frac{y_s - ym}{r_i}\right) - \arcsin\left(\frac{y_i - y_m}{r_i}\right). \tag{5.50}$$

As this is performed for every vertex v_i of the gear flank surface, there exists a possible contact angle α_i for every vertex. Based on these possible contact angles, the minimum contact angle finally results in the transmission error α^E (see Figure 5.78 (b)):

$$\alpha^E = \min(\alpha_i). \tag{5.51}$$

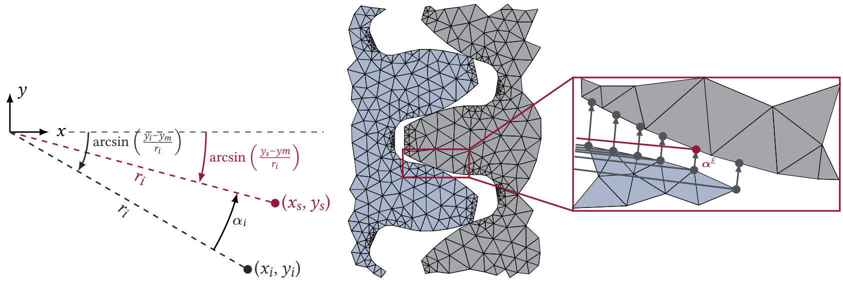

(a) Computation of the Contact Angle (b) Evaluation of the Transmission Error

Figure 5.78: Computation of the Contact Angle and Evaluation of the Transmission Error

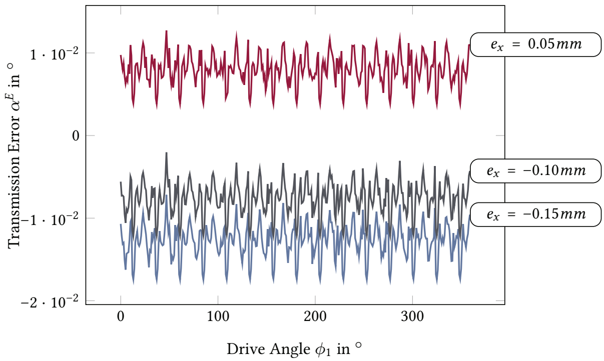

Figure 5.79: Results of the TCA considering Positioning Errors

Discussion and Selected Results The proposed TCA approach is employed to calculate the transmission errors of spur gears with data given in Table 5.3. The results for selected positioning errors e_x are shown in Figure 5.79. It can be seen, that the misalignment leads to piecewise parabolic functions of the transmission error as expected [LZLH90]. However, the results as well as the computing time of the approach depend on the density of the employed surface mesh. This can be seen from Figure 5.80, where the TCA approach is performed for a rough as well as for a finer surface mesh of the pinion and gear with nominal geometry. In this context, an increased mesh density leads to more accurate results due to the better surface approximation as illustrated in Figure 5.80, but also requires a higher computational effort. Thus, the surface mesh generation should be treated with attention to avoid degenerated results. Though, even for the finer surface mesh, a small scatter of the results for the transmission error can be observed, which arises from the discrete surface approximation and can be neglected for most applications.

However, the approach enables the tolerance analysis for rotating mechanism, which require a contact analysis algorithm, based on a discrete shape representation by surface meshes. Thereby, the results of various computer aided engineering tools, such as manufacturing pro-

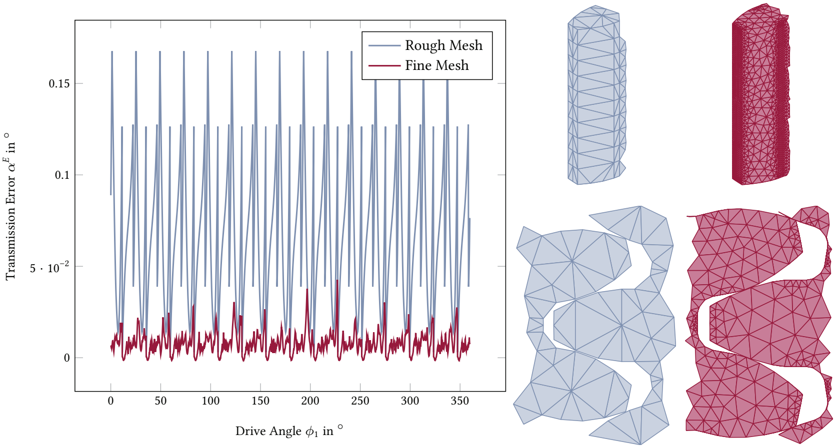

Figure 5.80: Results of the TCA for two nominal Surface Meshes

cess simulations, can be employed for the tolerance analysis. Furthermore, elastic deformations due to operating forces gathered from software tools for the structural analysis can be considered either by mapping the gathered results to the existing surface meshes or by directly employing the meshes used in these tools (e. g. for finite element analysis) for the tolerance analysis.

This allows the consideration of various sources of geometrical deviations, such as manufacturing deviations and elastic deformations, in the tolerance analysis. Moreover, the developed algorithm for the tooth contact analysis can also be used for the contact simulation of other rotating mechanism, such as valve gears (see Figure 5.81) or similar planar, spherical, and spatial mechanism.

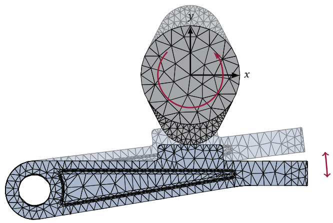

Figure 5.81: Application of the Contact Algorithm for a Valve Gear

Statistical Tolerance Analysis for Spur Gears In the following, the proposed TCA approach is used for a statistical tolerance analysis of spur gears. For this purpose, the Skin Model Shapes are generated randomly following the random field approach. Furthermore, also the positioning errors are chosen randomly following the Latin Hypercube Sampling [MBC79] assuming a uniform distribution in the interval $[-0.15; 0.05]$cm. As a consequence, the obtained results must be treated and evaluated statistically. However, it should be emphasized, that the approach can also be used for worst-case tolerance analysis when generating the non-ideal workpiece representatives deterministically and choosing constant values for the positioning error.

The results obtained by the Tooth Contact Analysis for non-ideal gears with positioning errors and gear deviations are visualized by a parallel coordinates plot in Figure 5.82 with the

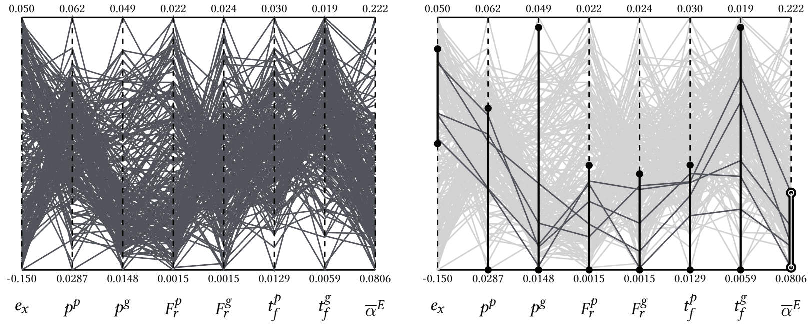

Figure 5.82: Parallel Coordinates Plot of the TCA Results without and with Tolerance Specifications

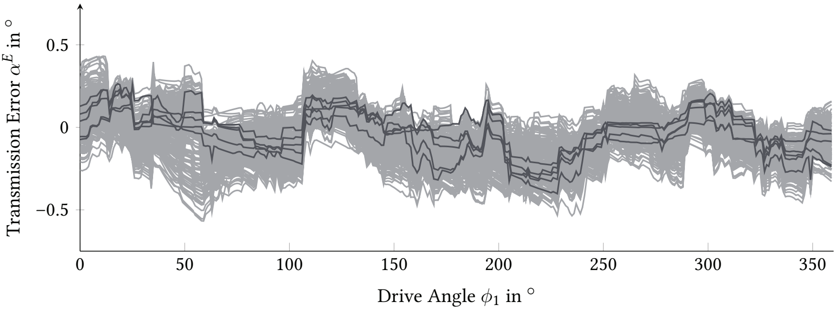

Figure 5.83: Transmission Error over the Drive Angle with and without Tolerance Specifications

superscript indicating pinion (p) and gear (g) tolerances (in *cm*). It can be seen, that there is a relationship between the mean transmission error and the pitch and runout deviations as well as the positioning error (see Figure 5.79). In contrast to that, no clear correspondence between the transmission error and the profile deviations can be identified. This is because the tooth form deviations are more likely to compensate each other, which does not hold for the other deviations. Though, the form deviations contribute to the scatter of the maximum transmission error, which can be seen from Figure 5.83, where the transmission error is plotted over the drive angle ϕ_1, and should therefore be decreased to ensure smooth transmission.

In this context, it is known, that the involute gear is hardly sensitive to positioning errors. Although apparently contradictory, the positioning error is a main contributor to the transmission error in this illustrative example. This can be explained by the broad range of e_x compared to the pitch, runout, and profile deviations. Furthermore, the level of the mean transmission error is comparably high, which is owed to the considerable geometrical deviations in this case study.

Based on the result visualization, required quality levels can be achieved by adjusting the gear and positioning tolerances. In this regard, the effects of these tolerance specifications can be appraised by the parallel coordinates plot and the plot of the transmission error over the drive angle. For example, in Figure 5.82, the parallel coordinates plot of the results with tolerance specifications for the positioning error as well as the gear deviations are shown, whereas Figure 5.83 shows the resulting transmission errors for these specifications. It can be seen, that these tolerance specifications help to improve the quality of the spur gears. This analysis based on the parallel coordinates plot can also be performed, if the results of a sensitivity analysis do not reveal explicit suggestions for tolerance improvements, as for example in [WBvdL13].

The obtained results can also be employed to estimate a surrogate model, which in turn can be used to quantify correlations between input and output parameters in a tolerance analysis and finally to optimize the tolerance specifications with regard to costs. For example, a quadratic regression model with interactions as:

$$\overline{\alpha}^E = \beta_0 + \sum_{i=1}^{N} \beta_i f_i + \sum_{i=1}^{N-1} \sum_{j=i+1}^{N} \beta_{ij} f_i f_j + \sum_{i=1}^{N} \beta_{ii} f_i^2 + \varepsilon \tag{5.52}$$

can be estimated from the obtained results for the mean (absolute) transmission error $\overline{\alpha}^E$, e. g. employing the least squares estimator, where the factors f_i are the positioning error as well as the gear deviations. Significant regression coefficients can then be identified by the analysis of variance (ANOVA), t-tests or F-tests. This procedure can also be performed for the standard deviation of the transmission error $sd(\alpha^E)$. In this regard, one can distinguish between geometrical deviations, which correlate to the mean transmission error, and deviations, which mainly affect the scatter of the transmission error.

For the results of the example gear pair, a quadratic regression model for both the mean transmission error and the standard deviation of the transmission error have been estimated. The coefficient of determination for the mean transmission error model is $R^2_{\max} = 90.70\%$, which suggests that the model approximates the underlying relationship between the considered geometrical deviations and the transmission error quite well. The quadratic model for the standard deviation of the transmission error achieves a coefficient of determination of $R^2_{sd} = 76.17\%$, which is low, but still acceptable. The comparison between the TCA simulation results and the predictions of the surrogate models for 200 simulation runs can be seen from Figure 5.84 for the mean transmission error and its standard deviation. The predictive quality is comparable to the results presented in [WBvdL13]. Based on these models, an impression of the influence of geometrical gear and positioning deviations to the mean transmission error and its scatter can be received.

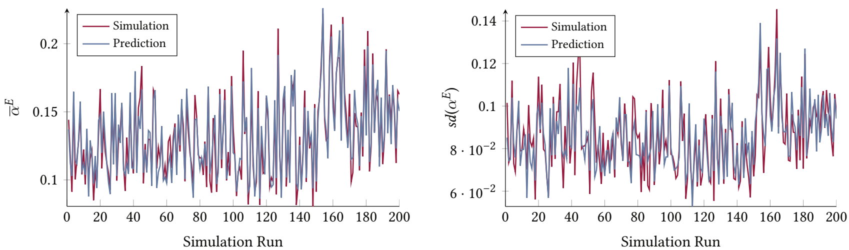

Figure 5.84: Comparison between the Simulation Results and the Surrogate Models

5.6 Measurement of Key Characteristics and Result Visualization

The last step in the tolerance analysis approach based on the concept of Skin Model Shapes is the measurement of key characteristics from the simulated assemblies as well as the visualization of the obtained results. In the following, these issues are briefly highlighted and methods for the evaluation of key characteristics from the obtained Skin Model Shape assemblies as well as selected visualization techniques are discussed.

5.6.1 Approaches for the Measurement of Key Characteristics

As the requirements on mechanical products continuously tighten, nowadays various geometrical product characteristics have to be considered in tolerance analyses. The application of the concept of Skin Model Shapes for the tolerance analysis employs point-based models and thus enables the definition and evaluation of these various characteristics, such as for example dimensional and geometrical tolerances, that have been specified on the assembly, minimal and maximal clearances and gaps in the assembly, and the size and location of contact zones between parts.

In order to evaluate such different assembly tolerance specifications, the approaches for the tolerance evaluation, that have been introduced in section 5.2, can be employed. They allow the identification of various dimensional and geometrical deviations based on the definition of different tolerances, such as tolerances of dimension, form, orientation, location, and runout, from Skin Model Shape assemblies.

Regarding the identification of minimal and maximal gaps as well as the size and location of contact zones between parts in the assembly, raytracing and point projection methods as described in section 5.3 and 5.5 can be applied, which allow the determination of signed distances between parts along pre-defined directions. Based on these signed distances, the contact situation between parts, i. e. floating, contact, or interpenetration, the contact quality, and the size and location of contact zones can be assessed.

Beside this, the x-, y-, and z-coordinates of specific points on parts in the assembly are of interest in certain applications, which can be easily obtained from the simulated assemblies.

5.6.2 Result Visualization Methods

Once the key characteristics are evaluated from the Skin Model Shape assemblies, these results have to be visualized in order to allow their proper and consistent interpretation as well as the derivation of adequate tolerancing decisions. In this regard, various approaches for the visualization of tolerance analysis results can be applied, for example statistical visualization methods, such as parallel coordinates plots, histograms, and plots of the kernel density estimates of the resulting characteristics. However, since the concept of Skin Model Shapes enables the consideration of form deviations in tolerance analysis, which have manifold and sometimes apparently contradictory effects on different key characteristics of assemblies, a particular focus should be laid on the visualization of the resulting assemblies with form deviations. For this purpose, the visualization approaches for Skin Model Shapes as discussed in section 4.2 can be applied, in which the colours can be chosen according to the part deviations or the accumulated deviations of the parts in the assembly compared to the nominal assembly position. Moreover, the effects of feature deviations, that have been brought in during the scaling of Skin Model Shapes, on the assembly characteristics can be visualized.

To illustrate this, a simple stack-up of two cubes as can be seen from Figure 5.85 is considered. Both cubes share the same simplified tolerancing scheme with two flatness tolerances applied to the bottom and top feature of each cube, respectively, as well as a parallelism tolerance of the top feature with reference to the bottom feature.

As it has been shown in Figure 5.16, the parallelism tolerance leads to a rhombic deviation domain of the top feature for each of the two cubes in the case when the form deviations are considered nil. These deviation domains for the two cubes are illustrated in Figure 5.86 and are plotted at different z-levels (bottom z-level refers to the bottom cube, middle z-level to the top cube). Moreover, the resulting rotational defects of the top feature of the top cube are plotted in the top z-level in Figure 5.86. By connecting the introduced feature deviations for each cube and the resulting observed deviation of the top feature for each of the 1,000 simulated Skin Model Shape assemblies, the effects of the single feature deviations on the assembly behaviour can be assessed and the part-related sources of deviations in the final assembly can be traced back. This can be seen from the Figure 5.86, where the sources of the maximal deviations of the top feature regarding the rotations around the x- and y-axis are traced back to the feature deviations of both cubes. Without considering form tolerances, this leads to straightforward results, since the feature rotations simply add up to the final deviations of the top feature (see Figure 5.86 (a)). In contrast to that, the situation is more complicated when considering form deviations, since the sources of the maximal deviations of the top feature are not necessarily located at the corners of the feature deviation domains (see Figure 5.86 (b)). Thus, the visualization of the introduced feature deviations and the resulting assembly deviations in the same plot can help to identify the part-related sources of critical assembly deviations.

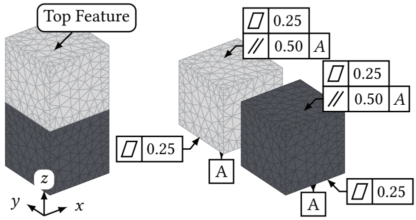

Figure 5.85: Stack-Up of two Cubes and simplified Tolerance Specifications for both Cubes

5.6.3 Application to the Example Case Study from Section 5.1

For the example case study (sec. 5.1), the evaluation of the key characteristics from the simulated assemblies is performed using approaches from computational geometry similarly to the evaluation of geometrical deviations on the part level. The resulting kernel density estimates of the functional key characteristic *pos* for the case study can be seen from Figure 5.87, where it can be found that the consideration of form deviations leads to a slightly increased position deviation *pos* in both the worst-case as well as the statistical analysis. This is because the form deviations, in fact, lead to decreased orientation defects on the part level (see also Figure 5.35), but to increased orientation defects on the assembly level due to irregular contact points between the parts.

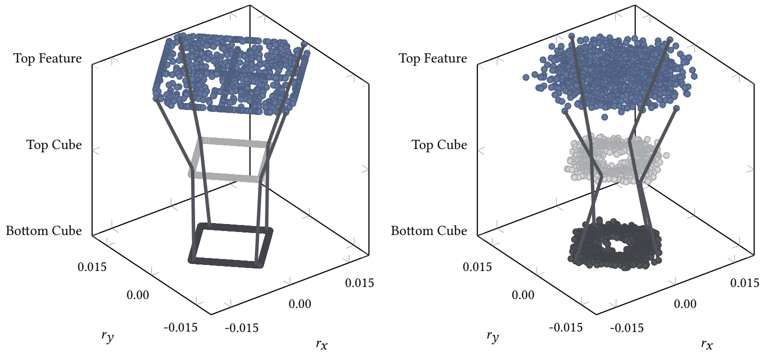

(a) No Consideration of Form Tolerances (b) With Consideration of Form Tolerances

Figure 5.86: Resulting Deviations of the Top Feature compared to the nominal Assembly without and with Consideration of Form Tolerances

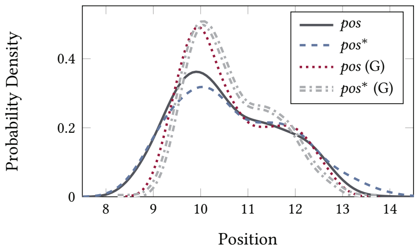

Figure 5.87: Probability Densities of the Pin Position *pos* with (*) and without Form Tolerances ((G) indicates the Statistical Tolerance Analysis)

This can also be seen from Figure 5.88, where the positions of a selected node on the bottom surface of the pin are shown. The consideration of form deviations leads to a wider range of position deviations due to increased orientation defects of the pin with reference to the base part. The two clusters of points for the worst-case analysis without form deviations (Figure 5.88, top left) result from the two possible results of the part scaling for the position tolerances of the base part and the beam (i. e. minimum part length vs. maximal part length). Moreover, Figure 5.88 reveals a large scatter of the pin location in the y-direction, particularly in negative y-direction. This is because the locating scheme of the beam, which is characterized by a comparably small contact zone for the two-point contact, is prone to feature defects regarding the mating features of the two-point contact, since their deviations are amplified by the long beam. Thus, small rotational defects of the two-point mating features of the base part and the beam lead to a rotation of the beam and finally to large location deviations of the pin in the y-direction. This effect is particularly significant in negative y-direction, since location errors in the positive y-direction are limited by the features of the one-point contact.

The deviations of the selected node on the bottom surface of the pin compared to its nominal position can also be traced back to the introduced location deviations of the features of the base part. Figure 5.89 illustrates these dependencies for the case of Gaussian input probabilities for the different tolerances under consideration of form deviations. It can be seen, that the extremal positions of the pin regarding the x- and y-deviation can be roughly backtracked to

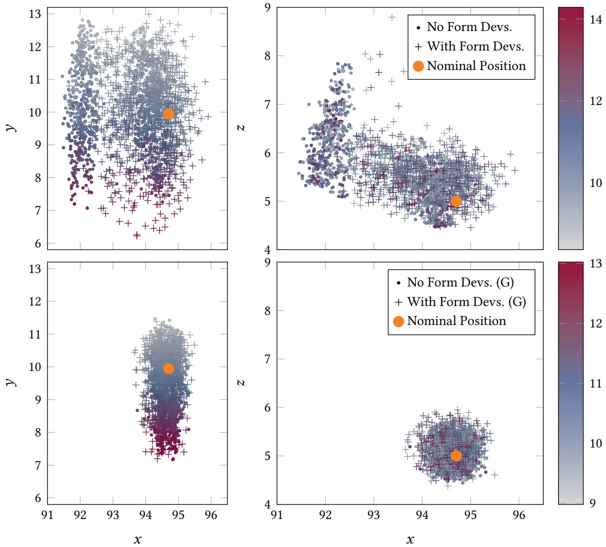

Figure 5.88: Coordinates of a selected Node on the bottom of the Pin in the global coordinate system: Top shows the Results of the Worst-Case and bottom of the Statistical Tolerance Analysis (Colours indicate the Position Deviation *pos* of the respective Sample)

the introduced location deviations of the base part features. However, again, the effects of the feature deviations are not as explicit as in the case when the form deviations are nil.

Moreover, the contact between the beam and the base part, which is determined using the difference surface approach for the 3-2-1 assembly simulation, has been analysed employing projected distances between the beam and the base part. The results can be seen from Figure 5.90 (a), where the mark colours in the scatter plot highlight the distance between the beam and the base part at the respective location in the direction of the corresponding assembly direction. Beside this, the contact points between the beam and the base part are highlighted as red dots. It can be found, that the assembly simulation leads to three contact points at the bottom surface, two contact points at the back surface, and one contact point on the side surface of the base part. Furthermore, the histograms of the corresponding distances for the three assembly steps (three-point, two-point, and one-point move) can be seen from Figure 5.90 (b), where it can be seen, that the three-point assembly step leads to a considerable tighter contact than the two-point and the one-point assembly step, since the projected part distances are smaller and the probability mass in the histogram is shifted to the left. Moreover, no part collision is detected, since all projected part distances are greater than zero.

In this context, it has been shown, that the Skin Model Shape paradigm enables the facile measurement of geometrical assembly characteristics as well as of physically relevant measures, such as minimal gaps or maximal distances. Furthermore, the contact quality can be evaluated using point projection methods to obtain the projected distances between the parts.

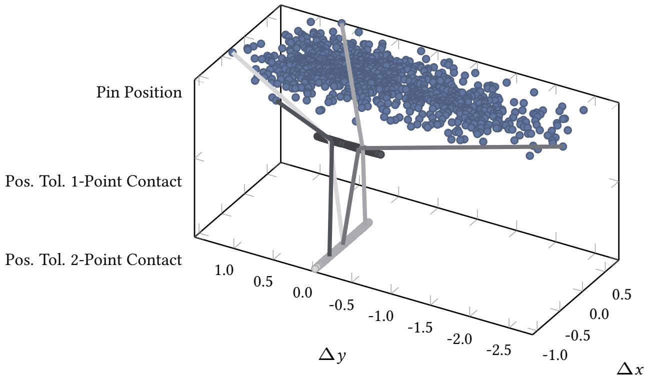

Figure 5.89: Multi-Dimensional Plot of the introduced Location Deviations of the Features of the Base Part and their Relations to the Deviations of a selected Node on the bottom of the Pin

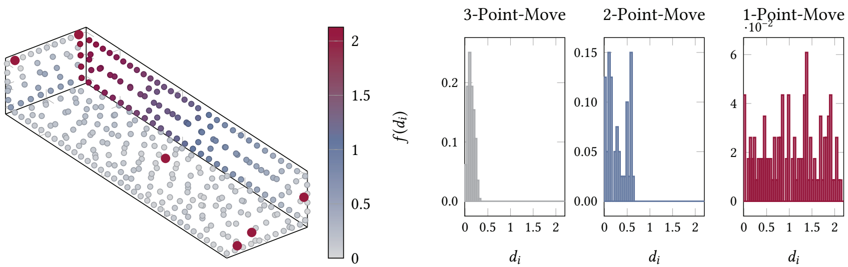

(a) Projected Point Distances between the Base Part and the Beam along the Assembly Directions

(b) Histograms of the Projected Point Distances for the Three Assembly Steps

Figure 5.90: Contact Analysis between the Beam and the Base Part for the Example Case Study

6 Prototype Implementation of a Tolerance Analysis Tool based on Skin Model Shapes

The aforementioned approaches for the generation, scaling, and assembly simulation of Skin Model Shapes as well as a software prototype called *tolSMS* have been implemented in MATLAB [Mat15] in order to demonstrate and validate this novel tolerance analysis approach in multiple case studies. In the following, the implementation and the functionalities of this software prototype are briefly highlighted, before the tolerance analysis results for multiple case studies are discussed in the next chapter.

6.1 General Architecture and Workflow

The general **architecture** of *tolSMS* comprises four modules, which will be briefly explained in the following, namely a part import module, a tolerance specification and assembly definition module, a tolerance simulation setting module, and a result visualization module. The overall **workflow** using *tolSMS* is highlighted in Figure 6.1 and starts with the import of all relevant parts of the assembly in the .stl file format. Thereafter, tolerance specifications as well as the assembly sequence and moves can be added to the simulation model. After that, relevant parameters for the tolerance simulation have to be defined in the tolerance simulation setting

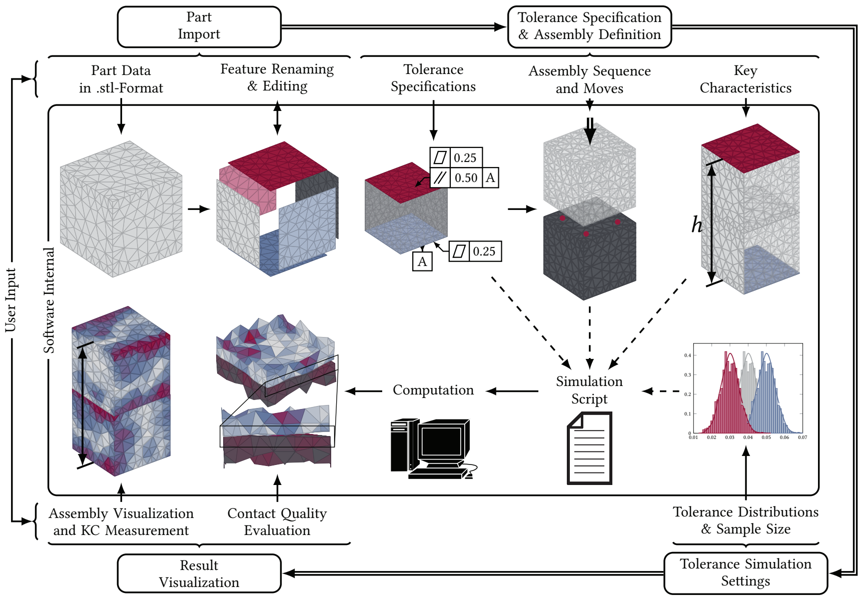

Figure 6.1: Overall Workflow using *tolSMS*

module. Based on the information about the tolerance specifications, the assembly sequence and moves, the key characteristics, as well as the tolerance simulation settings, a simulation script is automatically generated from *tolSMS*. This script may then be evaluated directly after its generation or at a later point in time (e. g. overnight in batch-mode). Furthermore, the simulation script may be edited, if custom measurements or complex assembly moves have to be performed. After the processing of the simulation script, the results can be visualized by the result visualization module.

For each of the four main modules, graphical user interfaces (GUI) have been implemented, which allow the easy preparation of tolerance simulation studies by few user inputs. The four main modules of *tolSMS* are briefly explained in the following.

6.2 Part Import Module

The part import module (see Figure 6.2) allows the import of mesh data in the .stl format, which offers a suitable and robust data exchange format for the description of solid models by triangle surface meshes [VWB+09]. The module allows the import of triangle surface meshes of the nominal part geometry as well as of results of manufacturing process simulations comprising part deviations. Right after the mesh import, an edge-based feature detection algorithm automatically extracts the features of the part surface mesh. For this purpose, the edges of the part are detected using the algorithm proposed in [PGK02, PKG03][56] and a growing neighbourhood algorithm is applied to identify the different features, which are separated by the identified edges. These different part features can then be renamed or edited by the user to ease the feature-based tolerance specification as well as the definition of assembly moves in the following steps of the workflow.

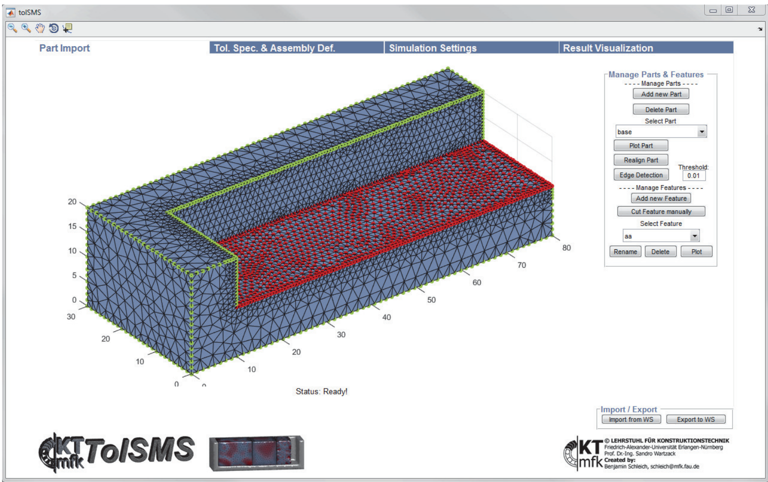

Figure 6.2: Part Import Module of *tolSMS* with imported Part, Part Edges (green), and highlighted Part Feature (red)

[56]More works on feature extraction can also be found in [SPP+02, LPJC04, DVVR07, DD15].

6.3 Tolerance Specification and Assembly Definition Module

After the parts of the assembly have been imported and their features have been labelled, the parts can be added to the assembly under consideration. Moreover, various tolerance specifications, such as dimensional tolerances (also with material modifiers), tolerances of form, of orientation, and of location, may be added to the features of the single parts of the assembly (see Figure 6.3 (a)). Furthermore, the assembly sequence and different assembly moves, such as the 3-2-1 positioning scheme or best-fit moves, can be defined (see Figure 6.3 (b)) by simply picking the relevant mating features for each assembly step. Additionally, various key characteristics may be defined, that are to be measured from the simulated assemblies.

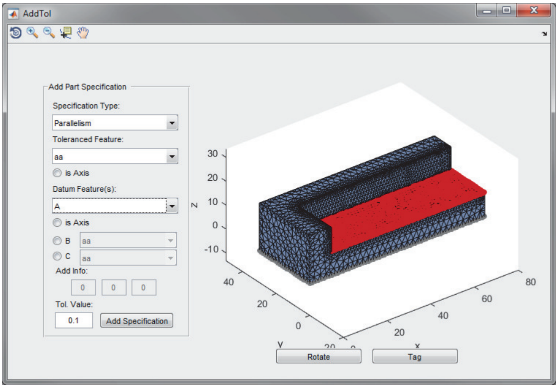

(a) Graphical User Interface for the Specification of Part Tolerances

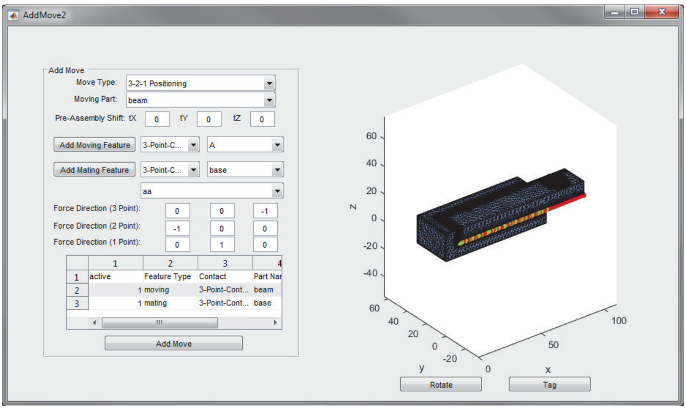

(b) Graphical User Interface for the Definition of Assembly Moves

Figure 6.3: *tolSMS*: GUIs for the Tolerance Specification and the Assembly Definition

6.4 Tolerance Simulation Module

As soon as all tolerance specifications, the assembly moves, and the key characteristics have been defined, the tolerance simulation settings can be specified. Among these settings are the number of samples, that should be performed, and whether form deviations and form tolerances should be considered in the tolerance simulation. Beside this, statistical distributions, such as uniform or Gaussian probability distributions, can be defined for the tolerances.

Once these parameters for the tolerance simulation are set, a simulation script is generated from *tolSMS*, with the general structure of such a script being shown in Table 6.1. This simulation script holds all relevant information and commands, that are necessary to perform the tolerance simulation. It may be evaluated immediately after its generation or at a later point in time (e. g. overnight) and may also be transferred to high-end workstations or servers to make use of available computing capacity and to reduce the required computation time. Moreover, the simulation script can be edited manually, if custom measurements or more complex assembly moves have to be considered in the tolerance simulation. After the processing of the simulation script, the results of the tolerance simulation are saved in a workspace, which in turn can be imported in *tolSMS* for the result visualization.

Table 6.1: General Structure of a Tolerance Simulation Script

Generate Skin Model Shapes {*Depending on whether form deviations are considered*}
Scale Skin Model Shapes {*The scaling sequence depends on the relationship between the different tolerance types and datum precedence*}
for each of the Samples **do**
  Perform the **assembly simulation** {*The order respects the assembly sequence*}
  Measure the KCs from the assemblies
end for
Save the results

6.5 Result Visualization and Export Module

In order to assess and interpret the tolerance simulation results, various visualization approaches have been implemented as parts of the result visualization module. In this context, for example kernel density estimates of the input tolerance distributions as well as of the distributions of the measured key characteristics are available. Moreover, a parallel coordinates plot (see Figure 6.4 (a)) and a multi-dimensional plot as described in 5.6.2 (see Figure 6.4 (b)) have been implemented. Furthermore, the resulting assemblies can be plotted (see Figure 6.4 (c)) and the contact quality can be assessed by visualizing the projected distances between the parts (see Figure 6.4 (d)). These various visualization approaches can be viewed directly in *tolSMS* or may be opened as separate figure windows. Moreover, the tolerance simulation results may be exported for documentation reasons or to perform the analysis using external spreadsheet or data analysis tools.

6.6 Additional Functionalities

Beside the ability to perform three-dimensional tolerance analyses considering form deviations in conformance to GPS standards based on the concept of Skin Model Shapes, the implemented software prototype offers also additional functionalities.

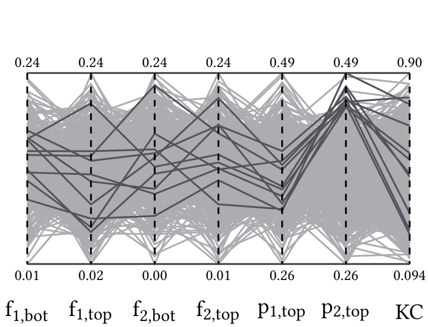

(a) Parallel Coordinates Plot

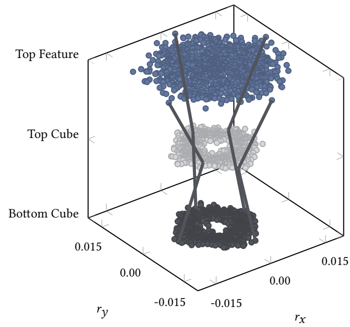

(b) Multi-Dimensional Plot

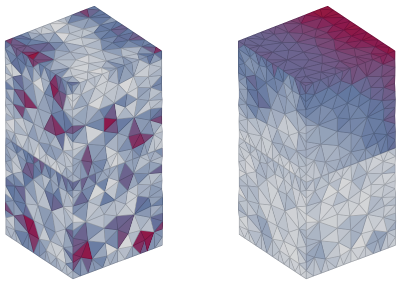

(c) Plot of a resulting Assembly: Colour Coding based on the Part Deviations after Scaling (left) and based on the accumulated Assembly Deviation (right)

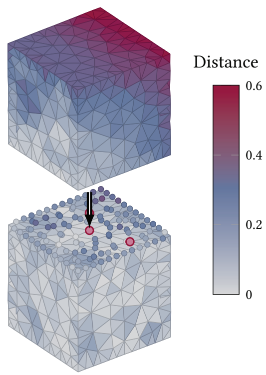

(d) Contact Quality Evaluation: The dots represent the Distance between the Parts in the Assembly Direction

Figure 6.4: Result Visualization Approaches implemented in *tolSMS*

One of these additional functionalities is the simplified computation of the deviation domain of a feature of interest by performing set operations (Minkowski sums) on the introduced feature defects (see Figure 6.5). In this regard, it has been highlighted in section 5.2, that the scaling of Skin Model Shapes for orientation and location tolerances is performed by introducing rotational and translational defects to the toleranced features. These feature defects are automatically propagated by set operations according to the assembly sequence and the assembly moves to obtain the (simplified) deviation domain of a feature of interest.

Moreover, two-dimensional tolerance simulations for certain cross-sections of the three-dimensional tolerance simulation model can be generated. For this purpose, the part surface meshes of the three-dimensional tolerance simulation model are cut along the defined analysis plane to obtain the nominal part geometries for the two-dimensional simulation as can be seen from Figure 6.6 (a). Furthermore, the tolerances, that have been specified on the relevant part

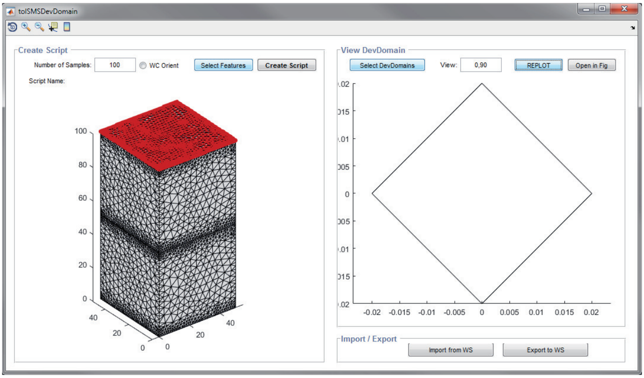

Figure 6.5: GUI for the simplified Computation of Deviation Domains

features, are transferred to corresponding two-dimensional counterparts following some basic rules (e. g. a flatness tolerance in the three-dimensional tolerance simulation model is transferred to a straightness tolerance for the two-dimensional tolerance simulation; see Figure 6.6 (b)). Similarly, the assembly moves are transferred. For this two-dimensional tolerance simulation, again a simulation script is generated, which may then be solved. For this purpose, the two-dimensional versions of the approaches and algorithms for the generation, scaling, and assembly simulation of Skin Model Shapes are used. Figure 6.6 (c) highlights an exemplary result of the two-dimensional tolerance simulation for the example case considering form deviations.

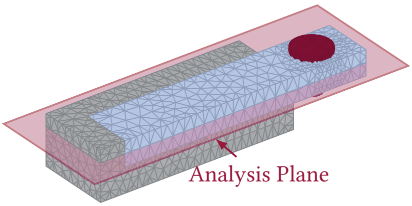

(a) Three-dimensional Model and considered Analysis Plane

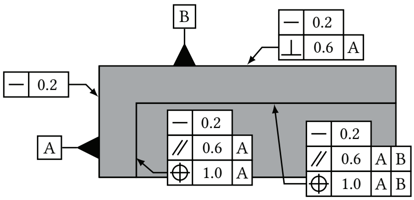

(b) Resulting Two-Dimensional Tolerancing Scheme (bottom) for the Base Part (compare Figure 5.2)

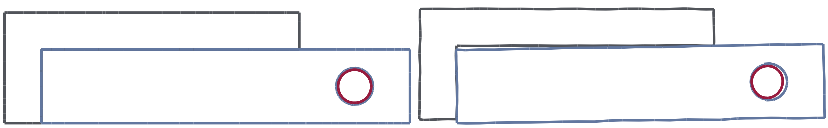

(c) Resulting Two-dimensional nominal Part Geometries (left) and exemplary resulting Assembly of the Two-dimensional Tolerance Simulation (right)

Figure 6.6: Generation of a Two-dimensional Tolerance Simulation Model based on an initially Three-dimensional Tolerance Simulation Model

7 Application and Benchmark of the Tolerance Analysis Approach based on Skin Model Shapes

As it has been highlighted, tolerance analysis is a main issue in the discrete goods industry and the studied tolerance analysis problems are consequently as manifold as the products being produced. In this regard, tolerance analysis has been applied to a wide variety of products from tiny components, such as contactors and relays [Abe15], to large assemblies, such as cars and aircrafts [CS95, FTCM16], as well as from large production batches, such as roller bearings [Röd15, AW16], to batch sizes of one, such as dental fits and implants [KSAL07, KSAL10]. Against this background, no single application example covers adequately all issues, that are possibly relevant in tolerance analysis. Thus, the framework for the tolerance analysis based on Skin Model Shapes is applied to multiple study cases in the following in order to provide a comprehensive overview of the possibilities offered by this novel tolerance analysis paradigm.

7.1 Tolerance Stack-Ups

The very basic and most often studied tolerance analysis examples in the literature are assemblies of simplified parts, that are vertically or horizontally stacked. Thus, as an introduction to this section, five different tolerance stack-up cases with increasing complexity are discussed.

7.1.1 Tolerance Stack-Up of two Cubes

The first example is a tolerance stack of two identically specified cubes, in which the first cube is positioned on an ideally even plane and the second cube is placed on top of the first one, with three-point moves being employed for both assembly steps. The key characteristics of the assembly are the parallelism and position deviation (par and pos, respectively) of the top feature of the second cube with reference to the ideally even plane. Figure 7.1 highlights the study case and the tolerancing scheme, which applies likewise to both cubes.

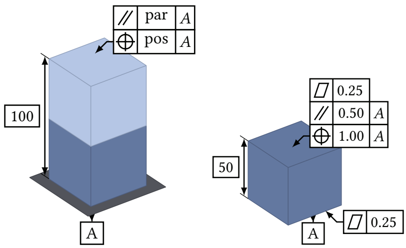

(a) Assembly (b) Tolerancing Scheme

Figure 7.1: Tolerance Stack-Up of two identically specified Cubes

In order to assess the influence of the density of the surface meshes of mating features on the tolerance analysis results obtained by the Skin Model Shape approach, the study case has been analysed using two different surface meshes of the cubes, which can be seen from Figure 7.2. The coarse surface mesh is characterized by triangle sizes between 8.7 mm^2 and 48.9 mm^2 (mean triangle size 22.3 mm^2), whereas the dense surface mesh has triangle sizes between 0.2 mm^2 and 1.3 mm^2 (mean triangle size 0.6 mm^2).

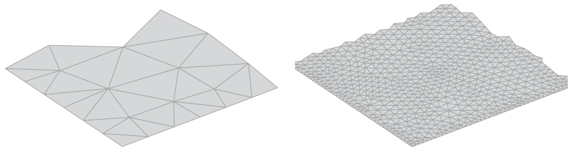

(a) Coarse Surface Mesh (b) Dense Surface Mesh

Figure 7.2: Details of the Different Surface Meshes of the Mating Features

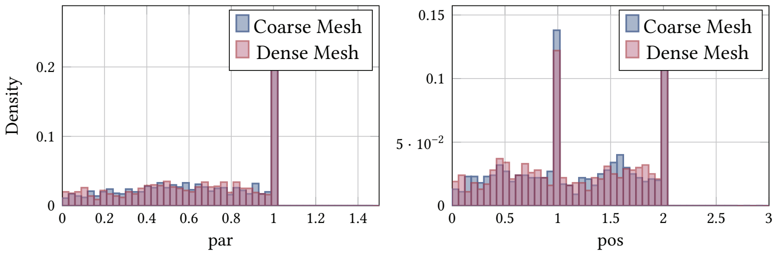

Figure 7.3: Histograms of the Key Characteristics without Consideration of Form Deviations

Without Consideration of Form Deviations Under the assumption, that the form deviations are nil (i. e. the flatness tolerances of the cubes are of value zero), the worst-case values of the key characteristics of the assembly can easily be obtained, since the admissible part deviations linearly accumulate through the assembly. Hence, the worst-case value of the parallelism deviation par is the sum of the parallelism tolerances of both cubes, i. e. $\max(\text{par}) = 2 \cdot 0.50 = 1.00$, and the worst-case value of the position deviation pos is the sum of the position tolerances of both cubes, i. e. $\max(\text{pos}) = 2 \cdot 1.00 = 2.00$. Their respective minimal values are zero, i. e. $\min(\text{par}) = \min(\text{pos}) = 0.00$, which refers to the situation when the part defects of the bottom and the top cube balance out. Moreover, values between the minimal and maximal value for each key characteristic may be observed, when the part defects of the cubes balance out only partially. This can be seen from the histograms of the key characteristics for 1,000 simulated Skin Model Shape assemblies without form deviations, which are given in Figure 7.3.

Moreover, without consideration of form deviations, the set of rotational and translational feature defects for each top feature of both cubes forms a regular deviation domain, which is illustrated in Figure 7.4. It can be seen, that a regular rhombus is obtained regarding the feature rotations r_x and r_y, which size is dependent on the parallelism tolerance, whereas a positive and a negative level for the feature translation t_z due to the position tolerance can be observed. Furthermore, no significant differences for the two different surface meshes can be found. These regular deviation domains may be "linearly" propagated by Minkowski sums when the form deviations are nil. As a result, the set of observed deviations of the top feature of the top cube with reference to the nominal assembly position is of twice the size of the individual deviation domains of the cubes, which can be seen from Figure 7.5. Again, no significant differences can be observed between the different surface meshes.

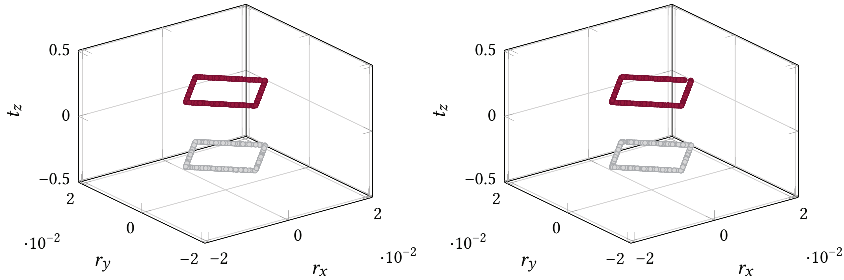

(a) Coarse Surface Mesh (b) Dense Surface Mesh

Figure 7.4: Introduced rotational and translational Defects for the top Feature of the bottom Cube without Consideration of Form Deviations

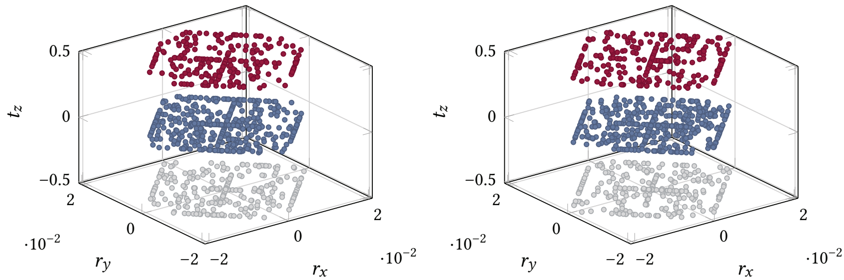

(a) Coarse Surface Mesh (b) Dense Surface Mesh

Figure 7.5: Observed Feature Defects of the top Feature of the top Cube after the Positioning compared to the nominal Assembly without Consideration of Form Deviations

With Consideration of Form Deviations In contrast to the case when the form deviations are nil, the key characteristics of the assembly may take values greater than their aforementioned theoretical worst-case limits when considering form deviations, which can be seen from the histograms of the key characteristics for 1,000 Skin Model Shape assemblies with form deviations (according to the flatness tolerances of 0.25) in Figure 7.6. This can be explained as follows. Indeed, the form deviations of the mating features decrease the admissible rotational feature defects, which can be seen from Figure 7.7, where the introduced rotational and translational feature defects of the top feature of the bottom cube are illustrated considering form deviations. It can be seen, that these introduced defects do not form regular deviation domains as it has been explained in section 5.2.5.1. However, the form deviations lead to irregular contact points between the parts and additional rotational and translational assembly deviations, which manifest in the observed feature defects after the assembly as shown in Figure 7.8.

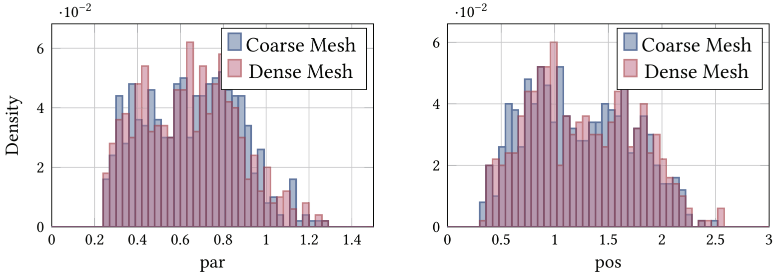

Figure 7.6: Histograms of the Key Characteristics with Consideration of Form Deviations

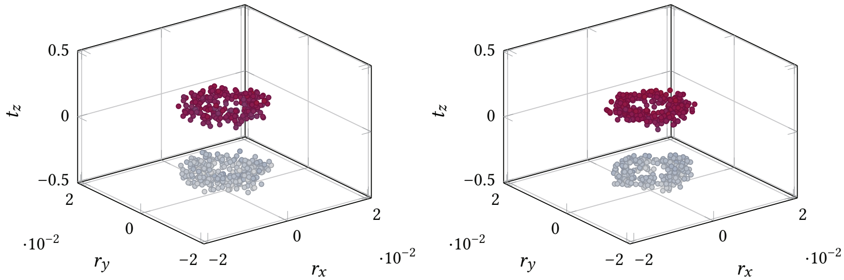

(a) Coarse Surface Mesh (b) Dense Surface Mesh

Figure 7.7: Introduced rotational and translational Defects for the top Feature of the bottom Cube with Consideration of Form Deviations

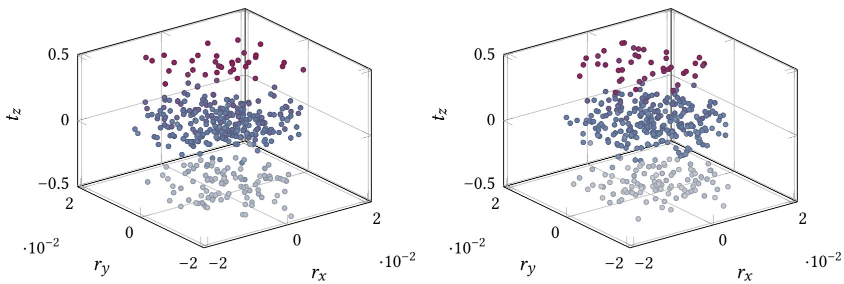

(a) Coarse Surface Mesh (b) Dense Surface Mesh

Figure 7.8: Observed Feature Defects of the top Feature of the top Cube after the Positioning compared to the nominal Assembly with Consideration of Form Deviations

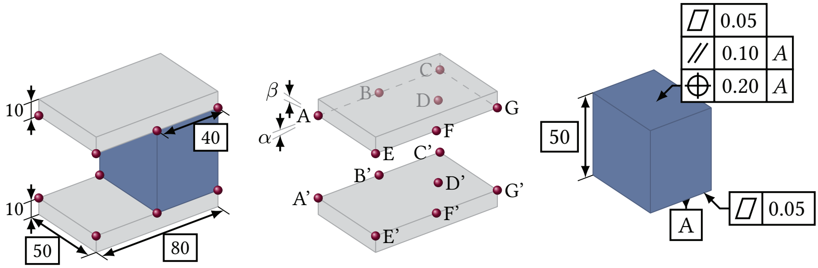

Figure 7.9: Tolerance Stack-Up of two ideal Plates and a specified Cube

7.1.2 Tolerance Stack-Up of two Plates and a Cube

The second study case has been described by Anselmetti and Mathieu in [AM01] and has been particularly designed to assess the conformance of a tolerance analysis tool to tolerancing standards. It is a stack-up of two identical plates and a cube as can be seen from Figure 7.9, where the two plates are considered to be ideal, whereas geometrical tolerances are assigned to the cube. The cube is placed on the bottom plate and top plate is placed on the cube subsequently, with three-point moves being employed for both assembly steps. The key characteristics of the assembly are the distances between the points A, B, ..., G on the top surface of the bottom plate and their correspondences A', B', ...,G' on the bottom surface of the top plate. Moreover, two angles α and β are analysed, with α being the angle between the line segments A'C' and AC and β between the segments A'E' and AE.

Both the theoretical limits of the point distances and of the angles as reported in [AM01] as well as the results obtained from each 1,000 samples using the Skin Model Shape approach are summarized in Table 7.1. In this regard, Table 7.1 (a) contains the results for the case without consideration of form and orientation tolerances (i. e. the flatness tolerances of the cube are of value zero and the parallelism tolerance is neglected). It can be seen, that no differences between the Skin Model Shape approach and the theoretical values can be reported. In contrast to that, Table 7.1 (b) highlights the results of the Skin Model Shape approach with consideration of form tolerances (but again without consideration of the orientation tolerance) for three different correlation lengths l_ρ of the form deviations (see Figure 7.10). The results reveal, that the effects of form deviations on the assembly behaviour depend on the characteristics of the form deviations. In this regard, form deviations with comparably short correlation lengths lead to clearly decreased part rotations of the top plate, which manifest in decreased angles α and β as well as decreased point distances AA' and EE'. In contrast to that, form deviations with larger correlation lengths result in increased ranges of the angles α and β. This effect can be understood from Figure 7.11, where a feature with form deviations of different correlation lengths, its orientation tolerance zone (dashed lines), the maximum rotation of a feature without form defects inside this tolerance zone (blue diagonal line), and the actual rotation of an ideal mating feature corresponding to the feature with form defects (red diagonal line) is illustrated. It can be seen, that the maximum rotation of the ideal mating feature is larger than the maximum rotations of the feature without form defects for large correlation

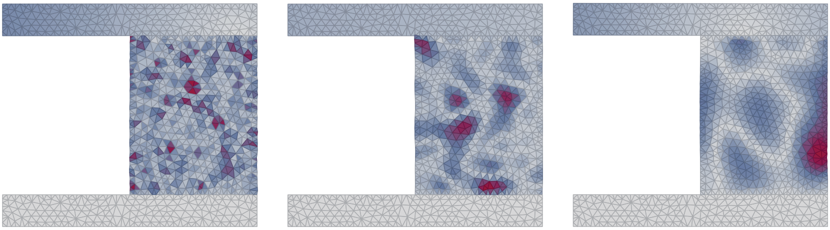

(a) l_ρ = 1mm (b) l_ρ = 5mm (c) l_ρ = 10mm

Figure 7.10: Skin Model Shape Assemblies with Different Form Deviation Correlation Lengths

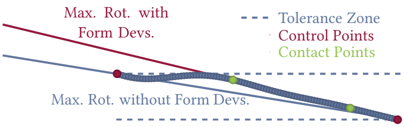

(a) Large Correlation Length and large Tolerance Zone

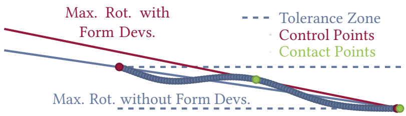

(b) Large Correlation Length and small Tolerance Zone

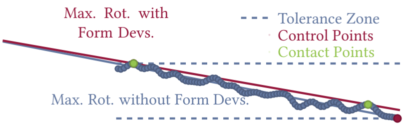

(c) Small Correlation Length and large Tolerance Zone

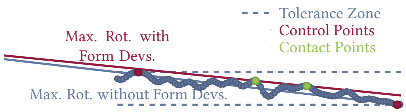

(d) Small Correlation Length and small Tolerance Zone

Figure 7.11: Effect of the Characteristic of the Form Deviations on the Assembly Behaviour: large Correlation Lengths of the Form Deviations lead to increased Part Rotations, whereas small Correlation Lengths lead to decreased Part Rotations

lengths, but smaller for small correlation lengths. Beside this effect, the consideration of form deviations generally results in increased point distances BB', CC', FF', and GG' due to irregular contact points between the cube and the two plates.

Moreover, Table 7.1 (c) shows the theoretical values and the results of the tolerance analysis based on Skin Model Shapes for the case when both the orientation and location tolerances are considered (no consideration of form tolerances). Similarly to the situation without consideration of orientation tolerances, no differences between the theoretical values and the tolerance analysis based on Skin Model Shapes can be observed. Furthermore, the results for the Skin Model Shape approach considering all specified tolerances of the cube are given in Table 7.1 (d). Again, it can be seen, that the consideration of form deviations with small correlation lengths leads to decreased ranges of the angles α and β, whereas form deviations with larger correlation lengths result in increased angle ranges.

Beside the worst-case computations, also statistical tolerance analyses considering all specified tolerances of the cube have been performed. In this context, truncated Gaussian probability distributions have been chosen for the tolerances, with their parameters, which relate to six sigma intervals inside the respective tolerance ranges, being shown in Table 7.2. The

Table 7.1: Maximal Differences between the nominal and the actual Point Distances and maximal Angles: Theoretical Values according to [AM01] and results obtained by the Tolerance Analysis Approach based on Skin Model Shapes

	AA'	BB'	CC'	DD'	EE'	FF'	GG'	α [mrad]	β [mrad]
Theoretical Values	0.60	0.20	0.20	0.20	0.60	0.20	0.20	$\pm$ 5.00	$\pm$ 4.00
Skin Model Shapes	0.60	0.20	0.20	0.20	0.60	0.20	0.20	$\pm$ 5.00	$\pm$ 4.00

(a) Results without Consideration of Form and Orientation Tolerances

	AA'	BB'	CC'	DD'	EE'	FF'	GG'	α [mrad]	β [mrad]
SMS (l_ρ = 1mm)	0.55	0.22	0.22	0.15	0.55	0.22	0.22	$\pm$ 4.52	$\pm$ 3.76
SMS (l_ρ = 5mm)	0.56	0.24	0.25	0.15	0.59	0.25	0.24	$\pm$ 4.65	$\pm$ 3.72
SMS (l_ρ = 10mm)	0.63	0.26	0.26	0.16	0.61	0.24	0.26	$\pm$ 5.10	$\pm$ 3.78

(b) Results with Consideration of Form Tolerances but without Consideration of Orientation Tolerances

	AA'	BB'	CC'	DD'	EE'	FF'	GG'	α [mrad]	β [mrad]
Theoretical Values	0.40	0.20	0.20	0.20	0.40	0.20	0.20	$\pm$ 2.50	$\pm$ 2.00
Skin Model Shapes	0.40	0.20	0.20	0.20	0.40	0.20	0.20	$\pm$ 2.50	$\pm$ 2.00

(c) Results without Consideration of Form Tolerances but with Consideration of Orientation Tolerances

	AA'	BB'	CC'	DD'	EE'	FF'	GG'	α [mrad]	β [mrad]
SMS (l_ρ = 1mm)	0.39	0.23	0.22	0.12	0.38	0.22	0.22	$\pm$ 2.30	$\pm$ 1.78
SMS (l_ρ = 5mm)	0.42	0.24	0.24	0.13	0.42	0.24	0.24	$\pm$ 2.81	$\pm$ 2.15
SMS (l_ρ = 10mm)	0.47	0.26	0.26	0.13	0.44	0.24	0.25	$\pm$ 3.03	$\pm$ 2.39

(d) Results with Consideration of Form and Orientation Tolerances for different Correlation Lengths

truncation of the probability distributions is necessary in order to ensure, that the pseudo-random values are inside meaningful intervals, i. e. that the values are inside the specified tolerance ranges and are non-negative. Figure 7.12 highlights the results of the statistical tolerance analysis based on Skin Model Shapes (l_ρ = 5) in comparison with results obtained by the commercial tolerance simulation tool 3DCS® by Dimensional Control Systems, Inc. as reported in [SAZ+14]. It can be seen, that the consideration of form deviations in conformance to international GPS standards leads to a decreased scatter of the point distances as well as the tilt angles. Moreover, a slight shift of the point distance distributions can be observed due to the consideration of the form deviations of the cubes datum plane.

Table 7.2: Truncated Input Probability Distributions for the different Tolerance Specifications

Tolerance	Type	Mean μ	St. Dev. σ	Min.	Max.
Flatness	Gaussian	0.0250	0.0083	0.0000	0.0500
Parallelism	Gaussian	0.0500	0.0167	0.0000	0.1000
Position	Gaussian	0.1000	0.0333	0.0000	0.2000

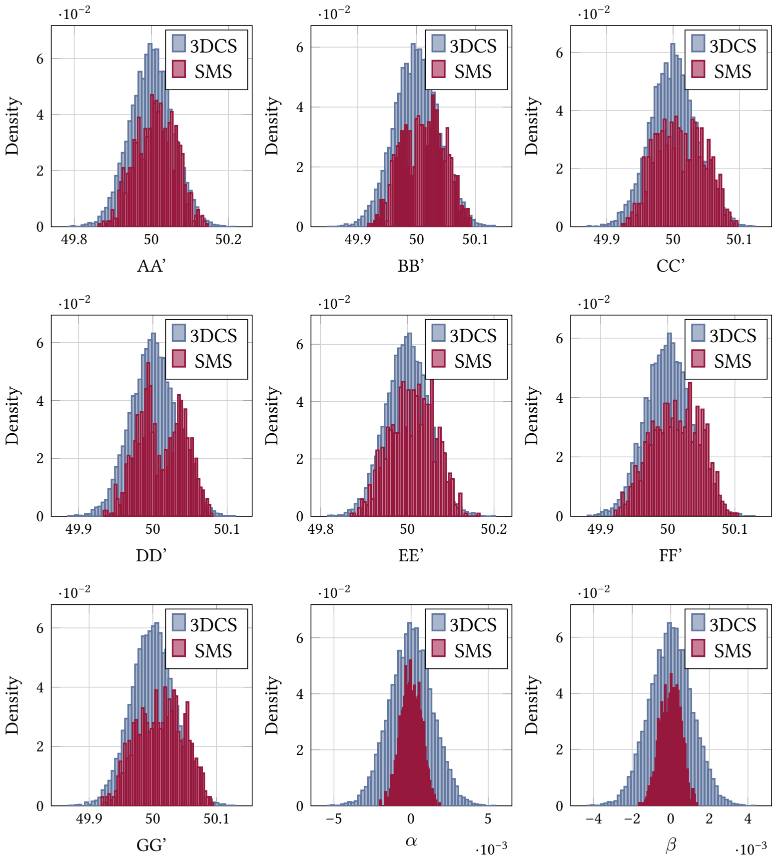

Figure 7.12: Comparison of the Results obtained by 3DCS® as reported in [SAZ+14] and the Skin Model Shape Approach (SMS) for the statistical Tolerance Analysis

7.1.3 Tolerance Stack-Up of four Parts

The third considered tolerance stack-up study case has been reported in [SW16] and can be seen from Figure 7.13. It consists of four parts, with the cubes being subsequently assembled on the clip employing a three-point-move in negative z-direction and a two-point-move in negative x-direction, which results in three contact points between the respective cube and the clip and two contact points between the respective cube and the previous cube or clip, respectively. The key characteristics are the position variation pos of the feature of interest with reference to the datums A and B on the clip and its parallelism variation par also with reference to A and B.

For this study case, the results of worst-case and statistical tolerance analyses employing different tolerance analysis approaches have been reported in [SW16], with Table 7.3 highlighting the considered tolerances in each approach.

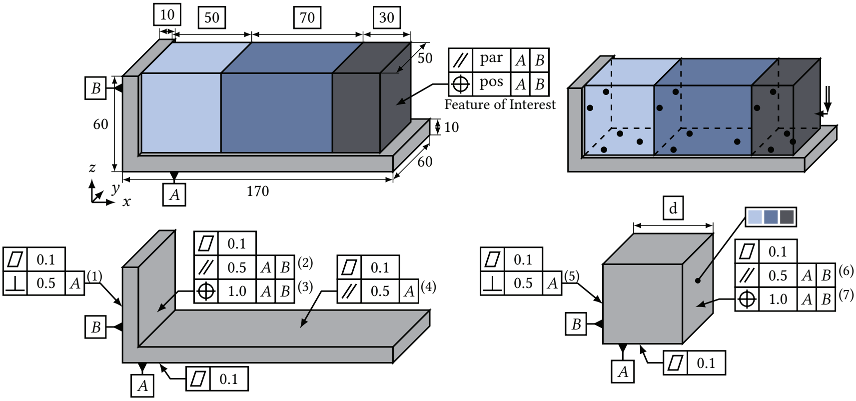

Figure 7.13: Tolerance Stack-Up of four Parts with geometrical Tolerances

In this regard, the worst-case results for the tolerance analysis employing tolerance stacks have been reported as min(pos) = 0.00 and max(pos) = 4.00 [SW16]. Similarly to this, the worst-case limits of the vector loop approach can be found as max(pos) = 4.00. In contrast to that, the tolerance analysis based on Skin Model Shapes without consideration of form deviations gives max(pos) = 4.26. This is because also the effect of the parallelism tolerance (4) is considered, which leads to a rotation of the assembly around the y-axis and hence to an increased position deviation of the feature of interest. In contrast to that, the consideration of form deviations leads up to max(pos) = 5.35, which can be explained by irregular contact points between the parts due to form deviations, that accumulate through the assembly leading to additional position deviations of the feature of interest. Furthermore, based on the results of the SDT approach for the worst possible feature rotations, the maximum parallelism deviation can be calculated as max(par) = 2.07, whereas it results from the tolerance analysis based on Skin Model Shapes as max(par) = 2.07 without and as max(par) = 1.76 with consideration of form deviations.

Beside the worst-case analysis, statistical evaluations have been performed, in which Gaussian input probability densities have been chosen with $\mu = 0.05, \sigma = 0.1/6$ for the form tolerances, $\mu = 0.3, \sigma = 0.4/6$ for the orientation tolerances, and $\mu = 0.75, \sigma = 0.5/6$ for the location tolerances. The results of the statistical tolerance analysis are shown in Figure 7.14 (a), with pos^*_G and par^*_G denoting the results of the tolerance analysis based on Skin Model Shapes with and pos_G and par_G without consideration of form deviations, $\text{pos}^\dagger_G$ are the position deviations calculated by tolerance stacks, and $\text{pos}^\ddagger_G$ using the vector loop approach. It can be found, that

Table 7.3: Considered Tolerances in the different Tolerance Analysis Approaches

Approach	Tolerances	Explanation
Stacks	(3),(7)	Conversion to Dim. Tolerances
Vector Loop	(1)–(3),(5)–(7)	Conversion to Gaps & Dim. Tolerances
SDT	(1),(2),(4)–(6)	Evaluation of Orientation Defects
SMS	(1)–(7) (+ Form)	With & without Form Tolerances

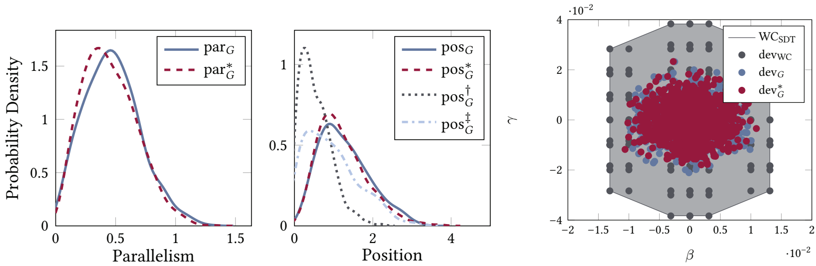

(a) Probability Densities of the KCs (b) Feature of Interest Rotation Defects

Figure 7.14: Results for the Tolerance Stack-Up of four Parts with geometrical Tolerances

tolerance stacks underestimate the position deviation pos, since gaps between the parts as a result of the orientation defects are not considered. Furthermore, it can be seen, that the consideration of form deviations leads to a slight negative shift of the probability densities for the parallelism deviation par. This is because the form deviations decrease the possible feature rotations and hence result in a decreased parallelism deviation of the feature of interest.

Moreover, the rotational defects around the y-axis (β) and around the z-axis (γ) of the feature of interest calculated by the approach based on Skin Model Shapes can be seen from Figure 7.14 (b), with WC_{SDT} indicating the deviation domain calculated by the SDT approach, dev_{WC} indicates the results of the worst-case analysis employing Skin Model Shapes, dev_G^* the results of the statistical tolerance analysis with, and dev_G without consideration of form deviations. It can be seen, that the tolerance analysis based on Skin Model Shapes also allows the worst-case analysis of orientation deviations. Beside this, it can be found, that the consideration of form deviations in the statistical tolerance analysis leads to a slightly decreased spread of the orientation defects of the feature of interest due to irregular contact points compared to the case when the form deviations are nil.

Furthermore, the effect of different tolerancing schemes with regard to the orientation and location tolerances has been analysed. For this purpose, the tolerancing schemes of the clip as well as of the cubes have been revised regarding the datums for the parallelism and position tolerances and the analysed key characteristic is the point-to-point distance between the center point of the right cube and its correspondence on the very left feature of the clip (see the red boxes in Figure 7.15).

Figure 7.16 highlights the results of statistical tolerance analyses (same Gaussian input probability distributions as explained before) for the study case with revised tolerancing scheme, with $\text{SMS}^\dagger$ indicating the results of the Skin Model Shape approach considering the initial tolerancing scheme from Figure 7.13, whereas SMS marks the results of the Skin Model Shape approach for the revised tolerancing scheme and VSA marks the results obtained by VSA® for the revised tolerancing scheme. From the obtained results without consideration of form deviations (Figure 7.16 (a)) it can be seen, that the initial tolerancing scheme (Figure 7.13) ensures the nominal point-to-point distance of 160.0, whereas the revised tolerancing scheme leads to a distinct mean shift towards larger values for the point-to-point distance. Thus, the initial tolerancing scheme is more suitable to ensure the functional requirement. This effect of the

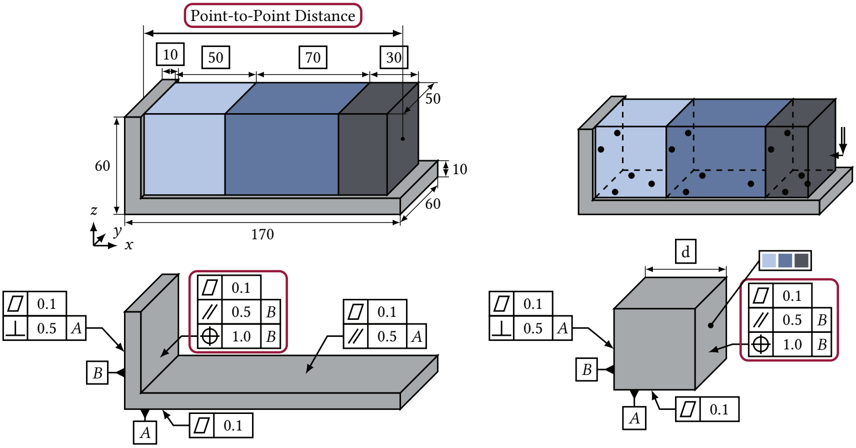

Figure 7.15: Tolerance Stack-Up of four Parts with revised Tolerancing Scheme

tolerancing scheme can also be seen from the results with consideration of form deviations in Figure 7.16 (b). Moreover, it can be found, that the consideration of form deviations leads to a mean shift towards smaller values of the point-to-point distance for both tolerancing schemes, which corresponds to the results discussed before. Beside this, it can be seen, that the results obtained by VSA® underestimate the variation of the point-to-point distance. Furthermore, it should be highlighted, that it was not possible to provide results by VSA® for the initial tolerancing scheme, since the orientation and location tolerances could not be entered with datums systems, though it is conform to tolerancing standards.

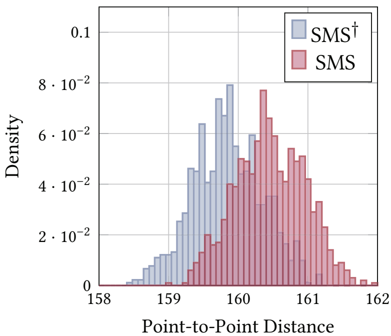

(a) No Consideration of Form Deviations

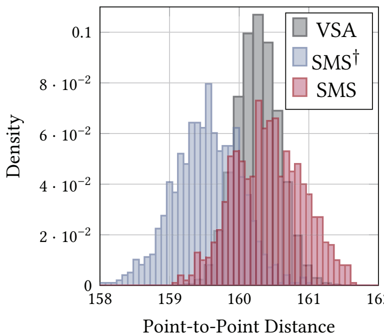

(b) With Consideration of Form Deviations

Figure 7.16: Results for the Tolerance Stack-Up of four Parts with revised Tolerancing Scheme: SMS† highlights the results of the Skin Model Shape approach for the initial Tolerancing Scheme, SMS the results for the revised Tolerancing Scheme, and VSA highlights the results obtained by VSA® for the revised Tolerancing Scheme

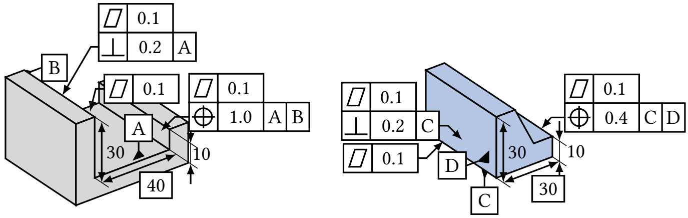

(a) Part Tolerancing Schemes

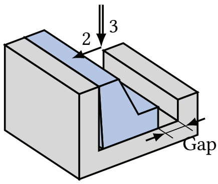

(b) First considered Positioning Scheme

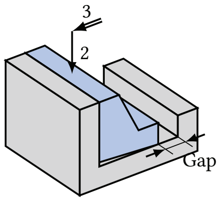

(c) Second considered Positioning Scheme

Figure 7.17: Tolerance Stack-Up considering different Positioning Schemes

7.1.4 Tolerance Stack-Up considering different Positioning Schemes

Similarly to the second case study, this example has been described in [AM01] and aims at analysing the effects of different assembly sequences on the key characteristic. It consists of two parts as illustrated in Figure 7.17 (a), which are assembled employing two different positioning schemes. In this context, the first considered positioning scheme is based on a primary contact between the datums A and C and a secondary contact between the datums B and D, whereas the second positioning scheme leads to a primary contact between the datum features B and D and a secondary contact between A and C (see Figure 7.17 (b) and (c)). The aim of the case study is to analyse if these two positioning schemes lead to different worst-case limits and distributions for the gap between the parts.

Similarly to the second considered study case, both the theoretical values and the results obtained from the Skin Model Shape approach are given in Table 7.4. It can be seen from Table 7.4 (a), that the tolerance analysis approach based on Skin Model Shapes leads to the expected worst-case limits for the gap in conformance to GPS standards when the form deviations are considered nil. In contrast to that, from Table 7.4 (b), it can be found, that the consideration of form deviations leads to slightly decreased worst-case gap values for both positioning schemes.

Beside the worst-case computations, also statistical tolerance analyses have been performed for this study case, in which the parameters for the tolerance distributions can be found in Table 7.5. Similarly to the second study case, the results for the statistical tolerance analysis obtained by the Skin Model Shape approach as well as the results obtained by 3DCS® as reported in [SAZ+14] and results obtained by VSA® are shown in Figure 7.18.

The results for the statistical tolerance analyses reveal little differences between the two considered positioning schemes using the commercial tolerance analysis tools. However, from the

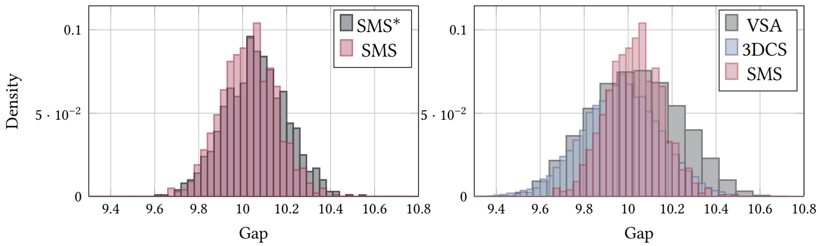

(a) Results for the First considered Positioning Scheme

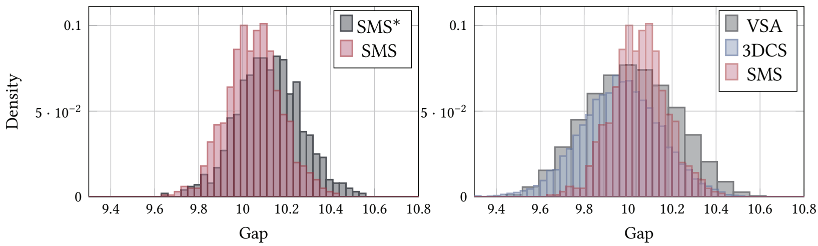

(b) Results for the Second considered Positioning Scheme

Figure 7.18: Comparison of the Results for the mean Gap obtained by 3DCS® as reported in [SAZ+14], obtained by VSA®, and employing the Skin Model Shape Approach (SMS with form deviations, SMS* without form deviations) for the statistical Tolerance Analysis

results of the Skin Model Shape approach, a mean shift of the gap probability towards larger mean gap values can be observed for the second positioning scheme. Moreover, the consideration of form deviations in the Skin Model Shape approach leads to a mean shift towards smaller gap values.

7.1.5 Tolerance Stack-Up of four Parts considering 3-2-1 Positioning Schemes

The last considered tolerance stack example is an extension of the third study case (see section 7.1.3) as a tolerance stack-up consisting of four parts with geometrical tolerances as can be seen from Figure 7.19. In this extension, the part locations of the cubes are additionally locked by a third one-point assembly move in the positive y-direction and the cubes are hence additionally aligned on the back of the gray support.

In order to assess the effects of the mesh density on such a more complex study case, tolerance analyses with three different surface mesh densities (coarse, normal, and dense) of the mating features have been performed. In this regard, the dense surface mesh is characterised by triangle sizes between 0.14 mm^2 and 1.32 mm^2 (mean triangle size of 0.61 mm^2), the normal surface mesh by triangle sizes between 0.43 mm^2 and 3.77 mm^2 (mean triangle size of 1.50 mm^2), and the coarse surface mesh by triangle sizes between 8.55 mm^2 and 51.12 mm^2 (mean triangle size of 21.93 mm^2). The results of the tolerance analyses with these three different surface mesh densities for the key characteristics par and pos can be seen from Figure 7.20, where it can be found, that the surface mesh density has no significant effect on the obtained

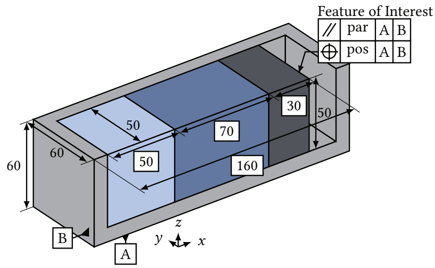

(a) Assembly Group and Key Characteristics

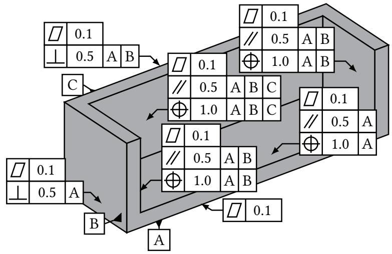

(b) Part Tolerancing Scheme of the Support

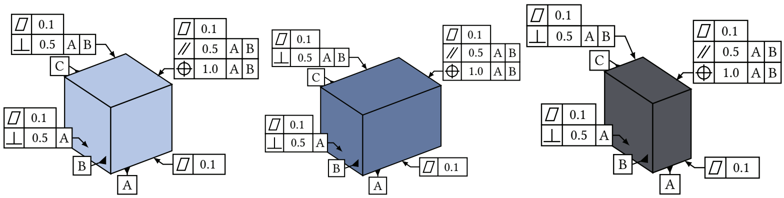

(c) Part Tolerancing Scheme of the Cubes

Figure 7.19: Tolerance Stack-Up of four Parts considering 3-2-1 Positioning Schemes

results in this particular study case neither without nor with consideration of form deviations (tolerance analysis considering a 3-2-1 positioning scheme of polyhedral parts). Tough, it can be seen, that the consideration of form deviations leads to a slightly larger scatter for the key characteristic par and pos. The same situation be seen from Figure 7.21, where the observed feature defects of the feature of interest are highlighted for the three analysed surface meshes. Again, no significant influence of the surface mesh density on the obtained feature defects can be constituted, but the consideration of form deviations leads to a larger scatter of the rotational defects of the feature of interest (compare Figure 7.21 (a, right) with (b, right)). Consequently, for the following tolerance analyses, the normal surface mesh is employed, since no significant accuracy improvements are expected when using the dense surface mesh.

With the aim to study the effects of the additional positioning step on the key characteristics, statistical tolerance analysis with the distribution values described in section 7.1.3 have been performed, with the results being shown in Figure 7.22 in comparison to the results of the study case from section 7.1.3. It can be found, that the adding of the third assembly step in positive y-direction has only minor effects on the key characteristics and on the rotational defects of the feature of interest of the third cube, which can be explained by the comparably small additional shift of the parts, that only slightly alter the resulting part positions.

7.2 Product Assemblability Evaluation

Part deviations not only influence the positions of parts in assemblies and tolerance stacks, but also affect the assemblability of parts in assembly groups. Consequently, assemblability eval-

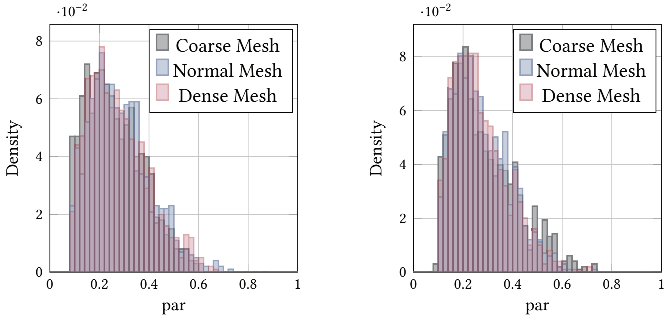

(a) Results for par without (left) and with (right) Consideration of Form Deviations

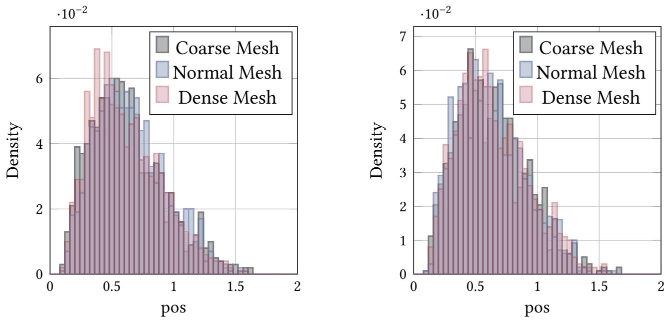

(b) Results for pos without (left) and with (right) Consideration of Form Deviations

Figure 7.20: Results of the Key Characteristics for the Tolerance Analyses with different Surface Mesh Densities for the Tolerance Stack-Up of four Parts considering 3-2-1 Positioning Schemes

uations are to be performed in order to ensure the product assemblability despite geometrical deviations of the mating parts. This section highlights two prominent assemblability analysis problems in tolerancing research and demonstrates the capabilities of the tolerance analysis approach based on Skin Model Shapes considering these specific problems.

7.2.1 Pin-Hole Assembly

A very basic example of part assemblability in tolerancing is the well-known pin-hole assembly problem (see e. g. [AKC96, DQ09]). In order to study the effects of dimensional tolerances of the pin and the hole on the assemblability of the pin, a study case as introduced in [AM01] is analysed (see Figure 7.23). It consists of a pin, which is assembled in a support according to “best-fit” and without application of mating forces. For the analysis, the diameter D of the hole in the support is varied between 11.975 and 12.075, whereas the diameter d of the cylindrical mating feature of the pin is varied between 11.925 and 12.025 (see Figures 7.24 (a) and (b)). Hence, there is a critical area (light red areas in Figures 7.24 (a) and (b)) where the

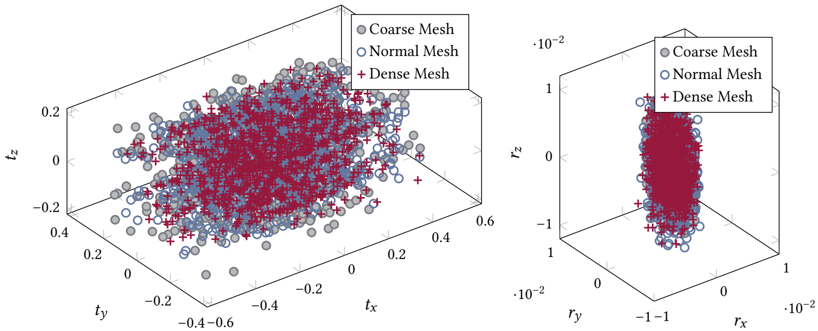

(a) Observed Feature Defects of the Feature of Interest without Consideration of Form Deviations

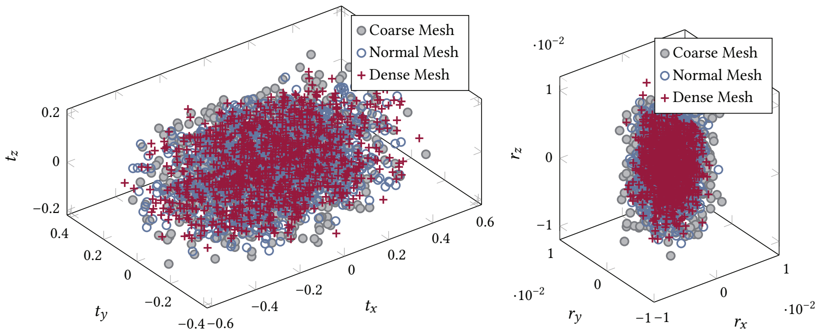

(b) Observed Feature Defects of the Feature of Interest with Consideration of Form Deviations

Figure 7.21: Observed Feature Defects of the Feature of Interest for the Tolerance Analyses with different Surface Mesh Densities for the Tolerance Stack-Up of four Parts considering 3-2-1 Positioning Schemes: Translational Defects left and Rotational Defects right

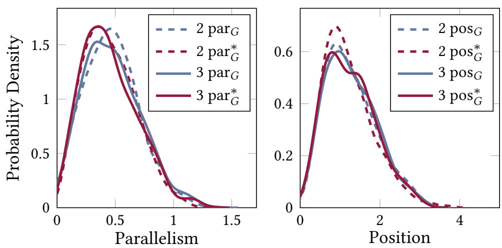

(a) Probability Densities of the Key Characteristics

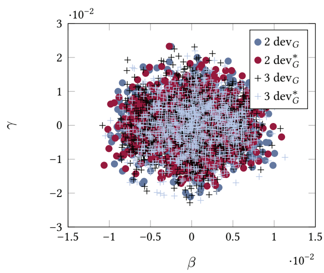

(b) Feature of Interest Rotational Defects

Figure 7.22: Results of the extended Tolerance Stack-Up of four Parts: 2 highlights the Results obtained for the Case Study in Figure 7.13, 3 highlights the Results for the current Extension in Figure 7.19, * highlights Consideration of Form Deviations

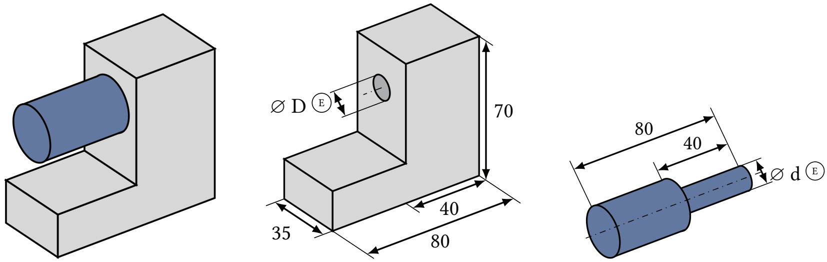

Figure 7.23: Pin-Hole Assembly and Part Specifications

assembly is not feasible, since the diameter D of the hole is smaller than the diameter d of the pin. Theoretically, this area corresponds to 12.5% of all considered diameter combinations.

In order to analyse this study case employing the tolerance analysis approach based on Skin Model Shapes, the assembly of the pin in the hole is simulated using the constrained registration approach, which employs numerical optimization algorithms to solve the assembly problem. Figure 7.24 (a) highlights the results of this analysis without consideration of form deviations, with the blue dots highlighting diameter combinations, that led to feasible solutions of the numerical optimization, whereas the red crosses imply diameter combinations, for which the optimization algorithm could not find feasible solutions. It can be seen, that the tolerance analysis based on Skin Model Shapes leads to reasonable results, even if the number of non-feasible diameter combinations is slightly larger (14.0%) than for the theoretical consideration. However, this effect could be reduced by using refined surface meshes of the mating features in order to minimize the discretization error.

Beside this, also the effects of form deviations have been studied by adding cylindricity tolerances of 0.05 to both the hole in the support and the cylindrical mating feature of the pin. The results for this situation are illustrated in Figure 7.24 (b). It can be found, that the number of non-feasible assemblies is distinctly smaller (8.8%) than for the case without form deviations and now also diameter combinations in the light red area are found to be feasible. This is because the form deviations of the mating cylinders partially balance out and lead to situations, where the diameter of the hull cylinder of the hole is smaller than the diameter of the hull cylinder of the pin, but the assembly is still feasible. Furthermore, there are some non-feasible diameter combinations in the light blue area, which can be traced back to discretization errors, which worsen when considering form deviations.

7.2.2 Two-Pin-Two-Hole Assembly

Beside the single pin-hole assembly problem, the two-pin-two-hole (TPTH) assembly is a prominent study case in tolerancing research (see e. g. [LY95, DBM08, BGDD13, DDG15, PM15a]). In order to study such as problem, an example case as described in [AM01] is analysed in the following. It consists of a plate, which is positioned on a base part by two pin-hole connections (see Figure 7.25), with the two pins and holes, respectively, being assigned with dimensional tolerances with material modifier as well as with location tolerances. Due to hole

Table 7.4: Theoretical Values of the minimum and maximum Gap according to [AM01] and results obtained by the Tolerance Analysis Approach based on Skin Model Shapes

First considered Positioning Scheme

	Gap Value
Theoretical Value	min 9.30 — max 10.90
Skin Model Shapes	min 9.30 — max 10.90

Second considered Positioning Scheme

	Gap Value
Theoretical Value	min 9.30 — max 11.10
Skin Model Shapes	min 9.30 — max 11.10

(a) Results without Consideration of Form Tolerances

First considered Positioning Scheme

	Gap Value
Skin Model Shapes	min 9.23 — max 10.88

Second considered Positioning Scheme

	Gap Value
Skin Model Shapes	min 9.21 — max 10.99

(b) Results with Consideration of Form Tolerances

Table 7.5: Truncated Input Probability Distributions for the different Tolerance Specifications

Tolerance	Type	Mean μ	St. Dev. σ	Min.	Max.
Flatness	Gaussian	0.0500	0.0167	0.0000	0.1000
Perpendicularity	Gaussian	0.1000	0.0333	0.0000	0.2000
Position (Support)	Gaussian	0.5000	0.1667	0.0000	1.0000
Position (Top Part)	Gaussian	0.2000	0.0667	0.0000	0.4000

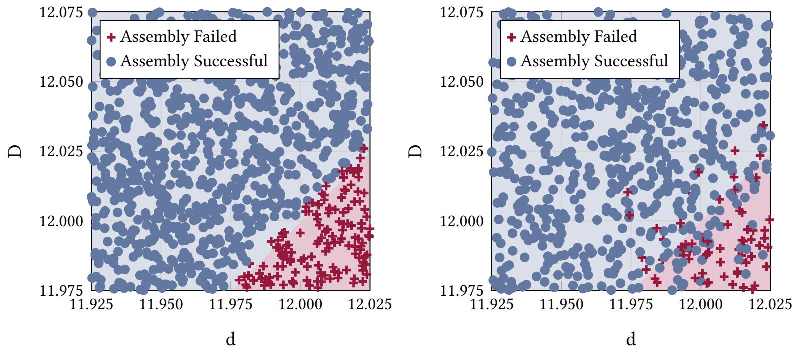

(a) Without Consideration of Form Deviations (b) With Consideration of Form Deviations

Figure 7.24: Results of the Assemblability Evaluation without and with Consideration of Form Deviations: The light-blue area highlights combinations of d and D, where the assembly is theoretically feasible, whereas the assembly is theoretically non-feasible in the light-red area.

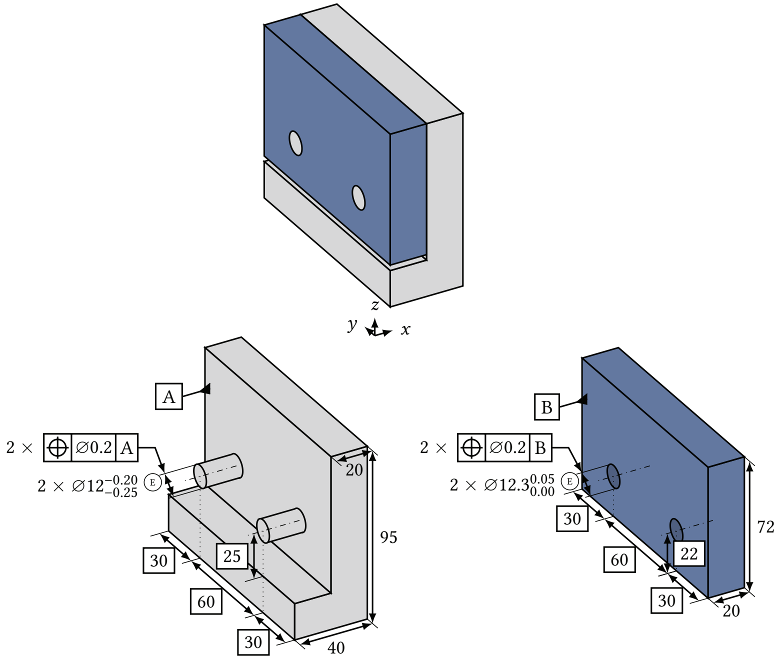

Figure 7.25: Two-Pin-Two-Hole Assembly with Part Specifications

clearance, the plate is subject to rotations, while the key characteristics of this study case are the point variations in z-direction of the points A, B, C, D, and E on the bottom of the plate as illustrated in Figure 7.26.

The worst-case point variations in z-direction considering maximal hole clearance, i. e. assuming pin diameters of 11.75 and hole diameters of 12.35, without consideration of location deviations of the pins and holes, respectively, have been calculated employing the gap hull estimation approach based on Skin Model Shapes and can be seen in comparison to the theoretical values reported in [AM01] in Table 7.6 (a). The small differences between the theoretical values and the values obtained from the gap hull estimation can be traced back to discretization errors of the surface meshes, which lead to slightly varying part rotations for this specific study case. Beside these small differences, good agreement between the theoretical values and the results of the Skin Model Shape approach can be concluded.

Moreover, the point variations considering location tolerances can be seen from Figure 7.27 and the worst-case point variations are given in Table 7.6 (b), with cylindricity tolerances of 0.02 having been added to both pins and holes to investigate the effects of form deviations of the mating features in the Skin Model Shape approach. It can be seen, that the consideration of location errors of the pins and holes leads to increased point variations and this effect is even amplified by form deviations regarding the point variations of the points B, C, and D.

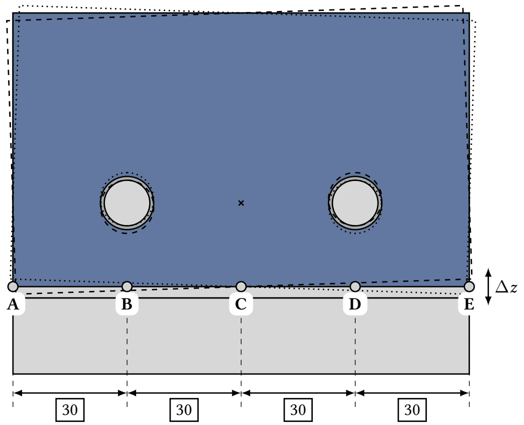

Figure 7.26: Two-Pin-Two-Hole Assembly: Point Variations due to Hole Clearance and Pin/Hole Positioning Errors

Table 7.6: Worst-Case Point Variations: Theoretical Values according to [AM01] and Results obtained by the Tolerance Analysis Approach based on Skin Model Shapes with and without Consideration of Form Deviations

	A	B	C	D	E
Theoretical Values	$\pm$ 0.60	$\pm$ 0.30	$\pm$ 0.30	$\pm$ 0.30	$\pm$ 0.60
Skin Model Shapes	$\pm$ 0.59	$\pm$ 0.31	$\pm$ 0.29	$\pm$ 0.30	$\pm$ 0.58

(a) Point Variations for Maximal Hole Clearance without Consideration of Location Tolerances

	A	B	C	D	E
Skin Model Shapes	$\pm$ 0.75	$\pm$ 0.57	$\pm$ 0.40	$\pm$ 0.57	$\pm$ 0.75
Skin Model Shapes (*)	$\pm$ 0.75	$\pm$ 0.63	$\pm$ 0.41	$\pm$ 0.66	$\pm$ 0.75

(b) With Consideration of Location Tolerances: (*) highlights the Consideration of Form Deviations

7.3 Further Applications and Additional Functionalities

Beside the analysis of typical tolerance stacks and the assemblability evaluation, some further application examples of the tolerance analysis approach based on Skin Model Shapes are provided in the following. In this regard, firstly an example study consisting of five parts with geometrical tolerances is studied, which is followed by two irregular tolerance stack examples.

7.3.1 Five-Piece Assembly

In order to apply the tolerance analysis approach based on Skin Model Shapes to a larger assembly, a study case as highlighted in [Dij05] is considered. It is build of five parts, which are subsequently stacked employing three-point moves in negative z-direction, two-point moves in negative x-directions, and one-point moves in positive y-direction as can be seen from Figure 7.28. The key characteristic is the position deviation of the hole feature of part 4 (red),

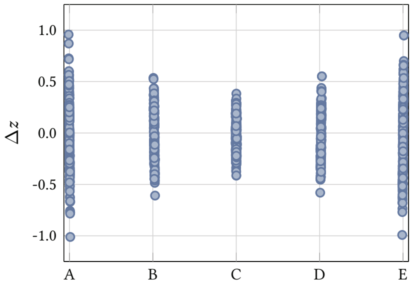

(a) Without Consideration of Form Deviations

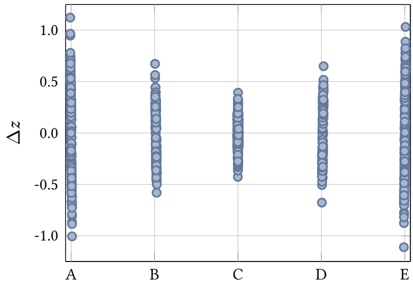

(b) With Consideration of Form Deviations

Figure 7.27: Two-Pin-Two-Hole Assembly: Resulting Point Variations

Table 7.7: Five-Piece Assembly: Truncated Input Probability Distributions

Tolerance	Type	Mean μ	St. Dev. σ	Min.	Max.
Form	Gaussian	0.0250	0.0083	0.0000	0.0500
Orientation	Gaussian	0.0750	0.0083	0.0500	0.1000
Location	Gaussian	0.1500	0.0167	0.1000	0.2000
Position (Hole)	Gaussian	0.3000	0.0333	0.2000	0.4000

which is to be ensured by a total number of 96 geometrical tolerance specifications, with the part tolerancing schemes having been obtained by CLIC [Ans06].

For this study case, worst-case as well as statistical tolerance analyses have been performed, where the assumed probability distributions for the statistical evaluations relate to a six-sigma assumption considering the well-known relationship between form, orientation, and location tolerances and are given in Table 7.7. The resulting probability distributions for the key characteristic for these worst-case and statistical tolerance analyses are highlighted in Figure 7.29. It can be seen, that the consideration of form deviations leads to an increased variation of the key characteristic due to irregular contact points between the parts under both worst-case and statistical conditions. Moreover, slightly tightened distributions of pos are obtained in the statistical case as expected.

In order to study these effects more in detail, the observed feature defects of the hole feature in part 4 are highlighted in Figure 7.30. In this regard, it can be found, that the consideration of form deviations leads to increased rotational and translational feature defects under both worst-case and statistical conditions. Moreover, it can be seen, that the translational feature defects t in y-direction are more distinct than in x- and z-direction, while the rotational feature defects r around the y-axis are considerably smaller than around the x- and z-direction.

With the aim to investigate the main contributors among the deviations of the part features, that are labelled in Figure 7.28, to these defects of the hole feature in part 4, a density-based sensitivity analysis as described in [PBS13] has been performed, to which the results are summarized in Figure 7.31. The bar plots in Figure 7.31 highlight the moment-independent sensitivity measures δ of the feature deviations of the different parts for each respective feature defect (translational t or rotational r). In this regard, for example the main contributor to the translational feature defect of the hole feature in x-direction (t_x, top left part of Figure 7.31

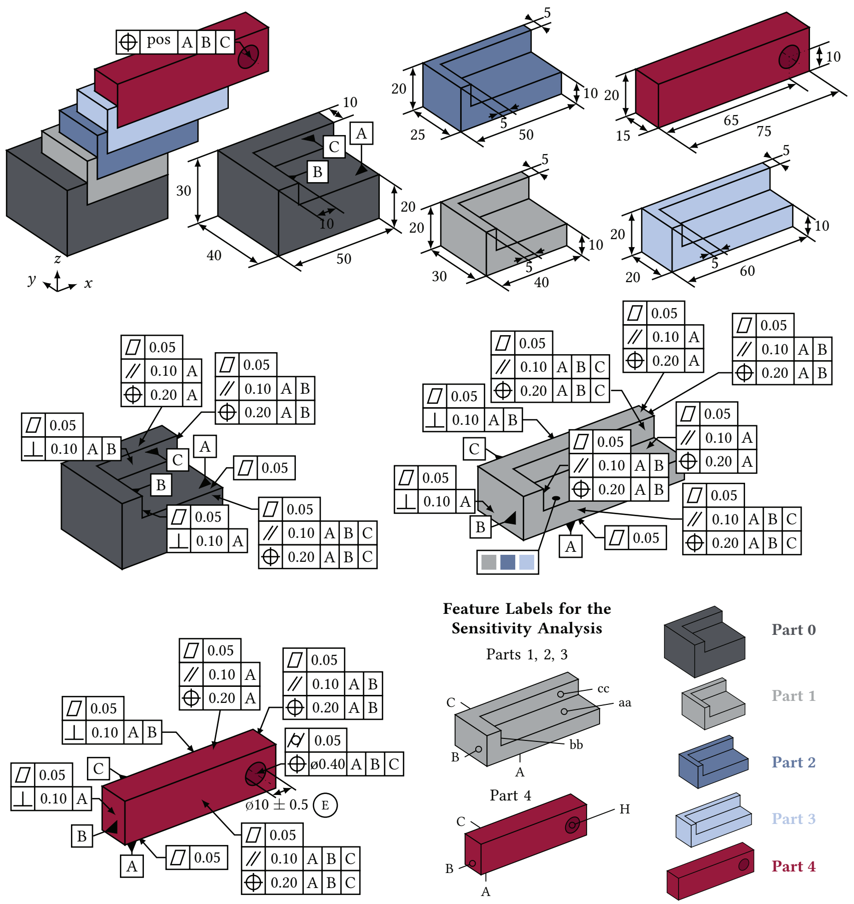

Figure 7.28: Five-Piece Assembly and Tolerancing Schemes

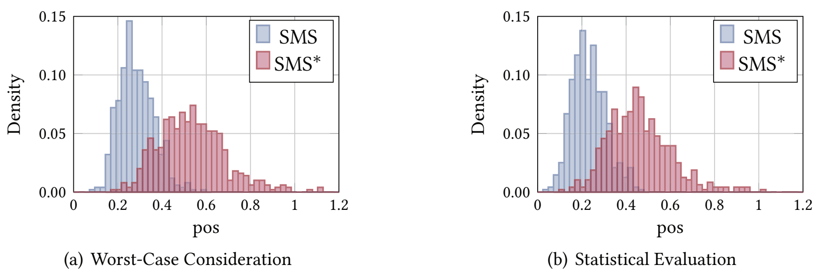

Figure 7.29: Five-Piece Assembly: Resulting Probability Distributions for the Key Characteristic, with (*) indicating the Consideration of Form Deviations

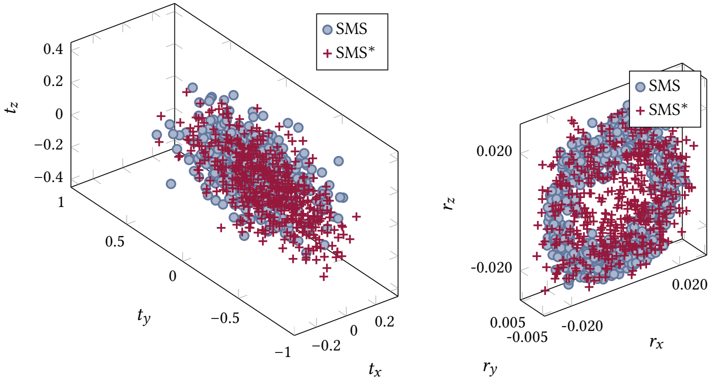

(a) Worst-Case Consideration

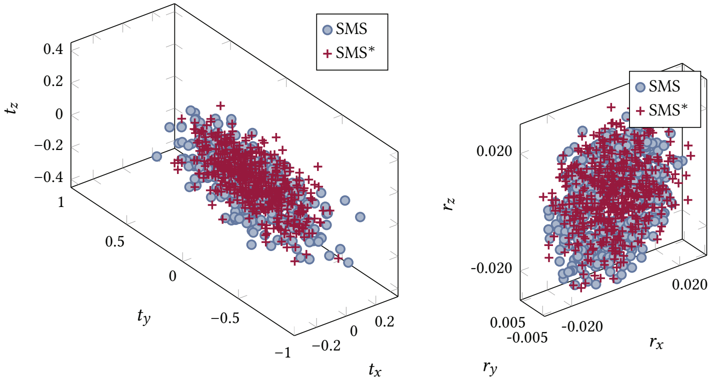

(b) Statistical Evaluation

Figure 7.30: Five-Piece Assembly: Observed Defects of the Hole Feature in Part 4

(a)) is $\oplus 3_{bb(t_x)}$, which marks the translational feature deviation in x-direction (t_x) of feature bb of part 3. This translational feature deviation is controlled by the position tolerance on this feature (see Figure 7.28). The other contributors to t_x in Figure 7.31 (a) are $\oplus 1_{bb(t_x)}$ and $\oplus 2_{bb(t_x)}$, which are the translational feature deviations of feature bb on part 1 and 2, which are both controlled by position tolerances, as well as $/\!/1_{aa(r_y)}$, which designates the rotational feature deviation around the y-axis of feature aa of part 1, which is controlled by a parallelism tolerance. This shows, that not only the translational deviations t_x of the bb features of the parts 1, 2, and 3 have an effect on the translational feature defect of the hole feature of part 4, but also the rotational deviation of feature aa of part 1, since it leads to a tilting of the whole assembly group. Similar effects can also be observed for the translational defects of the hole feature in z-direction (t_z), which are influenced by the translational feature deviations in z-direction of the aa features of parts 1, 2, and 3, but also by the rotational feature deviations around the y-axis (r_y) of the aa features of parts 1 and 2.

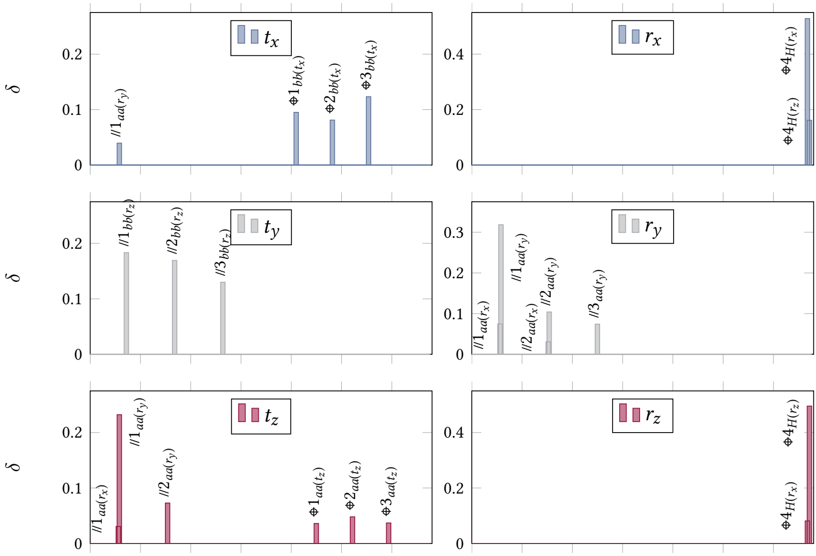

(a) Without Consideration of Form Deviations

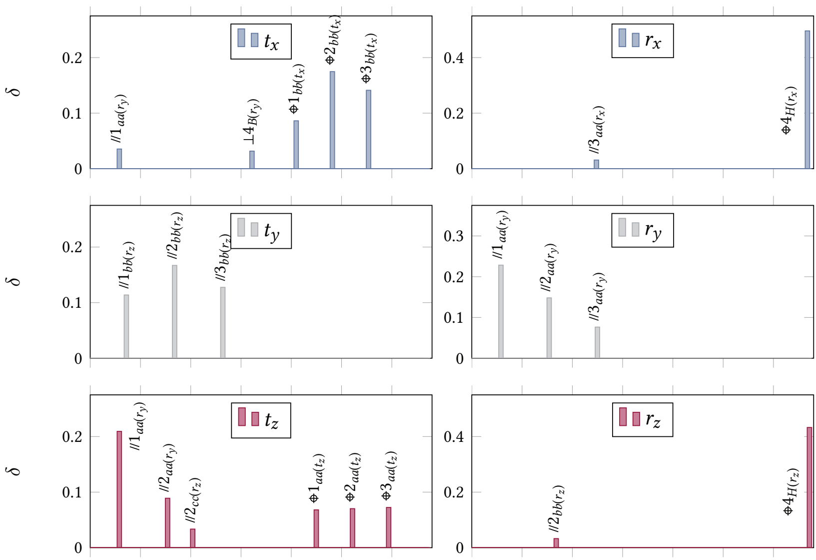

(b) With Consideration of Form Deviations

Figure 7.31: Five-Piece Assembly: Results of the Sensitivity Analysis based on Statistical Tolerance Analyses

However, when comparing Figures 7.31 (a) and (b), it can be found, that the consideration of form deviations has distinct effects on the results of the sensitivity analysis, since feature deviations, that are identified as contributors without consideration of form deviations, dissolve when form deviations are considered. Moreover, feature deviations, that have no effect when neglecting form deviations, influence the assembly behaviour when taking into account form defects.

7.3.2 Two Discs in a Box

The following study case has been employed in [MP09, MP11b, MP11a, Pol11, Pol12] to compare different tolerance analysis approaches, such as the vector loop approach, the variational model, the matrix approach, the Jacobian model, and the Torsor approach. It consists of two discs, which are positioned inside a box (see Figure 7.32). The discs and the box are specified with dimensional and geometrical tolerances and the key characteristic of the assembly is the vertical gap between the second disc and the top of the box. The solutions for this case study obtained by different tolerance analysis approaches considering these dimensional as well as geometrical tolerances have been provided in [Pol11] and can be seen from Table 7.8 compared to the results of the Skin Model Shape approach. In this regard, the two-dimensional variations of the proposed algorithms for the scaling and assembly simulation of Skin Model Shapes have been applied for the tolerance analysis based on Skin Model Shapes and Gaussian input probability distributions with centred mean and six sigma variation have been assumed for the statistical evaluations.

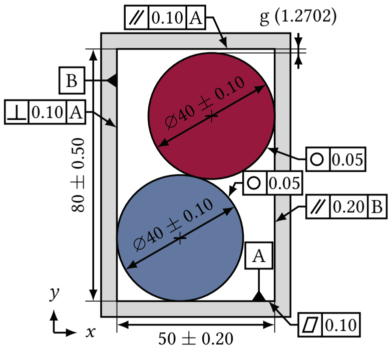

Figure 7.32: Two Discs in a Box as presented in [MP09, MP11b, MP11a, Pol11, Pol12]

From the results, it can be seen, that the tolerance analysis approach based on Skin Model Shapes leads to comparable levels regarding the gap variation as the other tolerance analysis

Table 7.8: Two Discs in a Box: Results for different Tolerance Analysis Approaches according to [Pol11] and for the Skin Model Shape Approach without (SMS) and with (SMS*) Consideration of Form Deviations

Approach	Worst-Case	Statistical
Vector Loop	$\pm$ 1.03	$\pm$ 0.54
Variational	$\pm$ 0.78	$\pm$ 0.50
Matrix	$\pm$ 0.69	–
Jacobian	$\pm$ 0.78	$\pm$ 0.53
Torsor	$\pm$ 0.78	–
SMS	$\pm$ 0.80	$\pm$ 0.62
SMS*	$\pm$ 0.85	$\pm$ 0.55

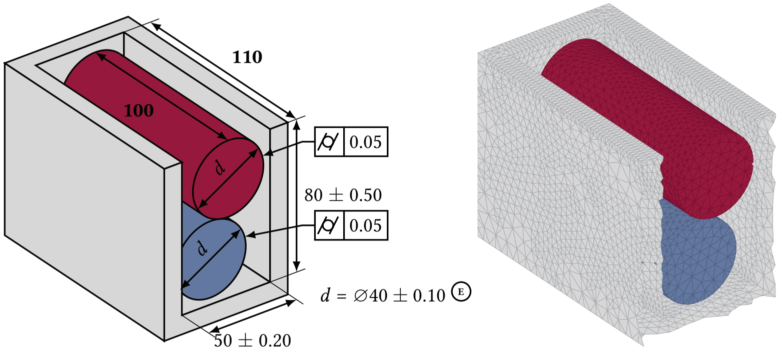

Figure 7.33: Three-Dimensional Extension of the Two Discs in a Box Study: Main Extensions compared to the initial Tolerancing Scheme in Figure 7.32 and Detail of the Surface Meshes

Table 7.9: Two Discs in a Box: Results for the Three-Dimensional Extension of the Study Case employing the Skin Model Shape Approach without (SMS) and with (SMS*) Consideration of Form Deviations

Approach	Worst Case	Statistical
SMS	± 0.81	± 0.58
SMS*	± 1.00	± 0.66

methods. However, it can also be seen, that the form deviations have partly contrary effects, since they lead to increased worst-case limits, but to decreased statistical limits for the gap value. This is because the form deviations may lead to more extreme part positions in worst-case consideration, but decrease the effects of dimensional variations in statistical evaluations.

Moreover, a three-dimensional extension of this study case as illustrated in Figure 7.33 has been analysed employing the Skin Model Shape approach. The results for worst-case and statistical evaluations (same distributional assumptions as before) can be seen from Table 7.9, where it can be found, that the three-dimensional tolerance analysis leads to comparable results as the two-dimensional tolerance simulation model for this study case. However, the consideration of form deviations results in slightly increased scatter for the gap values.

7.3.3 Irregular Tolerance Stack

The final study case is an irregular tolerance stack as originally proposed by Chase [Cha99], which has also been analysed in [BYWC13]. It consists of three parts (see Figure 7.34), namely a block (blue), which is placed on a frame (gray) and which is to position a cylinder (red). The key characteristic of the assembly is the gap G between the cylinder and the top of the frame. In order to analyse the effects of form deviations on such an irregular tolerance stack-up, the tolerancing scheme as proposed in [Cha99, BYWC13] is revised and geometrical tolerances are added as part specifications. Indeed, it should be noted, that for the sake of comprehensibility, the analysed tolerancing scheme as illustrated in Figure 7.34 is not fully complete and rigorous. Moreover, in contrast to the works in [Cha99, BYWC13], a three-dimensional tolerance analysis is performed.

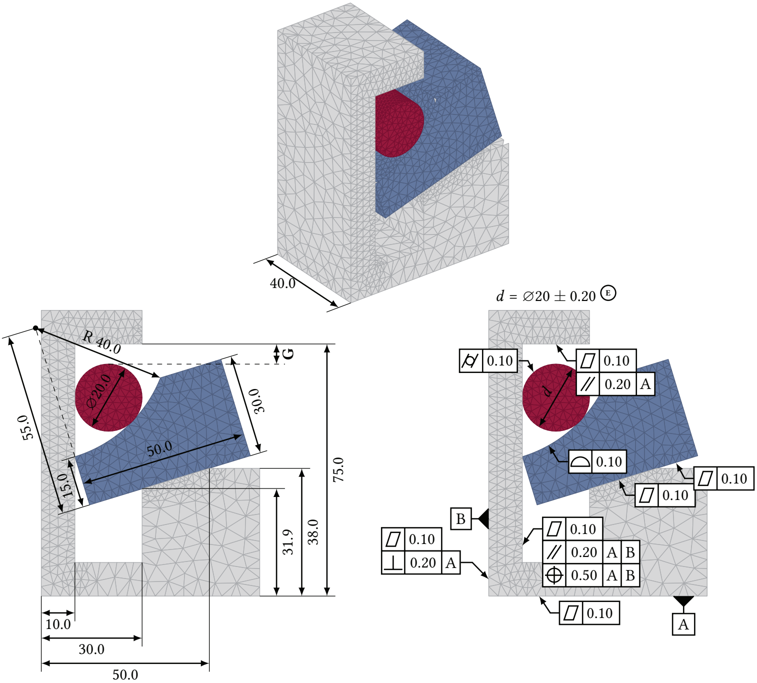

Figure 7.34: Irregular Tolerance Stack as adapted from [Cha99, BYWC13]

The results of the three-dimensional tolerance analysis based on Skin Model Shapes for the study case considering worst-case and statistical evaluations are given in Table 7.10 (b), where the distribution parameters from Table 7.10 (a) have been assumed for the statistical evaluations. It can be seen, that the consideration of form deviations leads to distinctly increased variations of the gap between the cylinder and the frame, which even amplifies under statistical assumptions.

Table 7.10: Irregular Tolerance Stack: Probability Distribution Parameters and Results for the Study Case employing the Skin Model Shape Approach without (SMS) and with (SMS*) Consideration of Form Deviations

Tolerance	Mean	St. Dev.	Min.	Max.
Dimension	0.2000	0.0667	0.0000	0.4000
Form	0.0500	0.0167	0.0000	0.1000
Orientation	0.1500	0.0167	0.1000	0.2000
Location	0.3500	0.0500	0.2000	0.5000

(a) Parameter Values of the Gaussian Probability Distributions for the Statistical Evaluations

Approach	Worst-Case	Statistical
SMS	$\pm$ 0.45	$\pm$ 0.37
SMS*	$\pm$ 0.62	$\pm$ 0.58

(b) Results of the Tolerance Analyses

7.4 Discussion of the obtained Results

The computer-aided tolerance analysis is a key tool for modern companies, since it helps to identify vast potentials for time and cost savings by enabling the virtual prediction of the effects of geometrical part deviations on assembly key characteristics as well as the evaluation of consequences of design decisions on the product quality. However, the benefits of tolerance analysis tools strongly depend on the assumptions, that are implicitly and explicitly made by these tools, as these assumptions distinctly influence the accuracy and validity of the obtained results. With the aim to assess the capabilities and limitations of the tolerance analysis approach based on Skin Model Shapes, various study cases have been analysed in the preceding sections and the obtained results have been compared to theoretical values reported in scientific literature as well as to the results of other tolerance analysis approaches and of commercial tolerance analysis software. In this context, the results for the highlighted tolerance analysis study cases reveal important insights, which are summarized in the following.

Impact of the Point and Mesh Density on the Tolerance Analysis Results The tolerance analysis based on the concept of Skin Model Shapes employs discrete geometry representation schemes, such as point clouds and surface meshes, for the modelling of parts considering geometrical deviations as well as for their scaling, the assembly simulation, the gap hull estimation, and the contact and mobility simulation. As it has been highlighted in chapter 4, the application of such discrete geometry representation schemes implies discretization errors, since point clouds and surface meshes only approximate the part surface. In this regard, it can for example be seen from the results of the tooth contact analysis for gears in section 5.5.2.3, that the accuracy of the obtained analysis results depends on the density of the employed surface meshes with dense meshes leading to more accurate results than coarse meshes. Moreover, the results of the assemblability evaluation for the pin-hole assembly (section 7.2.1) are influenced by the surface mesh density, which also applies to the gap hull estimation for the two-pin-two-hole problem (section 7.2.2). In contrast to that, the analysis results for the tolerance stack examples reveal no significant differences between coarse and dense surface meshes when considering 3-2-1 positioning schemes of polyhedral parts. Thus, it can be concluded, that the surface mesh density has an effect on the tolerance analysis results when considering curved and cylindrical part features. In such applications, careful attention should be paid to the surface mesh generation, while keeping in mind, that the discretization errors can be adjusted by the level of surface approximation. However, for many other applications, such as the analysis of tolerance stack-ups of polyhedral parts, coarse surface meshes not necessarily manifest in worsened tolerance analysis results.

Comparison with other Tolerance Analysis Approaches The obtained results of the tolerance analysis based on Skin Model Shapes have been elaborately compared to the results of other tolerance analysis approaches as well as of commercial software tools for various study cases. Based on these comparisons, it can be found, that the tolerance analysis employing Skin Model Shapes generally leads to comparable result levels for different analysis problems. However, distinct differences between the results of various tolerance analysis approaches have been identified, particularly when considering form deviations. This applies to the analysis of tolerance stack-ups, such as the stack-up of two plates and a cube (section 7.1.2) and the tolerance stack-up of four parts (sections 7.1.3 and 7.1.5), as well as the study of irregular stack-ups, such as the two discs in a box example (section 7.3.2). These differences can be observed for worst-case as well as for statistical tolerance analyses. Beside this, additional functionalities of the tolerance analysis approach based on Skin Model Shapes have been demonstrated, such as the assemblability evaluation, the two-dimensional tolerance analysis, as well as the gap hull estimation. These features offer further benefits in specific application examples.

Conformance to Tolerancing Standards In order to assess the conformance of the tolerance analysis approach based on Skin Model Shapes to international tolerancing standards, particularly to the standards for the geometrical product specification, the results obtained for several study cases have been compared to theoretical values provided in scientific literature. These study cases comprise the tolerance stack-up of parts with multiply toleranced features in section 7.1.2, the stack-up considering different part positioning schemes in section 7.1.4, and the assemblability evaluation for pin-hole assemblies in section 7.2.1 and for two-pin-two-hole problems in 7.2.2. From these comparisons, it can be found, that the tolerance analysis approach based on Skin Model Shapes is capable of adequately representing the theoretical effects of multiply toleranced features, of datum precedence, of material modifiers, as well as of form deviations. Though further comparisons could be performed for other relevant issues regarding the conformance to tolerancing standards, it can be argued, that the tolerance analysis based on Skin Model Shapes is conform to international tolerancing standards.

Effects of Form Deviations on Assembly Key Characteristics During the last decades, various tolerance analysis approaches have been proposed, which are predominantly based on the implicit or explicit assumption, that, due to their supposedly minor effects, form deviations can be neglected. However, motivated by the increasing relative importance of form deviations, which can be attributed to the advancements in manufacturing technology, the concept of Skin Model Shapes has been proposed, which enables the consideration of form deviations in the tolerance analysis and variation simulation. As it can be found based on the results of the analysed case studies, these form deviations of the mating parts have distinct effects on the key characteristics of mechanical assemblies and considerably influence the behaviour of physical products during use. However, it can also be seen, that the effects of form deviations are often contradictory and in spite of expert knowledge, they are seldom assessable based on mere reasoning. Thus, appropriate computer-aided tools are required, that allow the virtual prediction of these effects in order to optimize product and process development decisions. The proposed tolerance analysis approach based on Skin Model Shapes offers such as tool and is thus an important contribution to the computer-aided engineering environment in modern companies.

In conclusion, it can be found, that the concept of Skin Model Shapes as a new paradigm for the computer-aided tolerance analysis offers a sound theoretical framework and a tolerance analysis theory, which overcomes severe shortcomings of established tolerance analysis approaches.

8 Conclusion and Perspectives for future Research

The geometrical characteristics of mechanical products hugely influence their quality and functional compliance. Thus, quality-aware companies are strongly required to manage geometrical part variations, which can be observed on every manufactured artefact, and their manifold effects on various product quality attributes throughout the whole product life-cycle. In modern value added chains, which widely rely on specialisation, the concept of interchangeable parts, and external procurement, this comprises many different tasks and activities, that are performed by various actors. In this context, special attention should be paid to the tolerancing activities during design, since the decisions made in these early product development stages have far-reaching impacts on the product quality as well as on the product costs. In order to support these early tolerancing activities, tolerance simulation and tolerance analysis tools are increasingly applied in various industries, since they allow the virtual prediction of the effects on geometrical part deviations on geometrical product key characteristics without the need for time- and cost-expensive physical mock-ups. However, these tools and their underlying mathematical approaches for the tolerance representation and propagation have distinct weaknesses, such as the insufficient consideration of form deviations, which gain ascending importance for the function of high-precision mechanism, and the lacking conformance to international tolerancing standards, which evolved during the last century as the established means of communication between the various actors in geometrical variations management.

In order to overcome these important shortcomings, the concept of Skin Model Shapes as a novel paradigm for the modelling of geometrical deviations in mechanical engineering has been introduced (see Figure 8.1). It stems from basic concepts of the standards for the geometrical product specification and conveys the concept of the "Digital Twin" [Gri14] to geometrical variations management. The current work explored the fundamentals of the concept of Skin Model Shapes by providing a model conceptualisation, by investigating approaches for its representation and visualisation, by elaborating a framework for the generation of Skin Model Shapes, and by carving out possible applications and perspectives for this concept in mechanical engineering. Beside this, the work provided a comprehensive framework for the tolerance analysis based on Skin Model Shapes and proposed various computational algorithms for the scaling, the assembly simulation, the gap hull estimation, the contact and mobility simulation, and the key characteristics measurement for discrete geometry Skin Model Shapes. Moreover, the implementation of these algorithms in a software prototype has been illustrated and the tolerance analysis approach based on Skin Model Shapes has been applied to various study cases. Based on the obtained results, it can be found, that form deviations have significant effects on various key characteristics and must not be neglected in tolerance analyses of high-precision mechanical products.

However, perspectives for further research efforts are the consideration of novel manufacturing processes, such as additive manufacturing, as well as of various physical phenomena, such as thermal effects, in the generation and processing of Skin Model Shapes. In this regard, also the potentials of the concept of Skin Model Shapes for process-oriented tolerancing, that have already been sketched in [SW13b], need to be further investigated and exploited, which

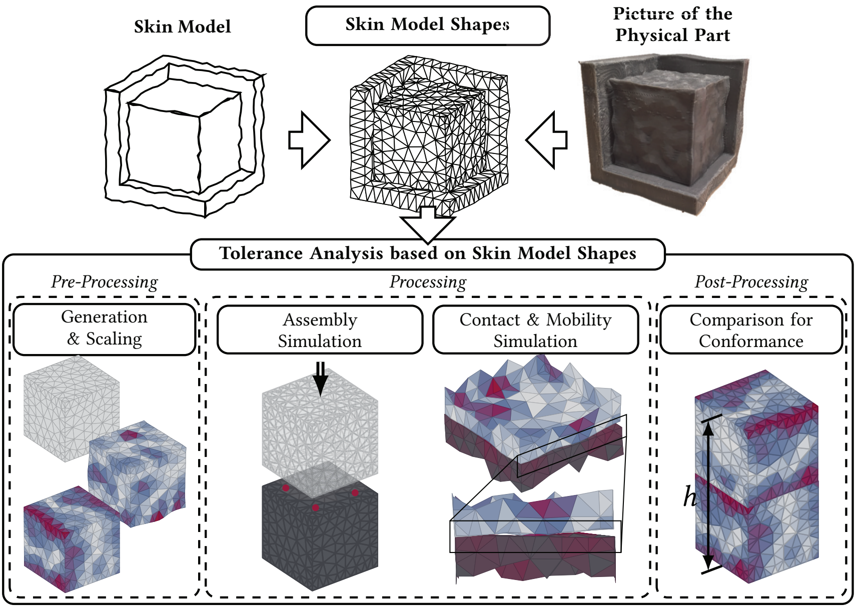

Figure 8.1: Main Contributions of the current Work: The Concept of Skin Model Shapes as a novel Paradigm for the Modelling of Geometrical Deviations and a Framework for the Tolerance Analysis based on Skin Model Shapes

is the objective of ongoing research projects. Moreover, the consideration of form deviations in tolerance analyses requires improved approaches for the worst-case and statistical evaluation of tolerance simulation models as well as for the sensitivity analysis in order to better support product development teams and manufacturing engineers in deriving adequate tolerancing decisions. A generic concept for the sensitivity analysis in geometrical variations management based on Skin Model Shapes has already been proposed in [SW15c], but further research is required to increase the explanatory power of these approaches and to reduce the required computational efforts. The accomplishment of these future research challenges has partly begun and will contribute to the establishment of the concept of Skin Model Shapes as a paradigm in computer-aided tolerancing and geometrical variations modelling.

In conclusion, it has been shown, that the concept of Skin Model Shapes offers a versatile and potent approach for the modelling and representation of geometrical variations in mechanical engineering and that the tolerance analysis based on Skin Model Shapes employing point-based geometry representation schemes allows the realistic prediction of the effects of geometrical part deviations on product key characteristics considering form deviations and in conformance to international standards for the geometrical product specification.

Appendix

In the following, further details about the employed assembly simulation models and the used surface meshes for the various study cases from section 7 are given.

Tolerance Stack-Up of two Cubes (Section 7.1.1)

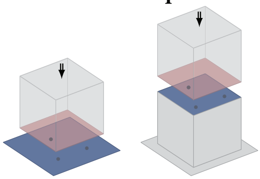

Type of Moves: 3-Point-Assembly
Assembly Model: Difference Surface
Mesh Statistics: Triangle Sizes (min. / max. / mean)
Coarse Mesh: 8.7 mm^2 / 48.9 mm^2 / 22.3 mm^2
Dense Mesh: 0.2 mm^2 / 1.3 mm^2 / 0.6 mm^2

Tolerance Stack-Up of two Plates and a Cube (Section 7.1.2)

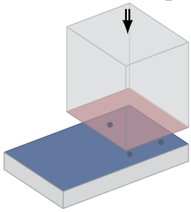

First Assembly Step
Type of Move: 3-Point-Assembly
Assembly Model: Difference Surface
Mesh Statistics: Triangle Sizes (min. / max. / mean)
= *Mating Feature:* 0.9 mm^2 / 5.7 mm^2 / 3.0 mm^2
= *Moving Feature:* 0.6 mm^2 / 3.9 mm^2 / 2.0 mm^2

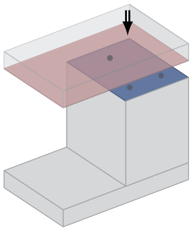

Second Assembly Step
Type of Move: 3-Point-Assembly
Assembly Model: Difference Surface
Mesh Statistics: Triangle Sizes (min. / max. / mean)
= *Mating Feature:* 0.6 mm^2 / 4.3 mm^2 / 2.1 mm^2
= *Moving Feature:* 0.7 mm^2 / 5.7 mm^2 / 3.0 mm^2

Tolerance Stack-Up of four Parts (Section 7.1.3)

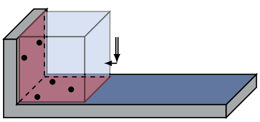

First Assembly Step
Type of Move: 3-2-Point-Assembly
Assembly Model: Difference Surface
Mesh Statistics: Triangle Sizes (min. / max. / mean)
= *Mating Features:* 1.9 mm^2 / 17.8 mm^2 / 7.9 mm^2
= *Moving Features:* 0.4 mm^2 / 3.6 mm^2 / 1.6 mm^2

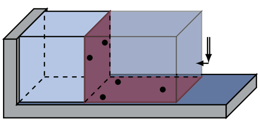

Second Assembly Step
Type of Move: 3-2-Point-Assembly
Assembly Model: Difference Surface
Mesh Statistics: Triangle Sizes (min. / max. / mean)
= *Mating Features:* 1.9 mm^2 / 17.8 mm^2 / 7.9 mm^2
= *Moving Features:* 0.5 mm^2 / 4.1 mm^2 / 2.0 mm^2

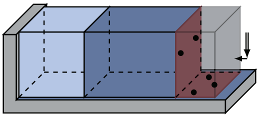

Third Assembly Step

Type of Move: 3-2-Point-Assembly
Assembly Model: Difference Surface
Mesh Statistics: Triangle Sizes (min. / max. / mean)
= *Mating Features:* 1.9 mm^2 / 17.8 mm^2 / 7.9 mm^2
= *Moving Features:* 0.3 mm^2 / 2.6 mm^2 / 1.3 mm^2

Tolerance Stack-Up considering different Positioning Schemes (Section 7.1.4)

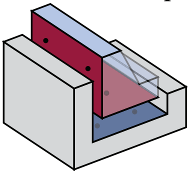

Type of Move: 3-2-Point-Assembly
Assembly Model: Difference Surface
Mesh Statistics: Triangle Sizes (min. / max. / mean)
= *Mating Features:* 0.1 mm^2 / 1.1 mm^2 / 0.5 mm^2
= *Moving Features:* 0.1 mm^2 / 0.6 mm^2 / 0.3 mm^2

Tolerance Stack-Up of four Parts considering 3-2-1 Positioning Schemes (Section 7.1.5)

First Assembly Step

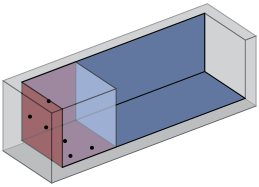

Type of Move: 3-2-1-Point-Assembly
Assembly Model: Difference Surface
Mesh Statistics: Triangle Sizes (min. / max. / mean)
= *Mating Features:* Coarse: 47.2 mm^2/ 223.2 mm^2/ 103.7 mm^2
Normal: 2.0 mm^2 / 19.1 mm^2 / 7.7 mm^2
Fine: 0.9 mm^2 / 7.8 mm^2 / 3.6 mm^2
= *Moving Features:* Coarse: 8.7 mm^2 / 39.6 mm^2 / 21.2 mm^2
Normal: 0.4 mm^2 / 3.6 mm^2 / 1.6 mm^2
Fine: 0.2 mm^2 / 1.3 mm^2 / 0.6 mm^2

Second Assembly Step

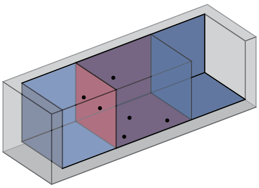

Type of Move: 3-2-1-Point-Assembly
Assembly Model: Difference Surface
Mesh Statistics: Triangle Sizes (min. / max. / mean)
= *Mating Features:* Coarse: 47.2 mm^2/ 223.2 mm^2/ 103.7 mm^2
Normal: 2.0 mm^2 / 19.1 mm^2 / 7.7 mm^2
Fine: 0.9 mm^2 / 7.8 mm^2 / 3.6 mm^2
= *Moving Features:* Coarse: 10.6 mm^2 / 61.7 mm^2 / 25.4 mm^2
Normal: 0.5 mm^2 / 4.1 mm^2 / 2.0 mm^2
Fine: 0.2 mm^2 / 1.7 mm^2 / 0.8 mm^2

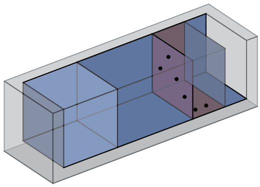

Third Assembly Step

Type of Move: 3-2-1-Point-Assembly
Assembly Model: Difference Surface
Mesh Statistics: Triangle Sizes (min. / max. / mean)
= *Mating Features:* Coarse: 47.2 mm^2/ 223.2 mm^2/ 103.7 mm^2
Normal: 2.0 mm^2 / 19.1 mm^2 / 7.7 mm^2
Fine: 0.9 mm^2 / 7.8 mm^2 / 3.6 mm^2
= *Moving Features:* Coarse: 6.7 mm^2 / 30.8 mm^2 / 15.3 mm^2
Normal: 0.3 mm^2 / 2.6 mm^2 / 1.3 mm^2
Fine: 0.1 mm^2 / 1.0 mm^2 / 0.5 mm^2

Pin-Hole Assembly (Section 7.2.1)

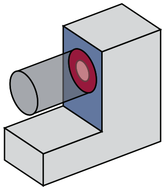

Optimization Feature

Type of Move: Best-Fit
Assembly Model: Constrained Registration
Mesh Statistics: Triangle Sizes (min. / max. / mean)
= *Mating Features:* 0.3 mm^2 / 7.0 mm^2 / 2.3 mm^2
= *Moving Features:* 0.1 mm^2 / 2.5 mm^2 / 0.7 mm^2

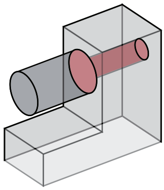

Constraint Feature

Type of Move: Best-Fit
Assembly Model: Constrained Registration
Mesh Statistics: Triangle Sizes (min. / max. / mean)
= *Mating Features:* 0.2 mm^2 / 1.1 mm^2 / 0.4 mm^2
= *Moving Features:* 0.1 mm^2 / 0.6 mm^2 / 0.2 mm^2

Two-Pin-Two-Hole Assembly (Section 7.2.2)

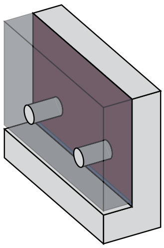

Optimization Feature

Type of Move: Best-Fit
Assembly Model: Constrained Registration
Mesh Statistics: Triangle Sizes (min. / max. / mean)
= *Mating Features:* 0.4 mm^2 / 4.5 mm^2 / 1.8 mm^2
= *Moving Features:* 0.3 mm^2 / 3.3 mm^2 / 1.6 mm^2

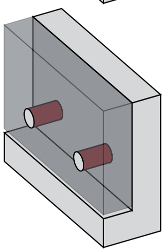

Constraint Feature

Type of Move: Best-Fit
Assembly Model: Constrained Registration
Mesh Statistics: Triangle Sizes (min. / max. / mean)
= *Mating Features:* 0.3 mm^2 / 1.6 mm^2 / 0.8 mm^2
= *Moving Features:* 0.3 mm^2 / 1.2 mm^2 / 0.6 mm^2

Five-Piece Assembly (Section 7.3.1)

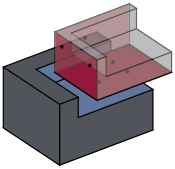

First Assembly Step

Type of Move:	3-2-1-Point-Assembly
Assembly Model:	Difference Surface
Mesh Statistics:	Triangle Sizes (min. / max. / mean)
= *Mating Features:*	0.3 mm^2 / 2.3 mm^2 / 1.0 mm^2
= *Moving Features:*	0.7 mm^2 / 4.9 mm^2 / 2.0 mm^2

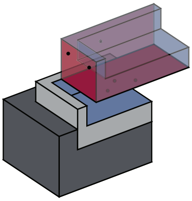

Second Assembly Step

Type of Move:	3-2-1-Point-Assembly
Assembly Model:	Difference Surface
Mesh Statistics:	Triangle Sizes (min. / max. / mean)
= *Mating Features:*	0.6 mm^2 / 5.1 mm^2 / 1.9 mm^2
= *Moving Features:*	0.8 mm^2 / 5.8 mm^2 / 2.4 mm^2

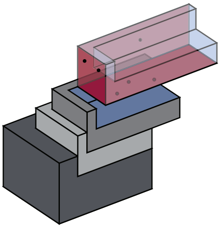

Third Assembly Step

Type of Move:	3-2-1-Point-Assembly
Assembly Model:	Difference Surface
Mesh Statistics:	Triangle Sizes (min. / max. / mean)
= *Mating Features:*	0.7 mm^2 / 5.0 mm^2 / 2.3 mm^2
= *Moving Features:*	0.8 mm^2 / 7.3 mm^2 / 3.3 mm^2

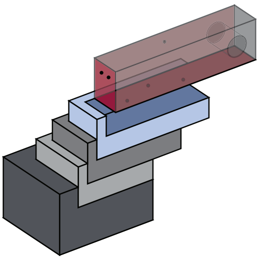

Fourth Assembly Step

Type of Move:	3-2-1-Point-Assembly
Assembly Model:	Difference Surface
Mesh Statistics:	Triangle Sizes (min. / max. / mean)
= *Mating Features:*	1.0 mm^2 / 5.5 mm^2 / 2.6 mm^2
= *Moving Features:*	0.4 mm^2 / 2.9 mm^2 / 1.2 mm^2

Two Discs in a Box (Section 7.3.2)

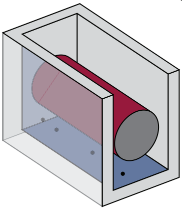

First Assembly Step

Type of Move:	2-2-Point-Assembly
Assembly Model:	Difference Surface
Mesh Statistics:	Triangle Sizes (min. / max. / mean)
= *Mating Features:*	1.8 mm^2 / 14.1 mm^2 / 6.2 mm^2
= *Moving Features:*	2.2 mm^2 / 14.0 mm^2 / 5.1 mm^2

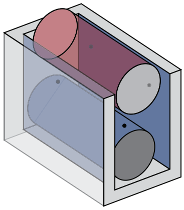

Second Assembly Step

Type of Move:	2-2-Point-Assembly
Assembly Model:	Difference Surface
Mesh Statistics:	Triangle Sizes (min. / max. / mean)
All Features:	$2.2\,mm^2$ / $14.0\,mm^2$ / $5.1\,mm^2$

Irregular Tolerance Stack (Section 7.3.3)

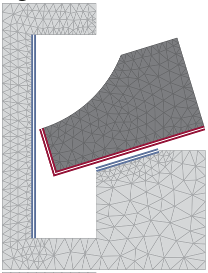

First Assembly Step

Type of Move:	3-2-Point-Assembly
Assembly Model:	Difference Surface
Mesh Statistics:	Triangle Sizes (min. / max. / mean)
= *Mating Features:*	$0.7\,mm^2$ / $5.9\,mm^2$ / $2.6\,mm^2$
= *Moving Features:*	$1.4\,mm^2$ / $10.1\,mm^2$ / $4.3\,mm^2$

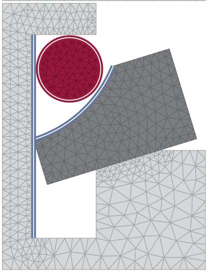

Second Assembly Step

Type of Move:	2-2-Point-Assembly
Assembly Model:	Difference Surface
Mesh Statistics:	Triangle Sizes (min. / max. / mean)
= *Mating Features:*	$0.8\,mm^2$ / $3.7\,mm^2$ / $1.8\,mm^2$
= *Moving Features:*	$0.3\,mm^2$ / $2.0\,mm^2$ / $0.9\,mm^2$

Bibliography

[ABC+99] Alvarez, A.; Barbero, J. I.; Carrillo, A. R.; Gutiérrez, T.; and Aizpitarte, M. TASys: A Computer Aided Tolerance System based on a Variational Geometry formulation. In Houten, F. and Kals, H., editors, *Global Consistency of Tolerances*, pages 207–214. Springer Netherlands, Dordrecht, 1999.

[Abe15] Abel, O. Toleranzanalyse in der Relaistechnik. In Wartzack, S., editor, *Summer School Toleranzmanagement – Beiträge zur 2. Summer School September 2015*, pages 58–65. Druck+Verlag Ernst Vögel GmbH Stamsried, 2015.

[ABM13] Anwer, N.; Ballu, A.; and Mathieu, L. The skin model, a comprehensive geometric model for engineering design. *CIRP Annals - Manufacturing Technology*, 62(1):143 – 146, 2013.

[ABW14] Ashhab, M.; Breitsprecher, T.; and Wartzack, S. Neural network based modeling and optimization of deep drawing – extrusion combined process. *Journal of Intelligent Manufacturing*, 25(1):77–84, 2014.

[ACYA10] Anselmetti, B.; Chavanne, R.; Yang, J.-X.; and Anwer, N. Quick GPS: A new CAT system for single-part tolerancing. *Computer-Aided Design*, 42(9):768 – 780, 2010.

[Ada21] Adams, J. Q. Report upon Weights and Measures. Report, United States, Dept. of State, 1821.

[Adr09] Adragna, P.-A. Respecting the loss-cost of a non-symmetrical functional requirement with a statistical tolerancing approach. In Giordano, M.; Villeneuve, F.; and Mathieu, L., editors, *Proceedings of the 11th CIRP International Conference on Computer Aided Tolerancing, Annecy*, 2009.

[AFSP08] Adragna, P.-A.; Favrelière, H.; Samper, S.; and Pillet, M. Statistical Assemblies with form Errors — A 2D Example. In Ratchev, S. and Koelemeijer, S., editors, *Micro-Assembly Technologies and Applications*, volume 260 of *IFIP — International Federation for Information Processing*, pages 23–33. Springer US, 2008.

[AG08] Arvidsson, M. and Gremyr, I. Principles of robust design methodology. *Quality and Reliability Engineering International*, 24(1):23–35, 2008.

[AJF15] Asadi, N.; Jackson, M.; and Fundin, A. Handling Product Variety in a Mixed-Product Assembly Line: A Case Study. In Weber, C.; Husung, S.; Cantamessa, M.; Cascini, G.; Marjanovic, D.; and Graziosi, S., editors, *Proceedings of the 20th International Conference on Engineering Design ICED15 Vol. 4: Design for X, Design to X, Milan*, pages 41–50, 2015.

[AKC96] Anantha, R.; Kramer, G. A.; and Crawford, R. H. Assembly modelling by geometric constraint satisfaction. *Computer-Aided Design*, 28(9):707 – 722, 1996.

[AL05] Anselmetti, B. and Louati, H. Generation of manufacturing tolerancing with ISO standards. *International Journal of Machine Tools and Manufacture*, 45(10):1124 – 1131, 2005.

[AM01] Anselmetti, B. and Mathieu, L. Evaluation des performances des logiciels d'aide au tolérancement. In *Integrated Design and Production CPI 2001, Fez (Maroc)*, Paper No. 8, 2001.

[And96] Andersson, P. A semi-analytic approach to robust design in the conceptual design phase. *Research in Engineering Design*, 8(4):229–239, 1996.

[ANLS13] Abellán-Nebot, J. V.; Liu, J.; and Subirón, F. R. Process-oriented tolerancing using the extended stream of variation model. *Computers in Industry*, 64(5):485 – 498, 2013.

[Ans06] Anselmetti, B. Generation of functional tolerancing based on positioning features. *Computer-Aided Design*, 38(8):902 – 919, 2006.

[Ans10] Anselmetti, B. Part optimization and tolerances synthesis. *The International Journal of Advanced Manufacturing Technology*, 48(9-12):1221–1237, 2010.

[Arm13] Armillotta, A. A method for computer-aided specification of geometric tolerances. *Computer-Aided Design*, 45(12):1604 – 1616, 2013.

[Arm15] Armillotta, A. Force analysis as a support to computer-aided tolerancing of planar linkages. *Mechanism and Machine Theory*, 93:11 – 25, 2015.

[Arm16] Armillotta, A. Tolerance Analysis Considering form Errors in Planar Datum Features. *Procedia CIRP – 14th CIRP Conference on Computer-Aided Tolerancing*, 43:64 – 69, 2016.

[AS05] Azariadis, P. N. and Sapidis, N. S. Drawing curves onto a cloud of points for point-based modelling. *Computer-Aided Design*, 37(1):109 – 122, 2005.

[AS13] Armillotta, A. and Semeraro, Q. Critical operating conditions for assemblies with parameter-dependent dimensions. *Proceedings of the Institution of Mechanical Engineers, Part B: Journal of Engineering Manufacture*, 227(5):735–744, 2013.

[AS14] Andrews, J. and Séquin, C. H. Type-Constrained Direct Fitting of Quadric Surfaces. *Computer-Aided Design and Applications*, 11(1):107–119, 2014.

[Asa09] Asante, J. N. A small displacement torsor model for tolerance analysis in a workpiece-fixture assembly. *Proceedings of the Institution of Mechanical Engineers, Part B: Journal of Engineering Manufacture*, 223(8):1005–1020, 2009.

[ASF10] Adragna, P.-A.; Samper, S.; and Favreliere, H. How Form Errors Impact on 2D Precision Assembly with Clearance? In Ratchev, S., editor, *Precision Assembly Technologies and Systems*, volume 315 of *IFIP Advances in Information and Communication Technology*, pages 50–59. Springer Berlin Heidelberg, 2010.

[ASG11] Ameta, G.; Samper, S.; and Giordano, M. Comparison of Spatial Math Models for Tolerance Analysis: Tolerance-Maps, Deviation Domain, and TTRS. *Journal of Computing and Information Science in Engineering*, 11(2):021004, 2011.

[ASM00] ASME. ASME B89.4.10:2000: Methods for Performance Evaluation of Coordinate Measuring System Software. Standard, 2000.

[ASM09] ASME. ASME Y14.5-2009: Dimensioning and Tolerancing. Standard, 2009.

[ASMW14] Anwer, N.; Schleich, B.; Mathieu, L.; and Wartzack, S. From solid modelling to skin model shapes: Shifting paradigms in computer-aided tolerancing. *CIRP Annals - Manufacturing Technology*, 63(1):137 – 140, 2014.

[ASP10] Adragna, P.-A.; Samper, S.; and Pillet, M. A proposition of 3D inertial tolerancing to consider the statistical combination of the location and orientation deviations. *International Journal of Product Development*, 10(1-2):26–45, 2010.

[AT07] Adler, R. J. and Taylor, J. E. *Random Fields and Geometry*. Number 1 in Springer Monographs in Mathematics. Springer New York Inc., 1 edition, 2007.

[ATLD14] Andolfatto, L.; Thiébaut, F.; Lartigue, C.; and Douilly, M. Quality- and cost-driven assembly technique selection and geometrical tolerance allocation for mechanical structure assembly. *Journal of Manufacturing Systems*, 33(1):103–115, 2014.

[AW16] Aschenbrenner, A. and Wartzack, S. A Concept for the Consideration of Dimensional and Geometrical Deviations in the Evaluation of the Internal Clearance of Roller Bearings. *Procedia CIRP – 14th CIRP Conference on Computer-Aided Tolerancing*, 43:256 – 261, 2016.

[Aza04] Azariadis, P. N. Parameterization of clouds of unorganized points using dynamic base surfaces. *Computer-Aided Design*, 36(7):607 – 623, 2004.

[BA11] Benichou, S. and Anselmetti, B. Thermal dilatation in functional tolerancing. *Mechanism and Machine Theory*, 46(11):1575 – 1587, 2011.

[Bau15] Bauer, L. Entwicklung eines Verfahrens für die mathematische Beschreibung von Fertigungsabweichungen. In Wartzack, S., editor, *Summer School Toleranzmanagement – Beiträge zur 2. Summer School September 2015*, pages 74–79. Druck+Verlag Ernst Vögel GmbH Stamsried, 2015.

[BB98] Ballot, E. and Bourdet, P. A Computation Method for the Consequences of Geometric Errors in Mechanisms. In ElMaraghy, H. A., editor, *Geometric Design Tolerancing: Theories, Standards and Applications*, pages 197–207. Springer US, 1998.

[BB08] Bischof, A. and Blessing, L. Guidelines for the Development of flexible Products. In Marjanovic, D.; Storga, M.; Pavkovic, N.; and Bojcetic, N., editors, *Proceedings of the 10th International Design Conference DESIGN 2008, Dubrovnik*, pages 289–300, 2008.

[BBM91] Ballu, A.; Bourdet, P.; and Mathieu, L. The Processing of Measured Points in Coordinates Metrology in Agreement with the Definition of Standardized Specifications. *CIRP Annals - Manufacturing Technology*, 40(1):491 – 494, 1991.

[BC76] Bourdet, P. and Clement, A. Controlling a complex Surface with a 3 Axis Measuring Machine. *CIRP Annals - Manufacturing Technology*, 25(1):359–361, 1976.

[BDBM07] Bruyère, J.; Dantan, J.-Y.; Bigot, R.; and Martin, P. Statistical tolerance analysis of bevel gear by tooth contact analysis and Monte Carlo simulation. *Mechanism and Machine Theory*, 42(10):1326 – 1351, 2007.

[BDH96] Barber, C. B.; Dobkin, D. P.; and Huhdanpaa, H. The Quickhull Algorithm for Convex Hulls. *ACM Trans. Math. Softw.*, 22(4):469–483, 1996.

[BDK94] Boothroyd, G.; Dewhurst, P.; and Knight, W. *Product Design for Manufacture and Assembly.* Marcel Dekker, Inc., New York, 1994.

[BDM10] Ballu, A.; Dantan, J.-Y.; and Mathieu, L. Language of Tolerancing: GeoSpelling. In Villeneuve, F. and Mathieu, L., editors, *Geometric Tolerancing of Products.* ISTE Ltd. and John Wiley & Sons, Inc., 2010.

[BDT07] Ballu, A.; Dufaure, J.; and Teissandier, D. An Adaptive Tolerance Model For Collaborative Design. In Cunha, P. and Maropoulos, P., editors, *Digital Enterprise Technology*, pages 233–240. Springer US, 2007.

[BEK07] Barari, A.; ElMaraghy, H. A.; and Knopf, G. K. Evaluation of Geometric Deviations in Sculptured Surfaces Using Probability Density Estimation. In Davidson, J. K., editor, *Models for Computer Aided Tolerancing in Design and Manufacturing*, pages 135–146. Springer Netherlands, 2007.

[Ben93] Bennich, P. Chain of Standards: A new Concept in Tolerancing and Engineering Drawing GPS-Standards – Geometrical Product Specification Standards. In Srinivasan, V. and Voelcker, H. B., editors, *Proceedings of the 1993 International Forum on Dimensional Tolerancing and Metrology, Dearborn, Michigan*, volume CRTD-Vol. 27, pages 269–278. ASME, 1993.

[Ben98] Bennich, P. International Standards for Design Tolerancing Review and Future Perspective. In ElMaraghy, H. A., editor, *Geometric Design Tolerancing: Theories, Standards and Applications*, pages 37–51. Springer US, Boston, MA, 1998.

[BFCM06] Ballu, A.; Falgarone, H.; Chevassus, N.; and Mathieu, L. A new Design Method based on Functions and Tolerance Specifications for Product Modelling. *CIRP Annals - Manufacturing Technology*, 55(1):139 – 142, 2006.

[BG70a] Bennett, G. and Gupta, L. C. LEAST-COST TOLERANCES – I. *International Journal of Production Research*, 8(1):65–74, 1970.

[BG70b] Bennett, G. and Gupta, L. C. LEAST-COST TOLERANCES – II. *International Journal of Production Research*, 8(2):169–182, 1970.

[BGDD13] Beaucaire, P.; Gayton, N.; Duc, E.; and Dantan, J.-Y. Statistical tolerance analysis of over-constrained mechanisms with gaps using system reliability methods. *Computer-Aided Design*, 45(12):1547 – 1555, 2013.

[BH13] Bohn, M. and Hetsch, K. *Toleranzmanagement im Automobilbau.* Carl Hanser Verlag, München, 1st edition, 2013.

[BHK98] Bialas, S.; Humienny, Z.; and Kiszka, K. Relations Between ISO 1101 Geometrical Tolerances and Vectorial Tolerances — Conversion Problems. In ElMaraghy, H. A., editor, *Geometric Design Tolerancing: Theories, Standards and Applications*, pages 88–99. Springer US, 1998.

[BLM94] Bourdet, P.; Lartigue, C.; and Mathieu, L. Mathematical method for tridimensional verification of the tolerances of location with degrees of freedom. In *Proceedings of the IMEKO Congress from Measurement to Innovation XIII, 5.-9. September, Torino, Italy*, 1994.

[BM92] Besl, P. and McKay, N. D. A method for registration of 3-D shapes. *IEEE Transactions on Pattern Analysis and Machine Intelligence*, 14(2):239–256, 1992.

[BM93] Ballu, A. and Mathieu, L. Analysis of dimensional and geometrical specifications: standards and models. In *Proceedings of the 3rd CIRP Seminar on Computer-Aided Tolerancing, Cachan, France*, pages 157–170, 1993.

[BM96] Ballu, A. and Mathieu, L. Univocal expression of functional and geometrical tolerances for design, manufacturing and inspection. In Kimura, F., editor, *Computer-aided Tolerancing*, pages 31–46. Springer Netherlands, 1996.

[BM99] Ballu, A. and Mathieu, L. Choice of functional specifications using graphs within the framework of education. In van Houten, F. and Kals, H., editors, *Global Consistency of Tolerances*, pages 197–206. Springer Netherlands, 1999.

[BMD03] Ballu, A.; Mathieu, L.; and Dantan, J.-Y. Global view of geometrical specifications. In Bourdet, P. and Mathieu, L., editors, *Geometric Product Specification and Verification: Integration of Functionality*, pages 13–24. Springer Netherlands, 2003.

[BMD15] Ballu, A.; Mathieu, L.; and Dantan, J.-Y. Formal Language for GeoSpelling. *Journal of Computing and Information Science in Engineering*, 15(2):021002, 2015.

[BMLB96] Bourdet, P.; Mathieu, L.; Lartigue, C.; and Ballu, A. The concept of the small displacement torsor in metrology. In Ciarlini, P.; Cox, M. G.; Pavese, F.; and Richter, D., editors, *Advanced Mathematical Tools in Metrology II*, pages 110–122. World Scientific Publishing Company, 1996.

[Boo63] Booker, P. J. *A History of Engineering Drawing*. Chatto & Windus, London, 1963.

[Bor07] Borgonovo, E. A new uncertainty importance measure. *Reliability Engineering & System Safety*, 92(6):771 – 784, 2007.

[BP16] Borgonovo, E. and Plischke, E. Sensitivity analysis: A review of recent advances. *European Journal of Operational Research*, 248(3):869 – 887, 2016.

[BPM08] Ballu, A.; Plantec, J.-Y.; and Mathieu, L. Geometrical reliability of overconstrained mechanisms with gaps. *CIRP Annals - Manufacturing Technology*, 57(1):159 – 162, 2008.

[Bre96] Brenner, A. E. The Computing Revolution and the Physics Community. *Physics Today*, 49(10):24–32, 1996.

[Bro01] Browning, T. R. Applying the design structure matrix to system decomposition and integration problems: a review and new directions. *IEEE Transactions on Engineering Management*, 48(3):292–306, 2001.

[BS27] Engineering Standards Committee BS27-1906: Report on Standard Systems of Limit Gauges For Running Fits. Standard, 1906.

[BS91] Boyer, M. and Stewart, N. Modeling Spaces for Toleranced Objects. *The International Journal of Robotics Research*, 10(5):570–582, 1991.

[BS308] British Engineering Standards Association BS308-1927: Engineering drawing office practice. Standard, 1927.

[Buc21] Buckingham, E. *Principles of Interchangeable Manufacturing – A Treatise on the basic Principles involved in successful interchangeable Manufacturing Practice covering Design, Tolerances, Drawings, Manufacturing Equipment, Gaging and Inspection.* The Industrial Press, New York, 1921.

[Buc09] Bucher, C. *Computational Analysis of Randomness in Structural Mechanics*, volume 3 of *Structures and Infrastructures Book Series.* CRC Press, 2009.

[BW99] Britten, W. and Weber, C. Transforming ISO 1101 Tolerances into Vectorial Tolerance Representations — A CAD-Based Approach. In Houten, F. and Kals, H., editors, *Global Consistency of Tolerances: Proceedings of the 6th CIRP International Seminar on Computer-Aided Tolerancing, University of Twente, Enschede, The Netherlands, 22–24 March, 1999*, pages 93–100. Springer Netherlands, Dordrecht, 1999.

[BYWC13] Bo, C.; Yang, Z.; Wang, L.; and Chen, H. A comparison of tolerance analysis models for assembly. *The International Journal of Advanced Manufacturing Technology*, 68(1-4):739–754, 2013.

[CA09] Chavanne, R. and Anselmetti, B. Quick GPS: Rapid tolerancing of an isolated Part. In Giordano, M.; Villeneuve, F.; and Mathieu, L., editors, *Proceedings of the 11th CIRP International Conference on Computer Aided Tolerancing, Annecy*, 2009.

[CA12] Chavanne, R. and Anselmetti, B. Functional tolerancing: Virtual material condition on complex junctions. *Computers in Industry*, 63(3):210 – 221, 2012.

[Cab90] Cabadaj, J. Theory of computer aided fixture design. *Computers in Industry*, 15(1):141 – 147, 1990.

[Cai08] Cai, W. A new tolerance modeling and analysis methodology through a two-step linearization with applications in automotive body assembly. *Journal of Manufacturing Systems*, 27(1):26 – 35, 2008.

[Can12] Cannavó, F. Sensitivity analysis for volcanic source modeling quality assessment and model selection. *Computers & Geosciences*, 44:52 – 59, 2012.

[CBA14a] Chahbouni, M.; Boutahari, S.; and Amegouz, D. Influence of form deviations on the tolerance analysis. *International Journal of Engineering & Technology*, 3(3):343–349, 2014.

[CBA14b] Chahbouni, M.; Boutahari, S.; and Amegouz, D. Statistical tolerance analysis by integrating form deviations. *International Journal of Innovation and Applied Studies*, 9(3):1281–1290, 2014.

[CBP12] Charpentier, F.; Ballu, A.; and Pailhes, J. A scientific point of view of a simple industrial tolerancing process. In Jiang, X. J., editor, *Proceedings of the 12th CIRP International Conference on Computer Aided Tolerancing, Huddersfield*, 2012.

[CBW05] Caro, S.; Bennis, F.; and Wenger, P. Tolerance Synthesis of Mechanisms: A Robust Design Approach. *Journal of Mechanical Design*, 127(1):86–94, 2005.

[CC01] Chou, C.-Y. and Chang, C.-L. Minimum-Loss Assembly Tolerance Allocation by Considering Product Degradation and Time Value of Money. *The International Journal of Advanced Manufacturing Technology*, 17(2):139–146, 2001.

[CCD+89] Charles, B.; Clement, A.; Desrochers, A.; Pelissou, P.; and Rivière, A. Toward a Computer Aided Functional Tolerancing Model. In Weill, R., editor, *Proceedings of the International Conference on CAD/CAM and AMT – Volume II: CIRP Sessions on Tolerancing for Function in a CAD/CAM Environment*, pages C–2–4, 1989.

[CCJC14] Camba, J.; Contero, M.; Johnson, M.; and Company, P. Extended 3D annotations as a new mechanism to explicitly communicate geometric design intent and increase CAD model reusability. *Computer-Aided Design*, 57:61 – 73, 2014.

[CCK+14] Chiffre, L. D.; Carmignato, S.; Kruth, J.-P.; Schmitt, R.; and Weckenmann, A. Industrial applications of computed tomography. *CIRP Annals - Manufacturing Technology*, 63(2):655 – 677, 2014.

[CDJC06] Chen, Y.; Ding, Y.; Jin, J.; and Ceglarek, D. Integration of Process-Oriented Tolerancing and Maintenance Planning in Design of Multistation Manufacturing Processes. *IEEE Transactions on Automation Science and Engineering*, 3(4):440–453, 2006.

[CDR91] Clément, A.; Desrochers, A.; and Rivière, A. Theory and Practice of 3-D Tolerancing for Assembly. In Weill, R., editor, *Proceedings of the CIRP Working Seminar on Computer-Aided Tolerancing, Penn State University*, pages 25–56, 1991.

[CF14] Curtis, M. and Farago, F. *Handbook of Dimensional Measurement*, volume 5. Industrial Press, South Norwalk, 2014.

[CG97] Chang, M. and Gossard, D. C. Modeling the assembly of compliant, non-ideal parts. *Computer-Aided Design*, 29(10):701 – 708, 1997.

[CG03] Chiesi, F. and Governi, L. Tolerance Analysis with eM-TolMate. *Journal of Computing and Information Science in Engineering*, 3(1):100–105, 2003.

[CGC07] Choi, S.-K.; Grandhi, R.; and Canfield, R. A. *Reliability-based Structural Design*. Springer London, 2007.

[CGLH90] Chase, K. W.; Greenwood, W. H.; Loosli, B. G.; and Hauglund, L. F. Least Cost Tolerance Allocation for Mechanical Assemblies with Automated Process Selection. *Manufacturing Review*, 3(1):49–59, 1990.

[CGMS96] Chase, K. W.; Gao, J.; Magleby, S. P.; and Sorensen, C. D. Including Geometric Feature Variations in Tolerance Analysis of Mechanical Assemblies. *IIE Transactions*, 28:795–807, 1996.

[Cha99] Chase, K. W. Tolerance Analysis of 2-D and 3-D Assemblies. Technical Report ADCATS Report No. 99-4, Mechanical Engineering Department, Brigham Young University, 1999.

[Cha13] Charpentier, F. *Handbook for the geometrical specification of products*. technologie – sciences & techniques industrielles. SCEREN-CNDP Cedex, 1st edition, 2013.

[Cha14] Charpentier, F. *Leitfaden für die Anwendung der Normen zur geometrischen Produktspezifikation (GPS) – ISO-GPS-Normen*. Beuth Verlag GmbH Berlin Wien Zürich, 1st edition, 2014.

[Cha15] Chattinnawat, W. Statistical tolerance design to minimize dual-responses of APFA height deviations with tolerance cost-quality loss model. *International Journal of Quality & Reliability Management*, 32(5):434-455, 2015.

[CHC03] Camelio, J.; Hu, S. J.; and Ceglarek, D. Modeling Variation Propagation of Multi-Station Assembly Systems With Compliant Parts. *Journal of Mechanical Design*, 125:673–681, 2003.

[CHC04] Camelio, J. A.; Hu, S. J.; and Ceglarek, D. Impact of fixture design on sheet metal assembly variation. *Journal of Manufacturing Systems*, 23(3):182 – 193, 2004.

[CHM04] Camelio, J. A.; Hu, S. J.; and Marin, S. P. Compliant Assembly Variation Analysis Using Component Geometric Covariance. *Journal of Manufacturing Science and Engineering*, 126(2):355–360, 2004.

[CHZ+04] Ceglarek, D.; Huang, W.; Zhou, S.; Ding, Y.; Kumar, R.; and Zhou, Y. Time-Based Competition in Multistage Manufacturing: Stream-of-Variation Analysis (SOVA) Methodology—Review. *International Journal of Flexible Manufacturing Systems*, 16(1):11–44, 2004.

[CJLL14] Chen, H.; Jin, S.; Li, Z.; and Lai, X. A comprehensive study of three dimensional tolerance analysis methods. *Computer-Aided Design*, 53:1 – 13, 2014.

[CJLL15a] Chen, H.; Jin, S.; Li, Z.; and Lai, X. A modified method of the unified Jacobian-Torsor model for tolerance analysis and allocation. *International Journal of Precision Engineering and Manufacturing*, 16(8):1789–1800, 2015.

[CJLL15b] Chen, H.; Jin, S.; Li, Z.; and Lai, X. A solution of partial parallel connections for the unified Jacobian–Torsor model. *Mechanism and Machine Theory*, 91:39 – 49, 2015.

[CK12] Cho, S. and Kim, J.-Y. Straightness and flatness evaluation using data envelopment analysis. *The International Journal of Advanced Manufacturing Technology*, 63(5-8):731–740, 2012.

[CLR12] Clozel, P.; Lacour, D.; and Rance, P. A. 3D Tolerances Analysis integrated to Digital Mock Up: MECAmaster for CATIA V5. In Jiang, X. J., editor, *Proceedings of the 12th CIRP International Conference on Computer Aided Tolerancing, Huddersfield*, 2012.

[CM88] Cheikh, A. and McGoldrick, P. F. The Influence of Cost, Function and Process Capability on Tolerance. *International Journal of Quality & Reliability Management*, 5(3):15–28, 1988.

[CM89] Cheikh, A. and McGoldrick, P. F. Functional Tolerancing in CAD/CAM. In Weill, R., editor, *Proceedings of the International Conference on CAD/CAM and AMT – Volume II: CIRP Sessions on Tolerancing for Function in a CAD/CAM Environment*, pages C–2–1, 1989.

[CMG98] Chase, K.; Magleby, S.; and Glancy, C. A Comprehensive System for Computer-Aided Tolerance Analysis of 2-D and 3-D Mechanical Assemblies. In ElMaraghy, H. A., editor, *Geometric Design Tolerancing: Theories, Standards and Applications*, pages 294–307. Springer US, 1998.

[CMJ15] Cao, Y.-l.; Mathieu, L.; and Jiang, J. Key research on computer aided tolerancing. *Journal of Zhejiang University SCIENCE A*, 16(5):335–340, 2015.

[Com16] European Commission. http://ec.europa.eu/growth/single-market/european-standards, European Standards, Retrieved in April 2016

[Con00] Council of the European Union Council Resolution of 28 October 1999 on the role of standardisation in Europe. *Official Journal of the European Communities*, C 141:1–4, 2000.

[Con13] Contreras, F. G. Maximization of process tolerances using an analysis of setup capability. *The International Journal of Advanced Manufacturing Technology*, 67(9-12):2171–2181, 2013.

[CoRUQ16] Chair of Risk, Safety and Uncertainty Quantification, ETH Zürich UQLab – The Framework for Uncertainty Quantification. http://www.uqlab.com, Retrieved in April 2016.

[CP91] Chase, K. and Parkinson, A. A survey of research in the application of tolerance analysis to the design of mechanical assemblies. *Research in Engineering Design*, 3(1):23–37, 1991.

[CP07] Colosimo, B. M. and Pacella, M. On the use of principal component analysis to identify systematic patterns in roundness profiles. *Quality and Reliability Engineering International*, 23(6):707–725, 2007.

[Cra96] Craig, M. Dimensional management versus tolerance assignment. *Assembly Automation*, 16(2):12–16, 1996.

[Cre97] Creveling, C. M. *Tolerance Design: A Handbook for developing optimal Specifications*. Addison Wesley Longman Inc., 1997.

[CS95] Ceglarek, D. and Shi, J. Dimensional Variation Reduction for Automotive Body Assembly Manufacturing. *Manufacturing Review*, 8(2):139–154, 1995.

[CS97] Ceglarek, D. and Shi, J. Tolerance analysis for sheet metal assembly using a beam-based model. In ASME, editor, *ASME Design Engineering Division Publication (1997 ASME International Mechanical Engineering Congress and Exposition)*, volume 94, pages 153–159, 1997.

[CS03] Carlson, J. S. and Söderberg, R. Assembly Root Cause Analysis: A Way to Reduce Dimensional Variation in Assembled Products. *International Journal of Flexible Manufacturing Systems*, 15(2):113–150, 2003.

[CT04] Cootes, T. and Taylor, C. Statistical Models of Appearance for Computer Vision. Technical report, Imaging Science and Biomedical Engineering, University of Manchester, 2004.

[CTBF07] Cid, G.; Thiebaut, F.; Bourdet, P.; and Falgarone, H. Geometrical Study of Assembly Behaviour, Taking into Accounts Rigid Components' Deviations, Actual Geometric Variations and Deformations. In Davidson, J., editor, *Models for Computer Aided Tolerancing in Design and Manufacturing*, pages 301–310. Springer Netherlands, 2007.

[CTCG95] Cootes, T.; Taylor, C.; Cooper, D.; and Graham, J. Active Shape Models-Their Training and Application. *Computer Vision and Image Understanding*, 61(1):38 – 59, 1995.

[CV08] Cressie, N. and Verzelen, N. Conditional-mean least-squares fitting of Gaussian Markov random fields to Gaussian fields. *Computational Statistics & Data Analysis*, 52(5):2794 – 2807, 2008.

[CW09] Chang, W.-T. and Wu, L.-I. Computerized tolerance analysis of disk cam mechanisms with a roller follower. *Engineering with Computers*, 25(3):247–260, 2009.

[CWL13] Chen, G.; Wang, H.; and Lin, Z. A unified approach to the accuracy analysis of planar parallel manipulators both with input uncertainties and joint clearance. *Mechanism and Machine Theory*, 64:1 – 17, 2013.

[CZC+06] Chen, G.; Zhou, J.; Cai, W.; Lai, X.; Lin, Z.; and Menassa, R. A framework for an automotive body assembly process design system. *Computer-Aided Design*, 38(5):531 – 539, 2006.

[CZM+11] Cao, Y.; Zhang, H.; Mao, J.; Xu, X.; and Yang, J. Study on tolerance modeling of complex surface. *The International Journal of Advanced Manufacturing Technology*, 53(9-12):1183–1188, 2011.

[DAM03] Dantan, J.-Y.; Anwer, N.; and Mathieu, L. Integrated Tolerancing Process for conceptual design. *CIRP Annals - Manufacturing Technology*, 52(1):135 – 138, 2003.

[Dan14] Dantan, J.-Y. Tolerancing. In Laperrière, L. and Reinhart, G., editors, *CIRP Encyclopedia of Production Engineering*, pages 1230–1237. Springer Berlin Heidelberg, 2014.

[Dan15] Dantan, J.-Y. Comparison of Skin Model Representations and Tooth Contact Analysis Techniques for Gear Tolerance Analysis. *Journal of Computing and Information Science in Engineering*, 15(2):021010, 2015.

[DB10] Dupac, M. and Beale, D. G. Dynamic analysis of a flexible linkage mechanism with cracks and clearance. *Mechanism and Machine Theory*, 45(12):1909 – 1923, 2010.

[DBBM07] Dantan, J.; Bruyere, J.; Baudouin, C.; and Mathieu, L. Geometrical Specification Model for Gear - Expression, Metrology and Analysis. *CIRP Annals - Manufacturing Technology*, 56(1):517 – 520, 2007.

[DBM08] Dantan, J.-Y.; Ballu, A.; and Mathieu, L. Geometrical product specifications — model for product life cycle. *Computer-Aided Design*, 40(4):493 – 501, 2008.

[DBVB08] Dantan, J.-Y.; Bruyere, J.; Vincent, J.-P.; and Bigot, R. Vectorial tolerance allocation of bevel gear by discrete optimization. *Mechanism and Machine Theory*, 43(11):1478 – 1494, 2008.

[DC94] Desrochers, A. and Clément, A. A dimensioning and tolerancing assistance model for CAD/CAM systems. *The International Journal of Advanced Manufacturing Technology*, 9(6):352–361, 1994.

[dC11] del Castillo, E. Statistical Shape Analysis of Manufacturing Data. In Colosimo, B. M. and Senin, N., editors, *Geometric Tolerances*, pages 215–234. Springer London, 2011.

[DD04] DiStefano, P. and DiAngelo, L. Geometric Modelling of Mechanical Parts affected by Shape Error. In Marjanovic, D., editor, *Proceedings of the 8th International Design Conference DESIGN 2004, Dubrovnik, Croatia*, pages 157–162, 2004.

[DD15] DiAngelo, L. and DiStefano, P. Geometric segmentation of 3D scanned surfaces. *Computer-Aided Design*, 62:44 – 56, 2015.

[DDG15] Dumas, A.; Dantan, J.-Y.; and Gayton, N. Impact of a behavior model linearization strategy on the tolerance analysis of over-constrained mechanisms. *Computer-Aided Design*, 62:152 – 163, 2015.

[Dem82] Deming, W. E. *Out of the Crisis.* MIT Press, 1982.

[Des07] Desrochers, A. Geometrical Variations Management in a Multi-Disciplinary Environment with the Jacobian-Torsor Model. In Davidson, J. K., editor, *Models for Computer Aided Tolerancing in Design and Manufacturing*, pages 75–84. Springer Netherlands, Dordrecht, 2007.

[DFC15] Das, A.; Franciosa, P.; and Ceglarek, D. Fixture Design Optimisation Considering Production Batch of Compliant Non-Ideal Sheet Metal Parts. In *Proceedings of the 43rd North American Manufacturing Research Conference (NAMRC) – ASME International Manufacturing Science and Engineering Conference (MSEC), Charlotte, NC*, volume 43, pages NAMRC43–28, 2015.

[DFO03] Desta, M. T.; Feng, H.-Y.; and OuYang, D. Characterization of general systematic form errors for circular features. *International Journal of Machine Tools and Manufacture*, 43(11):1069 – 1078, 2003.

[DGD+12] Dantan, J.-Y.; Gayton, N.; Dumas, A.; Etienne, A.; and Qureshi, A. J. Mathematical Issues in Mechanical Tolerance Analysis. In *Proceedings of the 13th Colloque National AIP PRIMECA, Le Mont Dore*, 2012.

[DGDS15] Dumas, A.; Gayton, N.; Dantan, J.-Y.; and Sudret, B. A new system formulation for the tolerance analysis of overconstrained mechanisms. *Probabilistic Engineering Mechanics*, 40:66 – 74, 2015.

[DHX94] Dong, Z.; Hu, W.; and Xue, D. New Production Cost-Tolerance Models for Tolerance Synthesis. *Journal of Engineering for Industry*, 116:199–206, 1994.

[Dia95] Diaz, C. Algorithm Testing and Evaluation Program for Coordinate Measuring Systems: Testing Methods. Technical Report NISTIR 5686, National Institute of Standards and Technology, 1995.

[Dij05] Dijon, F. Tolerancement Statistique: mise en place d'une Methode de Tolerancement Statistique Tridimensionnel. Master's thesis, Ecole normale supérieure de Cachan, 2005.

[DIN4760] DIN. DIN 4760:1982-06: Gestaltabweichungen; Begriffe, Ordnungssystem. Standard, 1982.

[DJCS00] Ding, Y.; Jin, J.; Ceglarek, D.; and Shi, J. Process-Oriented Tolerance Synthesis for Multistage Manufacturing Systems. In ASME, editor, *Proceedings of IMECE 2000, Nov. 5-10, 2000, Orlando*, 2000.

[DJCS02] Ding, Y.; Jin, J.; Ceglarek, D.; and Shi, J. Process-oriented Tolerancing for Multi-station Assembly Systems. Report 181, Center for Quality and Productivity Improvement, University of Wisconsin, 610 Walnut Street, Madison, Wisconsin, October 2002.

[DJCS05] Ding, Y.; Jin, J.; Ceglarek, D.; and Shi, J. Process-oriented tolerancing for multi-station assembly systems. *IIE Transactions*, 37(6):493–508, 2005.

[DL08] Dornfeld, D. and Lee, D.-E. Introduction to precision manufacturing. In *Precision Manufacturing*, pages 1–35. Springer US, 2008.

[DLSM07] Dantan, J.-Y.; Landmann, T.; Siadat, A.; and Martin, P. Information Modeling to Manage Tolerances during Product and Process Design. In Davidson, J., editor, *Models for Computer Aided Tolerancing in Design and Manufacturing*, pages 55–64. Springer Netherlands, 2007.

[DM98] Dryden, I. L. and Mardia, K. V. *Statistical Shape Analysis.* John Wiley & Sons, Inc., 1998.

[DMBM05] Dantan, J.-Y.; Mathieu, L.; Ballu, A.; and Martin, P. Tolerance synthesis: quantifier notion and virtual boundary. *Computer-Aided Design*, 37(2):231 – 240, 2005.

[DMS02] Davidson, J. K.; Mujezinović, A.; and Shah, J. J. A New Mathematical Model for Geometric Tolerances as Applied to Round Faces. *Journal of Mechanical Design*, 124(4):609–622, 2002.

[DQ09] Dantan, J.-Y. and Qureshi, A.-J. Worst-case and statistical tolerance analysis based on quantified constraint satisfaction problems and Monte Carlo simulation. *Computer-Aided Design*, 41(1):1 – 12, 2009.

[DQA+13] Dantan, J.; Qureshi, A.; Antoine, J.; Eisenbart, B.; and Blessing, L. Management of product characteristics uncertainty based on formal logic and characteristics properties model. *CIRP Annals - Manufacturing Technology*, 62(1):147 – 150, 2013.

[DR97] Desrochers, A. and Rivière, A. A matrix approach to the representation of tolerance zones and clearances. *The International Journal of Advanced Manufacturing Technology*, 13(9):630–636, 1997.

[DS10] Dawari, A. and Sen, D. Relation between part position and kinematic freedom: An expository survey. *Mechanism and Machine Theory*, 45(2):157 – 169, 2010.

[DSMW15] Dodd, C.; Scanlan, J.; Marsh, R.; and Wiseall, S. Improving profitability of optimal mean setting with multiple feature means for dual quality characteristics. *The International Journal of Advanced Manufacturing Technology*, 81(9-12):1767–1780, 2015.

[DT15a] Delos, V. and Teissandier, D. Minkowski sum of HV-polytopes in Rn. In *Proceedings of the 4th Annual International Conference on Computational Mathematics, Computational Geometry and Statistics*, Singapore, 2015.

[DT15b] Delos, V. and Teissandier, D. Minkowski Sum of Polytopes Defined by Their Vertices. *Journal of Applied Mathematics and Physics (JAMP)*, 3(1):62–67, 2015.

[DVGM10] Dantan, J.; Vincent, J.; Goch, G.; and Mathieu, L. Correlation uncertainty—Application to gear conformity. *CIRP Annals - Manufacturing Technology*, 59(1):509 – 512, 2010.

[DVVR07] Demarsin, K.; Vanderstraeten, D.; Volodine, T.; and Roose, D. Detection of closed sharp edges in point clouds using normal estimation and graph theory. *Computer-Aided Design*, 39(4):276 – 283, 2007.

[DW98] Dong, Z. and Wang, G. G. Automated Cost Modeling for Tolerance Synthesis Using Manufacturing Process Data, Knowledge Reasoning and Optimization. In ElMaraghy, H. A., editor, *Geometric Design Tolerancing: Theories, Standards and Applications*, pages 282–293. Springer US, 1998.

[DZ88] D'Errico, J. R. and Zaino, N. A. Statistical Tolerancing Using a Modification of Taguchi's Method. *Technometrics*, 30(4):397–405, 1988.

[ElM93] ElMaraghy, H. A. Evolution and Future Perspectives of CAPP. *CIRP Annals - Manufacturing Technology*, 42(2):739 – 751, 1993.

[EME+11] Eifler, T.; Mathias, J.; Engelhardt, R.; Kloberdanz, H.; Birkhofer, H.; and Bohn, A. Evaluation of Solution Variants in Conceptual Design by means of adequate Sensitivity Indices. In Maier, A.; Mougaard, K.; Howard, T.; and McAloone, T., editors, *Proceedings of the 18th International Conference on Engineering Design ICED 11, Lyngby/Copenhagen*, 2011.

[EN14] ElMaraghy, H. and Nassehi, A. Computer-Aided Process Planning. In Laperrière, L. and Reinhart, G., editors, *CIRP Encyclopedia of Production Engineering*, pages 266–271. Springer Berlin Heidelberg, 2014.

[Eva74] Evans, D. H. Statistical Tolerancing: The State of the Art. *Journal of Quality Technology*, 6(4):188–195, 1974.

[FA04] Flores, P. and Ambrósio, J. Revolute joints with clearance in multibody systems. *Computers & Structures*, 82(17–19):1359 – 1369, 2004.

[FB09] Fang, Q. and Boas, D. Tetrahedral mesh generation from volumetric binary and grayscale images. In *IEEE International Symposium on Biomedical Imaging: From Nano to Macro*, pages 1142–1145, 2009.

[FFS15] Feeney, A. B.; Frechette, S. P.; and Srinivasan, V. A Portrait of an ISO STEP Tolerancing Standard as an Enabler of Smart Manufacturing Systems. *Journal of Computing and Information Science in Engineering*, 15(2):021001, 2015.

[FG86] Farmer, L. and Gladman, C. Tolerance Technology — Computer-Based Analysis. *CIRP Annals - Manufacturing Technology*, 35(1):7 – 10, 1986.

[FG13] Feldhusen, J. and Grote, K.-H. *Pahl/Beitz Konstruktionslehre*. Springer Berlin Heidelberg, 2013.

[FGE91] Farmer, L.; Gladman, C.; and Edensor, K. The Scope of Tolerancing Problems in Engineering. In Weill, R., editor, *Proceedings of the CIRP Working Seminar on Computer-Aided Tolerancing, Penn State University*, pages 1–24, 1991.

[FGP10] Franciosa, P.; Gerbino, S.; and Patalano, S. Variational modeling and assembly constraints in tolerance analysis of rigid part assemblies: planar and cylindrical features. *The International Journal of Advanced Manufacturing Technology*, 49(1-4):239–251, 2010.

[FGP11] Franciosa, P.; Gerbino, S.; and Patalano, S. Simulation of variational compliant assemblies with shape errors based on morphing mesh approach. *The International Journal of Advanced Manufacturing Technology*, 53(1-4):47–61, 2011.

[FH10] Flöry, S. and Hofer, M. Surface fitting and registration of point clouds using approximations of the unsigned distance function. *Computer Aided Geometric Design*, 27(1):60 – 77, 2010.

[FKM11] Fu, S.; Kauppila, O.; and Mottonen, M. Measurement system escape and overkill rate analysis. *The International Journal of Advanced Manufacturing Technology*, 57(9):1079–1086, 2011.

[FKS13] Forslund, K.; Karlsson, M.; and Söderberg, R. Impacts of Geometrical Manufacturing Quality on the Visual Product Experience. *International Journal of Design*, 7(1), 2013.

[Flö09] Flöry, S. Fitting curves and surfaces to point clouds in the presence of obstacles. *Computer Aided Geometric Design*, 26(2):192 – 202, 2009.

[Flö10] Flöry, S. *Constrained Matching of Point Clouds and Surfaces*. PhD thesis, Fakultät für Mathematik und Geoinformation der Technischen Universität Wien, 2010.

[FM11] Forbes, A. B. and Minh, H. D. Form Assessment in Coordinate Metrology. In Georgoulis, E. H.; Iske, A.; and Levesley, J., editors, *Approximation Algorithms for Complex Systems*, volume 3 of *Springer Proceedings in Mathematics*, pages 69–90. Springer Berlin Heidelberg, 2011.

[For09] Forouraghi, B. Optimal tolerance allocation using a multiobjective particle swarm optimizer. *The International Journal of Advanced Manufacturing Technology*, 44(7):710–724, 2009.

[FS07] Formosa, F. and Samper, S. Modal Expression of Form Defects. In Davidson, J., editor, *Models for Computer Aided Tolerancing in Design and Manufacturing*, pages 13–22. Springer Netherlands, 2007.

[FS10] Forslund, K. and Söderberg, R. Effects of Geometric Variation on Perceived Quality. In Giordano, M.; Mathieu, L.; and Villeneuve, F., editors, *Product Lifecycle Management: Geometric Variations*, pages 503–519. John Wiley & Sons, Inc., 2010.

[FSPB11] Frisoli, A.; Solazzi, M.; Pellegrinetti, D.; and Bergamasco, M. A new screw theory method for the estimation of position accuracy in spatial parallel manipulators with revolute joint clearances. *Mechanism and Machine Theory*, 46(12):1929 – 1949, 2011.

[FTCM16] Falgarone, H.; Thiébaut, F.; Coloos, J.; and Mathieu, L. Variation Simulation During Assembly of Non-rigid Components. Realistic Assembly Simulation with ANATOLEFLEX Software. *Procedia CIRP – 14th CIRP Conference on Computer-Aided Tolerancing*, 43:202 – 207, 2016.

[FWB86] Fainguelernt, D.; Weill, R.; and Bourdet, P. Computer Aided Tolerancing and Dimensioning in Process Planning. *CIRP Annals - Manufacturing Technology*, 35(1):381 – 386, 1986.

[FZW+13] Fang, F.; Zhang, X.; Weckenmann, A.; Zhang, G.; and Evans, C. Manufacturing and measurement of freeform optics. *CIRP Annals - Manufacturing Technology*, 62(2):823 – 846, 2013.

[Gab93] Gabriele, G. A. A Perspective on Engineering Design Education: Where do Tolerances fit in? In Srinivasan, V. and Voelcker, H. B., editors, *Proceedings of the 1993 International Forum on Dimensional Tolerancing and Metrology, Dearborn, Michigan*, volume CRDT-Vol. 27, pages 279–290. ASME, 1993.

[Gad10] Gadelmawla, E. Simple and efficient algorithms for roundness evaluation from the coordinate measurement data. *Measurement*, 43(2):223 – 235, 2010.

[GAMQ14] Garaizar, O. R.; Anwer, N.; Mathieu, L.; and Qiao, L. Exploring the proceedings of Computer Aided Tolerancing CIRP Seminars and Conferences: A scientometric analysis. In *Proceedings of the 13th CIRP International Conference on Computer Aided Tolerancing, Hangzhou*, 2014.

[GB99] Graves, S. and Bisgaard, S. Integrated Tolerance Management. In Houten, F. and Kals, H., editors, *Global Consistency of Tolerances: Proceedings of the 6th CIRP International Seminar on Computer-Aided Tolerancing, University of Twente, Enschede, The Netherlands, 22–24 March, 1999*, pages 385–394. Springer Netherlands, 1999.

[GCM98] Gao, J.; Chase, K.; and Magleby, S. Generalized 3-D tolerance analysis of mechanical assemblies with small kinematic adjustments. *IIE Transactions*, 30(4):367–377, 1998.

[GCWL98] Gou, J.; Chu, Y.; Wu, H.; and Li, Z. Geometric formulation of orientation tolerances. In *Proceedings of the IEEE International Conference on Robotics and Automation 1998*, volume 3, pages 2728–2733, 1998.

[GD07] Guo, J. and Du, X. Sensitivity Analysis with Mixture of Epistemic and Aleatory Uncertainties. *AIAA Journal*, 45(9):2337–2349, 2007.

[GDTA92] Giordano, M.; Duret, D.; Tichadou, S.; and Arrieux, R. Clearance Space in Volumic Dimensioning. *CIRP Annals - Manufacturing Technology*, 41(1):565 – 568, 1992.

[GFLH13] Galovskyi, B.; Flessner, M.; Loderer, A.; and Hausotte, T. Systematic Form Deviations of additive manufactured Parts – Methods of their Identification and Correction. In *11th International Symposium on Measurement and Quality Control, September 11-13, 2013, Cracow-Kielce, Poland*, 2013.

[GFP15] Gerbino, S.; Franciosa, P.; and Patalano, S. Parametric Variational Analysis of Compliant Sheet Metal Assemblies with Shell Elements. *Procedia CIRP – 9th CIRP Conference on Intelligent Computation in Manufacturing Engineering - CIRP ICME '14*, 33:339 – 344, 2015.

[GFV12] Governi, L.; Furferi, R.; and Volpe, Y. A Genetic Algorithms-based Procedure for Automatic Tolerance Allocation Integrated in a Commercial Variation Analysis Software. *Journal of Artificial Intelligence*, 5(3):99–112, 2012.

[GG16] Ganji, Z. A. and Gildeh, B. S. A modified multivariate process capability vector. *The International Journal of Advanced Manufacturing Technology*, 83(5):1221–1229, 2016.

[GGL+15] Gröschl, A.; Götz, J.; Loderer, A.; Bills, P.; and Hausotte, T. Measures of Improvement MUVoT, a Blended Learning Course on the Topic of Measurement Uncertainty for Advanced Vocational Training. *Procedia CIRP – 13th CIRP Conference on Computer-Aided Tolerancing*, 27:111 – 116, 2015.

[Ghi10] Ghie, W. *Modeling Simulation and Optimization: Tolerance and Optimal Control*, Chapter 11: Tolerance Analysis Using Jacobian-Torsor Model: Statistical and Deterministic Applications. InTech, 2010.

[GHO+15] Geis, A.; Husung, S.; Oberänder, A.; Weber, C.; and Adam, J. Use of Vectorial Tolerances for Direct Representation and Analysis in CAD-systems. *Procedia CIRP – 13th CIRP Conference on Computer-Aided Tolerancing*, 27:230 – 240, 2015.

[GLD07] Ghie, W.; Laperrière, L.; and Desrochers, A. Re-Design of Mechanical Assemblies using the Unified Jacobian-Torsor Model for Tolerance Analysis. In Davidson, J. K., editor, *Models for Computer Aided Tolerancing in Design and Manufacturing*, pages 95–104. Springer Netherlands, Dordrecht, 2007.

[GLD10] Ghie, W.; Laperrière, L.; and Desrochers, A. Statistical tolerance analysis using the unified Jacobian–Torsor model. *International Journal of Production Research*, 48(15):4609–4630, 2010.

[GLLH15] Guo, J.; Liu, Z.; Li, B.; and Hong, J. Optimal tolerance allocation for precision machine tools in consideration of measurement and adjustment processes in assembly. *The International Journal of Advanced Manufacturing Technology*, 80(9-12):1625–1640, 2015.

[GLS11] Grandjean, J.; Ledoux, Y.; and Samper, S. Influence of form errors in plane surfaces assemblies.

In *Proceedings of the International Conference on Innovative Methods in Product Design IMProVe 2011, Venice, Italy*, 2011.

[GLS13] Grandjean, J.; Ledoux, Y.; and Samper, S. On the role of form defects in assemblies subject to local deformations and mechanical loads. *The International Journal of Advanced Manufacturing Technology*, 65(9-12):1769–1778, 2013.

[GLSF13] Grandjean, J.; Ledoux, Y.; Samper, S.; and Favrelière, H. Form Errors Impact in a Rotating Plane Surface Assembly. *Procedia CIRP – 12th CIRP Conference on Computer-Aided Tolerancing*, 10:178 – 185, 2013.

[Goc03] Goch, G. Gear Metrology. *CIRP Annals - Manufacturing Technology*, 52(2):659 – 695, 2003.

[Gou71] Gouraud, H. Continuous Shading of Curved Surfaces. *IEEE Transactions on Computers*, C-20(6):623–629, 1971.

[GRDN97] Gupta, S. K.; Regli, W. C.; Das, D.; and Nau, D. S. Automated manufacturability analysis: A survey. *Research in Engineering Design*, 9(3):168–190, 1997.

[Gri14] Grieves, M. Digital Twin: Manufacturing Excellence through Virtual Factory Replication. White-paper, 2014.

[GS09] González, I. and Sánchez, I. Statistical tolerance synthesis with correlated variables. *Mechanism and Machine Theory*, 44(6):1097 – 1107, 2009.

[GS12] Gust, P. and Schluer, C. Numerical investigation into the impact of dimensional and geometric tolerances on the long-life fatigue strength of mechanical components. In Jiang, X. J., editor, *Proceedings of the 12th CIRP International Conference on Computer Aided Tolerancing, Huddersfield*, 2012.

[GS13] Ge, Z. and Song, Z. *Multivariate Statistical Process Control – Process Monitoring Methods and Applications*. Advances in Industrial Control. Springer London, 2013.

[GS15] González, I. and Sánchez, I. Optimal centering and tolerance synthesis for non-independent and non-normal variables. *The International Journal of Advanced Manufacturing Technology*, 79(5-8):1171–1184, 2015.

[GSP07] Giordano, M.; Samper, S.; and Petit, J. Tolerance Analysis and Synthesis by Means of Deviation Domains, Axi-Symmetric Cases. In Davidson, J., editor, *Models for Computer Aided Tolerancing in Design and Manufacturing*, pages 85–94. Springer Netherlands, 2007.

[GT93a] Guilford, J. and Turner, J. Advanced Tolerance Analysis and Synthesis for Geometric Tolerances. In Srinivasan, V. and Voelcker, H. B., editors, *Proceedings of the 1993 International Forum on Dimensional Tolerancing and Metrology, Dearborn, Michigan*, volume CRTD-Vol. 27, pages 187–198. ASME, 1993.

[GT93b] Gupta, S. and Turner, J. Variational solid modeling for tolerance analysis. *Computer Graphics and Applications, IEEE*, 13(3):64–74, 1993.

[Gue11] Guenther, A. Interpretation of bevel gear topography measurements. *CIRP Annals - Manufacturing Technology*, 60(1):551 – 554, 2011.

[GWHK09] Gnezdilov, A.; Wittmann, S.; Helwig, S.; and Kokai, G. Acceleration of a Relative Positioning Framework. *International Journal of Computational Intelligence Research*, 5(2):130–140, 2009.

[GZS88] Gossard, D. C.; Zuffante, R. P.; and Sakurai, H. Representing dimensions, tolerances, and features in MCAE systems. *IEEE Computer Graphics and Applications*, 8(2):51–59, 1988.

[HAG09] Hasenkamp, T.; Arvidsson, M.; and Gremyr, I. A review of practices for robust design methodology. *Journal of Engineering Design*, 20(6):645–657, 2009.

[Hal13] Halsey, F. A. *Handbook for Machine Designers, Shop Men and Draftsmen.* McGraw-Hill Book Company, New York, 1913.

[Har14] Hartmann, W. D. *Mess- und Auswertestrategien zur modellbasierten Bewertung funktionaler Eigenschaften mikrostrukturierter Oberflächen.* PhD thesis, Technische Fakultät der Friedrich-Alexander-Universität Erlangen-Nürnberg, 2014.

[HB78] Hillyard, R. and Braid, I. Analysis of dimensions and tolerances in computer-aided mechanical design. *Computer-Aided Design*, 10(3):161 – 166, 1978.

[HB13] Humienny, Z. and Berta, M. New Multimedia Geometrical Tolerancing Course. *Procedia CIRP – 12th CIRP conference on Computer-Aided Tolerancing*, 10:312 – 316, 2013.

[HB15] Humienny, Z. and Berta, M. A Digital Application for Geometrical Tolerancing Concepts Understanding. *Procedia CIRP – 13th CIRP Conference on Computer-Aided Tolerancing*, 27:264 – 269, 2015.

[HC00] Hummel, S. R. and Chassapis, C. Configuration design and optimization of universal joints with manufacturing tolerances. *Mechanism and Machine Theory*, 35(3):463 – 476, 2000.

[HC02a] Hong, Y. and Chang, T. A comprehensive review of tolerancing research. *International Journal of Production Research*, 40(11):2425–2459, 2002.

[HC02b] Huang, W. and Ceglarek, D. Mode-based Decomposition of Part Form Error by Discrete-Cosine-Transform with Implementation to Assembly and Stamping System with Compliant Parts. *CIRP Annals - Manufacturing Technology*, 51(1):21 – 26, 2002.

[HCBS13] Hermansson, T.; Carlson, J. S.; Björkenstam, S.; and Söderberg, R. Geometric variation simulation and robust design for flexible cables and hoses. *Proceedings of the Institution of Mechanical Engineers, Part B: Journal of Engineering Manufacture*, 227(5):681–689, 2013.

[HCHC06] Hansen, H. N.; Carneiro, K.; Haitjema, H.; and Chiffre, L. D. Dimensional Micro and Nano Metrology. *CIRP Annals - Manufacturing Technology*, 55(2):721 – 743, 2006.

[HCLD06] Hamou, S.; Cheikh, A.; Linares, J. M.; and Daho, A. C. A stochastic concept for the optimization of manufacturing tolerances in computer aided process plan simulation. *International Journal of Computer Integrated Manufacturing*, 19(7):663–675, 2006.

[HDKS16] He, Y.; Davidson, J. K.; Kalish, N.; and Shah, J. Tolerance-Maps for Line-Profiles Formed by Intersecting Kinematically Transformed Primitive T-Map Elements. *Journal of Computing and Information Science in Engineering*, 16(2):021005, 2016.

[HDL16] Homri, L.; Dantan, J.-Y.; and Levasseur, G. Comparison of Optimization Techniques in a Tolerance Analysis Approach Considering Form Defects. *Procedia CIRP – 14th CIRP Conference on Computer-Aided Tolerancing*, 43:184 – 189, 2016.

[HDS13a] Hoffenson, S.; Dagman, A.; and Söderberg, R. Tolerance Optimization of a Mobile Phone considering Consumer Demand for Quality and Sustainability in China, Sweden, and the United States. In Lindemann, U.; Venkataraman, S.; Kim, Y.; and Lee, S., editors, *Proceedings of the 19th International Conference on Engineering Design ICED13, Seoul*, 2013.

[HDS13b] Hoffenson, S.; Dagman, A.; and Söderberg, R. Tolerance Specification Optimization for Economic and Ecological Sustainability. In Abramovici, M. and Stark, R., editors, *Smart Product Engineering*, Lecture Notes in Production Engineering, pages 865–874. Springer Berlin Heidelberg, 2013.

[HDS14] Hoffenson, S.; Dagman, A.; and Söderberg, R. Tolerance optimisation considering economic and environmental sustainability. *Journal of Engineering Design*, 25(10-12):367–390, 2014.

[HDS15] Hoffenson, S.; Dagman, A.; and Söderberg, R. Visual quality and sustainability considerations in tolerance optimization: A market-based approach. *International Journal of Production Economics*, 168:167 – 180, 2015.

[Hen73] Henriksen, E. K. *Jig and Fixture Design Manual.* Industrial Press Inc., New York, 1973.

[Hen91] Henzold, G. The new Principle of Independence and Geometric Tolerances. In Weill, R., editor, *Proceedings of the CIRP Working Seminar on Computer-Aided Tolerancing, Penn State University*, pages 151–190, 1991.

[Hen93] Henzold, G. Comparison of Vectorial Tolerancing and conventional Tolerancing. In Srinivasan, V. and Voelcker, H. B., editors, *Proceedings of the 1993 International Forum on Dimensional Tolerancing and Metrology, Dearborn, Michigan*, volume CRTD-Vol. 27, pages 147–160. ASME, 1993.

[Hen06] Henzold, G. *Geometrical Dimensioning and Tolerancing for Design, Manufacturing and Inspection.* Elsevier Science Publishers B. V., 2nd edition, 2006.

[Hen11] Henzold, G. *Anwendung der Normen über Form- und Lagetoleranzen in der Praxis.* Beuth Verlag GmbH Berlin Wien Zürich, 7th edition, 2011.

[HFG+06] Huang, Q.-X.; Flöry, S.; Gelfand, N.; Hofer, M.; and Pottmann, H. Reassembling fractured objects by geometric matching. *ACM Trans. Graph.*, 25(3):569–578, 2006.

[HG92] He, J. and Gibson, P. Computer-aided geometrical dimensioning and tolerancing for process-operation planning and quality control. *The International Journal of Advanced Manufacturing Technology*, 7(1):11–20, 1992.

[HH10] Havel, J. and Herout, A. Yet Faster Ray-Triangle Intersection (Using SSE4). *IEEE Transactions on Visualization and Computer Graphics*, 16(3):434–438, 2010.

[HHZX15] Huang, X.; Hu, S.; Zhang, Y.; and Xu, Y. A method to determine kinematic accuracy reliability of gear mechanisms with truncated random variables. *Mechanism and Machine Theory*, 92:200 – 212, 2015.

[HK97] Hu, S. and Koren, Y. Stream-of-Variation Theory for Automotive Body Assembly. *CIRP Annals - Manufacturing Technology*, 46(1):1 – 6, 1997.

[HK14] Hedlind, M. and Kjellberg, T. Kinematical product specifications in engineering design. *CIRP Annals - Manufacturing Technology*, 63(1):197 – 200, 2014.

[HK15] Hedlind, M. and Kjellberg, T. Design specifications with engineering terminology in a geometric context for CADCAM. *CIRP Annals - Manufacturing Technology*, 64(1):169 – 172, 2015.

[HLB+07] Huang, W.; Lin, J.; Bezdecny, M.; Kong, Z.; and Ceglarek, D. Stream-of-Variation Modeling—Part I: A Generic Three-Dimensional Variation Model for Rigid-Body Assembly in Single Station Assembly Processes. *Journal of Manufacturing Science and Engineering*, 129(4):821–831, 2007.

[HLC+14] Huang, W.; Liu, J.; Chalivendra, V.; Ceglarek, D.; Kong, Z.; and Zhou, Y. Statistical modal analysis for variation characterization and application in manufacturing quality control. *IIE Transactions*, 46(5):497–511, 2014.

[HLKC07] Huang, W.; Lin, J.; Kong, Z.; and Ceglarek, D. Stream-of-Variation (SOVA) Modeling II: A Generic 3D Variation Model for Rigid Body Assembly in Multistation Assembly Processes. *Journal of Manufacturing Science and Engineering*, 129(4):832–842, 2007.

[HMK+15] Haghighi, P.; Mohan, P.; Kalish, N.; Vemulapalli, P.; Shah, J. J.; and Davidson, J. K. Toward Automatic Tolerancing of Mechanical Assemblies: First-Order GD&T Schema Development and Tolerance Allocation. *Journal of Computing and Information Science in Engineering*, 15(4):041003, 2015.

[HNX+14] Huang, Q.; Nouri, H.; Xu, K.; Chen, Y.; Sosina, S.; and Dasgupta, T. Predictive modeling of geometric deviations of 3D printed products - A unified modeling approach for cylindrical and polygon shapes. In *2014 IEEE International Conference on Automation Science and Engineering (CASE)*, pages 25–30, 2014.

[HO04] Helton, J. and Oberkampf, W. Alternative representations of epistemic uncertainty. *Reliability Engineering & System Safety*, 85(1–3):1 – 10, 2004.

[Hol93] Holland, M. Systemkonzept zur prozeßgerechten Toleranzaufteilung bei Bauteilpaarungen. Technical Report 18, Institut für Maschinenwesen imw, TU Clausthal, 1993.

[Hol94] Holland, M. *Prozeßgerechte Toleranzfestlegung: Bereitstellung von Prozeßgenauigkeitsinformationen für die Konstruktion.* Number 137 in Fortschrittberichte, Reihe 20. VDI Verlag, Düsseldorf, 1994.

[Hon94] Honsinger, D. H. Geometric Dimensioning and Tolerancing – 1946 to 1982 The Differences in the Standards. Memorandum Report ARCCB-MR-94040, US Army Armament Research, Development and Engineering Center, Watervliet, N.Y., 1994.

[Hoo93] Hook, R. Interaction of Dimensioning, Tolerancing, and Metrology. In Srinivasan, V. and Voelcker, H. B., editors, *Proceedings of the 1993 International Forum on Dimensional Tolerancing and Metrology, Dearborn, Michigan*, volume CRTD-Vol. 27, pages 1–4. ASME, 1993.

[Hop92] Hopp, T. The Language of Tolerances. In Kuo, W. and Pierson, M. M., editors, *Quality Through Engineering Design*, number 16 in Advances in Industrial Engineering, pages 317–332. Elsevier Science Inc., 1992.

[Hop93] Hopp, T. H. Computational Metrology. In Srinivasan, V. and Voelcker, H. B., editors, *Proceedings of the 1993 International Forum on Dimensional Tolerancing and Metrology, Dearborn, Michigan*, volume CRTD-Vol. 27, pages 207–217. ASME, 1993.

[Hor87] Horn, B. K. P. Closed-form solution of absolute orientation using unit quaternions. *Journal of the Optical Society of America A*, 4:629–642, 1987.

[HOWG14] Husung, S.; Oberänder, A.; Weber, C.; and Geis, A. Use of Vectorial Tolerances in CAD during the Design Process. In Marjanovic, D.; Storga, M.; Pavkovic, N.; and Bojcetic, N., editors, *Proceedings of the 13th International Design Conference DESIGN 2014, Dubrovnik*, 2014.

[HP07] Hu, J. and Peng, Y. Tolerance modelling and robust design for concurrent engineering. *Proceedings of the Institution of Mechanical Engineers, Part C: Journal of Mechanical Engineering Science*, 221(4):455–465, 2007.

[HPC09] Huang, W.; Phoomboplab, T.; and Ceglarek, D. Process capability surrogate model-based tolerance synthesis for multi-station manufacturing systems. *IIE Transactions*, 41(4):309–322, 2009.

[HS03] Huang, Q. and Shi, J. Simultaneous Tolerance Synthesis through Variation Propagation Modeling of Multistage Manufacturing Processes. *NAMRI/SME Transactions*, 31:515–522, 2003.

[HSB+99] Henke, R.; Summerhays, K.; Baldwin, J.; Cassou, R.; and Brown, C. Methods for evaluation of systematic geometric deviations in machined parts and their relationships to process variables. *Precision Engineering*, 23(4):273 – 292, 1999.

[Hsi06] Hsieh, K.-L. The study of cost-tolerance model by incorporating process capability index into product lifecycle cost. *The International Journal of Advanced Manufacturing Technology*, 28(5):638–642, 2006.

[HTB15] Homri, L.; Teissandier, D.; and Ballu, A. Tolerance analysis by polytopes: Taking into account degrees of freedom with cap half-spaces. *Computer-Aided Design*, 62:112 – 130, 2015.

[HW92] Hu, S. J. and Wu, S. M. Identifying sources of variation in automobile body assembly using principal component analysis. *Transactions of NAMRI/SME*, 20:311–316, 1992.

[HXMP05] Hu, G.; Xu, J.; Miao, L.; and Peng, Q. *Computational Science and Its Applications – ICCSA 2005: International Conference, Singapore, May 9-12, 2005, Proceedings, Part I*, chapter Bilateral Estimation of Vertex Normal for Point-Sampled Models, pages 758–768. Springer Berlin Heidelberg, 2005.

[HYS03] Huang, Q.; Yuan, J.; and Shi, J. Part Dimensional Error and Its Propagation Modeling in Multi-Operational Machining Processes. *Journal of Manufacturing Science and Engineering*, 125:255–262, 2003.

[HZ08] Huang, M. and Zhong, Y. Dimensional and geometrical tolerance balancing in concurrent design. *The International Journal of Advanced Manufacturing Technology*, 35(7-8):723–735, 2008.

[HZ10] Huang, X. and Zhang, Y. Robust tolerance design for function generation mechanisms with joint clearances. *Mechanism and Machine Theory*, 45(9):1286 – 1297, 2010.

[HZS15] He, G.; Zhang, M.; and Song, Z. Error evaluation of free-form surface based on distance function of measured point to surface. *Computer-Aided Design*, 65:11 – 17, 2015.

[HZX05] Huang, M.; Zhong, Y.; and Xu, Z. Concurrent process tolerance design based on minimum product manufacturing cost and quality loss. *The International Journal of Advanced Manufacturing Technology*, 25(7-8):714–722, 2005.

[IMK95] Inui, M.; Miura, M.; and Kimura, F. Analysis of position uncertainties of parts in an assembly using configuration space in octree representation. In *Proceedings of the third ACM symposium on Solid modeling and applications*, pages 73–82, 1995.

[Ins09] Inselberg, A. *Parallel Coordinates – Visual Multidimensional Geometry and Its Applications*. Springer Dordrecht Heidelberg London New York, 2009.

[IP09] Imani, B. M. and Pour, M. Tolerance analysis of flexible kinematic mechanism using DLM method. *Mechanism and Machine Theory*, 44(2):445 – 456, 2009.

[Isl04] Islam, M. Functional dimensioning and tolerancing software for concurrent engineering applications. *Computers in Industry*, 54(2):169 – 190, 2004.

[Isl09a] Islam, M. A dimensioning and tolerancing methodology for concurrent engineering applications I: problem representation. *The International Journal of Advanced Manufacturing Technology*, 42(9-10):910–921, 2009.

[Isl09b] Islam, M. A dimensioning and tolerancing methodology for concurrent engineering applications II: comprehensive solution strategy. *The International Journal of Advanced Manufacturing Technology*, 42(9-10):922–939, 2009.

[ISO1] ISO/TC213. ISO 1:2002: Geometrical Product Specifications (GPS) – Standard reference temperature for geometrical product specification and verification. Standard, 2002.

[ISO129-1] ISO/TC10/SC1. ISO 129-1:2004: Technical drawings – Indication of dimensions and tolerances – Part 1: General principles. Standard, 2004.

[ISO230-1] ISO/TC39/SC2. ISO 230-1:2012: Test code for machine tools – Part 1: Geometric accuracy of machines operating under no-load or quasi-static conditions. Standard, 2012.

[ISO286-1] ISO/TC213. ISO 286-1:2010: Geometrical product specifications (GPS) – ISO code system for tolerances on linear sizes – Part 1: Basis of tolerances, deviations and fits. Standard, 2010.

[ISO286-2] ISO/TC213. ISO 286-2:2010: Geometrical product specifications (GPS) – ISO code system for tolerances on linear sizes – Part 2: Tables of standard tolerance classes and limit deviations for holes and shafts. Standard, 2010.

[ISO1101] ISO/TC213. ISO 1101:2012: Geometrical product specifications (GPS) – Geometrical tolerancing – Tolerances of form, orientation, location and run-out. Standard, 2012.

[ISO1660] ISO/TC213. ISO 1660:1987: Technical drawings – Dimensioning and tolerancing of profiles. Standard, 1987.

[ISO2692] ISO/TC213. ISO 2692:2014: Geometrical product specifications (GPS) – Geometrical tolerancing – Maximum material requirement (MMR), least material requirement (LMR) and reciprocity requirement (RPR). Standard, 2014.

[ISO2768-1] ISO/TC213. ISO 2768-1:1989: General tolerances – Part 1: Tolerances for linear and angular dimensions without individual tolerance indications. Standard, 1989.

[ISO2768-2] ISO/TC213. ISO 2768-2:1989: General tolerances – Part 2: Geometrical tolerances for features without individual tolerance indications. Standard, 1989.

[ISO4287] ISO/TC213. ISO 4287:1997: Geometrical Product Specifications (GPS) – Surface texture: Profile method – Terms, definitions and surface texture parameters. Standard, 1997.

[ISO5458] ISO/TC213. ISO 5458:1998: Geometrical Product Specifications (GPS) – Geometrical tolerancing – Positional tolerancing. Standard, 1998.

[ISO5459] ISO/TC213. ISO 5459:2011: Geometrical product specifications (GPS) – Geometrical tolerancing – Datums and datum systems. Standard, 2011.

[ISO7870-1] ISO/TC69/SC4. ISO 7870-1:2014: Control charts – Part 1: General guidelines. Standard, 2014.

[ISO8015] ISO/TC213. ISO 8015:2011: Geometrical product specifications (GPS) – Fundamentals – Concepts, principles and rules. Standard, 2011.

[ISO8062-1] ISO/TC213. ISO 8062-1:2007: Geometrical product specifications (GPS) – Dimensional and geometrical tolerances for moulded parts – Part 1: Vocabulary. Standard, 2007.

[ISO8062-2] ISO/TC213. ISO/TS 8062-2:2013: Geometrical product specifications (GPS) – Dimensional and geometrical tolerances for moulded parts – Part 2: Rules. Standard, 2013.

[ISO8062-3] ISO/TC213. ISO 8062-3:2007: Geometrical product specifications (GPS) – Dimensional and geometrical tolerances for moulded parts – Part 3: General dimensional and geometrical tolerances and machining allowances for castings. Standard, 2007.

[ISO8785] ISO/TC213. ISO 8785:1998: Geometrical Product Specification (GPS) – Surface imperfections – Terms, definitions and parameters. Standard, 1998.

[ISO10360-6] ISO/TC213. ISO 10360-6:2001: Geometrical Product Specifications (GPS) – Acceptance and reverification tests for coordinate measuring machines (CMM) – Part 6: Estimation of errors in computing Gaussian associated features. Standard, 2001.

[ISO10579] ISO/TC213. ISO 10579:2010: Geometrical product specifications (GPS) – Dimensioning and tolerancing – Non-rigid parts. Standard, 2010.

[ISO11462-1] ISO/TC69/SC4. ISO 11462-1:2001: Guidelines for implementation of statistical process control (SPC) – Part 1: Elements of SPC. Standard, 2001.

[ISO11462-2] ISO/TC69/SC4. ISO 11462-2:2010: Guidelines for implementation of statistical process control (SPC) – Part 2: Catalogue of tools and techniques. Standard, 2010.

[ISO12180-1] ISO/TC213. ISO 12180-1:2011: Geometrical product specifications (GPS) – Cylindricity – Part 1: Vocabulary and parameters of cylindrical form. Standard, 2011.

[ISO12180-2] ISO/TC213. ISO 12180-2:2011: Geometrical product specifications (GPS) – Cylindricity – Part 2: Specification operators. Standard, 2011.

[ISO12181-1] ISO/TC213. ISO 12181-1:2011: Geometrical product specifications (GPS) – Roundness – Part 1: Vocabulary and parameters of roundness. Standard, 2011.

[ISO12181-2] ISO/TC213. ISO 12181-2:2011: Geometrical product specifications (GPS) – Roundness – Part 2: Specification operators. Standard, 2011.

[ISO12780-1] ISO/TC213. ISO 12780-1:2011: Geometrical product specifications (GPS) – Straightness – Part 1: Vocabulary and parameters of straightness. Standard, 2011.

[ISO12780-2] ISO/TC213. ISO 12780-2:2011: Geometrical product specifications (GPS) – Straightness – Part 2: Specification operators. Standard, 2011.

[ISO12781-1] ISO/TC213. ISO 12781-1:2011: Geometrical product specifications (GPS) – Flatness – Part 1: Vocabulary and parameters of flatness. Standard, 2011.

[ISO12781-2] ISO/TC213. ISO 12781-2:2011: Geometrical product specifications (GPS) – Flatness – Part 2: Specification operators. Standard, 2011.

[ISO13920] ISO/TC44/SC10. ISO 13920:1996: Welding – General tolerances for welded constructions – Dimensions for lengths and angles – Shape and position. Standard, 1996.

[ISO14253-1] ISO/TC213. ISO 14253-1:2013: Geometrical product specifications (GPS) – Inspection by measurement of workpieces and measuring equipment – Part 1: Decision rules for proving conformity or nonconformity with specifications. Standard, 2013.

[ISO14405-1] ISO/TC213. ISO 14405-1:2010: Geometrical product specifications (GPS) – Dimensional tolerancing – Part 1: Linear sizes. Standard, 2010.

[ISO14405-2] ISO/TC213. ISO 14405-2:2011: Geometrical product specifications (GPS) – Dimensional tolerancing – Part 2: Dimensions other than linear sizes. Standard, 2011.

[ISO14638] ISO/TC213. ISO 14638:2015: Geometrical product specifications (GPS) – Matrix model. Standard, 2015.

[ISO17450-1] ISO/TC213. ISO 17450-1:2011: Geometrical product specifications (GPS) – General concepts – Part 1: Model for geometrical specification and verification. Standard, 2011.

[ISO17450-2] ISO/TC213. ISO 17450-2:2012: Geometrical product specifications (GPS) – General concepts – Part 2: Basic tenets, specifications, operators, uncertainties and ambiguities. Standard, 2012.

[ISO22432] ISO/TC213. ISO 22432:2011: Geometrical product specifications (GPS) – Features utilized in specification and verification. Standard, 2011.

[ISO22514-1] ISO/TC69/SC4. ISO 22514-1:2014: Statistical methods in process management – Capability and performance – Part 1: General principles and concepts. Standard, 2014.

[ISO22514-2] ISO/TC69/SC4. ISO 22514-2:2013: Statistical methods in process management – Capability and performance – Part 2: Process capability and performance of time-dependent process models. Standard, 2013.

[ISO22514-7] ISO/TC69/SC4. ISO 22514-7:2012: Statistical methods in process management – Capability and performance – Part 7: Capability of measurement processes. Standard, 2012.

[ISO25178-2] ISO/TC213. ISO 25178-2:2012: Geometrical product specifications (GPS) – Surface texture: Areal – Part 2: Terms, definitions and surface texture parameters. Standard, 2012.

[ISO25378] ISO/TC213. ISO 25378:2011: Geometrical product specifications (GPS) – Characteristics and conditions – Definitions. Standard, 2011.

[ISOTC16] ISO. ISO TC 213: http://www.iso.org/iso/home/standards_development/list_of_iso_technical_committees/iso_technical_committee.htm?commid=54924 Retrieved in April 2016.

[ITK97] Ikonomov, P. G.; Tanaka, F.; and Kishinami, T. A model of the constraint substitute element for geometrical tolerances verification. *International Journal of Machine Tools and Manufacture*, 37(10):1465 – 1473, 1997.

[Jai12] Jaishankar, L. N. Tolerance Analysis of Parallel Assemblies using Tolerance-Maps and a Functional Map Derived from Induced Deformations. Master's thesis, Arizona State University, 2012.

[JBL+11] Jaballi, K.; Bellacicco, A.; Louati, J.; Riviere, A.; and Haddar, M. Rational method for 3D manufacturing tolerancing synthesis based on the TTRS approach "R3DMTSyn". *Computers in Industry*, 62(5):541 – 554, 2011.

[JC02] Jeang, A. and Chang, C.-L. Combined Robust Parameter and Tolerance Design Using Orthogonal Arrays. *The International Journal of Advanced Manufacturing Technology*, 19(6):442–447, 2002.

[JCG08] JCGM/WG1 of the Bureau International des Poids et Mesures. Evaluation of measurement data – Guide to the expression of uncertainty in measurement. Guideline, 2008.

[JCLL15] Jin, S.; Chen, H.; Li, Z.; and Lai, X. A small displacement torsor model for 3D tolerance analysis of conical structures. *Proceedings of the Institution of Mechanical Engineers, Part C: Journal of Mechanical Engineering Science*, 229(14):2514–2523, 2015.

[JD08] Jérome, D. and Denis, T. A tolerancing framework to support geometric specifications traceability. *The International Journal of Advanced Manufacturing Technology*, 36(9-10):894–907, 2008.

[JDLS14] Jiang, K.; Davidson, J. K.; Liu, J.; and Shah, J. J. Using tolerance maps to validate machining tolerances for transfer of cylindrical datum in manufacturing process. *The International Journal of Advanced Manufacturing Technology*, 73(1):465–478, 2014.

[Jea99] Jeang, A. Robust Tolerance Design by Response Surface Methodology. *The International Journal of Advanced Manufacturing Technology*, 15(6):399–403, 1999.

[JHC02] Jeang, A.; Hwan, C.-L.; and Chen, T.-K. A Statistical Dimension and Tolerance Design for Mechanical Assembly Under Thermal Impact. *The International Journal of Advanced Manufacturing Technology*, 20(12):907–915, 2002.

[JLMC00] Ji, S.; Li, X.; Ma, Y.; and Cai, H. Optimal Tolerance Allocation Based on Fuzzy Comprehensive Evaluation and Genetic Algorithm. *The International Journal of Advanced Manufacturing Technology*, 16(7):461–468, 2000.

[JLW15] Jin, Q.; Liu, S.; and Wang, P. Optimal tolerance design for products with non-normal distribution based on asymmetric quadratic quality loss. *The International Journal of Advanced Manufacturing Technology*, 78(1-4):667–675, 2015.

[JS00] Johannesson, H. and Söderberg, R. Structure and Matrix Models for Tolerance Analysis from Configuration to Detail Design. *Research in Engineering Design*, 12(2):112–125, 2000.

[JS14] Jorden, W. and Schütte, W. *Form- und Lagetoleranzen – Handbuch für Studium und Praxis.* Carl Hanser Verlag, München, 8th edition, 2014.

[JSS97] Joskowicz, L.; Sacks, E.; and Srinivasan, V. Kinematic tolerance analysis. *Computer-Aided Design*, 29(2):147 – 157, 1997.

[JST11] Jayaprakash, G.; Sivakumar, K.; and Thilak, M. Integration of thermo mechanical strains into optimal tolerance design of mechanical assembly using NSGA II and FE simulation. *Journal of Mechanical Engineering Research*, 3(6):168–180, 2011.

[Jur62] Juran, J. M. Specification of Quality. In Juran, J. M.; Seder, L. A.; and Gryna, F. M., editors, *Quality Control Handbook.* McGraw-Hill Book Company, New York, 2nd edition, 1962.

[KA12] Krogstie, L. and Andersson, P. A Case Study on Reuse of Manufacturing Knowledge - Comparing Defense Practices with Automotive & Aerospace Practices. *Procedia CIRP – 45th CIRP Conference on Manufacturing Systems*, 3(0):430 – 435, 2012.

[KAV13] Krogstie, L.; Andersen, B.; and Verberne, C. J. Performance Measurement supporting Closed Loop Tolerance Engineering – an Industrial Case on Tolerance and Variation Collaboration. In

Lindemann, U.; Venkataraman, S.; Kim, Y.; and Lee, S., editors, *Proceedings of the 19th International Conference on Engineering Design ICED13, Seoul*, 2013.

[KEH15] Krogstie, L.; Ebro, M.; and Howard, T. J. How to implement and apply robust design: insights from industrial practice. *Total Quality Management & Business Excellence*, 26(11-12):1387–1405, 2015.

[KGA14] Krogstie, L.; Gaarder, A.; and Andersen, B. Variation Analysis in Collaborative Engineering; an Industrial Case Study of Rocket Motor Development. *Procedia CIRP – 24th CIRP Design Conference*, 21:306 – 311, 2014.

[KH06] Krzykacz-Hausmann, B. An approximate sensitivity analysis of results from complex computer models in the presence of epistemic and aleatory uncertainties. *Reliability Engineering & System Safety*, 91(10–11):1210 – 1218, 2006.

[Kle05] Klein, R. *Algorithmische Geometrie.* Springer Berlin Heidelberg, 2005.

[Kle11] Klein, B. *Prozessorientierte Statistische Tolerierung im Maschinen- und Fahrzeugbau.* expert-Verlag Renningen, 2011.

[Kle12] Klein, B. *Toleranzmanagement im Maschinen- und Fahrzeugbau.* Oldenbourg Verlag München, 2012.

[KM99] Krimmel, O. and Martinsen, K. Industrial application of Vectorial Tolerancing to improve clamping of forged workpieces in machining. In van Houten, F. and Kals, H., editors, *Global Consistency of Tolerances*, pages 101–110. Springer Netherlands, 1999.

[KM11] Khodaygan, S. and Movahhedy, M. Tolerance analysis of assemblies with asymmetric tolerances by unified uncertainty–accumulation model based on fuzzy logic. *The International Journal of Advanced Manufacturing Technology*, 53(5-8):777–788, 2011.

[KM12a] Khodaygan, S. and Movahhedy, M. R. Fuzzy-based analysis of process capability for assembly quality assessment in mechanical assemblies. *International Journal of Production Research*, 50(12):3395–3415, 2012.

[KM12b] Krogstie, L. and Martinsen, K. Closed Loop Tolerance Engineering – A Relational Model Connecting Activities of Product Development. *Procedia CIRP – 45th CIRP Conference on Manufacturing Systems*, 3:519 – 524, 2012.

[KM16] Khodaygan, S. and Movahhedy, M. A comprehensive fuzzy feature-based method for worst case and statistical tolerance analysis. *International Journal of Computer Integrated Manufacturing*, 29(1):42–63, 2016.

[KMA14] Krogstie, L.; Martinsen, K.; and Andersen, B. Approaching the Devil in the Details; A Survey for Improving Tolerance Engineering Practice. *Procedia CIRP – Variety Management in Manufacturing: Proceedings of the 47th CIRP Conference on Manufacturing Systems*, 17:230 – 235, 2014.

[KMF11] Khodaygan, S.; Movahhedy, M.; and Foumani, M. S. Fuzzy-small degrees of freedom representation of linear and angular variations in mechanical assemblies for tolerance analysis and allocation. *Mechanism and Machine Theory*, 46(4):558 – 573, 2011.

[Koc06] Koch, A. *Entwicklung einer Methode zur Visualisierung der Auswirkungen von Form- und Lagetoleranzen auf die Bauteilgestalt.* PhD thesis, Technische Fakultät der Friedrich-Alexander-Universität Erlangen-Nürnberg, 2006.

[KPB16] Kumar, L. R.; Padmanaban, K. P.; and Balamurugan, C. Least cost–tolerance allocation based on Lagrange multiplier. *Concurrent Engineering*, 24(2):164 – 177, 2016.

[KPMW03] Kethara Pasupathy, T. M.; Morse, E. P.; and Wilhelm, R. G. A Survey of Mathematical Methods for the Construction of Geometric Tolerance Zones. *Journal of Computing and Information Science in Engineering*, 3(1):64–75, 2003.

[KRY03a] Kang, Y.; Rong, Y.; and Yang, C. J. Computer-Aided Fixture Design Verification. Part 1. The Framework and Modelling. *The International Journal of Advanced Manufacturing Technology*, 21(10):827–835, 2003.

[KRY03b] Kang, Y.; Rong, Y.; and Yang, C. J. Computer-Aided Fixture Design Verification. Part 2. Tolerance Analysis. *The International Journal of Advanced Manufacturing Technology*, 21(10):836–841, 2003.

[KRY03c] Kang, Y.; Rong, Y.; and Yang, C. J. Computer-Aided Fixture Design Verification. Part 3. Stability Analysis. *The International Journal of Advanced Manufacturing Technology*, 21(10):842–849, 2003.

[KSAL07] Kero, T.; Söderberg, R.; Andersson, M.; and Lindkvist, L. Process Optimization Regarding Geometrical Variation and Sensitivity Involving Dental Drill- and Implant-Guided Surgeries. In *Proceedings of World Academy of Science, Engineering and Technology*, volume 24, 2007.

[KSAL10] Kero, T.; Söderberg, R.; Andersson, M.; and Lindkvist, L. A Method for Improving Dental Crown Fit – Increasing the Robustness. *International Journal of Medical, Health, Biomedical, Bioengineering and Pharmaceutical Engineering*, 4(3):62–69, 2010.

[KSD01] Kandikjan, T.; Shah, J.; and Davidson, J. A mechanism for validating dimensioning and tolerancing schemes in CAD systems. *Computer-Aided Design*, 33(10):721 – 737, 2001.

[KSS13] Kumaraswamy, U.; Shunmugam, M.; and Sujatha, S. A unified framework for tolerance analysis of planar and spatial mechanisms using screw theory. *Mechanism and Machine Theory*, 69:168 – 184, 2013.

[Kum83] Kumar, V. Optimization of tolerance for minimum manufacturing cost of satisfactory journal bearings. *Wear*, 86(1):21 – 27, 1983.

[KUWA14] Krogstie, L.; Ulonska, S.; Welo, T.; and Andersen, B. On Knowledge-based Development: How Documentation Practice Represents a Strategy for Closing Tolerance Engineering Loops. *Procedia CIRP – 24th CIRP Design Conference*, 21:318 – 323, 2014.

[Kwa11] Kwan, A. Vernier scales and other early devices for precise measurement. *American Journal of Physics*, 79(4):368–373, 2011.

[LABH06] Louati, J.; Ayadi, B.; Bouaziz, Z.; and Haddar, M. Three-dimensional modelling of geometric defaults to optimize a manufactured part setting. *The International Journal of Advanced Manufacturing Technology*, 29(3-4):342–348, 2006.

[LAS02] Linares, J. M.; Anthierens, C.; and Sprauel, J. M. Synthesis of tolerancing by functional group. *Journal of Manufacturing Systems*, 21(4):260 – 275, 2002.

[LC96] Lai, J.-Y. and Chen, I.-H. Minimum zone evaluation of circles and cylinders. *International Journal of Machine Tools and Manufacture*, 36(4):435 – 451, 1996.

[LCE+14] Lorin, S.; Cromvik, C.; Edelvik, F.; Lindkvist, L.; and Söderberg, R. Variation Simulation of Welded Assemblies Using a Thermo-Elastic Finite Element Model. *Journal of Computing and Information Science in Engineering*, 14(3):031003, 2014.

[LDB05] Lavoué, G.; Dupont, F.; and Baskurt, A. A new CAD mesh segmentation method, based on curvature tensor analysis. *Computer-Aided Design*, 37(10):975 – 987, 2005.

[LDP+00] Litvin, F.; Donno, M.; Peng, A.; Vorontsov, A.; and Handschuh, R. Integrated computer program for simulation of meshing and contact of gear drives. *Computer Methods in Applied Mechanics and Engineering*, 181(1–3):71 – 85, 2000.

[Lee09] Lee, M.-K. An enhanced convex-hull edge method for flatness tolerance evaluation. *Computer-Aided Design*, 41(12):930 – 941, 2009.

[LF04] Litvin, F. L. and Fuentes, A. *Gear Geometry and Applied Theory*. Cambridge University Press, 2nd edition, 2004.

[LFW06] Lu, C.; Fuh, J. Y. H.; and Wong, Y. S. Evaluation of product assemblability in different assembly sequences using the tolerancing approach. *International Journal of Production Research*, 44(23):5037–5063, 2006.

[LGD02] Laperrière, L.; Ghie, W.; and Desrochers, A. Statistical and Deterministic Tolerance Analysis and Synthesis Using a Unified Jacobian-Torsor Model. *CIRP Annals - Manufacturing Technology*, 51(1):417 – 420, 2002.

[LH94] Lin, P. D. and Hwang, S. G. Modeling for error analysis of cam mechanisms by using 4 × 4 homogeneous transformation matrix. *Mathematical and Computer Modelling*, 19(5):33 – 42, 1994.

[LH97] Liu, S. C. and Hu, S. J. Variation Simulation for Deformable Sheet Metal Assemblies Using Finite Element Methods. *Journal of Manufacturing Science and Engineering*, 119(3):368–374, 1997.

[LH09] Liu, Q. and Homma, T. A new computational method of a moment-independent uncertainty importance measure. *Reliability Engineering & System Safety*, 94(7):1205 – 1211, 2009.

[Li10] Li, Q. Measurement of surface roughness from fractal theory. In *2010 International Conference on Computer, Mechatronics, Control and Electronic Engineering*, volume 2, pages 180–182, 2010.

[LIK+08] Li, Z.; Izquierdo, L. E.; Kokkolaras, M.; Hu, S. J.; and Papalambros, P. Y. Multiobjective Optimization for Integrated Tolerance Allocation and Fixture Layout Design in Multistation Assembly. *Journal of Manufacturing Science and Engineering*, 130(4):044501, 2008.

[LJLX08] Lu, W. L.; Jiang, X.; Liu, X. J.; and Xu, Z. G. Compliance uncertainty of diameter characteristic in the next-generation geometrical product specifications and verification. *Measurement Science and Technology*, 19(10):105103, 2008.

[LJZ+14] Lin, J.; Jin, S.; Zheng, C.; Li, Z.; and Liu, Y. Compliant assembly variation analysis of aeronautical panels using unified substructures with consideration of identical parts. *Computer-Aided Design*, 57:29 – 40, 2014.

[LK93] Li, C. and Kiureghian, A. D. Optimal Discretization of Random Fields. *Journal of Engineering Mechanics*, 119(6):1136–1154, 1993.

[LL99a] Lafond, P. and Laperriere, L. Jacobian-based modeling of dispersions affecting pre-defined functional requirements of mechanical assemblies. In *Proceedings of the 1999 IEEE International Symposium on Assembly and Task Planning*, pages 20–25, 1999.

[LL99b] Laperrière, L. and Lafond, P. Modeling Dispersions Affecting Pre-Defined Functional Requirements of Mechanical Assemblies Using Jacobian Transforms. In Batoz, J.-L.; Chedmail, P.; Cognet, G.; and Fortin, C., editors, *Integrated Design and Manufacturing in Mechanical Engineering '98: Proceedings of the 2nd IDMME Conference held in Compiègne, France, 27–29 May 1998*, pages 381–388. Springer Netherlands, Dordrecht, 1999.

[LL15] Lipman, R. and Lubell, J. Conformance checking of PMI representation in CAD model STEP data exchange files. *Computer-Aided Design*, 66:14 – 23, 2015.

[LLAS13] Lindau, B.; Lindkvist, L.; Andersson, A.; and Söderberg, R. Statistical shape modeling in virtual assembly using PCA-technique. *Journal of Manufacturing Systems*, 32(3):456 – 463, 2013.

[LLB14] Lê, H.-N.; Ledoux, Y.; and Ballu, A. Experimental and Theoretical Investigations of Mechanical Joints With Form Defects. *Journal of Computing and Information Science in Engineering*, 14(4):041004, 2014.

[LLDM15] Li, Y.; Lu, H.; Daniel, W.; and Meehan, P. Investigation and optimization of deformation energy and geometric accuracy in the incremental sheet forming process using response surface methodology. *The International Journal of Advanced Manufacturing Technology*, 79(9-12):2041–2055, 2015.

[LLH99] Lin, A. C.; Lin, M.-Y.; and Ho, H.-B. CAPP and its integration with tolerance charts for machining of aircraft components. *Computers in Industry*, 38(3):263 – 283, 1999.

[LLK98a] Liu, W.; Li, L.; and Kochhar, A. K. A method for assessing geometrical errors in layered manufacturing. Part 1: Error interaction and transfer mechanisms. *The International Journal of Advanced Manufacturing Technology*, 14(9):637–643, 1998.

[LLK98b] Liu, W.; Li, L.; and Kochhar, A. K. A method for assessing geometrical errors in layered manufacturing. Part 2: Mathematical modelling and numerical evaluation. *The International Journal of Advanced Manufacturing Technology*, 14(9):644–650, 1998.

[LLS07] Lööf, J.; Lindkvist, L.; and Söderberg, R. Envelope of Rotating Parts Based on Motion and Variation Simulation Data. In Weckenmann, A., editor, *Proceedings of the 10th CIRP International Seminar on Computer Aided Tolerancing, Erlangen*, 2007.

[LPG13] Leonard, P.; Pairel, E.; and Giordano, M. A Simpler and More Formal Geometric Tolerancing Model. *Procedia CIRP – 12th CIRP Conference on Computer-Aided Tolerancing*, 10:30 – 36, 2013.

[LPJC04] Lee, Y.; Park, S.; Jun, Y.; and Choi, W. A robust approach to edge detection of scanned point data. *The International Journal of Advanced Manufacturing Technology*, 23(3-4):263–271, 2004.

[LPY+06] Liu, Y.-S.; Paul, J.-C.; Yong, J.-H.; Yu, P.-Q.; Zhang, H.; Sun, J.-G.; and Ramani, K. Automatic least-squares projection of points onto point clouds with applications in reverse engineering. *Computer-Aided Design*, 38(12):1251 – 1263, 2006.

[LR01] Li, B. and Roy, U. Relative positioning of toleranced polyhedral parts in an assembly. *IIE Transactions*, 33(4):323–336, 2001.

[LSL06] Lööf, J.; Söderberg, R.; and Lindkvist, L. Visualization of Variation in early Design Phases: A Convex Hull Approach. In Marjanovic, D., editor, *Proceedings of the 9th International Design Conference DESIGN 2006, Dubrovnik*, pages 905–912, 2006.

[LSRC15] Liu, R.; Serré, P.; Rameau, J.-F.; and Clément, A. Generic Approach for the Generation of Symbolic Dimensional Variations Based on Gröbner Basis for Over-constrained Mechanical Assemblies. *Procedia CIRP – 13th CIRP Conference on Computer-Aided Tolerancing*, 27:223 – 229, 2015.

[LT15] Lépine, M. J. and Tahan, A. S. The Relationship Between Geometrical Complexity and Process Capability. *Journal of Manufacturing Science and Engineering*, 138(5):051009, 2015.

[LTBT15] Louhichi, B.; Tlija, M.; Benamara, A.; and Tahan, A. An algorithm for CAD tolerancing integration: Generation of assembly configurations according to dimensional and geometrical tolerances. *Computer-Aided Design*, 62:259 – 274, 2015.

[Lut14a] Lutters, E. Computer-Aided Design. In Laperrière, L. and Reinhart, G., editors, *CIRP Encyclopedia of Production Engineering*, pages 252–254. Springer Berlin Heidelberg, 2014.

[Lut14b] Lutters, E. Product Development. In Laperrière, L. and Reinhart, G., editors, *CIRP Encyclopedia of Production Engineering*, pages 991–992. Springer Berlin Heidelberg, 2014.

[LV03] Legoff, O. and Villeneuve, F. Three-dimensional geometrical tolerancing: quantification of machining defects. In Bourdet, P. and Mathieu, L., editors, *Geometric Product Specification and Verification: Integration of Functionality: Selected Conference Papers of the 7th CIRP International Seminar on Computer-Aided Tolerancing, held at the École Normale Supérieure de Cachan, France, 24–25 April 2001*, pages 185–196. Springer Netherlands, Dordrecht, 2003.

[LvHB+14] Lutters, E.; van Houten, F. J.; Bernard, A.; Mermoz, E.; and Schutte, C. S. Tools and techniques for product design. *CIRP Annals - Manufacturing Technology*, 63(2):607 – 630, 2014.

[LWG97] Latombe, J.-C.; Wilson, R. H.; and Gazals, F. Assembly sequencing with toleranced parts. *Computer-Aided Design*, 29(2):159 – 174, 1997.

[LX08] Liu, Y. and Xiong, Y. Automatic segmentation of unorganized noisy point clouds based on the Gaussian map. *Computer-Aided Design*, 40(5):576 – 594, 2008.

[LY95] Lee, S. and Yi, C. Assemblability evaluation based on tolerance propagation. In *Proceedings of the IEEE International Conference on Robotics and Automation*, volume 2, pages 1593–1598, 1995.

[LY98a] Lee, S. and Yi, C. An analytic approach to assemblability analysis. In *Proceedings of the IEEE International Conference on Robotics and Automation*, volume 2, pages 1484–1489, 1998.

[LY98b] Lee, S. and Yi, C. Statistical representation and computation of tolerance and clearance for assemblability evaluation. *Robotica*, 16(3):251–264, 1998.

[LYHZ09] Li, B.; Yang, X.; Hu, Y.; and Zhang, D. Quality design of tolerance allocation for sheet metal assembly with resistance spot weld. *International Journal of Production Research*, 47(6):1695–1711, 2009.

[LZ01] Lin, E. and Zhang, H.-C. Theoretical Tolerance Stackup Analysis Based on Tolerance Zone Analysis. *The International Journal of Advanced Manufacturing Technology*, 17(4):257–262, 2001.

[LZC07] Loose, J.-P.; Zhou, S.; and Ceglarek, D. Kinematic Analysis of Dimensional Variation Propagation for Multistage Machining Processes With General Fixture Layouts. *IEEE Transactions on Automation Science and Engineering*, 4(2):141–152, 2007.

[LZLH90] Litvin, F. L.; Zhang, J.; Lee, H.-T.; and Handschuh, R. F. Transmission Errors and Bearing Contact of Spur, Helical, and Spiral Bevel Gears. *Gear Technology*, July/August:8–13/44–45, 1990.

[LZLH14] Li, H.; Zhu, H.; Li, P.; and He, F. Tolerance analysis of mechanical assemblies based on small displacement torsor and deviation propagation theories. *The International Journal of Advanced Manufacturing Technology*, 72(1-4):89–99, 2014.

[LZW01] Liu, Q.; Zhang, C.; and Wang, H.-P. On the effects of CMM measurement error on form tolerance estimation. *Measurement*, 30(1):33 – 47, 2001.

[LZZ+16] Li, H.; Zhu, H.; Zhou, X.; Li, P.; and Yu, Z. A new computer-aided tolerance analysis and optimization framework for assembling processes using DP-SDT theory. *The International Journal of Advanced Manufacturing Technology*, pages 1–12, 2016. doi:10.1007/s00170-015-8266-9.

[MA98] Mullins, S. and Anderson, D. Automatic identification of geometric constraints in mechanical assemblies. *Computer-Aided Design*, 30(9):715 – 726, 1998.

[MAM05] Mejbri, H.; Anselmetti, B.; and Mawussi, K. Functional tolerancing of complex mechanisms: Identification and specification of key parts. *Computers & Industrial Engineering*, 49(2):241 – 265, 2005.

[Man04] Mannewitz, F. Komplexe Toleranzanalysen einfach durchführen. *Konstruktion*, 7/8:69–74, 2004.

[Man05a] Mannewitz, F. Baugruppenfunktions- und prozessorientierte Toleranzaufweitung (Teil 1) – Sub-Assembly Functionality and Process-Oriented Tolerance Expansion (Part 1). *Konstruktion*, (10):87–93, 2005.

[Man05b] Mannewitz, F. Baugruppenfunktions- und prozessorientierte Toleranzaufweitung (Teil 2) – Sub-Assembly Functionality and Process-Oriented Tolerance Expansion (Part 2). *Konstruktion*, (11/12):57–62, 2005.

[Man05c] Mannewitz, F. Toleranzanalysen an beliebigen physikalischen Systemen. *ATZ*, 107:896–903, 2005.

[Man15] Mannewitz, F. Toleranzmanagement aus Sicht eines Engineering-Dienstleisters. In Wartzack, S., editor, *Summer School Toleranzmanagement – Beiträge zur 2. Summer School September 2015*, pages 68–73. Druck+Verlag Ernst Vögel GmbH Stamsried, 2015.

[Mar93] Martinsen, K. Vectorial Tolerancing for all types of surfaces. In Gilmore, B. J., editor, *Advances in Design Automation 1993: Proceedings of the 1993 ASME Design Technical Conferences – 19th Design Automation Conference, Albuquerque, New Mexico, September 19-22, 1993*, volume 2, pages 187–198. ASME, New York, 1993.

[Mar96] Martinsen, K. Statistical Process Control using Vectorial Tolerancing. In Kimura, F., editor, *Computer-aided Tolerancing*, pages 173–186. Springer Netherlands, 1996.

[Mat97] Matthiassen, B. *Design for Robustness and Reliability – Improving the Quality Consciousness in Engineering Design.* PhD thesis, Department of Control and Engineering Design, Technical University of Denmark, 1997.

[Mat08] Matuszyk, T. I. *Shape Characterisation of Sheet Metal Assembly Variation with a View to Quality Assessment and Dimensional Control.* PhD thesis, Australian National University, 2008.

[Mat15] The MathWorks, Inc.. MATLAB Release 2015b. Software, 2015.

[MB03] Mathieu, L. and Ballu, A. GEOSPELLING: a common language for Geometrical Product Specification and Verification to express method uncertainty. In Wilhelm, R. G., editor, *Proceedings of the 8th CIRP International Seminar on Computer Aided Tolerancing – Managing Geometric Uncertainty in the Product Lifecycle*, pages 70–79, 2003.

[MB07] Mathieu, L. and Ballu, A. A Model for a Coherent and Complete Tolerancing Process. In Davidson, J., editor, *Models for Computer Aided Tolerancing in Design and Manufacturing*, pages 35–44. Springer Netherlands, 2007.

[MB12] Mickaël, C. and Bernard, A. 3D ISO manufacturing specifications with vectorial representation of tolerance zones. *The International Journal of Advanced Manufacturing Technology*, 60(5-8):577–588, 2012.

[MBC79] McKay, M. D.; Beckman, R. J.; and Conover, W. J. A Comparison of Three Methods for Selecting Values of Input Variables in the Analysis of Output from a Computer Code. *Technometrics*, 21(2):239–245, 1979.

[MBK96] Mattikalli, R.; Baraff, D.; and Khosla, P. Finding all stable orientations of assemblies with friction. *IEEE Transactions on Robotics and Automation*, 12(2):290–301, 1996.

[MBKR95] Mattikalli, R.; Baraff, D.; Khosla, P.; and Repetto, B. Gravitational stability of frictionless assemblies. *IEEE Transactions on Robotics and Automation*, 11(3):374–388, 1995.

[MC10] Maropoulos, P. and Ceglarek, D. Design verification and validation in product lifecycle. *CIRP Annals - Manufacturing Technology*, 59(2):740 – 759, 2010.

[MCB98] Mathieu, L.; Clement, A.; and Bourdet, P. Modeling, Representation and Processing of Tolerances, Tolerance Inspection: a Survey of Current Hypothesis. In ElMaraghy, H. A., editor, *Geometric Design Tolerancing: Theories, Standards and Applications*, pages 1–33. Springer US, 1998.

[MCHR10] Matuszyk, T. I.; Cardew-Hall, M. J.; and Rolfe, B. F. The kernel density estimate/point distribution model (KDE-PDM) for statistical shape modeling of automotive stampings and assemblies. *Robotics and Computer-Integrated Manufacturing*, 26(4):370 – 380, 2010.

[MCLY09] Mao, J.; Cao, Y.; Liu, S.; and Yang, J. Manufacturing environment-oriented robust tolerance optimization method. *The International Journal of Advanced Manufacturing Technology*, 41(1-2):57–65, 2009.

[MDS09] Muthu, P.; Dhanalakshmi, V.; and Sankaranarayanasamy, K. Optimal tolerance design of assembly for minimum quality loss and manufacturing cost using metaheuristic algorithms. *The International Journal of Advanced Manufacturing Technology*, 44(11-12):1154–1164, 2009.

[Mee94] Meerkamm, H. Design for X – A Core Area of Design Methodology. *Journal of Engineering Design*, 5(2):165–181, 1994.

[MGD13] Mansuy, M.; Giordano, M.; and Davidson, J. K. Comparison of Two Similar Mathematical Models for Tolerance Analysis: T-Map and Deviation Domain. *Journal of Mechanical Design*, 135(10):101008, 2013.

[MGH11] Mansuy, M.; Giordano, M.; and Hernandez, P. A new calculation method for the worst case tolerance analysis and synthesis in stack-type assemblies. *Computer-Aided Design*, 43(9):1118 – 1125, 2011.

[MGH13] Mansuy, M.; Giordano, M.; and Hernandez, P. A Generic Method for the Worst Case and Statistical Tridimensional Tolerancing Analysis. *Procedia CIRP – 12th CIRP Conference on Computer-Aided Tolerancing*, 10:276 – 282, 2013.

[MHSD15] Mohan, P.; Haghighi, P.; Shah, J.; and Davidson, J. Development of a library of feature fitting algorithms for CMMs. *International Journal of Precision Engineering and Manufacturing*, 16(10):2101–2113, 2015.

[Mil92] Miller, S. Statistical tolerance modeling in the framework of concurrent engineering. In *Combined Proceedings of the 1990 and 1991 Leesburg Workshops on Reliability and Maintainability Computer-Aided Engineering in Concurrent Engineering, 1990 and 1991*, pages 143–152, 1992.

[Mio09] Miotti, H. The economic Impact of Standardization – Technological Change, Standards Growth in France. Technical report, afnor Normalisation, 2009.

[MKI11] Muvengei, O.; Kihiu, J.; and Ikua, B. Dynamic Analysis of Multi-Body Mechanical Systems with Imperfect Kinematic Joints: A Literature Survey and Review. *Sustainable Research and Innovation Proceedings*, 3:61 – 76, 2011.

[MM01] Mathieu, L. and Marguet, B. Integrated Design Method to Improve Producibility based on Product Key Characteristics and Assembly Sequences. *CIRP Annals - Manufacturing Technology*, 50(1):85 – 88, 2001.

[MM03] Marguet, B. and Mathieu, L. Method for Geometric Variation Management from Key Characteristics to Specification. In Bourdet, P. and Mathieu, L., editors, *Geometric Product Specification and Verification: Integration of Functionality*, pages 217–226. Springer Netherlands, Dordrecht, 2003.

[MMLS10] Morière, S.; Mailhé, J.; Linares, J.-M.; and Sprauel, J.-M. Assembly Method Comparison Including form Defect. In Giordano, M.; Mathieu, L.; and Villeneuve, F., editors, *Product Lifecycle Management: Geometric Variations*, pages 245–257. John Wiley & Sons, Inc., 2010.

[Mor98] Morse, E. P. More on the Effects of Non-Normal Statistics in Geometric Tolerancing. In ElMaraghy, H. A., editor, *Geometric Design Tolerancing: Theories, Standards and Applications*, pages 254–261. Springer US, 1998.

[MP08] Moroni, G. and Petrò, S. Geometric tolerance evaluation: A discussion on minimum zone fitting algorithms. *Precision Engineering*, 32(3):232 – 237, 2008.

[MP09] Marziale, M. and Polini, W. A review of two models for tolerance analysis of an assembly: vector loop and matrix. *The International Journal of Advanced Manufacturing Technology*, 43(11-12):1106–1123, 2009.

[MP11a] Marziale, M. and Polini, W. Review of variational models for tolerance analysis of an assembly. *Proceedings of the Institution of Mechanical Engineers, Part B: Journal of Engineering Manufacture*, 225(3):305–318, 2011.

[MP11b] Marziale, M. and Polini, W. A review of two models for tolerance analysis of an assembly: Jacobian and torsor. *International Journal of Computer Integrated Manufacturing*, 24(1):74–86, 2011.

[MP14] Moroni, G. and Petrò, S. Optimal inspection strategy planning for geometric tolerance verification. *Precision Engineering*, 38(1):71 – 81, 2014.

[MPT11] Moroni, G.; Petrò, S.; and Tolio, T. Early cost estimation for tolerance verification. *CIRP Annals - Manufacturing Technology*, 60(1):195 – 198, 2011.

[MS13a] Mölzer, B. and Strobelt, M. Dimensional Management in Vehicle Development – A preventive quality assurance method. *Porsche Engineering Magazin*, 01:24–29, 2013.

[MS13b] Morse, E. P. and Srinivasan, V. Size tolerancing revisited: A basic notion and its evolution in standards. *Proceedings of the Institution of Mechanical Engineers, Part B: Journal of Engineering Manufacture*, 227(5):662–671, 2013.

[MSD05] Martin, P.; Schneider, F.; and Dantan, J.-Y. Optimal adjustment of a machine tool for improving the geometrical quality of machined parts. *The International Journal of Advanced Manufacturing Technology*, 26(5-6):559–564, 2005.

[MSP14] Moroni, G.; Syam, W. P.; and Petrò, S. Towards Early Estimation of Part Accuracy in Additive Manufacturing. *Procedia CIRP – 24th CIRP Design Conference*, 21:300 – 305, 2014.

[MTA05] Murphy, T.; Tsui, K.-L.; and Allen, J. A review of robust design methods for multiple responses. *Research in Engineering Design*, 16(3):118–132, 2005.

[MTB+11] Mounaud, M.; Thiébaut, F.; Bourdet, P.; Falgarone, H.; and Chevassus, N. Assembly sequence influence on geometric deviations propagation of compliant parts. *International Journal of Production Research*, 49(4):1021–1043, 2011.

[MW98] Mantripragada, R. and Whitney, D. E. The Datum Flow Chain: A systematic approach to assembly design and modeling. *Research in Engineering Design*, 10(3):150–165, 1998.

[MW99] Mantripragada, R. and Whitney, D. E. Modeling and controlling variation propagation in mechanical assemblies using state transition models. *IEEE Transactions on Robotics and Automation*, 15(1):124–140, 1999.

[MZ11] Ma, X. and Zabaras, N. Kernel principal component analysis for stochastic input model generation. *Journal of Computational Physics*, 230(19):7311 – 7331, 2011.

[NB14] Nouira, H. and Bourdet, P. Evaluation of roundness error using a new method based on a small displacement screw. *Measurement Science and Technology*, 25(4):044012, 2014.

[NBK80] Nagel, R. N.; Braithwaite, W. W.; and Kennicott, P. R. Initial Graphics Exchange Specification IGES Version 1.0. Technical Report NBSIR 80-1978, National Bureau of Standards, Washington D.C., 1980.

[Nic99] Nickolaisen, R. H. Dimensional Management. In Drake, P. J., editor, *Dimensioning and Tolerancing Handbook*. McGraw-Hill Book Company, New York, 1999.

[Nie03] Nielsen, H. S. Specifications, Operators and Uncertainties. In Wilhelm, R. G., editor, *Proceedings of the 8th CIRP International Seminar on Computer Aided Tolerancing – Managing Geometric Uncertainty in the Product Lifecycle*, pages 1–6, 2003.

[Nie06] Nielsen, H. S. New concepts in specifications, operators and uncertainties and their impact on measurement and instrumentation. *Measurement Science and Technology*, 17(3):541–544, 2006.

[Nie12] Nielsen, H. S. Vision of the international GPS-Standards. In Michael Dietzsch, S. G., editor, *Proceedings of the XIII. Internationales Oberflächenkolloquium*, pages 1–14, 2012.

[Nie13] Nielsen, H. S. Recent developments in International Organization for Standardization geometrical product specification standards and strategic plans for future work. *Proceedings of the Institution of Mechanical Engineers, Part B: Journal of Engineering Manufacture*, 227(5):643–649, 2013.

[NLS07] Niu, J.; Li, Z.; and Salvendy, G. *Digital Human Modeling: First International Conference on Digital Human Modeling, ICDHM 2007, Held as Part of HCI International 2007, Beijing, China, July 22-27, 2007. Proceedings*, chapter Mathematical Methods for Shape Analysis and form Comparison in 3D Anthropometry: A Literature Review, pages 161–170. Springer Berlin Heidelberg, 2007.

[NO98] Ngoi, B. and Ong, C. Product and process dimensioning and tolerancing techniques. A state-of-the-art review. *The International Journal of Advanced Manufacturing Technology*, 14(12):910–917, 1998.

[NRFK14] Nelaturi, S.; Rangarajan, A.; Fritz, C.; and Kurtoglu, T. Automated fixture configuration for rapid manufacturing planning. *Computer-Aided Design*, 46:160 – 169, 2014.

[NT95] Nigam, S. D. and Turner, J. U. Review of statistical approaches to tolerance analysis. *Computer-Aided Design*, 27(1):6 – 15, 1995.

[OBB01] Ohtake, Y.; Belyaev, A.; and Bogaevski, I. Mesh regularization and adaptive smoothing. *Computer-Aided Design*, 33(11):789 – 800, 2001.

[OBJ05] Ostrovsky-Berman, Y. and Joskowicz, L. Tolerance envelopes of planar mechanical parts with parametric tolerances. *Computer-Aided Design*, 37(5):531 – 544, 2005.

[OBJ06] Ostrovsky-Berman, Y. and Joskowicz, L. Relative Position Computation for Assembly Planning With Planar Toleranced Parts. *The International Journal of Robotics Research*, 25(2):147–170, 2006.

[OBJ07] Ostrovsky-Berman, Y. and Joskowicz, L. Relative Positioning of Planar Parts in Toleranced Assemblies. In Davidson, J., editor, *Models for Computer Aided Tolerancing in Design and Manufacturing*, pages 65–74. Springer Netherlands, 2007.

[ORE+14] Okholm, A. B.; Rask, M.; Ebro, M.; Eifler, T.; Holmberg, M.; and Howard, T. J. Improving Process Capability Database Usage for Robust Design Engineering by Generalising Measurement Data. In Marjanovic, D.; Storga, M.; Pavkovic, N.; and Bojcetic, N., editors, *Proceedings of the 13th International Design Conference DESIGN 2014, Dubrovnik*, 2014.

[PA15] Pierre, L. and Anselmetti, B. Comparison of Analysis Line and Polytopes Methods to Determine the Result of a Tolerance Chain. *Journal of Computing and Information Science in Engineering*, 15(2):021007, 2015.

[Pag14] Pagano, C. Positioning. In Laperrière, L. and Reinhart, G., editors, *CIRP Encyclopedia of Production Engineering*, pages 962–968. Springer Berlin Heidelberg, 2014.

[PBS13] Plischke, E.; Borgonovo, E.; and Smith, C. L. Global sensitivity measures from given data. *European Journal of Operational Research*, 226(3):536 – 550, 2013.

[PCV05] Parenti-Castelli, V. and Venanzi, S. Clearance influence analysis on mechanisms. *Mechanism and Machine Theory*, 40(12):1316 – 1329, 2005.

[PE94] Pimmler, T. U. and Eppinger, S. D. Integration Analysis of Product Decompositions. In *Proceedings of the ASME Design Theory and Methodology Conference*, pages 343–351, 1994.

[Pet70] Peters, J. Tolerancing the Components of an Assembly for Minimum Cost. *Journal of Engineering for Industry*, 92(3):677–682, 1970.

[PG02] Prisco, U. and Giorleo, G. Overview of current CAT systems. *Integrated Computer-Aided Engineering*, 9:373–387, 2002.

[PG03] Pairel, E. and Giordano, M. A Formal Dimensioning and Tolerancing Model: The Linked Tolerance Zones. In Wilhelm, R. G., editor, *Proceedings of the 8th CIRP International Seminar on Computer Aided Tolerancing – Managing Geometric Uncertainty in the Product Lifecycle*, pages 80–91, 2003.

[PGK02] Pauly, M.; Gross, M.; and Kobbelt, L. Efficient simplification of point-sampled surfaces. In *IEEE Visualization VIS 2002, Boston, MA, USA*, pages 163–170, 2002.

[Pha89] Phadke, M. S. *Quality Engineering Using Robust Design.* Prentice Hall, Englewood Cliffs, NJ, 1989.

[PJH+14] Plowucha, W.; Jakubiec, W.; Humienny, Z.; Hausotte, T.; Savio, E.; Dragomir, M.; Bills, P.; Marxer, M.; Wisla, N.; and Mathieu, L. Geometrical Product Specification and Verification as toolbox to meet up-to-date technical requirements. In *Proceedings of the 11th International Scientific Conference "COORDINATE MEASURING TECHNIQUE" CMT2014, Bielsko-Biala*, pages 131–139, 2014.

[PK06] Pearn, W. L. and Kotz, S. *Encyclopedia and Handbook of Process Capability Indices*, volume 12 of *Series on Quality, Reliability and Engineering Statistics*. World Scientific Publishing Company, 2006.

[PKG03] Pauly, M.; Keiser, R.; and Gross, M. Multi-scale Feature Extraction on Point-Sampled Surfaces. *Computer Graphics Forum*, 22(3):281–289, 2003.

[PL97] Park, S. and Lee, K. Mathematical Foundation for Representing Propagation of Geometric Tolerances. In *Proceedings of the Fourth ACM Symposium on Solid Modeling and Applications*, pages 240–247, 1997.

[PLH02] Pottmann, H.; Leopoldseder, S.; and Hofer, M. Simultaneous registration of multiple views of a 3D object. In *Intl. Archives of the Photogrammetry, Remote Sensing and Spatial Information Sciences, Vol. XXXIV, Part 3A, Commission III*, pages 265–270, 2002.

[PLH04] Pottmann, H.; Leopoldseder, S.; and Hofer, M. Registration Without ICP. *Computer Vision and Image Understanding*, 95(1):54–71, 2004.

[PLH+05] Pottmann, H.; Leopoldseder, S.; Hofer, M.; Steiner, T.; and Wang, W. Industrial geometry: recent advances and applications in CAD. *Computer-Aided Design*, 37(7):751 – 766, 2005.

[Pli10] Plischke, E. An effective algorithm for computing global sensitivity indices (EASI). *Reliability Engineering & System Safety*, 95(4):354 – 360, 2010.

[PM15a] Polini, W. and Marziale, M. To model bolted parts for tolerance analysis using variational model. *International Journal of Engineering & Technology*, 4(1):139–148, 2015.

[PM15b] Polini, W. and Moroni, G. Manufacturing Signature for Tolerance Analysis. *Journal of Computing and Information Science in Engineering*, 15(2):021005, 2015.

[Pol11] Polini, W. Geometric Tolerance Analysis. In Colosimo, B. M. and Senin, N., editors, *Geometric Tolerances*, pages 39–68. Springer London, 2011.

[Pol12] Polini, W. Taxonomy of models for tolerance analysis in assembling. *International Journal of Production Research*, 50(7):2014–2029, 2012.

[Pol14] Polini, W. To model joints with clearance for tolerance analysis. *Proceedings of the Institution of Mechanical Engineers, Part B: Journal of Engineering Manufacture*, 228(12):1689–1700, 2014.

[PPA15] Petitcuenot, M.; Pierre, L.; and Anselmetti, B. ISO Specifications of Complex Surfaces: Application on Aerodynamic Profiles. *Procedia CIRP – 13th CIRP Conference on Computer-Aided Tolerancing*, 27:16 – 22, 2015.

[PPC04] Pearce, E.; Parkinson, A.; and Chase, K. Tolerance analysis and design of nesting forces for exactly constrained mechanical assemblies. *Research in Engineering Design*, 15(3):182–191, 2004.

[PR07a] Pierce, R. S. and Rosen, D. A Method for Integrating Form Errors Into Geometric Tolerance Analysis. *Journal of Mechanical Design*, 130(1):011002, 2007.

[PR07b] Pierce, R. S. and Rosen, D. Simulation of Mating Between Nonanalytic Surfaces Using a Mathematical Programing Formulation. *Journal of Computing and Information Science in Engineering*, 7(4):314–321, 2007.

[PRA07] Prabhaharan, G.; Ramesh, R.; and Asokan, P. Concurrent optimization of assembly tolerances for quality with position control using scatter search approach. *International Journal of Production Research*, 45(21):4959–4988, 2007.

[PS10] Pfeifer, T. and Schmitt, R. *Fertigungsmesstechnik*. Oldenbourg Verlag München, 2010.

[PSW15] Pianosi, F.; Sarrazin, F.; and Wagener, T. A Matlab toolbox for Global Sensitivity Analysis. *Environmental Modelling & Software*, 70:80 – 85, 2015.

[PTN09a] Pierre, L.; Teissandier, D.; and Nadeau, J. P. Integration of multiple physical behaviours into a geometric tolerancing approach. In Giordano, M.; Villeneuve, F.; and Mathieu, L., editors, *Proceedings of the 11th CIRP International Conference on Computer Aided Tolerancing, Annecy*, 2009.

[PTN09b] Pierre, L.; Teissandier, D.; and Nadeau, J. P. Integration of thermomechanical strains into tolerancing analysis. *International Journal on Interactive Design and Manufacturing*, 3(4):247–263, 2009.

[PTN14] Pierre, L.; Teissandier, D.; and Nadeau, J. P. Variational tolerancing analysis taking thermo-mechanical strains into account: Application to a high pressure turbine. *Mechanism and Machine Theory*, 74:82 – 101, 2014.

[PW10] Poniatowska, M. and Werner, A. Fitting Spatial Models of Geometric Deviations of Free-Form Surfaces determined in Coordinate Measurements. *Metrology and Measurement Systems*, 17(4):599–610, 2010.

[PW15] Pianosi, F. and Wagener, T. A simple and efficient method for global sensitivity analysis based on cumulative distribution functions. *Environmental Modelling & Software*, 67:1 – 11, 2015.

[PWW08] Penzkofer, F.; Wittmann, S.; and Winter, M. Visual Analysis Methods for non-ideal Assemblies. In Marjanovic, D.; Storga, M.; Pavkovic, N.; and Bojcetic, N., editors, *Proceedings of the 10th International Design Conference DESIGN 2008, Dubrovnik*, 2008.

[QDS+12] Qureshi, A. J.; Dantan, J.-Y.; Sabri, V.; Beaucaire, P.; and Gayton, N. A statistical tolerance analysis approach for over-constrained mechanism based on optimization and Monte Carlo simulation. *Computer-Aided Design*, 44(2):132 – 142, 2012.

[QKFS13] Quattelbaum, B.; Knispel, J.; Falk, B.; and Schmitt, R. Tolerancing subjective and uncertain customer requirements regarding perceived product quality. *Proceedings of the Institution of Mechanical Engineers, Part B: Journal of Engineering Manufacture*, 227(5):702–708, 2013.

[QLMW16] Qu, X.; Li, X.; Ma, Q.; and Wang, X. Variation propagation modeling for locating datum system design in multi-station assembly processes. *The International Journal of Advanced Manufacturing Technology*, pages 1–10, 2016.

[QRP+10] Quintana, V.; Rivest, L.; Pellerin, R.; Venne, F.; and Kheddouci, F. Will Model-based Definition replace engineering drawings throughout the product lifecycle? A global perspective from aerospace industry. *Computers in Industry*, 61(5):497 – 508, 2010.

[QSJL14] Qi, Q.; Scott, P. J.; Jiang, X.; and Lu, W. Design and implementation of an integrated surface texture information system for design, manufacture and measurement. *Computer-Aided Design*, 57:41 – 53, 2014.

[RA96] Rhee, J. and Akay, A. Dynamic response of a revolute joint with clearance. *Mechanism and Machine Theory*, 31(1):121 – 134, 1996.

[RA10] Ramaswami, H. and Anand, S. Accurate size evaluation of cylindrical components. *The International Journal of Advanced Manufacturing Technology*, 49(9-12):1079–1092, 2010.

[RA16] Royer, M. and Anselmetti, B. 3D manufacturing tolerancing with probing of a local work coordinate system. *The International Journal of Advanced Manufacturing Technology*, 84(9):2151 – 2165, 2016.

[RABL11] Rossi, A.; Antonetti, M.; Barloscio, M.; and Lanzetta, M. Fast genetic algorithm for roundness evaluation by the minimum zone tolerance (MZT) method. *Measurement*, 44(7):1243 – 1252, 2011.

[Req80] Requicha, A. A. G. Representations for Rigid Solids: Theory, Methods, and Systems. *Computing Surveys*, 12(4):437–464, 1980.

[Req83] Requicha, A. A. G. Toward a Theory of Geometric Tolerancing. *The International Journal of Robotics Research*, 2(45):45–60, 1983.

[RFM94] Rivest, L.; Fortin, C.; and Morel, C. Tolerancing a solid model with a kinematic formulation. *Computer-Aided Design*, 26(6):465 – 476, 1994.

[RH05] Rong, Y. and Huang, S. H. *Advanced Computer-Aided Fixture Design.* Academic Press, 2005.

[RHK+01] Rong, Y.; Hu, W.; Kang, Y.; Zhang, Y.; and Yen, D. W. Locating error analysis and tolerance assignment for computer-aided fixture design. *International Journal of Production Research*, 39(15):3529–3545, 2001.

[RHSD14] Rao, S. S.; Haghighi, P.; Shah, J. J.; and Davidson, J. K. Library of T-Maps for Dimensional and Geometric Tolerances. In ASME, editor, *Proceedings of the ASME 2014 International Design En-*

gineering Technical Conferences and Computers and Information in Engineering Conference, Buffalo, New York*, volume 4, Paper no. DETC2014–35273, 2014.

[RL98] Roy, U. and Li, B. Representation and interpretation of geometric tolerances for polyhedral objects—I. Form tolerances. *Computer-Aided Design*, 30(2):151 – 161, 1998.

[RL99] Roy, U. and Li, B. Representation and interpretation of geometric tolerances for polyhedral objects. II.: Size, orientation and position tolerances. *Computer-Aided Design*, 31(4):273 – 285, 1999.

[RL01] Rusinkiewicz, S. and Levoy, M. Efficient variants of the ICP algorithm. In *Proceedings of the Third International Conference on 3-D Digital Imaging and Modeling, Quebec City*, pages 145–152, 2001.

[RLW91] Roy, U.; Liu, C.; and Woo, T. Review of dimensioning and tolerancing: representation and processing. *Computer-Aided Design*, 23(7):466 – 483, 1991.

[Röd15] Rödel, P. Statistische Toleranzanalyse bei Wälzlagern – Grenzen statistischer Verteilungsmodelle und Vorschläge zur Erweiterung. In Wartzack, S., editor, *Summer School Toleranzmanagement – Beiträge zur 2. Summer School September 2015*, pages 20–25. Druck+Verlag Ernst Vögel GmbH Stamsried, 2015.

[Ros60] Ross, D. T. Computer-Aided Design: A Statement of Objectives. Technical Memorandum 8436-TM-4, Electronic Systems Laboratory, Massachusetts Institute of Technology, 1960.

[Roy95] Roy, U. Computational methodologies for evaluating form and positional tolerances in a computer integrated manufacturing system. *The International Journal of Advanced Manufacturing Technology*, 10(2):110–117, 1995.

[RPS+01] Roy, U.; Pramanik, N.; Sudarsan, R.; Sriram, R.; and Lyons, K. Function-to-form mapping: model, representation and applications in design synthesis. *Computer-Aided Design*, 33(10):699 – 719, 2001.

[RR86] Rossignac, J. R. and Requicha, A. A. G. Offsetting operations in solid modelling. *Computer Aided Geometric Design*, 3:129–148, 1986.

[RSBMG+13] Ricci, F.; Sauza Bedolla, J.; Martinez Gomez, J.; Ruffa, S.; Maddis, M.; and Chiabert, P. A Case Study on the Integration of GPS Concepts in a PLM Based Industrial Context. In Bernard, A.; Rivest, L.; and Dutta, D., editors, *Product Lifecycle Management for Society: Proceedings of the 10th IFIP WG 5.1 International Conference, PLM 2013, Nantes, France, July 6-10, 2013*, pages 336–345. Springer Berlin Heidelberg, 2013.

[RT02] RUE, H. and TJELMELAND, H. Fitting Gaussian Markov Random Fields to Gaussian Fields. *Scandinavian Journal of Statistics*, 29(1):31–49, 2002.

[RV83] Requicha, A. A. G. and Voelcker, H. B. Solid modeling: current status and research directions. *IEEE Computer Graphics and Applications*, 3(7):25–37, 1983.

[SACS03] Shiu, B. W.; Apley, D. W.; Ceglarek, D.; and Shi, J. Tolerance allocation for compliant beam structure assemblies. *IIE Transactions*, 35(4):329–342, 2003.

[SAFP09] Samper, S.; Adragna, P.-A.; Favreliere, H.; and Pillet, M. Modeling of 2D and 3D Assemblies Taking Into Account Form Errors of Plane Surfaces. *Journal of Computing and Information Science in Engineering*, 9(4):041005, 2009.

[Sal02] Saltelli, A. Sensitivity Analysis for Importance Assessment. *Risk Analysis*, 22(3):579–590, 2002.

[SAMW14] Schleich, B.; Anwer, N.; Mathieu, L.; and Wartzack, S. Skin Model Shapes: A new paradigm shift for geometric variations modelling in mechanical engineering. *Computer-Aided Design*, 50:1 – 15, 2014.

[SAMW15] Schleich, B.; Anwer, N.; Mathieu, L.; and Wartzack, S. Contact and Mobility Simulation for Mechanical Assemblies Based on Skin Model Shapes. *Journal of Computing and Information Science in Engineering*, 15(2):021009, 2015.

[SAMW16] Schleich, B.; Anwer, N.; Mathieu, L.; and Wartzack, S. Status and Prospects of Skin Model Shapes for Geometric Variations Management. *Procedia CIRP – 14th CIRP Conference on Computer Aided Tolerancing*, 43:154 – 159, 2016.

[San99] Sanderson, A. Assemblability based on maximum likelihood configuration of tolerances. *IEEE Transactions on Robotics and Automation*, 15(3):568–572, 1999.

[SASD05] Shen, Z.; Ameta, G.; Shah, J. J.; and Davidson, J. K. A Comparative Study Of Tolerance Analysis Methods. *Journal of Computing and Information Science in Engineering*, 5(3):247–256, 2005.

[SASD07] Shah, J. J.; Ameta, G.; Shen, Z.; and Davidson, J. Navigating the Tolerance Analysis Maze. *Computer-Aided Design and Applications*, 4(5):705–718, 2007.

[SAZ+14] Schleich, B.; Anwer, N.; Zhu, Z.; Qiao, L.; Mathieu, L.; and Wartzack, S. A Comparative Study on Tolerance Analysis Approaches. In Howard, T. J. and Eifler, T., editors, *Proceedings of the International Symposium on Robust Design – ISoRD14, Copenhagen, Denmark*, pages 29–39, 2014.

[SBD11] Sahoo, P.; Barman, T.; and Davim, J. P. *Fractal Analysis in Machining*, volume 3 of *SpringerBriefs in Applied Sciences and Technology*. Springer Berlin Heidelberg, 2011.

[SBF+10] Sergent, A.; Bui, M.-H.; Favreliere, H.; Duret, D.; Samper, S.; and Villeneuve, F. Identification of machining defects by Small Displacement Torsor and form parameterization method. In *Proceedings of IDMME – Virtual Concept 2010, Bordeaux*, 2010.

[SBR11a] Sivakumar, K.; Balamurugan, C.; and Ramabalan, S. Concurrent multi-objective tolerance allocation of mechanical assemblies considering alternative manufacturing process selection. *The International Journal of Advanced Manufacturing Technology*, 53(5-8):711–732, 2011.

[SBR11b] Sivakumar, K.; Balamurugan, C.; and Ramabalan, S. Simultaneous optimal selection of design and manufacturing tolerances with alternative manufacturing process selection. *Computer-Aided Design*, 43(2):207 – 218, 2011.

[SC86] Smith, R. C. and Cheeseman, P. On the Representation and Estimation of Spatial Uncertainty. *The International Journal of Robotics Research*, 5(4):56–68, 1986.

[SC04] Shakarji, C. and Clement, A. Reference Algorithms for Chebyshev and One-Sided Data Fitting for Coordinate Metrology. *CIRP Annals - Manufacturing Technology*, 53(1):439 – 442, 2004.

[Sch95] Scholz, F. Tolerance Stack Analysis Methods. Technical report, Research and Technology Boeing Information & Support Services, Seattle, 1995.

[SCT+12] Stricher, A.; Champaney, L.; Thiébaut, F.; Fricero, B.; and Chevassus, N. Tolerance Analysis of Compliant Assemblies Using FEM Simulations and Modal Description of Shape Defects. In ASME, editor, *Proceedings of the ASME 2012 11th Biennial Conference on Engineering Systems Design and Analysis, Nantes*, number ESDA2012-83002, pages 307–314, 2012.

[SDP95] Sfantsikopoulos, M.; Diplaris, S.; and Papazoglou, P. Concurrent dimensioning for accuracy and cost. *The International Journal of Advanced Manufacturing Technology*, 10(4):263–268, 1995.

[SF06] Samper, S. and Formosa, F. Form Defects Tolerancing by Natural Modes Analysis. *Journal of Computing and Information Science in Engineering*, 7(1):44–51, 2006.

[SF12] Scott, P. J. and Forbes, A. B. Mathematics for modern precision engineering. *Philosophical Transactions of the Royal Society of London A: Mathematical, Physical and Engineering Sciences*, 370(1973):4066–4088, 2012.

[SG98] Samper, S. and Giordano, M. Taking into account elastic displacements in 3D tolerancing: Models and application. *Journal of Materials Processing Technology*, 78(1–3):156 – 162, 1998.

[SG02] Stegmann, M. B. and Gomez, D. D. A Brief Introduction to Statistical Shape Analysis. Lecture Notes, Informatics and Mathematical Modelling, Technical University of Denmark, 2002.

[Sha91] Shah, J. Conceptual development of form features and feature modelers. *Research in Engineering Design*, 2(2):93–108, 1991.

[SHB+02] Summerhays, K. D.; Henke, R. P.; Baldwin, J. M.; Cassou, R. M.; and Brown, C. W. Optimizing discrete point sample patterns and measurement data analysis on internal cylindrical surfaces with systematic form deviations. *Precision Engineering*, 26(1):105 – 121, 2002.

[She30] Shewart, W. A. Economic Quality Control of Manufactured Product. *Bell System Technical Journal*, 9(2):364–389, 1930.

[She31] Shewart, W. A. *Economic Control of Quality of Manufactured Product*. D. van Nostrand Company, New York, 1931.

[She39] Shewart, W. A. *Statistical Method from the Viewpoint of Quality Control*. Graduate School of Agriculture, Washington, 1939.

[SHP+96] Salomons, O.; Haalboom, F.; Poerink, H.; van Slooten, F.; van Houten, F.; and Kals, H. A computer aided tolerancing tool II: Tolerance analysis. *Computers in Industry*, 31(2):175 – 186, 1996.

[Sim07] Simon, V. Computer simulation of tooth contact analysis of mismatched spiral bevel gears. *Mechanism and Machine Theory*, 42(3):365 – 381, 2007.

[SJ97] Sacks, E. and Joskowicz, L. Parametric kinematic tolerance analysis of planar mechanisms. *Computer-Aided Design*, 29(5):333 – 342, 1997.

[SJ98a] Sacks, E. and Joskowicz, L. Parametric kinematic tolerance analysis of general planar systems. *Computer-Aided Design*, 30(9):707 – 714, 1998.

[SJ98b] Sacks, E. and Joskowicz, L. Parametric Kinematic Tolerance Analysis of Planar Mechanisms. In ElMaraghy, H. A., editor, *Geometric Design Tolerancing: Theories, Standards and Applications*, pages 308–324. Springer US, 1998.

[SJ99] Söderberg, R. and Johannesson, H. Tolerance Chain Detection by Geometrical Constraint Based Coupling Analysis. *Journal of Engineering Design*, 10(1):5–24, 1999.

[SJJ05] Singh, P. K.; Jain, S. C.; and Jain, P. K. Advanced optimal tolerance design of mechanical assemblies with interrelated dimension chains and process precision limits. *Computers in Industry*, 56(2):179 – 194, 2005.

[SK00] Sudret, B. and Kiureghian, A. D. Stochastic Finite Element Methods and Reliability: A State-of-the-Art Report. Technical Report UCB/SEMM2000/08, Department of Civil & Environmental Engineering, University of California, Berkeley, 2000.

[SKC10] Shin, S.; Kongsuwon, P.; and Cho, B. R. Development of the parametric tolerance modeling and optimization schemes and cost-effective solutions. *European Journal of Operational Research*, 207(3):1728 – 1741, 2010.

[SKH+08] Schwenke, H.; Knapp, W.; Haitjema, H.; Weckenmann, A.; Schmitt, R.; and Delbressine, F. Geometric error measurement and compensation of machines—An update. *CIRP Annals - Manufacturing Technology*, 57(2):660 – 675, 2008.

[SL99] Söderberg, R. and Lindkvist, L. Computer Aided Assembly Robustness Evaluation. *Journal of Engineering Design*, 10(2):165–181, 1999.

[SL02] Söderberg, R. and Lindkvist, L. Stability and seam variation analysis for automotive body design. *Journal of Engineering Design*, 13(2):173–187, 2002.

[SL03] Söderberg, R. and Lindkvist, L. Automated Seam Variation and Stability Analysis for Automotive Body Design. In Bourdet, P. and Mathieu, L., editors, *Geometric Product Specification and Verification: Integration of Functionality*, pages 255–264. Springer Netherlands, Dordrecht, 2003.

[Sla16] Sladek, J. A. *Coordinate Metrology : Accuracy of Systems and Measurements*, chapter Introduction, pages 1–13. Springer Berlin Heidelberg, 2016.

[SLC06a] Söderberg, R.; Lindkvist, L.; and Carlson, J. S. Managing physical dependencies through location system design. *Journal of Engineering Design*, 17(4):325–346, 2006.

[SLC06b] Söderberg, R.; Lindkvist, L.; and Carlson, J. S. Virtual Geometry Assurance for effective Product Realization. In *Proceedings of the 1st Nordic Conference on Product Lifecycle Management NordPLM, Göteborg*, 2006.

[SLD06] Söderberg, R.; Lindkvist, L.; and Dahlström, S. Computer-aided robustness analysis for compliant assemblies. *Journal of Engineering Design*, 17(5):411–428, 2006.

[SLMW10] Stoll, T.; Lauks, C.; Meerkamm, H.; and Wartzack, S. Calculating the Impact of Form Variations on the Position of Parts. In Dagman, A. and Söderberg, R., editors, *Proceedings of NordDesign 2010, the 8th International NordDesign Conference, Göteborg, Sweden, 25.-27.08.2010*, pages 539–548, 2010.

[SM09] Stuppy, J. and Meerkamm, H. Tolerance analysis of a crank mechanism by taking into account different kinds of deviation. In Giordano, M.; Villeneuve, F.; and Mathieu, L., editors, *Proceedings of the 11th CIRP International Conference on Computer Aided Tolerancing, Annecy*, 2009.

[SM16] Šibalija, T. V. and Majstorović, V. D. *Advanced Multiresponse Process Optimisation – An Intelligent and Integrated Approach.* Springer International Publishing, 2016.

[Smi97] Smith, R. The historical roots of concurrent engineering fundamentals. *IEEE Transactions on Engineering Management*, 44(1):67–78, 1997.

[SMM02] Schwab, A.; Meijaard, J.; and Meijers, P. A comparison of revolute joint clearance models in the dynamic analysis of rigid and elastic mechanical systems. *Mechanism and Machine Theory*, 37(9):895 – 913, 2002.

[SMW09] Stoll, T.; Meerkamm, H.; and Wartzack, S. Simulation möglicher nicht-idealer Fugenmaße in der Virtual Reality. *Zeitschrift für wirtschaftlichen Fabrikbetrieb ZWF*, 104(12):1167–1171, 2009.

[Sob01] Sobol, I. M. Global sensitivity indices for nonlinear mathematical models and their Monte Carlo estimates. *Mathematics and Computers in Simulation*, 55(1–3):271 – 280, 2001.

[Soh92] Sohlenius, G. Concurrent Engineering. *CIRP Annals - Manufacturing Technology*, 41(2):645 – 655, 1992.

[Spe72] Speckhart, F. H. Calculation of Tolerance Based on a Minimum Cost Approach. *Journal of Engineering for Industry*, 94(2):447–453, 1972.

[SPG07] Samper, S.; Petit, J.-P.; and Giordano, M. Elastic Clearance Domain and Use Rate Concept Applications to Ball Bearings and Gears. In Davidson, J., editor, *Models for Computer Aided Tolerancing in Design and Manufacturing*, pages 331–340. Springer Netherlands, 2007.

[SPH+96] Salomons, O.; Poerink, H.; Haalboom, F.; van Slooten, F.; van Houten, F.; and Kals, H. A computer aided tolerancing tool I: Tolerance specification. *Computers in Industry*, 31(2):161 – 174, 1996.

[SPL+15] Shen, W.; Pang, K.; Liu, C.; Ge, M.; Zhang, Y.; and Wang, X. The quality control method for remanufacturing assembly based on the Jacobian-torsor model. *The International Journal of Advanced Manufacturing Technology*, 81(1):253–261, 2015.

[Spo73] Spotts, M. F. Allocation of Tolerances to Minimize Cost of Assembly. *Journal of Engineering for Industry*, 95(3):762–764, 1973.

[SPP+02] Sun, Y.; Page, D.; Paik, J.; Koschan, A.; and Abidi, M. Triangle mesh-based edge detection and its application to surface segmentation and adaptive surface smoothing. In *Proceedings of the 2002 International Conference on Image Processing*, volume 3, pages 825–828, 2002.

[SR00] Sudarsan, R. and Roy, U. Information Models for Design Tolerancing: From Conceptual to the Detailed Design. Report NISTIR 6524, National Institute of Standards and Technology, Gaithersburg, MD, 2000.

[SRA+08] Saltelli, A.; Ratto, M.; Andres, T.; Campolongo, F.; Cariboni, J.; Gatelli, D.; Saisana, M.; and Tarantola, S. *Global Sensitivity Analysis: The Primer.* John Wiley & Sons, Inc., 2008.

[Sri91] Srinivasan, V. A Geometer grapples with Tolerancing Standards. In Weill, R., editor, *Proceedings of the CIRP Working Seminar on Computer-Aided Tolerancing, Penn State University*, pages 191–200, 1991.

[Sri94] Srinivasan, R. S. *A Theoretical Framework for Functional Form Tolerances in Design for Manufacturing.* PhD thesis, University of Texas, 1994.

[Sri99] Srinivasan, V. A geometrical product specification language based on a classification of symmetry groups. *Computer-Aided Design*, 31(11):659 – 668, 1999.

[Sri03] Srinivasan, V. An Integrated View of Geometrical Product Specification and Verification. In Bourdet, P. and Mathieu, L., editors, *Geometric Product Specification and Verification: Integration of Functionality*, pages 1–11. Springer Netherlands, 2003.

[Sri05] Srinivasan, V. Elements of Computational Metrology. In Janardan, R.; Smid, M.; and Dutta, D., editors, *Geometric and Algorithmic Aspects of Computer-Aided Design and Manufacturing*, volume 67 of *DIMACS Series in Discrete Mathematics and Theoretical Computer Science*, pages 79–116. American Mathematical Society, 2005.

[Sri06] Srinivasan, V. Computational Metrology for the Design and Manufacture of Product Geometry: A

Classification and Synthesis. *Journal of Computing and Information Science in Engineering*, 7(1):3–9, 2006.

[Sri08] Srinivasan, V. Standardizing the specification, verification, and exchange of product geometry: Research, status and trends. *Computer-Aided Design*, 40(7):738 – 749, 2008.

[Sri13] Srinivasan, V. Reflections on the role of science in the evolution of dimensioning and tolerancing standards. *Proceedings of the Institution of Mechanical Engineers, Part B: Journal of Engineering Manufacture*, 227(1):3–11, 2013.

[Sri15] Srinivasan, V. Geometrical Product Specification. In CIRP; Laperrière, L. and Reinhart, G., editors, *CIRP Encyclopedia of Production Engineering – Living Reference Work Entry*, doi:10.1007/978-3-642-35950-7_16757-1. Springer Berlin Heidelberg, 2015.

[SRR14] Sarigecili, M. I.; Roy, U.; and Rachuri, S. Interpreting the semantics of GD&T specifications of a product for tolerance analysis. *Computer-Aided Design*, 47:72 – 84, 2014.

[SRSB16] Sharma, G. V. S. S.; Rao, P. S.; and Surendra Babu, B. Process-based tolerance assessment of connecting rod machining process. *Journal of Industrial Engineering International*, 12(2):211 – 220, 2016.

[SRW99] Shan, A.; Roth, R. N.; and Wilson, R. J. A New Approach to Statistical Geometrical Tolerance Analysis. *The International Journal of Advanced Manufacturing Technology*, 15(3):222–230, 1999.

[SSM11] Srinivasan, V.; Shakarji, C. M.; and Morse, E. P. On the Enduring Appeal of Least-Squares Fitting in Computational Coordinate Metrology. *Journal of Computing and Information Science in Engineering*, 12(1):011008, 2011.

[SSW11] Stoll, T.; Stockinger, A.; and Wartzack, S. Geometric Manipulation Method for Evaluation of aesthetic Quality in early Design Phases. In Maier, A.; Mougaard, K.; Howard, T.; and McAloone, T., editors, *Proceedings of the 18th International Conference on Engineering Design ICED 11, Lyngby/Copenhagen*, 2011.

[Ste81] Steward, D. V. The design structure system: A method for managing the design of complex systems. *IEEE Transactions on Engineering Management*, EM-28(3):71–74, 1981.

[Sto06] Stoll, T. Generieren von nichtidealer Geometrie. In Meerkamm, H., editor, *Proceedings of the 17th Symposium on Design for X, Neukirchen/Erlangen*, 2006.

[Sto10] Stockinger, A. *Computer Aided Robust Design – Verknüpfung rechnerunterstützter Entwicklung und virtueller Fertigung als Baustein des Toleranzmanagements.* PhD thesis, Technische Fakultät der Friedrich-Alexander-Universität Erlangen-Nürnberg, 2010.

[Sto12] Stoll, T. *Einsatzmöglichkeiten von virtuellen, nichtidealen Prototypen in der Toleranzsynthese und -analyse.* PhD thesis, Technische Fakultät der Friedrich-Alexander-Universität Erlangen-Nürnberg, 2012.

[SvHK98] Salomons, O. W.; van Houten, F. J. A. M.; and Kals, H. J. J. Current Status of CAT Systems. In ElMaraghy, H. A., editor, *Geometric Design Tolerancing: Theories, Standards and Applications*, pages 438–452. Springer US, 1998.

[SW95] Srinivasan, R. S. and Wood, K. L. Geometric Tolerancing in Mechanical Design Using Fractal-Based Parameters. *Journal of Mechanical Design*, 117(1):203–206, 1995.

[SW97] Srinivasan, R. S. and Wood, K. L. A Form Tolerancing Theory Using Fractals and Wavelets. *Journal of Mechanical Design*, 119(2):185–193, 1997.

[SW13a] Schleich, B. and Wartzack, S. How to determine the influence of geometric deviations on elastic deformations and the structural performance? *Proceedings of the Institution of Mechanical Engineers, Part B: Journal of Engineering Manufacture*, 227(5):754–764, 2013.

[SW13b] Schleich, B. and Wartzack, S. Process-oriented Tolerancing – A Discrete Geometry Framework. In Lindemann, U.; Venkataraman, S.; Kim, Y.; and Lee, S., editors, *Proceedings of the 19th International Conference on Engineering Design ICED13, Seoul*, 2013.

[SW14] Schleich, B. and Wartzack, S. A discrete geometry approach for tolerance analysis of mechanism. *Mechanism and Machine Theory*, 77:148 – 163, 2014.

[SW15a] Schleich, B. and Wartzack, S. Approaches for the assembly simulation of skin model shapes. *Computer-Aided Design*, 65:18 – 33, 2015.

[SW15b] Schleich, B. and Wartzack, S. Evaluation of geometric tolerances and generation of variational part representatives for tolerance analysis. *The International Journal of Advanced Manufacturing Technology*, 79(5-8):959–983, 2015.

[SW15c] Schleich, B. and Wartzack, S. A generic Approach to Sensitivity Analysis in Geometric Variations Management. In Weber, C.; Husung, S.; Cantamessa, M.; Cascini, G.; Marjanovic, D.; and Graziosi, S., editors, *Proceedings of the 20th International Conference on Engineering Design ICED15 Vol. 4: Design for X, Design to X, Milan*, pages 343–352, 2015.

[SW15d] Schleich, B. and Wartzack, S. Tolerance Analysis of Rotating Mechanism Based on Skin Model Shapes in Discrete Geometry. *Procedia CIRP – 13th CIRP Conference on Computer-Aided Tolerancing*, 27:10 – 15, 2015.

[SW16] Schleich, B. and Wartzack, S. A Quantitative Comparison of Tolerance Analysis Approaches for Rigid Mechanical Assemblies. *Procedia CIRP – 14th CIRP Conference on Computer-Aided Tolerancing*, 43:172 – 177, 2016.

[SWHP07] Stoll, T.; Wittmann, S.; Helwig, S.; and Paetzold, K. Registration of measured and simulated non-ideal geometry using optimization methods. In Weckenmann, A., editor, *Proceedings of the 10th CIRP International Seminar on Computer Aided Tolerancing, Erlangen*, 2007.

[SWM96] Srinivasan, R. S.; Wood, K. L.; and McAdams, D. A. Functional tolerancing: A design for manufacturing methodology. *Research in Engineering Design*, 8(2):99–115, 1996.

[SWM09] Stoll, T.; Wittmann, S.; and Meerkamm, H. Tolerance Analysis with detailed Part Modeling including Shape Deviations. In Giordano, M.; Villeneuve, F.; and Mathieu, L., editors, *Proceedings of the 11th CIRP International Conference on Computer Aided Tolerancing, Annecy*, 2009.

[SWM+10a] Stockinger, A.; Wittmann, S.; Martinek, M.; Meerkamm, H.; and Wartzack, S. Virtual Assembly Analysis: Standard Tolerance Analysis compared to Manufacturing Simulation and Relative Positioning. In Marjanovic, D.; Storga, M.; Pavkovic, N.; and Bojcetic, N., editors, *Proceedings of the 11th International Design Conference DESIGN 2010, Dubrovnik*, 2010.

[SWM10b] Stoll, T.; Wittmann, S.; and Meerkamm, H. Tolerance Analysis with detailed Part Modeling. In Giordano, M.; Mathieu, L.; and Villeneuve, F., editors, *Product Lifecycle Management: Geometric Variations*, pages 231–243. John Wiley & Sons, Inc., 2010.

[SWW+12] Schleich, B.; Walter, M.; Wartzack, S.; Anwer, N.; and Mathieu, L. A Comprehensive Framework for Skin Model Simulation. In ASME, editor, *Proceedings of the ASME 2012 11th Biennial Conference on Engineering Systems Design and Analysis, Nantes*, number ESDA2012-82204, pages 567–576, 2012.

[Swy01] Swyt, D. A. Length and Dimensional Measurements at NIST. *Journal of the Research of the National Institute of Standards and Technology*, 106(1):1–23, 2001.

[SZ12] Sui, W. and Zhang, D. Four Methods for Roundness Evaluation. *Physics Procedia*, 24(Part C):2159 – 2164, 2012.

[SZCZ08] Schmitz, T. L.; Ziegert, J. C.; Canning, J. S.; and Zapata, R. Case study: A comparison of error sources in high-speed milling. *Precision Engineering*, 32(2):126 – 133, 2008.

[Tag86] Taguchi, G. *Introduction to Quality Engineering: Designing Quality into Products and Processes*. Asian Productivity Organization, Tokyo, 1986.

[Tan83] Taniguchi, N. Current Status in, and Future Trends of, Ultraprecision Machining and Ultrafine Materials Processing. *CIRP Annals - Manufacturing Technology*, 32(2):573 – 582, 1983.

[Tau95] Taubin, G. A Signal Processing Approach to Fair Surface Design. In *Proceedings of the 22Nd Annual Conference on Computer Graphics and Interactive Techniques*, SIGGRAPH '95, pages 351–358, 1995.

[TC12] Tahan, A. S. and Cauvier, J. Capability Estimation of Geometrical Tolerance With a Material Modifier by a Hasofer–Lind Index. *Journal of Manufacturing Science and Engineering*, 134(2):021007, 2012.

[TCD99] Teissandier, D.; Couetard, Y.; and Delos, V. Operations on polytopes: application to tolerance analysis. In van Houten, F. and Kals, H., editors, *Global Consistency of Tolerances*, pages 425–434. Springer Netherlands, 1999.

[TCG14] Tannous, M.; Caro, S.; and Goldsztejn, A. Sensitivity analysis of parallel manipulators using an interval linearization method. *Mechanism and Machine Theory*, 71:93 – 114, 2014.

[TD11] Teissandier, D. and Delos, V. Algorithm to calculate the Minkowski sums of 3-polytopes based on normal fans. *Computer-Aided Design*, 43(12):1567 – 1576, 2011.

[TD13] Tönshoff, H. and Denkena, B. Surface and Subsurface Properties. In *Basics of Cutting and Abrasive Processes*, Lecture Notes in Production Engineering, pages 349–370. Springer Berlin Heidelberg, 2013.

[TDE00] Thornton, A. C.; Donnelly, S.; and Ertan, B. More than Just Robust Design: Why Product Development Organizations Still Contend with Variation and its Impact on Quality. *Research in Engineering Design*, 12(3):127–143, 2000.

[TF00] Thomke, S. and Fujimoto, T. The effect of "front-loading" problem-solving on product development performance. *Journal of Product Innovation Management*, 17(2):128 – 142, 2000.

[Tho98] Thomke, S. H. Simulation, learning and R&D performance: Evidence from automotive development. *Research Policy*, 27(1):55 – 74, 1998.

[Tho99a] Thornton, A. C. Variation Risk Management Using Modeling and Simulation. *Journal of Mechanical Design*, 121(2):297–304, 1999.

[Tho99b] Thornton, A. C. A Mathematical Framework for the Key Characteristic Process. *Research in Engineering Design*, 11(3):145–157, 1999.

[TL04] Tsai, M.-J. and Lai, T.-H. Kinematic sensitivity analysis of linkage with joint clearance based on transmission quality. *Mechanism and Machine Theory*, 39(11):1189 – 1206, 2004.

[TL09] Tahan, S.-A. and Levesque, S. Exploiting the process capability of position geometric tolerance according GD&T ASME Y14.5M. In *International Conference on Computers Industrial Engineering, CIE 2009, Troyes*, pages 1267–1272, 2009.

[TT04] Tseng, R.-T. and Tsay, C.-B. Contact characteristics of cylindrical gears with curvilinear shaped teeth. *Mechanism and Machine Theory*, 39(9):905 – 919, 2004.

[TT05] Tseng, J.-T. and Tsay, C.-B. Undercutting and Contact Characteristics of Cylindrical Gears With Curvilinear Shaped Teeth Generated by Hobbing. *Journal of Mechanical Design*, 128(3):634–643, 2005.

[Tur88] Turner, J. New methods for tolerance analysis in solid modeling. In *International Conference on Computer Integrated Manufacturing, Troy*, pages 306–314, 1988.

[Tur93] Turner, J. Current Tolerancing Packages. In Srinivasan, V. and Voelcker, H. B., editors, *Proceedings of the 1993 International Forum on Dimensional Tolerancing and Metrology, Dearborn, Michigan*, volume CRTD-Vol. 27, pages 241–248. ASME, 1993.

[TW87] Turner, J. and Wozny, M. Tolerances in computer-aided geometric design. *The Visual Computer*, 3(4):214–226, 1987.

[TZW00] Ting, K.-L.; Zhu, J.; and Watkins, D. The effects of joint clearance on position and orientation deviation of linkages and manipulators. *Mechanism and Machine Theory*, 35(3):391 – 401, 2000.

[UE12] Ulrich, K. T. and Eppinger, S. D. *Product Design and Development.* McGraw-Hill Book Company, New York, 5th edition, 2012.

[VDA06] VDA. Wirtschaftliche Tolerierung. In *VDA-Band 4: Qualitätsmanagement in der Automobilindustrie – Sicherung der Qualität vor Serieneinsatz*. Verband der Automobilindustrie e.V. (VDA), 1st edition, 2006.

[VDI2235] VDI. VDI 2235:1987: Wirtschaftliche Entscheidungen beim Konstruieren; Methoden und Hilfen. Guideline, 1987.

[VDI2613] VDI/VDE. VDI/VDE 2613:2003: Pitch and runout testing on gearings - Cylindrical gears, whormwheels, bevel gears. Guideline, 2003.

[Vec06] VECCHIATO, D. Tooth contact analysis of a misaligned isostatic planetary gear train. *Mechanism and Machine Theory*, 41(6):617 – 631, 2006.

[VHD13] VALENTINI, P. P. and HASHEMI-DEHKORDI, S.-M. Effects of dimensional errors on compliant mechanisms performance by using dynamic splines. *Mechanism and Machine Theory*, 70:106 – 115, 2013.

[Vim07] VIMERCATI, M. Mathematical model for tooth surfaces representation of face-hobbed hypoid gears and its application to contact analysis and stress calculation. *Mechanism and Machine Theory*, 42(6):668 – 690, 2007.

[VL08] VALLET, B. and LÉVY, B. Spectral Geometry Processing with Manifold Harmonics. *Computer Graphics Forum*, 27(2):251–260, 2008.

[VMW10] VOSS, R.; MEERKAMM, H.; and WARTZACK, S. Manufacturing Process Driven Tolerance Analysis of Casting Parts. In DAGMAN, A. and SÖDERBERG, R., editors, *Proceedings of NordDesign 2010, the 8th International NordDesign Conference, Göteborg, Sweden, 25.-27.08.2010*, pages 11–20, 2010.

[VNA06] VASILIS, D.; NECTARIOS, V.; and ARISTOMENIS, A. Advanced Computer Aided Design Simulation of Gear Hobbing by Means of Three-Dimensional Kinematics Modeling. *Journal of Manufacturing Science and Engineering*, 129(5):911–918, 2006.

[Voe93] VOELCKER, H. B. A current Perspective on Tolerancing and Metrology. In SRINIVASAN, V. and VOELCKER, H. B., editors, *Proceedings of the 1993 International Forum on Dimensional Tolerancing and Metrology, Dearborn, Michigan*, volume CRTD-Vol. 27, pages 49–60. ASME, 1993.

[Voe98] VOELCKER, H. B. The current state of affairs in dimensional tolerancing: 1997. *Integrated Manufacturing Systems*, 9(4):205–217, 1998.

[VR77] VOELCKER, H. B. and REQUICHA, A. A. G. Geometric Modeling of Mechanical Parts and Processes. *Computer*, 10(12):48–57, 1977.

[VW86] VEITSCHEGGER, W. and WU, C.-H. Robot accuracy analysis based on kinematics. *IEEE Journal on Robotics and Automation*, 2(3):171–179, 1986.

[VWB+09] VAJNA, S.; WEBER, C.; BLEY, H.; ZEMAN, K.; and HEHENBERGER, P. *CAx für Ingenieure – Eine praxisbezogene Einführung*. Springer Berlin Heidelberg, 2009.

[War00] WARTZACK, S. *Predictive Engineering – Assistenzsystem zur multikriteriellen Analyse alternativer Produktkonzepte*. PhD thesis, Technische Fakultät der Friedrich-Alexander-Universität Erlangen-Nürnberg, 2000.

[WB06] WECK, M. and BRECHER, C. Geometrisches und kinematisches Verhalten von Werkzeugmaschinen. In *Werkzeugmaschinen 5*, VDI-Buch, pages 77–162. Springer Berlin Heidelberg, 2006.

[WBvdL13] WATRIN, S.; BINZ, H.; and VAN DE LINDELOOF, B. Methodology for Requirement-driven Tolerance Specification of Bevel Gears. *Procedia CIRP – 12th CIRP Conference on Computer-Aided Tolerancing*, 10:299 – 305, 2013.

[WCH+88] WEILL, R.; CLÉMENT, A.; HOCKEN, R.; FARMER, L.; GLADMAN, C.; WIRTZ, A.; BOURDET, P.; FRECKLETON, J.; KUNZMANN, H.; HAM, I.; TRUMPOLD, H.; and MATTHIAS, E. Tolerancing for Function. *CIRP Annals - Manufacturing Technology*, 37(2):603 – 610, 1988.

[WCH04] WITTWER, J. W.; CHASE, K. W.; and HOWELL, L. L. The direct linearization method applied to position error in kinematic linkages. *Mechanism and Machine Theory*, 39(7):681 – 693, 2004.

[WCS16] WÄRMEFJORD, K.; CARLSON, J. S.; and SÖDERBERG, R. Controlling Geometrical Variation Caused by Assembly Fixtures. *Journal of Computing and Information Science in Engineering*, 16(1):011007, 2016.

[WCT98] WU, C.-C.; CHEN, Z.; and TANG, G.-R. Component tolerance design for minimum quality loss and manufacturing cost. *Computers in Industry*, 35(3):223 – 232, 1998.

[WDA93] WILSON, P. F.; DELL, L. D.; and ANDERSON, G. F. *Root Cause Analysis: A Tool for Total Quality Management*. ASQC Quality Press, Milwaukee, Wisconsin, 1993.

[Wec14] WECKENMANN, A. A. Form Error. In LAPERRIÈRE, L. and REINHART, G., editors, *CIRP Encyclopedia of Production Engineering*, pages 535–539. Springer Berlin Heidelberg, 2014.

[WEE88] Wu, Z.; ElMaraghy, W. H.; and ElMaraghy, H. A. Evaluation of Cost-Tolerance Algorithms for Design Tolerance Analysis and Synthesis. *Manufacturing Review*, 1(3):168–179, 1988.

[Wei88] Weill, R. Integrating dimensioning and tolerancing in computer-aided process planning. *Robotics and Computer-Integrated Manufacturing*, 4(1):41 – 48, 1988.

[Wei15a] Weidenhiller, F. Statistische Toleranzsimulation – Werkzeug des Toleranzmanagements zur Absicherung von Produkt und Prozess. In Wartzack, S., editor, *Summer School Toleranzmanagement – Beiträge zur 2. Summer School September 2015*, pages 116–121. Druck+Verlag Ernst Vögel GmbH Stamsried, 2015.

[Wei15b] Weidenhiller, F. Toleranzmanagement in der Produktentwicklung: Methoden und Werkzeuge zur frühzeitigen Optimierung von Qualität, Geometrie und Montageprozess. Lecture Notes, Friedrich-Alexander-Universität Erlangen-Nürnberg, 2015.

[Wen10] Wenzlhuemer, R. The History of Standardisation in Europe. *European History Online (EGO)*, http://www.ieg-ego.eu/wenzlhuemerr-2010-en, Published 2010, Retrieved in April 2016.

[WG98] Wisniewski, D. M. and Gomer, P. Tolerance Analysis Using VSA-3D® for Engine Applications. In ElMaraghy, H. A., editor, *Geometric Design Tolerancing: Theories, Standards and Applications*, pages 453–464. Springer US, 1998.

[WGJ94] Whitney, D. E.; Gilbert, O. L.; and Jastrzebski, M. Representation of geometric variations using matrix transforms for statistical tolerance analysis in assemblies. *Research in Engineering Design*, 6(4):191–210, 1994.

[WH01] Weckenmann, A. and Humienny, Z. *Geometrical product specifications (GPS): course for technical universities.* Universität Erlangen-Nürnberg, Lehrstuhl für Qualitätsmanagement und Fertigungsmeßtechnik QFM, 2001.

[Wil03] Wilhelm, R. G. Trends in Tolerancing Research. In Wilhelm, R. G., editor, *Proceedings of the 8th CIRP International Seminar on Computer Aided Tolerancing – Managing Geometric Uncertainty in the Product Lifecycle*, pages 7–13, 2003.

[Wir88] Wirtz, A. Vektorielle Tolerierung zur Qualitätssteuerung in der mechanischen Fertigung. *CIRP Annals - Manufacturing Technology*, 37(1):493 – 498, 1988.

[Wir89] Wirtz, A. Vectorial Tolerancing. In Weill, R., editor, *Proceedings of the International Conference on CAD/CAM and AMT – Volume II: CIRP Sessions on Tolerancing for Function in a CAD/CAM Environment*, pages C–1–4, 1989.

[Wir91] Wirtz, A. Vectorial Tolerancing for Production Quality Control and Functional Analysis in Design. In Weill, R., editor, *Proceedings of the CIRP Working Seminar on Computer-Aided Tolerancing, Penn State University*, pages 77–84, 1991.

[Wit11] Wittmann, S. *Verfahren zur Simulation und Analyse der Auswirkungen toleranzbedingter Bauteilabweichungen.* PhD thesis, Technische Fakultät der Friedrich-Alexander-Universität Erlangen-Nürnberg, 2011.

[WK09] Weckenmann, A. and Krämer, P. Application of Computed Tomography in Manufacturing Metrology. *tm – Technisches Messen*, 76(7-8):340–346, 2009.

[WM00] Wartzack, S. and Meerkamm, H. Durchgängige Rechnerunterstützung in der Produktentwicklung aufgrund des Einsatzes von semantisch hochwertiger Features (Continuous computer support in the product development process by the use of high grade semantic features). *Konstruktion*, 3:24–26, 2000.

[WMAR99] Whitney, D. E.; Mantripragada, R.; Adams, J. D.; and Rhee, S. J. Toward a Theory for Design of Kinematically Constrained Mechanical Assemblies. *The International Journal of Robotics Research*, 18(12):1235–1248, 1999.

[WMS+11] Wartzack, S.; Meerkamm, H.; Stockinger, A.; Stoll, T.; Stuppy, J.; Voss, R.; Walter, M.; and Wittmann, S. Lebenszyklusorientierte Toleranzsimulation zur funktionalen und ästhetischen Produktabsicherung (Lifecycle-oriented Tolerance Simulation). *Konstruktion*, 6:63–74, 2011.

[Woo60] Woodbury, R. S. The Legend of Eli Whitney and Interchangeable Parts. *Technology and Culture*, 1(3):235–253, 1960.

[WS93] Walker, R. K. and Srinivasan, V. Creation and Evolution of the ASME Y14.5.1M Standard. In Srinivasan, V. and Voelcker, H. B., editors, *Proceedings of the 1993 International Forum on Dimensional Tolerancing and Metrology, Dearborn, Michigan*, volume CRTD-Vol. 27, pages 19–30. ASME, 1993.

[WS04] Wickman, C. and Söderberg, R. Comparison of Non-Nominal Geometry Models Represented in Physical Versus Virtual Environments. *Journal of Computing and Information Science in Engineering*, 4(3):171–177, 2004.

[WS06] Wittmann, S. and Stockinger, A. Volumenvisualisierung von abweichungsbehafteter Geometrie. In Meerkamm, H., editor, *Proceedings of the 17th Symposium on Design for X, Neukirchen/Erlangen*, 2006.

[WS07] Wickman, C. and Söderberg, R. Perception of gap and flush in virtual environments. *Journal of Engineering Design*, 18(2):175–193, 2007.

[WS08] Waldron, K. and Schmiedeler, J. Kinematics. In Siciliano, B. and Khatib, O., editors, *Springer Handbook of Robotics*, pages 9–33. Springer Berlin Heidelberg, 2008.

[WSD03] Wu, Y.; Shah, J. J.; and Davidson, J. K. Improvements to algorithms for computing the Minkowski sum of 3-polytopes. *Computer-Aided Design*, 35(13):1181 – 1192, 2003.

[WSH16] Wartzack, S.; Schleich, B.; and Heling, B. DFG-Forschergruppe “Prozessorientiertes Toleranzmanagement” an der FAU gestartet. *WiGeP News*, 2:6, November 2016.

[WSL13] Wärmefjord, K.; Söderberg, R.; and Lindkvist, L. Simulation of Variation in Assembly Forces Due to Variation in Spot Weld Position. In Abramovici, M. and Stark, R., editors, *Smart Product Engineering*, Lecture Notes in Production Engineering, pages 473–482. Springer Berlin Heidelberg, 2013.

[WSP07] Wittmann, S.; Stoll, T.; and Paetzold, K. Volume Visualization of Geometric Deviations. In Bocquet, J.-C., editor, *Proceedings of the 16th International Conference on Engineering Design ICED07, Paris*, 2007.

[WSW13] Walter, M.; Sprügel, T.; and Wartzack, S. Tolerance analysis of systems in motion taking into account interactions between deviations. *Proceedings of the Institution of Mechanical Engineers, Part B: Journal of Engineering Manufacture*, 227(5):709–719, 2013.

[WSW15] Walter, M.; Sprügel, T.; and Wartzack, S. Least Cost Tolerance Allocation for Systems with Time-variant Deviations. *Procedia CIRP – 13th CIRP Conference on Computer-Aided Tolerancing*, 27:1 – 9, 2015.

[WT98] Wu, C. C. and Tang, G. Tolerance design for products with asymmetric quality losses. *International Journal of Production Research*, 36(9):2529–2541, 1998.

[WT15] Wang, Y. and Tian, D. A weighted assembly precedence graph for assembly sequence planning. *The International Journal of Advanced Manufacturing Technology*, 83(1):99–115, 2015.

[Wu97] Wu, Z. Sensitive factor for position tolerance. *Research in Engineering Design*, 9(4):228–234, 1997.

[WW00] Weber, C. and Wernr, H. Klassifizierung von CAx-Werkzeugen für die Produktentwicklung auf der Basis eines neuartigen Produkt- und Prozessmodells. In Meerkamm, H., editor, *Proceedings of the 11th Symposium on Design for X, Schnaittach*, 2000.

[WW13] Walter, M. and Wartzack, S. Statistical Tolerance-Cost-Optimization of Systems in Motion Taking into Account Different Kinds of Deviations. In Abramovici, M. and Stark, R., editors, *Smart Product Engineering*, Lecture Notes in Production Engineering, pages 705–714. Springer Berlin Heidelberg, 2013.

[WWP09] Wittmann, S.; Winter, M.; and Paetzold, K. Assembly Simulation for Toleranced Parts: an adapted Path Planning Approach. In Norell Bergendahl, M.; Grimheden, M.; Leifer, L.; Skogstad, P.; and Lindemann, U., editors, *Proceedings of the 17th International Conference on Engineering Design ICED09, Palo Alto*, 2009.

[WYWSC16] Wang, G.-d.; Yang, Y.; Wang, W.; and Si-Chao, L. V. Variable coefficients reciprocal squared model based on multi-constraints of aircraft assembly tolerance allocation. *The International Journal of Advanced Manufacturing Technology*, 82(1):227–234, 2016.

[XDW08] Xia, H.; Ding, Y.; and Wang, J. Gaussian process method for form error assessment using coordinate measurements. *IIE Transactions*, 40(10):931–946, 2008.

[XJ14] Xiuming, L. and Jingcai, Z. Evaluation for the minimum circumscribed circle based on the rotation method. *Measurement Science and Technology*, 25(9):097001, 2014.

[Yau97] Yau, H.-T. Evaluation and uncertainty analysis of vectorial tolerances. *Precision Engineering*, 20(2):123 – 137, 1997.

[YB16] Yan, X. and Ballu, A. Toward an Automatic Generation of Part Models with Form Error. *Procedia CIRP – 14th CIRP Conference on Computer-Aided Tolerancing*, 43:23 – 28, 2016.

[YM96] Yau, H.-T. and Menq, C.-H. A unified least-squares approach to the evaluation of geometric errors using discrete measurement data. *International Journal of Machine Tools and Manufacture*, 36(11):1269 – 1290, 1996.

[YWLY12] Yan, D.-M.; Wang, W.; Liu, Y.; and Yang, Z. Variational mesh segmentation via quadric surface fitting. *Computer-Aided Design*, 44(11):1072 – 1082, 2012.

[ZAB13] Zhao, H.; Anwer, N.; and Bourdet, P. Curvature-based Registration and Segmentation for Multisensor Coordinate Metrology. *Procedia CIRP – 12th CIRP Conference on Computer-Aided Tolerancing*, 10:112 – 118, 2013.

[ZAMZ11] Zhang, M.; Anwer, N.; Mathieu, L.; and Zhao, H. B. A Discrete Geometry Framework for Geometrical Product Specifications. In Thompson, M. K., editor, *Proceedings of the 21st CIRP Design Conference, Kaist*, 2011.

[ZAS+13] Zhang, M.; Anwer, N.; Stockinger, A.; Mathieu, L.; and Wartzack, S. Discrete shape modeling for skin model representation. *Proceedings of the Institution of Mechanical Engineers, Part B: Journal of Engineering Manufacture*, 227(5):672–680, 2013.

[ZCWY13] Zhang, H.; Cao, Y.; Wei, Y.; and Yang, J. A Concurrent Design Method for Functional Tolerance and Structure based on the Principle of Decomposition and Reconstitution. *Procedia CIRP – 12th CIRP Conference on Computer-Aided Tolerancing*, 10:194 – 202, 2013.

[ZD02] Zhu, X. and Ding, H. Flatness tolerance evaluation: an approximate minimum zone solution. *Computer-Aided Design*, 34(9):655 – 664, 2002.

[Zha10] Zhao, H. *Multisensor Integration and discrete Geometry Processing for Coordinate Metrology.* PhD thesis, École normale supérieure de Cachan - ENS Cachan, 2010.

[Zha11] Zhang, M. *Discrete shape modeling for geometrical product specification : contributions and applications to skin model simulation.* PhD thesis, École normale supérieure de Cachan - ENS Cachan, 2011.

[ZJF+13] Zhang, X.; Jiang, X.; Forbes, A. B.; Minh, H. D.; and Scott, P. J. Evaluating the form errors of spheres, cylinders and cones using the primal–dual interior point method. *Proceedings of the Institution of Mechanical Engineers, Part B: Journal of Engineering Manufacture*, 227(5):720–725, 2013.

[ZLB+10] Zhang, J.; Li, S.; Bao, N.; Zhang, G.; Xue, D.; and Gu, P. A robust design approach to determination of tolerances of mechanical products. *CIRP Annals - Manufacturing Technology*, 59(1):195 – 198, 2010.

[ZLGH11] Zhang, Y.; Li, Z.; Gao, J.; and Hong, J. New reasoning algorithm for assembly tolerance specifications and corresponding tolerance zone types. *Computer-Aided Design*, 43(12):1606 – 1628, 2011.

[ZLT15] Zeng, C.; Liao, W.-H.; and Tian, W. Influence of initial fit tolerance and squeeze force on the residual stress in a riveted lap joint. *The International Journal of Advanced Manufacturing Technology*, 81(9-12):1643–1656, 2015.

[ZLW15] Zhao, Y. M.; Liu, D. S.; and Wen, Z. J. Optimal tolerance design of product based on service quality loss. *The International Journal of Advanced Manufacturing Technology*, 82(9):1715–1724, 2015.

[ZM95] Zhang, H. C. and Mei, J. Automated tolerance analysis for CAPP system. *The International Journal of Advanced Manufacturing Technology*, 10(4):219–224, 1995.

[ZM04] Zou, Z. and Morse, E. P. A gap-based approach to capture fitting conditions for mechanical assembly. *Computer-Aided Design*, 36(8):691 – 700, 2004.

[ZPW06] Zhao, X.; Pasupathy, T. K.; and Wilhelm, R. G. Modeling and representation of geometric tolerances information in integrated measurement processes. *Computers in Industry*, 57(4):319 – 330, 2006.

[ZQ15] Zhu, Z. and Qiao, L. Analysis and Control of Assembly Precision in Different Assembly Sequences. *Procedia CIRP – 13th CIRP Conference on Computer-Aided Tolerancing*, 27:117 – 123, 2015.

[ZQH+13] Zhong, Y.; Qin, Y.; Huang, M.; Lu, W.; Gao, W.; and Du, Y. Automatically generating assembly tolerance types with an ontology-based approach. *Computer-Aided Design*, 45(11):1253 – 1275, 2013.

[ZQH+14] Zhong, Y.; Qin, Y.; Huang, M.; Lu, W.; and Chang, L. Constructing a meta-model for assembly tolerance types with a description logic based approach. *Computer-Aided Design*, 48:1 – 16, 2014.

[ZW15a] Ziegler, P. and Wartzack, S. Sensitivity Analysis of features in tolerancing based on constraint function level sets. *Reliability Engineering & System Safety*, 134:324 – 333, 2015.

[ZW15b] Ziegler, P. and Wartzack, S. A statistical method to identify main contributing tolerances in assemblability studies based on convex hull techniques. *Journal of Zhejiang University SCIENCE A*, 16(5):361–370, 2015.

[Zwi11] Zwillinger, D. *Standard Mathematical Tables and Formulae*. CRC Press, 32nd edition, 2011.

[ZZL16] Zhu, H.; Zhou, X.; and Li, H. A novel tolerance analysis for mechanical assemblies based on Convex Method and non-probabilistic set theory. *The International Journal of Advanced Manufacturing Technology*, 83(9):1649–1657, 2016.

Publications by the Author

2016

- **Schleich, B.**; Anwer, N.; Mathieu, L.; and Wartzack, S.: Status and Prospects of Skin Model Shapes for Geometric Variations Management. *Procedia CIRP – 14th CIRP CAT 2016 - CIRP Conference on Computer Aided Tolerancing*, 43:154 – 159, 2016.
- **Schleich, B.** and Wartzack, S.: A Quantitative Comparison of Tolerance Analysis Approaches for Rigid Mechanical Assemblies. *Procedia CIRP – 14th CIRP CAT 2016 - CIRP Conference on Computer Aided Tolerancing*, 43:172 – 177, 2016.
- Wartzack, S.; **Schleich, B.**; and Heling, B.: DFG-Forschergruppe "Prozessorientiertes Toleranzmanagement" an der FAU gestartet. *WiGeP News*, 2016(2):6, 2016.

2015

- **Schleich, B.**; Anwer, N.; Mathieu, L.; and Wartzack, S.: Contact and Mobility Simulation for Mechanical Assemblies Based on Skin Model Shapes. *Journal of Computing and Information Science in Engineering*, 15(2):021009-1–021009-7, 2015.
- **Schleich, B.** and Wartzack, S.: Approaches for the assembly simulation of skin model shapes. *Computer-Aided Design*, 65:18 – 33, 2015.
- **Schleich, B.** and Wartzack, S.: Evaluation of geometric tolerances and generation of variational part representatives for tolerance analysis. *The International Journal of Advanced Manufacturing Technology*, 79(5-8):959–983, 2015.
- **Schleich, B.** and Wartzack, S.: A generic Approach to Sensitivity Analysis in Geometric Variations Management. In Weber, C.; Husung, S.; Cantamessa, M.; Cascini, G.; Marjanovic, D.; and Graziosi, S., editors, *Proceedings of the 20th International Conference on Engineering Design ICED15, Milan*, Volume 4: Design for X, Design to X, Pages 343–352, 2015.
- **Schleich, B.** and Wartzack, S.: Tolerance Analysis of Rotating Mechanism Based on Skin Model Shapes in Discrete Geometry. *Procedia CIRP – 13th CIRP Conference on Computer-Aided Tolerancing*, 27:10 – 15, 2015.
- **Schleich, B.**; Wartzack, S.; Anwer, N.; and Mathieu, L.: Skin Model Shapes: Offering New Potentials for Modelling Product Shape Variability. In ASME, editor, *Proceedings of the ASME 2015 International Design Engineering Technical Conferences and Computers and Information in Engineering Conference, Boston, Massachusetts, USA, August 2–5, 2015*, Volume 1A: 35th Computers and Information in Engineering Conference, Paper no. DETC2015–46701, 2015.
- Wartzack, S.; Walter, M.; **Schleich, B.**; Aschenbrenner, A.; and Heling, B.: Der KTmfk und die Arbeitsgruppe "Toleranzmanagement". In Wartzack, S., editor, *Summer School Toleranzmanagement – Beiträge zur 2. Summer School September 2015*, Pages 3–8. Druck+Verlag Ernst Vögel GmbH Stamsried, 2015.

2014

- Anwer, N.; **Schleich, B.**; Mathieu, L.; and Wartzack, S.: From solid modelling to skin model shapes: Shifting paradigms in computer-aided tolerancing. *CIRP Annals - Manufacturing Technology*, 63(1):137 – 140, 2014.
- **Schleich, B.**; Anwer, N.; Mathieu, L.; and Wartzack, S.: Skin Model Shapes: A new paradigm shift for geometric variations modelling in mechanical engineering. *Computer-Aided Design*, 50:1 – 15, 2014.
- **Schleich, B.** and Wartzack, S.: A discrete geometry approach for tolerance analysis of mechanism. *Mechanism and Machine Theory*, 77:148 – 163, 2014.

- **Schleich, B.**; Anwer, N.; Zhang, W.; Mathieu, L.; and Wartzack, S.: Skin Model Based Simulation of Contact and Mobility for Mechanical Assemblies. In Yanlong, C. and Jianrong, T., editors, *Proceedings of the 13th CIRP Conference on Computer Aided Tolerancing, Hangzhou*, Paper no. 13, 2014.
- **Schleich, B.**; Anwer, N.; Zhu, Z.; Qiao, L.; Mathieu, L.; and Wartzack, S.: A Comparative Study on Tolerance Analysis Approaches. In Howard, T. J. and Eifler, T., editors, *Proceedings of the International Symposium on Robust Design – ISoRD14, Copenhagen, Denmark*, Pages 29–39, 2014.
- **Schleich, B.** and Wartzack, S.: How can Computer Aided Tolerancing Support Closed Loop Tolerance Engineering? *Procedia CIRP – 24th CIRP Design Conference*, 21:312 – 317, 2014.

2013

- Grottke, M. and **Schleich, B.**: How does testing affect the availability of aging software systems? *Performance Evaluation*, 70:179–196, 2013.
- **Schleich, B.** and Wartzack, S.: How to determine the influence of geometric deviations on elastic deformations and the structural performance? *Proceedings of the Institution of Mechanical Engineers, Part B: Journal of Engineering Manufacture*, 227(5):754–764, 2013.
- Wartzack, S.; Walter, M.; and **Schleich, B.**: So eng wie nötig, so breit wie möglich. *Konstruktionspraxis*, Pages 14–16, 2013.
- Luft, T.; **Schleich, B.**; and Wartzack, S.: Concept development for innovative products – A challenge for engineering design education. In Lindemann, U.; V, S.; Kim, Y. S.; Lee, S. W.; Clarkson, J.; and Cascini, G., editors, *Proceedings of the 19th International Conference on Engineering Design (ICED13), Design for Harmonies, Seoul, Korea, 19-22.08.2013*, Volume 8: Design Education, Pages 105–114, 2013.
- **Schleich, B.** and Wartzack, S.: Ein methodisches Framework für das prozessorientierte Toleranzmanagement. In Spath, D.; Binz, H.; and Bertsche, B., editors, *Stuttgarter Symposium für Produktentwicklung SSP2013*. Fraunhofer Verlag, 2013.
- **Schleich, B.** and Wartzack, S.: The Implications of the Skin Model Concept for Computer Aided Tolerancing. In Abramovici, M. and Stark, R., editors, *Smart Product Engineering*, Lecture Notes in Production Engineering, Pages 573–582. Springer Berlin Heidelberg, 2013.
- **Schleich, B.** and Wartzack, S.: Process-oriented Tolerancing – A Discrete Geometry Framework. In Lindemann, U.; V, S.; Kim, Y. S.; Lee, S. W.; Clarkson, J.; and Cascini, G., editors, *Proceedings of the 19th International Conference on Engineering Design (ICED13) Design For Harmonies, Seoul, Korea 19-22.08.2013*, Volume 5: Design for X, Design to X, Pages 61–70, 2013.
- Wartzack, S.; **Schleich, B.**; Walter, M.; and Ziegler, P.: Die Einbettung des Toleranzmanagements in den Produktentwicklungsprozess. In Wartzack, S., editor, *Summer School Toleranzmanagement – Beiträge zur 1. Summer School September 2013*, Pages 63–67. TuTech Verlag, Hamburg, 2013.
- Wartzack, S.; **Schleich, B.**; Walter, M.; and Ziegler, P.: Toleranzmanagement am KTmfk. In Wartzack, S., editor, *Summer School Toleranzmanagement – Beiträge zur 1. Summer School September 2013*, Pages 2–5. TuTech Verlag, Hamburg, 2013.

2012

- Grottke, M. and **Schleich, B.**: Cost Optimality in Testing and Rejuvenation. In *IEEE 23rd International Symposium on Software Reliability Engineering Workshops, Dallas*, Pages 259–264, 2012.
- **Schleich, B.**; Stockinger, A.; and Wartzack, S.: On the impact of geometric deviations on structural performance. In Jiang, X. J., editor, *Proceedings of the 12th CIRP International Conference on Computer Aided Tolerancing, Huddersfield*, 2012.
- **Schleich, B.** and Wartzack, S.: Generation of deviated geometry based on manufacturing process simulations. In Dynardo, editor, *Proceedings of the Weimarer Optimierungs- und Stochastiktage WOST 9.0, Weimar*, 2012.
- **Schleich, B.** and Wartzack, S.: Virtuelle Toleranzbeurteilung abweichungsbehafteter Bauteile. In

Wartzack, S., editor, *Proceedings of the 23rd Symposium on Design for X, Bamberg/Erlangen*, 2012. (This paper received the **ENmfk-Preis 2012**).

- **Schleich, B.**; Walter, M.; Wartzack, S.; Anwer, N.; and Mathieu, L.: A Comprehensive Framework for Skin Model Simulation. In ASME, editor, *Proceedings of the ASME 2012 11th Biennial Conference on Engineering Systems Design and Analysis, Nantes*, Paper no. ESDA2012-82204, Pages 567–576, 2012.

Awards

- **ASME CAPPD Technical Committee 2015 Prakash Krishnaswami Best Paper Award** for the paper *"Skin Model Shapes: Offering New Potentials for Modelling Product Shape Variability"* by B. Schleich, S. Wartzack, N. Anwer, and L. Mathieu at the 35th ASME Computers and Information in Engineering Conference 2015.
- **Reviewers Favourite Recognition** (top 10% papers) for the paper *"A generic Approach to Sensitivity Analysis in Geometric Variations Management"* by B. Schleich and S. Wartzack at the 20th International Conference on Engineering Design (ICED15).
- **Luise Prell-Preis 2013** in recognition of the outstanding diploma thesis *"Generation of non-ideal geometry in order to robustly simulate random shapes within tolerance zones using random fields"*.
- **ENmfk-Preis** for the best contribution at the 23rd DfX-Symposium 2012 for the paper *"Virtuelle Toleranzbeurteilung abweichungsbehafteter Bauteile"* by B. Schleich and S. Wartzack.

Die Reihen der Fortschritt-Berichte VDI:

1 Konstruktionstechnik/Maschinenelemente
2 Fertigungstechnik
3 Verfahrenstechnik
4 Bauingenieurwesen
5 Grund- und Werkstoffe/Kunststoffe
6 Energietechnik
7 Strömungstechnik
8 Mess-, Steuerungs- und Regelungstechnik
9 Elektronik/Mikro- und Nanotechnik
10 Informatik/Kommunikation
11 Schwingungstechnik
12 Verkehrstechnik/Fahrzeugtechnik
13 Fördertechnik/Logistik
14 Landtechnik/Lebensmitteltechnik
15 Umwelttechnik
16 Technik und Wirtschaft
17 Biotechnik/Medizintechnik
18 Mechanik/Bruchmechanik
19 Wärmetechnik/Kältetechnik
20 Rechnerunterstützte Verfahren (CAD, CAM, CAE CAQ, CIM ...)
21 Elektrotechnik
22 Mensch-Maschine-Systeme
23 Technische Gebäudeausrüstung

ISBN 978-3-18-3**43801**-3